Rhodium-catalysed Stereoselective Carbocyclisation Reactions for the Synthesis of Bicyclopentenone Derivatives

Thesis submitted in accordance with the requirements of the University of Liverpool for the degree of Doctor in Philosophy

Paolo Ricci

September 2011

Rhodium-catalysed Stereoselective Carbocyclisation Reactions for the Synthesis of Bicyclopentenone Derivatives

Dedication

This thesis is dedicated to Italia, Salvatore, Orlando and Vanda.

"Faber est suae quisque fortunae" (Appius Claudius Caecus)

"Every man is the maker of his own fortune" (Appius Claudius Caecus)

Acknowledgments

Whenever you are going to fly, it's good news to know that the pilot is experienced and able to solve any possible issue during the flight. In a similar way, during these four years of PhD, I have been incredibly lucky and honoured to have a supervisor like Prof. P. Andrew Evans, whose knowledge and experience in Chemistry is undoubtedly great. I express to him all my gratitude for the continuous support, advice and patience throughout my academic career. I would like to thank Katie Evans for her precious help and support to me and other people in this group with every sort of problem we had, you are a really nice person. I would like to thank all the past and present members of the Evans group, in good and bad times, in serious and less serious moments, I really enjoyed your company and I am so grateful for our continuous exchange of ideas and criticism. I would like to express my sincere gratitude to my neighbours in the bay No. 2. Dr Sanil Sreekumar, I wish you all the best for your new chemistry adventure in California; Dr Deju-Shang and Dr Mu-Hua Huang, good luck for your academic career, wish you all the best. Thank you all, Alex, Sergio, Stephen, Sean, Phill, Helen, Sam and Ryan. I also would like to thank some members of the Department of Chemistry, Moya, Jim, Keith and Sandra, you've always been incredibly helpful and kind with me. Since I was born I have been so lucky to have the best family in the world. Mom and dad, you only know how much you helped me in my entire life. If I am here today it's because of your sacrifices and your good advice. I hope you will always be proud of me and be by my side, I love you from the depth of my heart. Alessandro, you're not just my big brother, you are the coolest brother ever and a wonderful person, I can't wait to go to the stadium together and watch our hometown team playing football. My last acknowledgement is probably the most important. You've seen my tears, you've seen my joy, and a lifetime won't be enough to thank you for your love, dedication and support. My best smile is for you, Martina.

Abstract

Among the classes of organic transformations, cycloaddition reactions constitute a powerful and versatile strategy for the rapid assembly of complex polycyclic scaffolds in a highly stereoselective fashion. A unique feature of this class of reactions resides in the possibility to alter the geometry and coordination number of the metal centre in order to increase the reactivity and selectivity of the process. Hence, the development of this strategy highlighted the opportunity to synthesize complex molecular architectures in a highly convergent and stereoselective manner using mild operating conditions, thereby improving the efficiency with respect to atom-economy and environmentally benign synthesis. Among the metal-catalysed carbocyclisation reactions, the Pauson-Khand (PK) methodology enables the straightforward construction of cyclopentenone derivatives from readily available synthons. Distinguishing feature of this reaction is the incorporation of a carbon monoxide unit into a polycyclic framework with the production of carbonyl systems that are amenable of further functionalisation. In this context, we performed a detailed computational analysis of the mechanism of the Rh-catalysed diastereoselective PK reaction. This study outlined the possibility to enhance the reactivity of 1,6-enynes towards the carbocyclisation through the incorporation of electron-withdrawing substituents on the alkyne terminus. Further experimental analysis revealed that the employment of a chlorine substituent on the alkyne moiety exerted a beneficial effect on the reactivity of 1,6-enynes and thereby provided a novel highly diastereoselective Rh-catalysed PK reaction at room temperature. The enhanced reactivity of chlorinated 1,6-enynes was subsequently exploited in the Rh-catalysed asymmetric PK reaction. A detailed optimisation study revealed that the electronic and geometric properties of

chiral bisphosphine ligands exerted a remarkable influence on the reactivity of 1,6-enynes towards the carbocyclisation process. Hence, the synergic combination of chlorinated 1,6-enynes and SEGPHOS-type bisphosphine ligands allowed a highly enantioselective rhodium-catalysed PK reaction of substrates that are generally unreactive, such as 1,6-enynes bearing substituents on the alkene position. Hence, methodology expanded the synthetic potential of the PK reaction and moreover, provided a highly enantioselective construction of bicyclopentenone scaffolds under extremely mild operating conditions.

Table of Contents

List of Schemes

Chapter 1 **EXPERIMENTAL AND COMPUTATIONAL STUDIES ON RHODIUM(I)-CATALYSED [2+2+1] DIASTEREOSELECTIVE PAUSON-KHAND CARBOCYCLISATIONS AT ROOM TEMPERATURE.**

List of Tables

Chapter 1 **EXPERIMENTAL AND COMPUTATIONAL STUDIES ON RHODIUM(I)-CATALYSED [2+2+1] DIASTEREOSELECTIVE PAUSON-KHAND CARBOCYCLISATIONS AT ROOM TEMPERATURE.**

Chapter 2 **RHODIUM(I)-CATALYSED [2+2+1] ENANTIOSELECTIVE PAUSON-KHAND CARBOCYCLISATIONS OF CHLORINATED 1,6-ENYNES AT ROOM TEMPERATURE.**

List of Figures

Chapter 1 **EXPERIMENTAL AND COMPUTATIONAL STUDIES ON RHODIUM(I)-CATALYSED [2+2+1] DIASTEREOSELECTIVE PAUSON-KHAND CARBOCYCLISATIONS AT ROOM TEMPERATURE.**

Chapter 2 **RHODIUM(I)-CATALYSED [2+2+1] ENANTIOSELECTIVE PAUSON-KHAND CARBOCYCLISATIONS OF CHLORINATED 1,6-ENYNES AT ROOM TEMPERATURE.**

List of Abbreviations

°C	degrees Celsius
Å	angstrom
ABCN	1,1'-azobis(cyclohexanecarbonitrile)
Ac	acetate
Acac	acetylacetonate
Atm	atmosphere
BINAP	2,2'-bis(diphenylphosphino)-1,1'-binaphthyl
BIPHEP	2,2'-bis(diphenylphosphino)-1,1'-biphenyl
Bn	benzyl
BOC	*tert*-butyloxycarbonyl
BPE	1,2-bis(2,5-diethylphospholano)
Bu	butyl
COD	1,5-cyclooctadiene
COSY	COrrelation SpectroscopY
Cp	cyclopentadienyl
Cy	cyclohexyl
DABCO	1,4-diazabicyclo[2.2.2]octane
DCB	1,4-dichlorobenzene
DCE	1,2-dichloroethane
DCM	dichloromethane
DEAD	diethyl azodicarboxylate
DFT	density functional theory
DIFLUORPHOS	5,5'-bis(diphenylphosphino)-2,2,2',2'-tetrafluoro-4,4'-bi-1,3-benzodioxole
DIOP	(-)-4,5-bis(diphenylphosphinomethyl)-2,2-dimethyl-1,3-dioxolane

DIPAMP	ethane-1,2-diylbis[(2-methoxyphenyl)phenylphosphane]
DM	3,5-dimethyl
DME	dimethoxyethane
DMF	dimethylformamide
DMSO	dimethyl sulfoxide
dpdb	2-dicyclohexylphosphino-2',6'- dimethoxybiphenyl
dppp	1,3-bis(diphenylphosphino)propane
dr	diastereoisomeric ratio
DUPHOS	1,2-(bisphospholano)benzene
EBTHI	ethylene- bistetrahydroindenyl
EDG	electron-donating
ee	enantiomeric excess
Et	ethyl
EWG	electron-withdrawing
HMAF	hydroxymethylacylfulvene
HMDS	bis(trimethylsilyl)amide
Me	methyl
mg	milligram
MHz	megahertz
MOM	methoxymethyl ether
NMO	*N*-methylmorpholine *N*-oxide
NMR	nuclear magnetic resonance
NOE	nuclear Overhauser effect
NOESY	nuclear Overhauser effect spectroscopy
Oct	octane
P-Phos	2,2',6,6'-tetramethoxy-4,4'-bis(diphenylphosphino)-3,3'-bipyridine
Ph	phenyl
PK	Pauson-Khand

ppm	parts per million
Pr	propyl
Psi	pounds per square Inch
RCM	ring closing metathesis
RT	room temperature
Samp	1-amino-2-(methoxymethyl)pyrrolidine
SDP	7,7'-bis(diphenylphosphino)-2,2',3,3'-tetrahydro-1,1'-spirobiindane
SEGPHOS	5,5′-bis(diphenylphosphino)-4,4′-bi-1,3-benzodioxole
SEM	[2-(trimethylsilyl)ethoxy]methyl
SIPHOS	(11a)-(+)-10,11,12,13-Tetrahydrodiindeno[7,1-de:1',7'-fg][1,3,2]dioxaphosphocin-5-dimethylamine
SOS	sodium octyl sulfate
SPIROP	1,6-bis(diphenylphosphinoxy)spiro[4.4]-nonane)
SYNPHOS	(5,6),(5′,6′)-bis(ethylenedioxy) biphenyl-2,2′-diyl]bis(diphenylphosphine
TBAF	tetra-*n*-butylammonium fluoride
TBDPS	*tert*-butyldiphenylsilyl
TBS	*tert*-butyldimethylsilyl
TEB	triethylborane
TES	triethylsilyl
Tf	trifluoromethansulfonate
THF	tetrahydrofuran
THP	tetrahydropyran
TIPS	triisopropylsilyl
TMANO	trimethylamine *N*-oxide
TMS	trimethylsilyl
TMTU	tetramethyl thiourea
Tol	tolyl

TON	turnover number
Ts	toluenesulfonyl
TTMSS	tris(trimethylsilyl)silane
TPPTS	3,3′,3″-phosphinidynetris(benzenesulfonic acid) trisodium salt
Tunephos	1,13-bis(diphenylphosphino)-7,8-dihydro-6*H*-dibenzo[f,h][1,5]dioxonin
UV	ultraviolet
VCP	vinylcyclopropane
xyl	xylyl

CHAPTER 1

EXPERIMENTAL AND COMPUTATIONAL STUDIES ON RHODIUM(I)-CATALYSED [2+2+1] DIASTEREOSELECTIVE PAUSON-KHAND CARBOCYCLISATIONS AT ROOM TEMPERATURE

1.1 Introduction.

1.1.1. Transition Metal-catalysed Carbocyclisation Reactions.

Among the classes of organic transformations, cycloaddition reactions provide an efficient and versatile tool for the direct assembly of complex polycyclic scaffolds from simple starting materials in a single operation.[1] The discovery and implementation of transition metal-catalysed cycloaddition reactions has broadened the scope and the versatility of this powerful strategy. This allows synthetic processes that either do not occur *via* classic pericyclic reactions or are difficult to accomplish in the absence of a catalyst. A unique feature of this class of reactions is the opportunity to tune the geometry and coordination number of the metal centre in order to increase the reactivity and selectivity of the process. Hence, the development of this strategy highlights the construction of complex molecular architectures in a highly convergent and stereoselective manner using milder reaction conditions, thereby improving the efficiency with respect to atom-economy and making the process more environmentally benign.

In this context, the Pauson-Khand (PK) reaction[2] provides an effective strategy for the rapid construction of cyclopentenone derivatives from readily available synthons. A distinguishing feature of this methodology is the incorporation of a carbon monoxide unit into a polycyclic framework with the production of carbonyl systems that are amenable to further synthetic elaboration. Since its inception in 1971, the Pauson-Khand reaction[3,4] has undergone extensive development, thereby gaining wide acceptance as a powerful strategy for the

expeditious synthesis of polycyclic structures. A unique feature in the development of this method is the ability for rhodium(I) complexes to overcome the use of stoichiometric transition metal and promote PK reactions with a high degree of reactivity and stereoselectivity. The following dissertation will highlight the overall advancements in this process and describe the development of novel computationally-designed and experimentally confirmed stereoselective rhodium(I)-catalysed PK reactions.

1.2. The Pauson-Khand Reaction.

1.2.1. Historical Background.

In a preliminary study, Pauson and coworkers disclosed the ability of (alkynyl)-hexacarbonyldicobalt complexes to react in presence of norbornadiene and promote the formation of arenecobalt derivatives **3** and **4** by reverse Diels-Alder type cleavage or displacement of an apical carbon monoxide moiety by the aromatic solvent (**Scheme 1.1**).[4]

Scheme 1.1. Synthesis of arenecobalt products from (alkynyl)hexacarbonyldicobalt complexes.

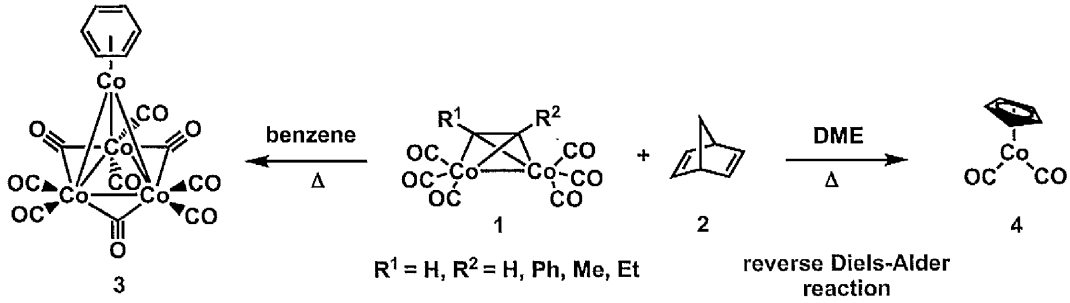

In addition to the abovementioned products, further detailed studies revealed the concurrent cobalt-catalysed formation of "*hydrocarbon and ketonic products from norbornadiene, acetylene and carbon monoxide*" (Eq. 1.1).[4]

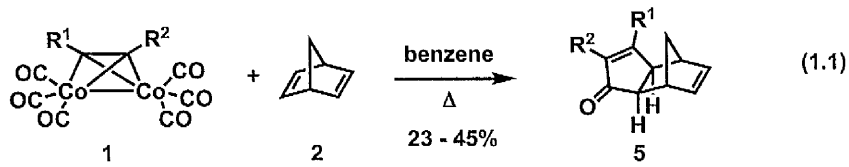

1 2 5 (1.1)

a) R^1 = H, R^2 = H, Me, Ph
b) R^1 = R^2 = Ph
c) R^1 = R^2 = Et

The reaction generally provided a single *exo* adduct and a single regioisomer was detected when monosubstituted alkynes were employed (R^1 = H, R^2 = Me, Ph).[3b] However, irreversible *exo-endo* isomerisation was observed on norbornadiene derivatives and further confirmed by prolonged heating of the originally isolated *exo*-adduct in presence of dicobalt octacarbonyl.[3] Despite the low intrinsic reactivity and limited substrate scope to symmetrical strained alkenes (norbornene and norbornadiene), this unexpected formal [2+2+1] cycloaddition of an alkyne, alkene and carbon monoxide furnished an intriguing approach for the construction of bicyclopentenone derivatives from readily available starting materials.[3b] The abovementioned process, which is commonly referred to as the Pauson-Khand reaction, has been the subject of intensive synthetic studies. The opportunity to exploit a wide array of substituted starting materials and, thus, enhance the degree of complexity of the resulting adducts provided a significant driving force in the development of new methodologies towards target-oriented total synthesis. Nonetheless, the critical challenge to overcome the requirement of stoichiometric transition metals and harsh reaction conditions prompted the synthetic organic community to explore alternative transition metals and more viable reaction conditions.

In this context, rhodium complexes played a primary role in offering a valid alternative to stoichiometric protocols and confer enhanced reactivity and selectivity to the overall methodology. This chapter will discuss the relevant aspects related to the pivotal work of Pauson and Khand, as well highlighting further advancements within this field. This will include the development of catalytic processes, use of alternative transition metals and implementation of the Pauson-Khand reaction towards the total synthesis of biologically active natural products.

1.2.2. Proposed Mechanism of the Pauson-Khand Reaction.

The ability to accurately determine the mechanism of the cobalt-mediated PK reaction has been the subject of extensive theoretical and synthetic studies. A critical limitation in the understanding of the mechanism resided in the lack of any observable intermediate in the process, albeit the initial (alkynyl)hexacarbonyldicobalt species can be isolated as a stable tetrahedral bimetallic cluster.[5]

Scheme 1.2. Postulated mechanism of the cobalt-mediated Pauson-Khand reaction.

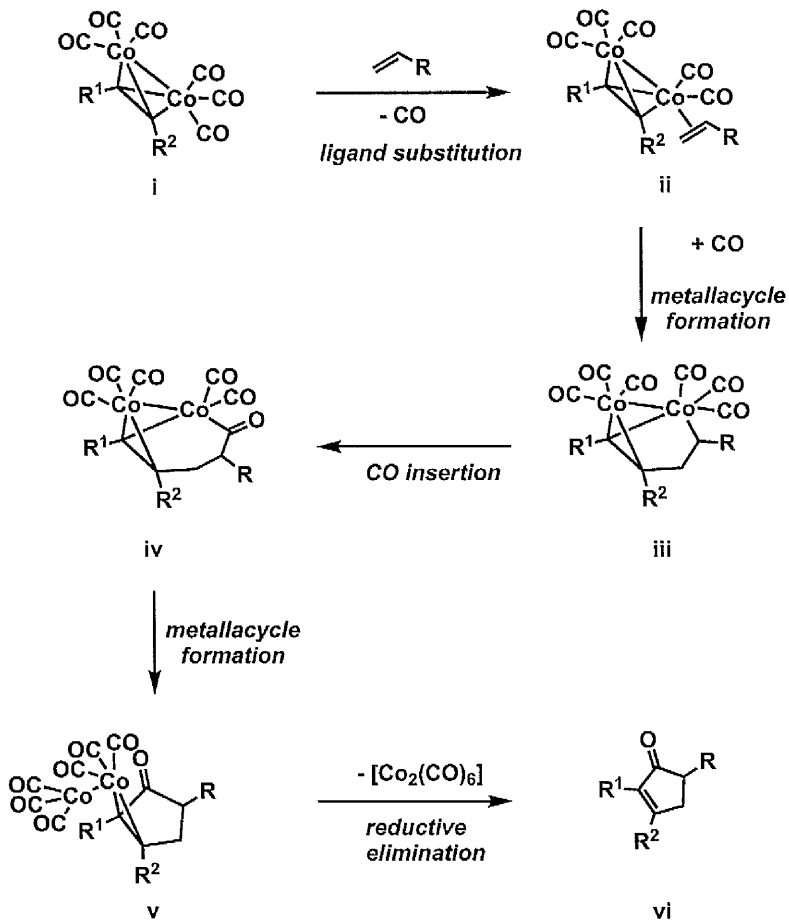

Despite the limited experimental mechanistic data, pivotal studies by Magnus[6] and Schore[7] set the basis for the current and widely accepted mechanism of the Co-mediated Pauson-Khand reaction (**Scheme 1.2**). The aforementioned postulated pathway confirmed the initial

experimental findings by Pauson and Khand and successfully rationalised the stereochemical outcome of the PKR in the context of the total synthesis of polycyclic natural products.[6] The initial step of the reaction involved displacement of a carbon monoxide molecule from the (alkynyl)hexacarbonyldicobalt complex **i** and the formation of a vacant coordination site. Dissociative loss of CO is a highly endothermic process and is commonly regarded as the rate-determining step. The olefin insertion step to provide **iii** is considered to be the stereo- and regiochemistry-determining step in the reaction. Additional mechanistic studies by Nakamura,[8a] Pericas[8b] and Gimbert[8c] provided further insights into the energy of the reaction intermediates (**Scheme 1.3**) and confirmed the validity of the mechanism hypothesised by Magnus and Schore.

Scheme 1.3. Mechanistic energy profile of the dicobaltacycle formation.

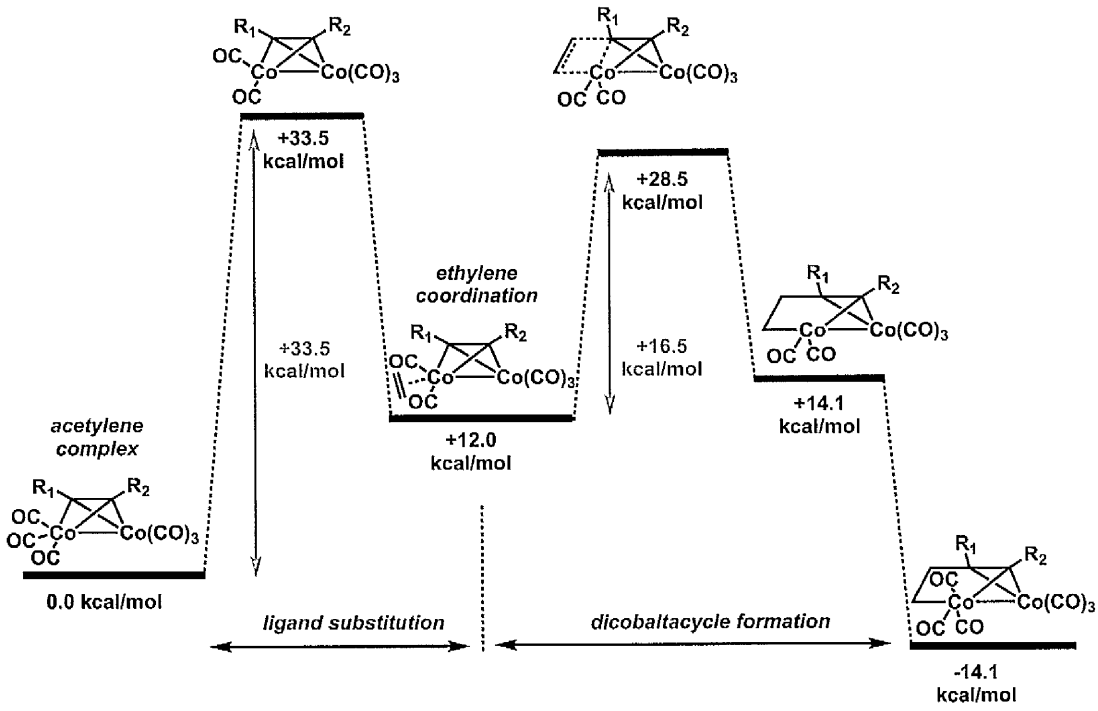

Notably, further examination of natural charges of the cobalt atoms throughout the process clarified the role of the two metal centres in the reaction.[8a] Despite the fact that all the bond-forming events occurs on a single metal centre, the second cobalt atom did not act as a mere

spectator, but exerted a remarkable electronic effect by balancing the variation of natural charge of the first cobalt atom throughout the process.

1.2.3. Cobalt-catalysed Pauson-Khand Reaction.

Despite the importance of the seminal work by Pauson and Khand, the reaction suffered from severe limitations, including low reactivity, stoichiometric use of metal catalyst and substrate scope. The first significant attempt to overcome the reaction drawbacks was accomplished by Schore and Croudace in 1981 (**Scheme 1.4**).[9] In this context, they utilised tethered enynes as reaction precursors, which effectively improved the reactivity of the system, and thus allowed the exploitation of unstrained alkenes to be utilised under an atmospheric pressure of carbon monoxide.

Scheme 1.4. Schore's intramolecular cobalt-catalysed PK reaction of 1,*n*-enynes.

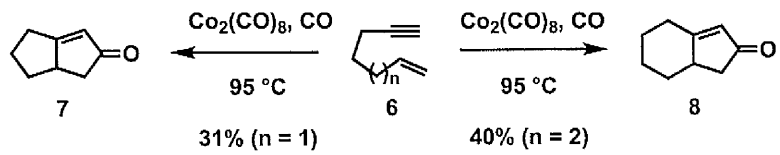

The ability of tethered enynes to circumvent alkene regioselectivity issues, coupled with the abundance of bicyclopentane scaffolds in natural products defined the intramolecular Pauson-Khand reaction as a privileged methodology for the total synthesis of polycyclic natural targets. Despite the significant improvement regarding substrate scope and optimisation of operational conditions, many of these reaction use stoichiometric cobalt, which coupled to the moderate reactivity still constitute a major drawback in the process.[9]

The next sections will highlight the recent advances in the development of a general approach to the cobalt-mediated Pauson-Khand reaction.

1.2.3.1. Use of Additives.

As previously mentioned, the rate determining step of the reaction involves displacement of a carbon monoxide molecule from the hexacarbonyldicobalt complex, which results in the formation of an unstable complex that has a vacant coordination site. According to these predictions, an increase in rate could be achieved by lowering the activation barrier energy of the dissociative step. The first major breakthrough was accomplished by Jeong and Schreiber, who independently examined the influence of amine *N*-oxide additives, such as TMANO[10] and NMO,[11] in the cobalt-mediated PKR. As outlined in **Scheme 1.5**, amine *N*-oxides could efficiently facilitate the formation of a vacant coordination site by oxidation of a CO ligand to CO_2 and subsequent decarboxylation. As a result of enhanced reactivity, exploitation of these additives could finally overcome thermal process limitations and circumvent the issue of prolonged reaction times. Widespread acceptance of the beneficial effect of *N*-oxides additives prompted further investigations into the potential development of this strategy.

Scheme 1.5. Mechanism of CO displacement catalysed by amine *N*-oxides.

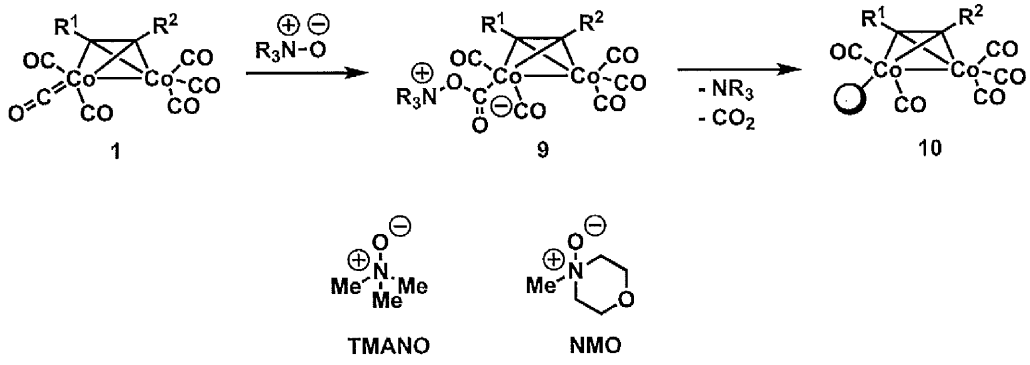

An effective strategy to promote the carbon monoxide dissociation was the preliminary treatment of the initial cobalt complex with a Lewis base. Coordination of the base was believed to enhance the electron density on the metal centre and the lability of the metal-CO

δ bond, thereby favouring the subsequent alkene insertion.[12] Leveraging this concept, a wide range of additives have been employed as promoters in the cobalt-catalysed reaction.

Scheme 1.6. Primary amines as promoters in the intramolecular PK reaction.

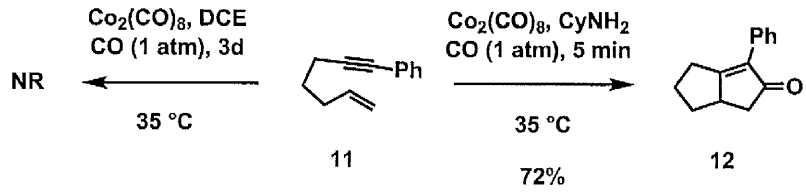

Elegant studies by Sugihama and coworkers demonstrated the ability of hard Lewis bases, such as aliphatic primary amines **(Scheme 1.6)**, to enhance CO dissociation and dramatically increase the rate of the reaction.[13] A seminal report by Krafft et *al.*,[14] which was inspired by the enhanced reactivity of homopropargylic alkynyl sulfides, prompted the group to probe the utilisation of sulfur derivatives as potential promoters in the cobalt-catalysed PK reaction (Eq. 1.2).[15] Aliphatic sulfides as additives proved to exert a significant influence on the catalyst, thereby allowing the construction of polycyclic structures that are not generally accessible *via* the thermal PK reaction.

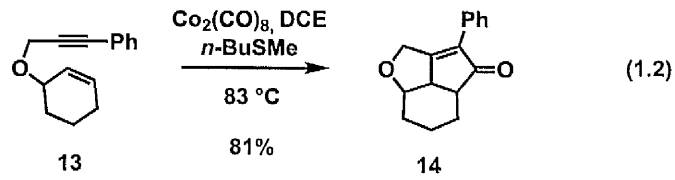

1.2.3.2. Development of the Catalytic Cobalt-catalysed Pauson-Khand Reaction.

The use of promoters provided an attractive methodology in terms of addressing the issues of limited substrate scope and extended reaction times. In light of these promising results, further investigations focused on the development of a general catalytic process. In this context, seminal studies by Rautenstrauch (Eq. 1.3) reported the first effective catalytic PK

reaction.[16] Despite the impressive TON (turnover number) of 110 by employing 0.022 mol% of catalyst, the reaction suffered from severe limitations in terms of operating conditions and reproducibility.

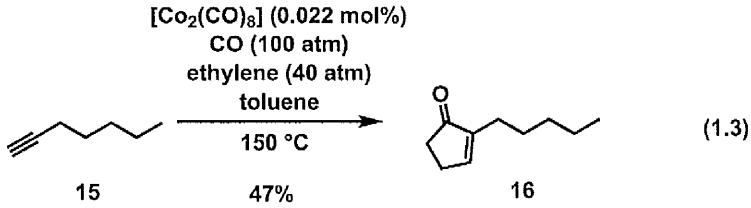

Based on his previous work regarding the beneficial effect of amine *N*-oxides as promoters,[10] Jeong successfully developed a practical catalytic protocol employing phosphites as coligands (Eq. 1.4).[17] Remarkable features were the applicability of the methodology to a wide range of substituted enynes and reduced catalyst loading, albeit high CO pressure (3 atm.) was essential to achieve useful levels of conversion.

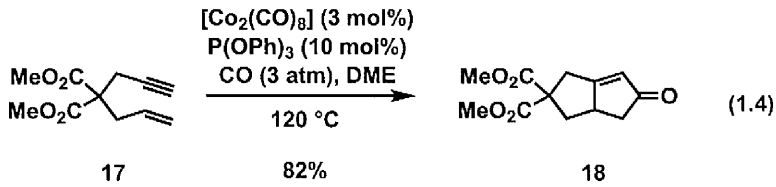

Scheme 1.7. Dicobalt hexacarbonyl complexes a catalytic precursor for the PK reaction.

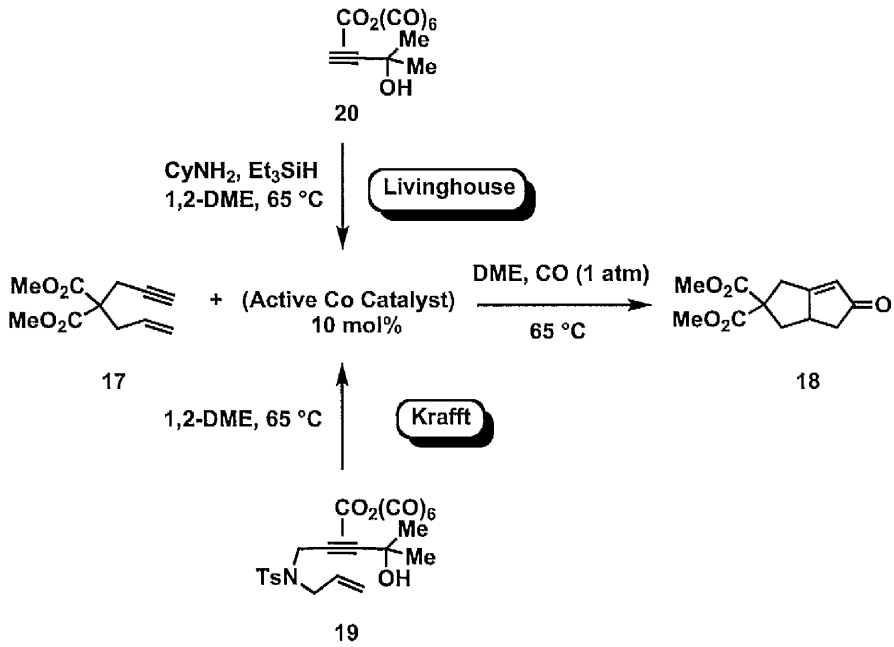

Additional studies by Livinghouse[18] and Krafft[19] provided the first photochemical and thermal catalytic PK reaction, thus avoiding the use of promoters. As outlined in the aforementioned studies, the use of high purity dicobalt octacarbonyl was crucial to achieve high yields under catalytic reaction conditions. This limitation prompted a re-evaluation of the catalytic system with the development of an air-stable catalyst surrogate. In this context, Livinghouse[20] showed that air-stable $Co_2(CO)_6$-alkyne complex **20** underwent reductive decomplexation by treatment with Et_3SiH and the resulting (carbonyl)cobalt byproduct displayed catalytic activity towards the PK reaction (**Scheme 1.7**). Subsequent studies by Krafft[21] described that air-stable and crystalline $Co_2(CO)_8$-enyne **19** could act as catalyst precursor without the requirement of Et_3SiH and Lewis-base promoters (**Scheme 1.7**). Additionally, the Gibson group developed of an economical and air-stable triphenylphosphine dicobalt catalyst, which displayed good reactivity for both the inter- and intramolecular PK reaction (Eq. 1.5).[22]

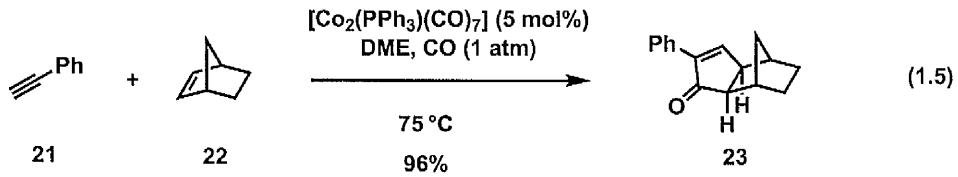

Perez-Castells envisioned that a CO-pretreated "paste" of powdered molecular sieves and *tert*-BuOH could subsequently determine a slow release of CO during the course of the PK reaction (**Scheme 1.8**).[23] Hence, the employment of this "paste" in the catalytic PKR could effectively eliminate the requirement of toxic CO operating environment, which previously proved to be imperative for catalyst turnover.

Scheme 1.8. Effect of the CO-pretreated molecular sieves on the Co-catalysed PK reaction.

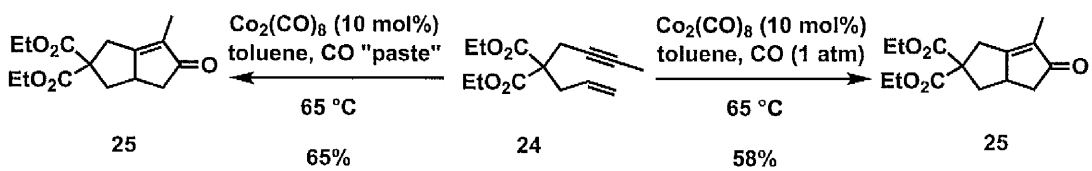

Since the inception of the cobalt-catalysed PK reaction, considerable effort has been devoted towards the establishment of an efficient and general methodology. Major accomplishments have been achieved with respect to reactivity, stereoselectivity and development of catalytic variants. Nonetheless, severe substrate limitations and lack of overall reactivity provided the impetus to examine alternative transition metals that enable general and efficient catalytic process.

1.2.4. Transition Metal Catalysed Pauson-Khand Reactions.

1.2.4.1. Molybdenum.

Early work by Hanaoka and Mukai on PK reactions focused on the ability of group 6 elements (Cr, Mo, W) to form isoelectronic complexes of hexacarbonyldicobalt congeners (Eq. 1.6).[24] Consequently, experimental studies demonstrated the ability of molybdenum complexes to catalyse the PK reaction, thus providing a valid alternative to the classic cobalt-catalysed process.[25]

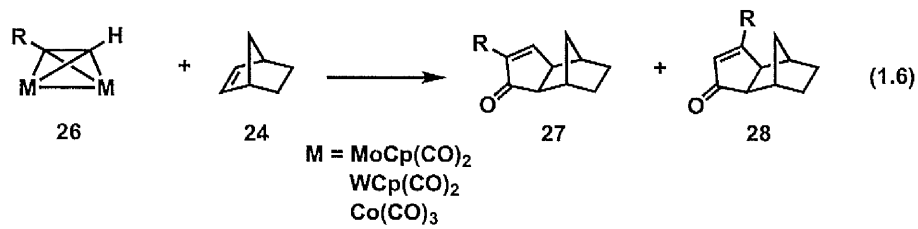

(1.6)

As previously established for the cobalt-catalysed protocol, the ability of promoters to displace a CO ligand proved to be essential for substrate coordination.[11-13,15] Similarly, low-valent organotransition metal carbonyl complexes could extrude a CO ligand in the presence of coordinating hard Lewis bases and allow the formation of a vacant coordination site. Rationalising these experimental observations, Jeong envisioned the ability of promoters to generate a coordination vacancy on carbonyl molybdenum complexes and thereby enhance the interaction between the metal centre and enyne (**Scheme 1.9**).[26,27]

Scheme 1.9. Mo-mediated PK reaction.

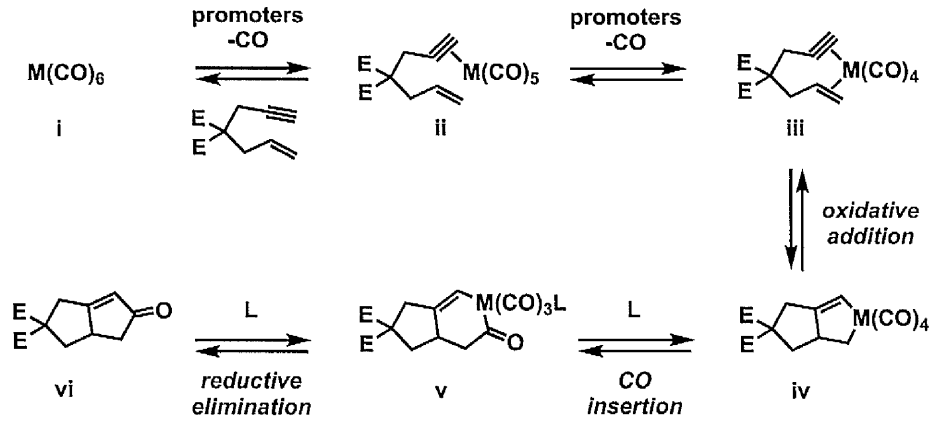

Extensive screening of promoters revealed that DMSO was crucial to promote CO decomplexation and thereby achieve high levels of reactivity (Eq. 1.7).

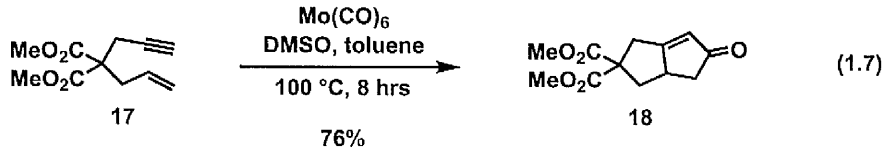

Additional studies focused on the examination of catalytic process under an atmosphere of carbon monoxide. In contrast to the cobalt-catalysed manifold, amine *N*-oxides promoters had a detrimental effect on the systems reactivity.[26] In the context of developing an efficient methodology, Carretero sought to address the issue of poor reactivity and lack of beneficial additives by altering the ligand environment around the metal centre.

Partial replacement of the carbon monoxide ligands with more labile DMF ligands proved to be essential to circumvent the disfavoured CO decomplexation step, thus providing a spontaneous room temperature cyclocarbonylation in the absence of additives or promoters

(Eq. 1.8).[28] Despite the impressive advancements in the molybdenum-mediated PK reaction of 1,6-enynes, the inability to develop a catalytic process has prompted the development of alternative methodologies in terms of atom economy and applicability in total synthesis. Nonetheless, molybdenum catalysis provides a suitable alternative due to its exceptional and unique reactivity in the context of the allenic and hetero-Pauson-Khand reactions.

1.2.4.1.1. Allenic Pauson-Khand Reaction.

A significant initial drawback for the development of an allene-type Pauson-Khand lay in the propensity of dicobalt octacarbonyl to catalyse allene polymerisation.[29]

Scheme 1.10. Regioselectivity in the Mo-catalysed PK reaction of allenynes.

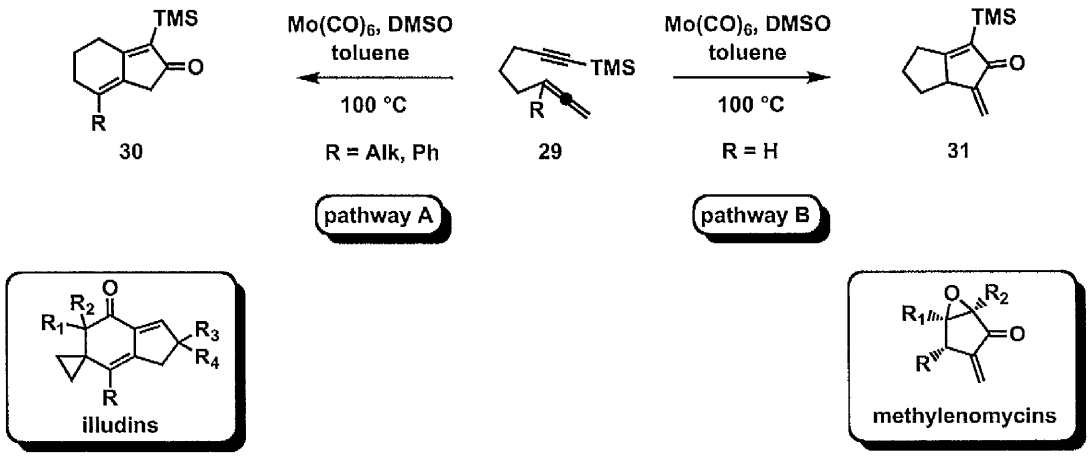

However, the high reactivity profile provided by the unique structural and electronic arrangement of the cumulated diene moiety inspired the Brummond group to probe the catalytic activity of alternative transition metals in the context of the allenic Pauson-Khand reaction. Treatment of allenynes under conditions reported by Jeong,[26] resulted in the regioselective formation of α-methylene cyclopentenones (**Scheme 1.10**, pathway B).[30] The intrinsic value of this methodology relied on the unprecedented preferential reactivity of the internal π-bond of the allene and the ubiquity of α-methylene motifs in biologically active

compounds. Additional studies focused on the allene substitution pattern in order to direct the regiochemical outcome towards terminal π-bond. Notably, internal substituted allenes dramatically influenced the regiochemical pathway and promote the selective formation of the bicyclo[4.3.0]nonane ring system (**Scheme 1.10**, pathway A).[31] Hence, the allenic moiety provided regioselective access to polycyclic motifs that are generally not accessible *via* the classic PK reaction of 1,6-enynes, and established the molybdenum-catalysed PKR of allenynes as a complementary and powerful strategy for the synthesis of biologically active compounds (**Scheme 1.10**).[32]

1.2.4.1.2. Hetero-Pauson-Khand Reaction.

The hetero-Pauson-Khand reaction recently emerged as a powerful strategy for the rapid construction of butenolide derivatives.

Scheme 1.11. Ti-mediated hetero-PK reaction of unsaturated carbonyl derivatives.

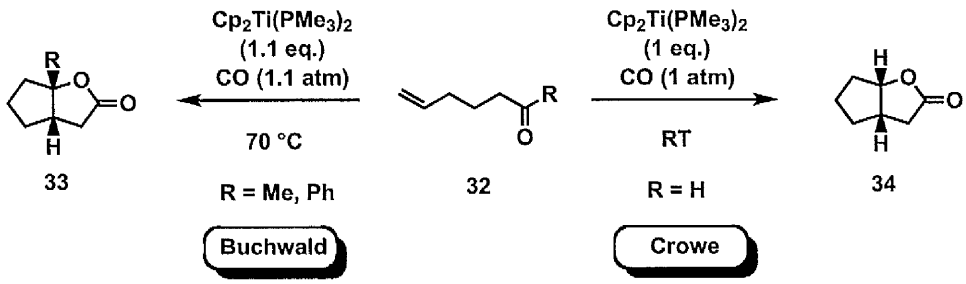

Independent studies by Buchwald[33] and Crowe[34] demonstrated that titanium metallacycles promote the formation of γ-butyrolactones *via* tandem reductive cyclisation/carbonylation of tethered unsaturated carbonyl derivatives (**Scheme 1.11**). Interestingly,the replacement of the alkene moiety with an alkyne led to a dramatic drop in reactivity, which was attributed to the unfavoured CO insertion into the hindered Ti-C(sp^2) bond.[33,34] The first catalytic method for the conversion of yne-aldehydes into bicyclic α,β-unsaturated lactones was achieved by

Murai and Chatani,[35] albeit very harsh thermal conditions. In this process, the substitution on the alkyne moiety proved to be critical to promote CO insertion into the Ru-C(sp^2) metallacycle bond (Eq. 1.9).

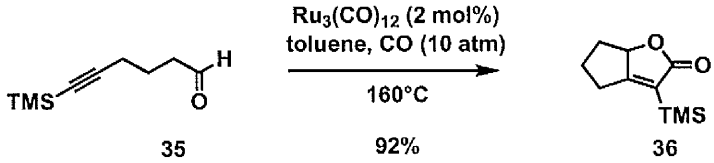

(1.9)

In light of the catalytic activity of molybdenum hexacarbonyl in allene-type hetero-PK reactions,[30,31] Carretero envisioned that enhanced catalytic activity of $Mo(CO)_3(DMF)_3$[28] could effectively overcome the poor reactivity of yne-aldehydes in the hetero-PK reaction.[36] This resulted in the development of a room temperature Mo-mediated carbocyclisation of 1,6 and 1,7-yne aldehydes, which, in contrast to previous protocols, could overcome the drawback of thermal processes and prolonged reaction times, to provide a highly convergent approach to bicyclic butenolides (**Scheme 1.12**).[36]

Scheme 1.12. Butenolide synthesis by Mo-mediated hetero-PK reaction of yne-aldehydes.

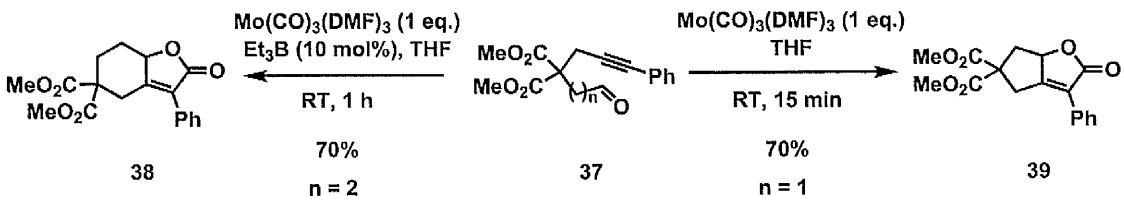

1.2.4.2. Iron and Ruthenium.

The acknowledged ability of pentacarbonyl iron to promote intramolecular carbonylative coupling of enynes provided the rationale to pursue its suitability for iron-catalysed Pauson-Khand reactions. Early reports by Pearson and Dubbert confirmed the viability of the

approach, albeit stoichiometric, and the necessity of high temperature and pressure (Eq. 1.10).[37]

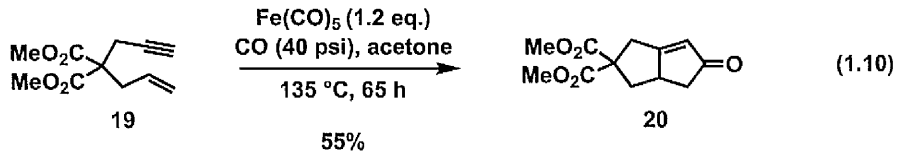

(1.10)

In a recent development, Murai[38] and Matsudo[39] reported the catalytic ruthenium-catalysed cyclocarbonylation of 1,6-diynes[40] using $Ru_3(CO)_{12}$ for the Pauson-Khand reaction (Eq. 1.11). Although high CO pressure and harsh temperatures remained an intrinsic limitation, experimental investigations demonstrated that $Ru_3(CO)_{12}$ has higher catalytic activity relative to its iron congener (2 mol%).[38-39]

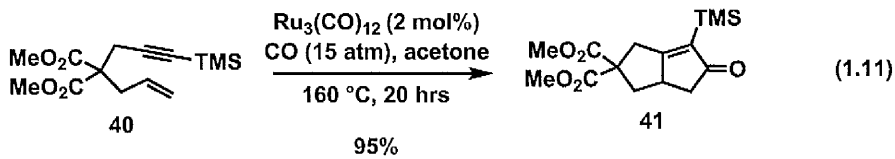

(1.11)

Additional studies focused on the applicability of the methodology towards the intermolecular reaction. In this context, the efficiency of the intermolecular PK reaction relied on a reactive strained alkene and the alkyne counterpart in order to promote a regioselective transformation. Inspired by seminal studies by Krafft,[14] Yoshida envisioned that tethering a coordinating heteroatom to the alkene counterpart could perform a dual role of enhancing the substrate reactivity and simultaneously act as a stereodirecting group by interaction with the metal centre. Consequent experimental investigations demonstrated the ability of alkenyl(2-pyridyl)silanes to undergo Ru-catalysed intermolecular PK reaction and deliver a highly convergent cyclopentenone synthesis (Eq. 1.12).[41a]

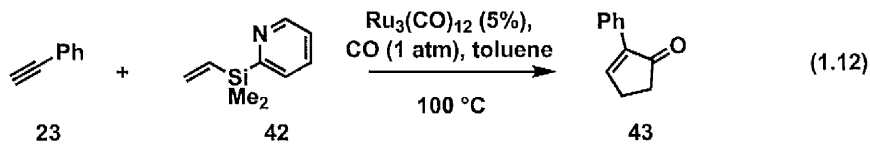

(1.12)

The mechanism of the reaction is thought to involve the initial dissociation of the ruthenium cluster **i** and formation of Ru(alkenylsilane) complex **iii** (**Scheme 1.13**).[41b]

Scheme 1.13. Mechanism of the Ru-catalysed intermolecular PK reaction of vinylpyridylsilanes.

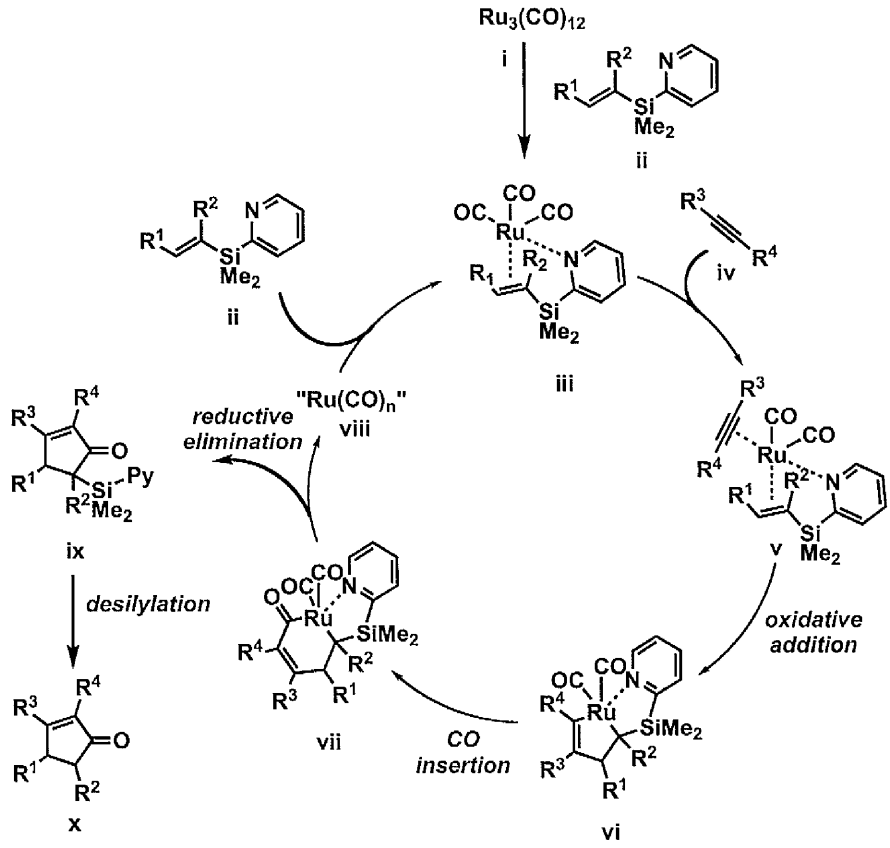

Alkyne coordination and stereospecific oxidative addition provides metallacycle **vi**. Retention of the pyridyl-Ru coordination directs a stereospecific CO migratory insertion into the Ru-C(sp^2) bond and provides ruthenacycle **vii**. Reductive elimination and desilylation of intermediate **ix** affords cyclopentenone **x**. Further mechanistic studies clarified the beneficial role of the pyridyl moiety in terms of dissociation of the initial unreactive ruthenium cluster and enhancement of the coordinating aptitude of the alkene group for oxidative addition.[41b] As a result, the overall process required low catalyst loading and atmospherical CO pressure. Although very little effort has been devoted towards the synthetic application of the Ru-catalysed PK reaction, the recent development of a tandem RCM/hetero-Pauson-Khand

reaction demonstrated the ability of this strategy for the construction of complex molecular targets (Eq. 1.13).[42]

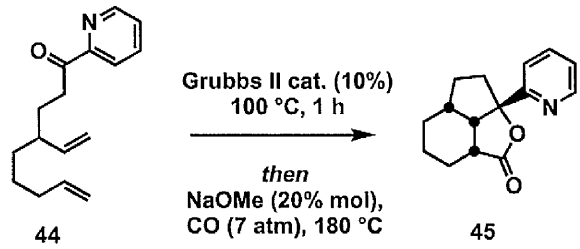

(1.13)

1.2.4.3 Nickel and Palladium.

Early reports on Ni-catalysed allene cycloadditions disclosed the ability of isocyanides to insert into a Ni-C(sp^3) bond and serve as a π-component for the synthesis of iminocyclopentenes that, upon hydrolysis, provided the corresponding cyclopentenone adducts.[43] The ability of isocyanides to serve as a CO surrogate, provided Buchwald and coworkers the impetus to develop the first example of a Ni-catalysed Pauson-Khand reaction (Eq. 1.14).[44] The choice of trialkylsilyl cyanides was crucial in terms of avoiding the formation of unreactive Ni-isocyanide species and increasing the reactivity of the cycloadducts to hydrolysis.

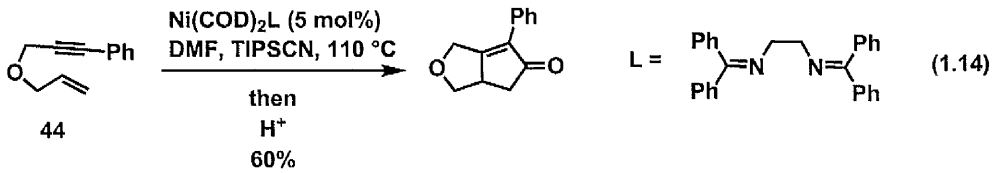

(1.14)

Despite its role in metal-catalysed reactions, palladium had not been extensively explored in the [2+2+1] reactions, until in 2005 the Yang group developed the first example of a Pd-catalysed PK reaction (Eq. 1.15).[45a,b] The synthetic value of this effective methodology lay in the mild operating conditions and employment of a readily available catalyst, which provides wide substrate scope.

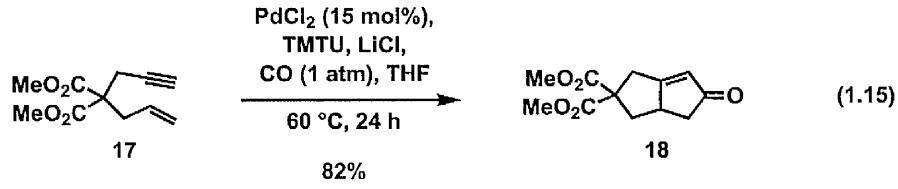

Moreover, the thiourea ligand[46] and lithium chloride were critical for an efficient catalyst turnover, which prompted additional investigations into the reaction mechanism.[45c] Experimentally confirmed computational studies clarified the key role of the above mentioned additives and outlined the unique mechanistic pathway of the Pd-catalysed PK reaction (**Scheme 1.14**).[45c] The mechanism of the reaction involves initial coordination of the enyne **ii** to $PdCl_2L_2$, followed by a stereospecific *syn*-addition of the Pd-Cl bond to the alkyne moiety. After subsequent alkene and carbon monoxide insertion to provide intermediate **v**, palladium oxidatively inserts into the vinyl-chloride bond leading to the formation of palladacycle **vii**. Reductive elimination affords the desired bicyclopentenone adduct **viii**.

Scheme 1.14. Proposed mechanistic pathway of the Pd-catalysed PK reaction.

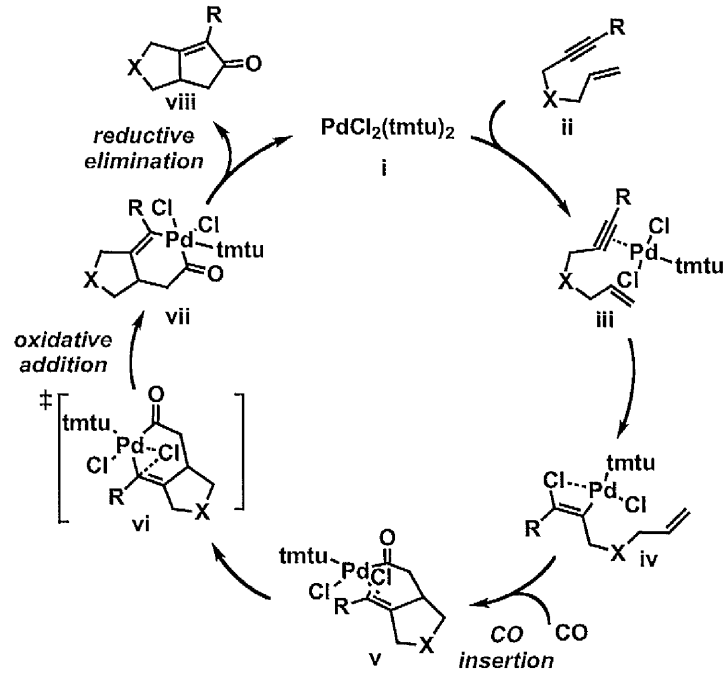

The investigation of the electronic influence of ligands in the reaction outlined the ability of the thiourea ligands to dramatically decrease the energy barrier for the intramolecular oxidative addition and stabilise the transition state **vi'** for the formation of Pd(IV) species **vii'** (**Scheme 1.15**).[45c] Additionally, the chelating effect of the lithium atom further stabilise the octahedral geometry of the resulting oxidative addition product **vii'**, thereby enhancing the reactivity the overall transformation.

Scheme 1.15. Chelation-based stabilisation in the transition state of the Pd-catalysed PKR.

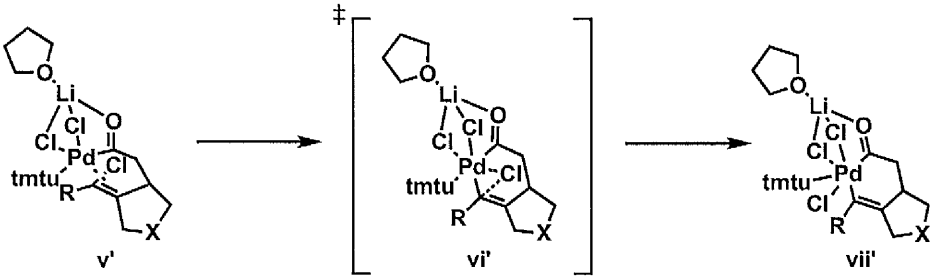

1.2.4.4. Rhodium and Iridium.

Prior to the development of the first rhodium-catalysed approach, the PK reaction had undergone extensive development and was successfully exploited with a wide array of transition metals. Nonetheless, previously discussed limitations in terms of operating reaction conditions and substrate scope failed to satisfy the potential of the methodology. Livinghouse and Wender estabilished the ability of rhodium catalysts in [4+2][47] and [5+2][48] cycloaddition reactions to provide elegant access to six- and seven-membered bicyclic scaffolds. Hence, acknowledged catalytic activity and aptitude of this metal to selectively assemble multiple π-components prompted the investigation of a rhodium-catalysed [2+2+1] carbocyclisation in order to overcome the previously encountered limitations. Narasaka[49] and Jeong[50] independently reported the first rhodium-catalysed PK reaction in 1998 (**Scheme 1.16**). Remarkable features of these methodologies included low catalyst loading and the ability to

conduct the process under an atmospheric pressure of CO. Additionally, high catalytic activity displayed by phosphine-substituted rhodium complexes[50] provided a concrete opportunity to generate a chiral environment in the system and deliver an asymmetric variant of the process.[51]

Scheme 1.16. Rh-catalysed PK reaction of 1,6-enynes.

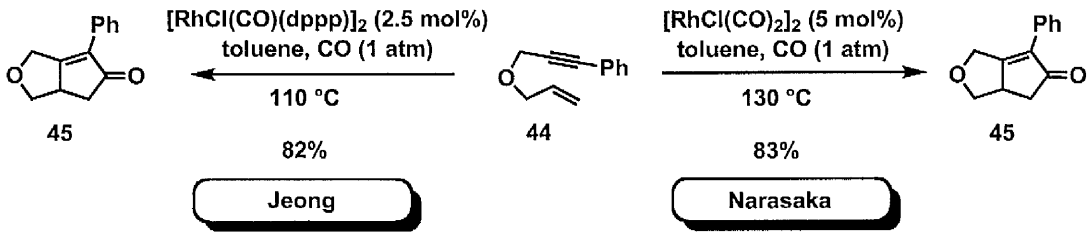

Further discussion in this chapter will provide additional insight into the Rh-catalysed diastereoselective PK reaction and describe the optimisation and achievement of an efficient diastereoselective methodology. Chapter 2 will examine the asymmetric variant of the process and describe the development of a highly enantioselective variant. The investigation of the iridium-catalysed process has been exclusively carried out in the context of the asymmetric PK process and will be thus highlighted in the second chapter.

1.3. Rhodium-Catalysed Cyclocarbonylation Reactions.

1.3.1 Allenic [2+2+1] Pauson-Khand Reaction.

The exquisite reactivity of allenynes in the Mo-mediated PK reaction,[30,31] prompted the Brummond[52] and Mukai[53] groups to probe the feasibility of a rhodium-catalysed process. These studies confirmed the enhanced reactivity of the allene moiety in Rh-catalysed cycloadditions and provided a highly convergent strategy for the assembly of bicyclo[4.3.0] skeletons (**Scheme 1.17**).

Scheme 1.17. Rh-catalysed PK reaction of allenynes.

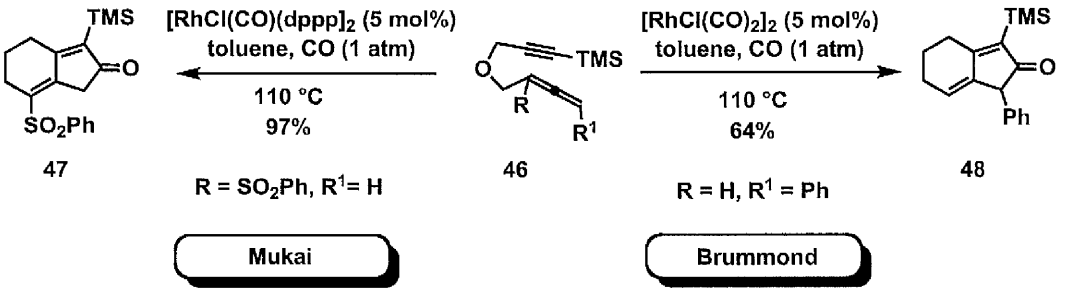

Additionally, the allene moiety broadened the scope of the methodology to the unprecedented construction of novel bicyclo[5.3.0] scaffolds, thereby expanding the applicability of the process towards the synthesis of seven-membered ring containing target molecules (**Scheme 1.18**).[53a,b]

Scheme 1.18. Synthesis of bicyclo[4.3.0] and [5.3.0] scaffolds by Rh-catalysed allenic PK reaction.

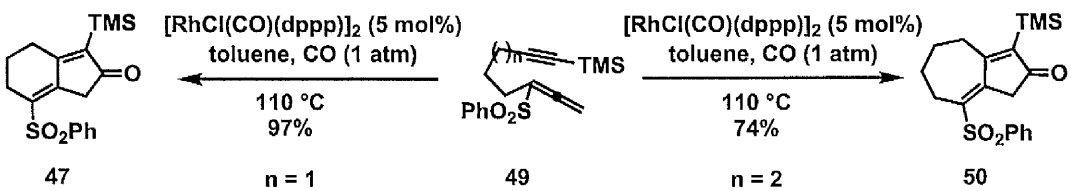

Early reports by Itoh[54] prompted Mukai to investigate the reactivity of allene-enes in the context of a PK reaction.[53c] A remarkable limitation with the process was the diminished reactivity of the alkene compared to the alkyne.

Nonetheless, controlling the carbon monoxide pressure provided optimal reactivity and allowed the stereoselective formation of bicyclo[4.3.0] and [5.3.0] bicyclic adducts (**Scheme 1.19**).[53c] The outstanding reactivity of the allene moiety in the context of Rh-catalysed cyclocarbonylation reactions was further demonstrated with a [2+2+1] cycloaddition of a *bis*-

allene to generate bicyclo[6.3.0] and [7.3.0] skeletons, thereby overcoming the inherent limitations of 1,8- and 1,9-enynes to construct these type of scaffolds (**Scheme 1.20**).[53d]

Scheme 1.19. Rh-catalysed PK reaction of 1,*n*-allenes.

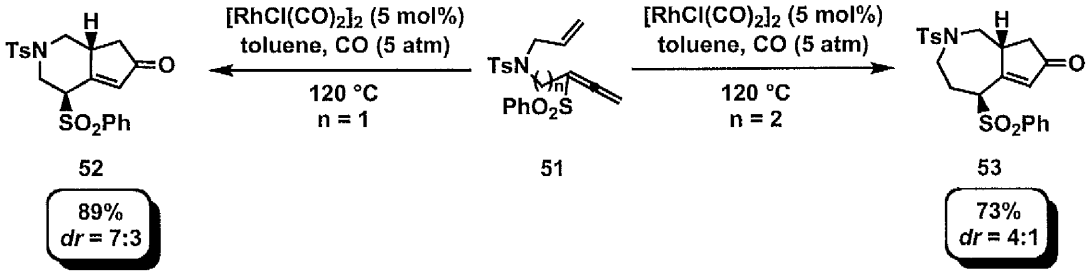

Scheme 1.20. Rh-catalysed PK reaction of 1,*n*-bisallenes.

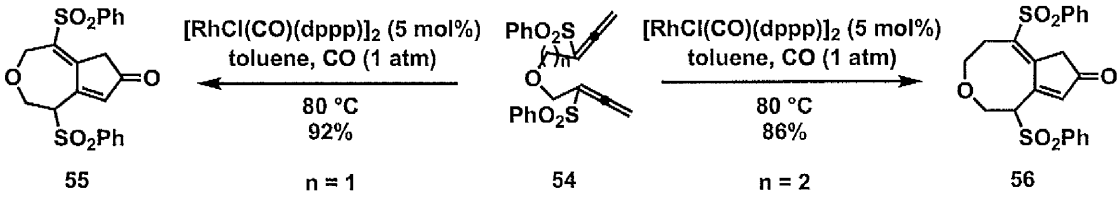

1.3.2. Dienyl [2+2+1] Pauson-Khand Reaction.

Wender and coworkers recognised the possibility of replacing the alkene counterpart with a more reactive diene moiety and to facilitate the Rh-catalysed [4+2+1] cycloaddition. Experimental observations demonstrated that the diene moiety behaves as a 2π component and results in the development of the first Rh-catalysed dienyl PK reaction (Eq. 1.16).[55a]

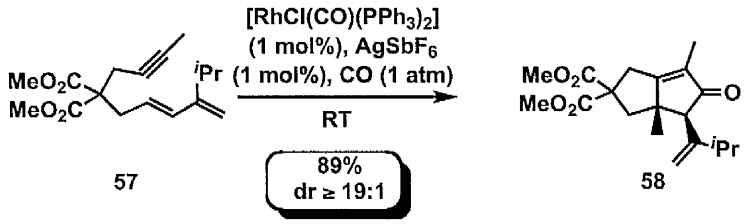

(1.16)

Detailed optimisation of the solvent system and substrate concentration proved to be crucial in order to avoid the undesired formation of [4+2] adducts and provided a diastereoselective synthesis of bicyclopentenone derivatives under mild operating conditions. The inherent reactivity of diene and alkyne components in the intramolecular PK reaction provided the basis for the development of the corresponding intermolecular manifold (Eq. 1.17).[55b] Careful control of thermal conditions was required in order to circumvent the formation of [4+2] and [2+2+2] adducts and, moreover, significant excess of the diene component was crucial to achieve excellent reactivity.

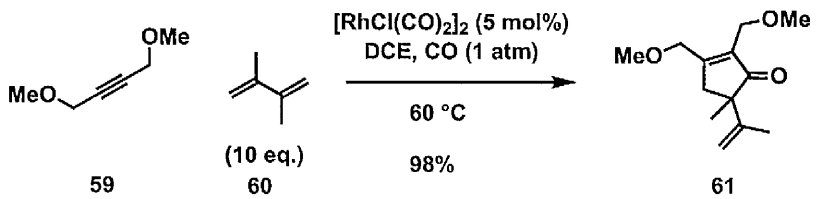

(1.17)

Additional studies demonstrated the ability of 1,3-dienes to display reactivity comparable to the alkyne moiety and culminated in the development of the first Rh-catalysed diene-ene [2+2+1] cycloaddition (Eq. 1.18).[55c] Distinguishing features of the methodology included high degrees of diastereocontrol and simultaneous formation of three contiguous stereogenic centres.

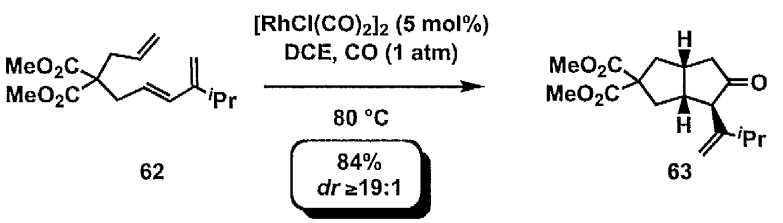

(1.18)

Elegant computational studies by Baik[56] provided additional insight into the role of the diene moiety in the reaction. These studies demonstrated that the oxidative addition process requires a high electron density on the metal centre and is disfavoured by the presence of π-electron

withdrawing CO ligands. In this context, $\eta^2 \rightarrow \eta^4$ reorganisation of the diene moiety in **i** drives the expulsion of the CO ligand from the metal centre with concomitant formation of a coordinatively saturated electron-rich Rh(I) species **ii**, thereby enhancing the rate of oxidative addition in the process (**Scheme 1.21**).[56]

Scheme 1.21. Oxidative addition step in the Rh-catalysed PK reaction of diene-enes.

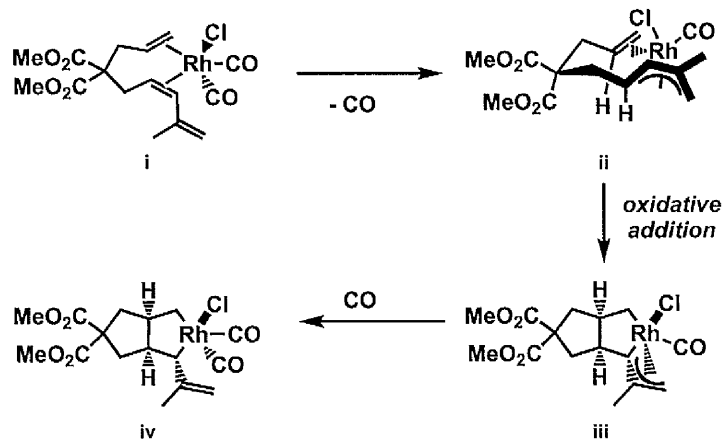

1.3.3. [3+2+1] and [3+3+1] Cycloadditions.

Extensive studies by Wender and coworkers outlined the ability of vinylcyclopropanes to act as a reactive component in Rh-catalysed [5+2] cycloaddition reactions.[48] In contrast, the employment of cyclopropanes as a 3_{2s} component in metal-catalysed cycloadditions remained largely unexplored, due to propensity of the corresponding metallocyclobutanes to undergo β-hydride elimination.[57]

Scheme 1.22. Postulated mechanism for the [3+2+1] cycloaddition of yne-cyclopropanes.

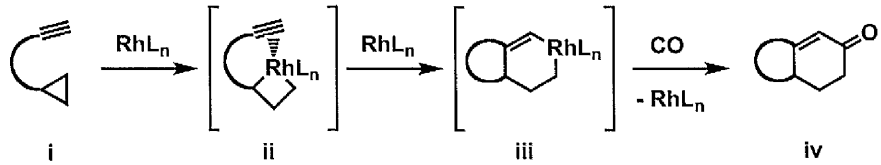

However, Narasaka envisioned that incorporation of a cyclopropane component into an enyne-type structure could favour preferential alkyne coordination to the metallacyclobutane, which would suppress competitive β-hydride elimination and promote the formation of six-membered metallacycle. Subsequent CO insertion and reductive elimination would afford the desired adduct (**Scheme 1.22**).[58] Rationalisation of the mechanistic hypothesis provided the first example of a Rh-catalysed [3+2+1] carbocyclisation reaction (Eq. 1.19). The methodology provided a unique approach to the synthesis of bicyclohexenone derivatives, albeit with the requirement of harsh thermal conditions and high CO pressure.[58]

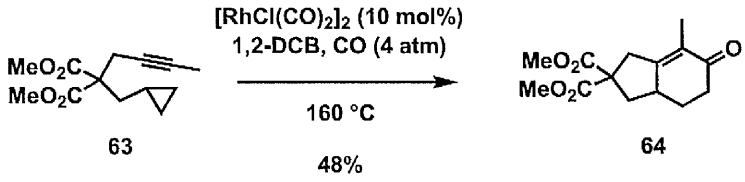

63 64 (1.19)

Renewed interest in the strategy by Yu and coworkers originated from the exploitation of a *trans*-vinylcyclopropane moiety to provide a [$3C_{2\delta}$] synthon in the Rh-catalysed [3+2] cycloaddition reaction.[59] Hence, employment of the latter in the corresponding Rh-catalysed [3+2+1] process could effectively overcome the poor reactivity of cyclopropanes and provide a mild approach to the synthesis of bicyclohexenone adducts (Eq. 1.20).[60]

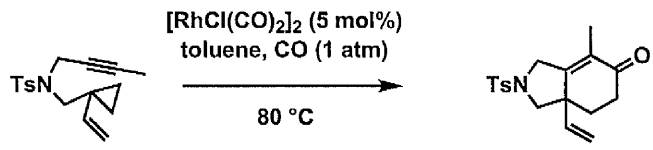

65 66 (1.20)

Additional experimental studies revealed that minor modifications in the operating conditions could alter the mechanistic pathway of the aforementioned [3+2+1] process and provide alternative formation of tricyclic derivatives, as outlined in **Scheme 1.23**.[61]

Scheme 1.23. Different mechanistic pathways in the Rh-catalysed cycloaddition of VCP-ynes.

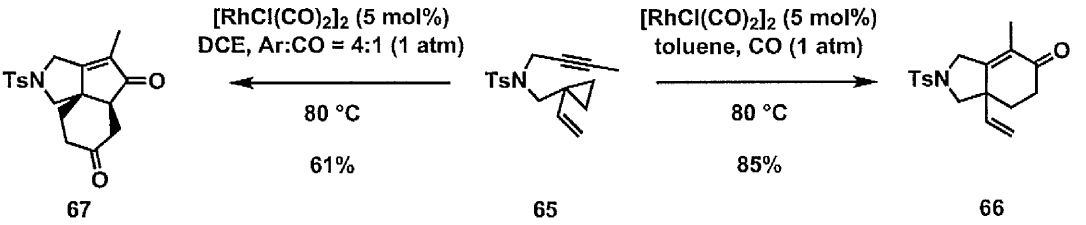

Scheme 1.24. Mechanistic pathway of the Rh-catalysed [5+1]/[2+2+1] cycloaddition reactions of yne-vinylcyclopropanes.

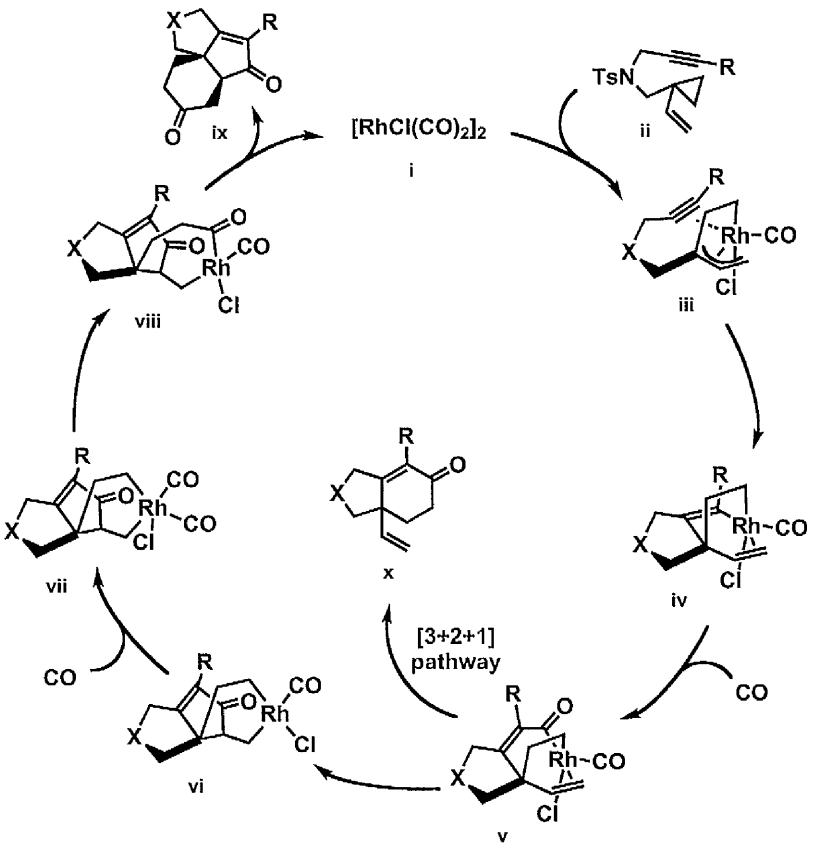

The initial step involved coordination of the rhodium catalyst **i** to the ene-cyclopropane **ii** and oxidative addition into the VCP moiety to afford **iii**. Subsequent alkyne and CO insertion provided metallacycle **v**. Reductive elimination of **v** afforded [3+2+1] bicyclic adduct **xi**

whereas alternative alkene insertion provides metallacycle **vii**. This latter intermediate is amenable to CO insertion and reductive elimination to afford angular tricyclic derivative **ix**. Studies by Wang outlined the investigation of cyclopropenes as an alternative reactive [$3C_{2s}$] component in the Rh-catalysed [3+2+1] cycloaddition (Eq. 1.21-1.22).[62]

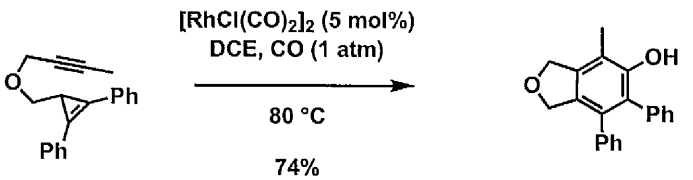

(1.21)

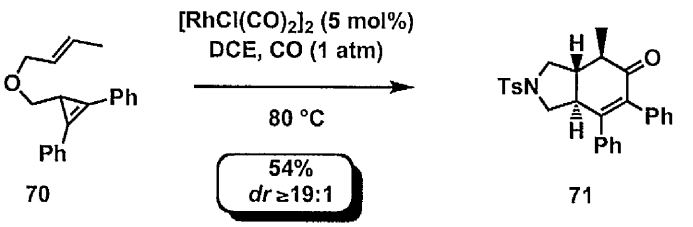

(1.22)

Higher strain energy of cyclopropenes compared to the parent cyclopropane and VCP allowed the cyclopropenes to react efficiently with an alkene and alkyne counterpart and thereby furnish bicyclohexenone or phenol-type derivatives (Eq. 1.21-1.22). An intriguing feature of this approach involved the exclusive formation of *trans*-fused bicyclic adducts and antithetical *cis*-stereochemistry of the corresponding [3+2] derivatives.[62] This interesting dichotomy provided the basis for a working hypothesis for the divergent [3+2] and [3+2+1] cycloaddition reactions of cyclopropen-ene substrates (**Scheme 1.25**). Initial coordination of cyclopropen-ene **ii** to the rhodium catalyst, followed by oxidative addition into the cyclopropene provides common metallacyclobutane **iv**. Alkene insertion in the [3+2] pathway affords *cis*-metallacyclopentene **ix** which undergoes reductive elimination to provide adduct **x**. In the [3+2+1] pathway, on the contrary, alkene insertion is preceded by CO insertion and formation of intermediate **v**. Stereospecific alkene insertion provides the *trans*-bridged metallacycle **vii** and subsequent reductive elimination supplies bicyclohexenone adduct **viii** (**Scheme 1.25**).[62]

Scheme 1.25. Mechanistic pathways for [3+2] and [3+2+1] cycloaddition reactions of cyclopropene-enes.

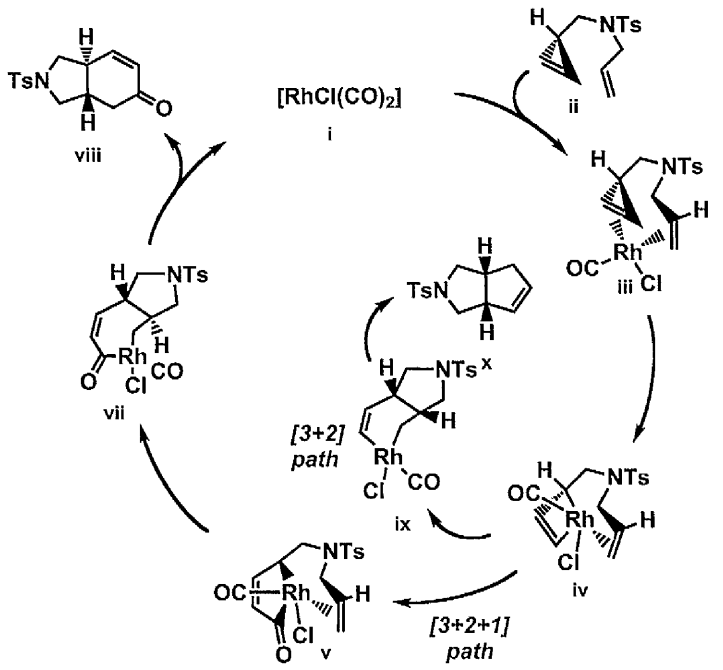

The development of the metal-catalysed [3+3+1] carbocylisation reactions has not been investigated extensively due to the low reactivity of cyclopropanes. Nonetheless, a unique report by Chung demonstrated the ability of unsymmetrical biscylopropanes to undergo a carbocyclisation reaction and provide synthetically useful bicycloheptanone derivatives (Eq. 1.23).[63]

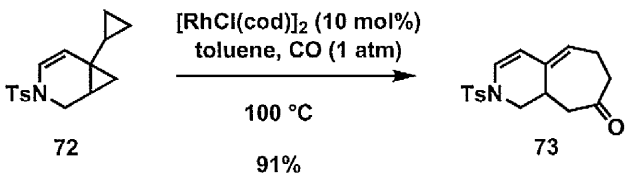

(1.23)

1.3.4. [4+1] and [5+1] Cycloadditions.

Early studies by Eaton[64] reported the ability of iron carbonyl complexes to catalyse [4+1] cycloadditions of conjugated allenes under a carbon monoxide atmosphere. Inspired by these

studies, Murakami and Ito probed the feasibility of a Rh-catalysed [4+1] carbonylative cyclisation of vinylallenes derivatives.[65] A postulated mechanism involved initial η^4 coordination of the vinylallene moiety to the rhodium centre and subsequent oxidative addition for the formation of metallacycle **iii** (**Scheme 1.26**). Subsequent CO insertion and reductive elimination provides dienone **vi**. This mechanistic hypothesis rationalised the development of the Rh-catalysed [4+1] cycloaddition (Eq. 1.24).[65] A significant drawback with the methodology was the concomitant formation of an isomeric mixture of cyclopentenones **75a** and **75b**. Further optimisation of the methodology demonstrated that bisphospholane ligand DuPhos and high CO pressure exerts a beneficial effect and prevents the isomerisation process, thus providing the exclusive formation of dienone **75a**.[66]

Scheme 1.26. Putative mechanism of the Rh-catalysed [4+1] cycloaddition of vinylallenes.

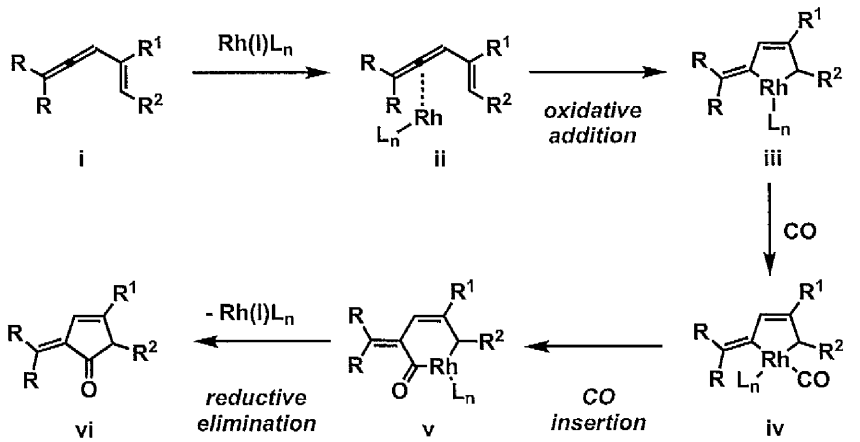

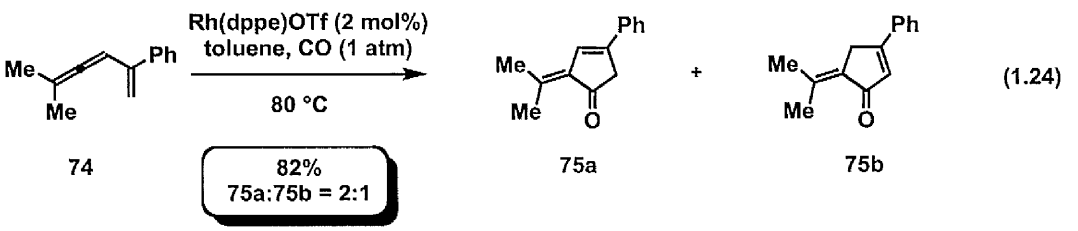

Later studies by Liebeskind described the Rh-catalysed [5+1] cycloaddition of conjugated cyclopropene derivatives under a carbon monoxide atmosphere.[67] This protocol provided an

interesting methodology for the regioselective synthesis of functionalised phenol and pyrone adducts (**Scheme 1.27**).

Scheme 1.27. Rh-catalysed [5+1] cycloaddition reaction of conjugated cyclopropenes.

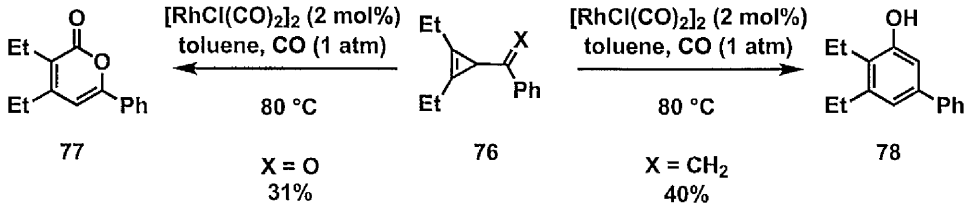

The proposed mechanism for this process is thought to involve the initial formation of the metallocyclobutene **ii** and regiospecific CO insertion, which results in metallacyclopentenone **iii** (**Scheme 1.28**). Subsequent alkene insertion and reductive elimination provides the corresponding pyrone **v** or phenol **vi**.

Scheme 1.28. Mechanistic pathway of the Rh-catalysed [5+1] cycloaddition reaction.

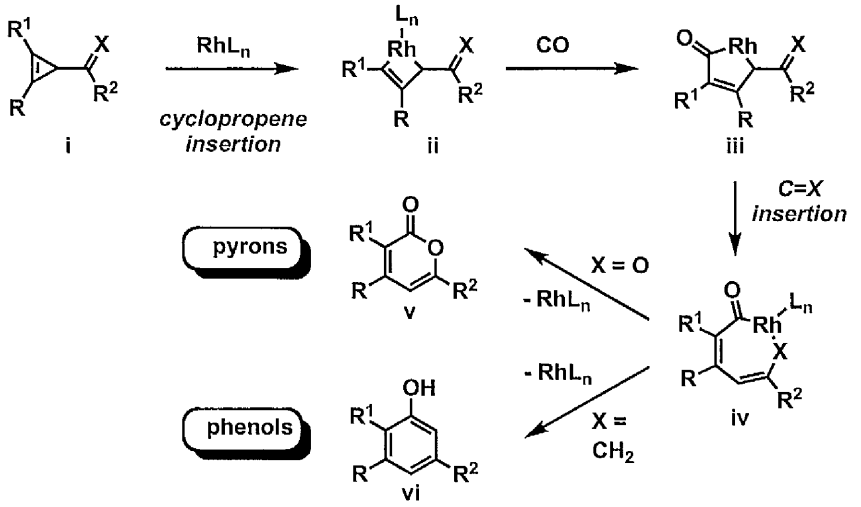

Additional investigations prompted the De Meijere group to expand the strategy to vinylcyclopropanes and develop a convergent approach to cyclohexanone derivatives,

although the crucial requirement of an additional cyclopropane moiety partially limited the synthetic utility of the process (Eq. 1.25).[68]

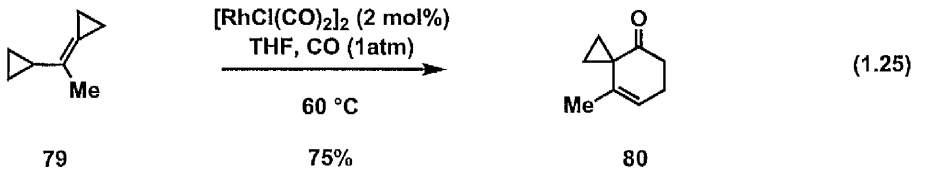

79 75% 80 (1.25)

Recent work by Malacria and Fensterbank disclosed the opportunity to carry out a [5+1] cycloaddition without the necessity of a cyclopropane-type 5C component. Treatment of 3-acyloxy-1,4-enyne **81** under carbonylative conditions resulted in a regioselective synthesis of resorcinol derivative **82** (Eq. 1.26).[69]

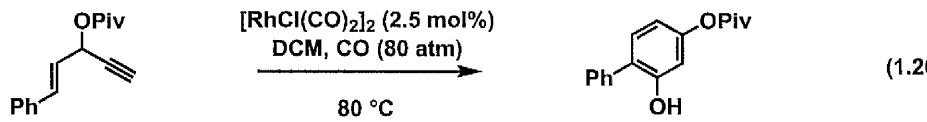

81 76% 82 (1.26)

Scheme 1.29. Postulated mechanism of the Rh-catalysed [5+1] cycloaddition reaction of 3-acyloxyenynes.

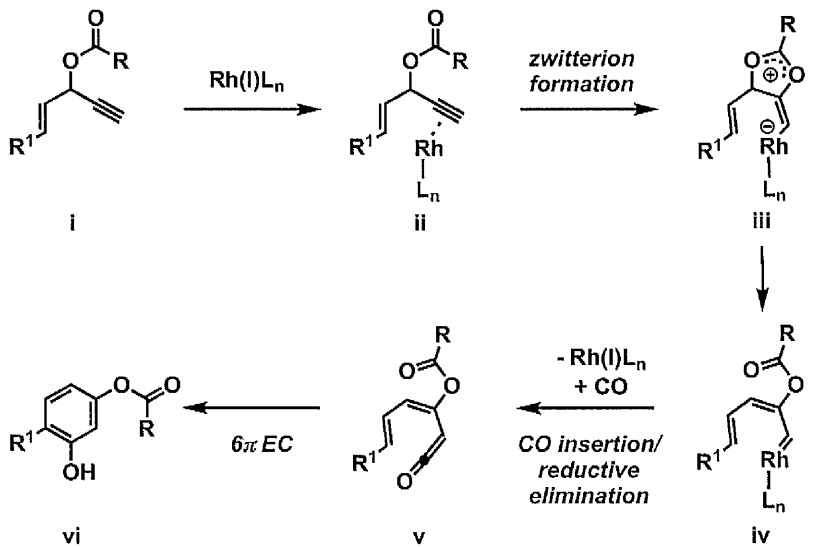

Additional studies supported an unusual mechanistic pathway, which involves formation of a conjugated ketene intermediate **v** to permit a thermal 6π electrocyclisation, which delivers the aromatic adduct **vi** (**Scheme 1.29**).[69]

1.3.5. [5+2+1] Cycloadditions.

Extensive studies by Wender highlighted the ability of VCP to undergo Rh-catalysed [5+2] cycloaddition with a wide variety of 2C synthons, thus providing a valuable approach for the construction of cycloheptane scaffolds.[48] In this context, it was envisioned that the incorporation of a carbon monoxide unit in the cycloaddition could deliver a powerful method for the construction of cyclooctenone derivatives. Preliminary studies revealed the intrinsic instability of the cyclooctenone ring, which resulted in the formation of bicyclic derivatives.[70] Hence, the appropriate choice of alkyne counterpart with hydrolytic work-up allowed the exclusive formation of transannular adducts (**Scheme 1.30**). A remarkable feature with the process includes the high regioselectivity in the alkyne insertion step and the latent functionalities in the cycloadducts.

Scheme 1.30. Intermolecular Rh-catalysed [5+2+1] cycloaddition reaction of vinylcyclopropanes, alkynes and CO.

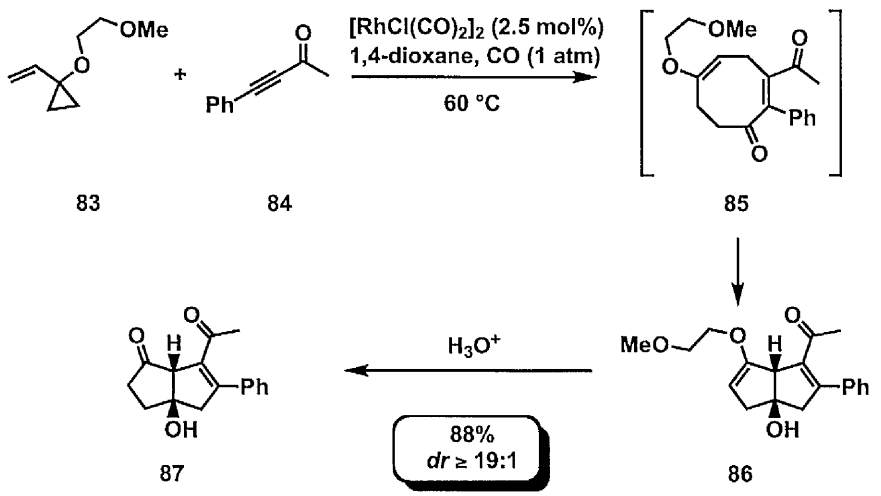

Previous studies on the [5+2] cycloaddition of VCP/ene substrates demonstrated that $[RhCl(CO)_2]_2$ failed to efficiently promote the process (**Scheme 1.31**).[71] The lack of reactivity was attributed to the low aptitude of the catalyst to promote reductive elimination (RE) and consequent $C(sp^3)$-$C(sp^3)$ bond formation (**Scheme 1.31**). On the other hand, the mechanistic pathway of the corresponding [5+2+1] involved migratory reductive elimination (MRE) and $C(sp^2)$-$C(sp^3)$ bond formation. Related computational studies indicated a lower activation energy for this step, thereby assessing the ability of $[RhCl(CO)_2]_2$ to promote a [5+2+1] carbocyclisation reaction.

Scheme 1.31. Reductive elimination step in Rh-catalysed [5+2] and [5+2+1] cycloadditions.

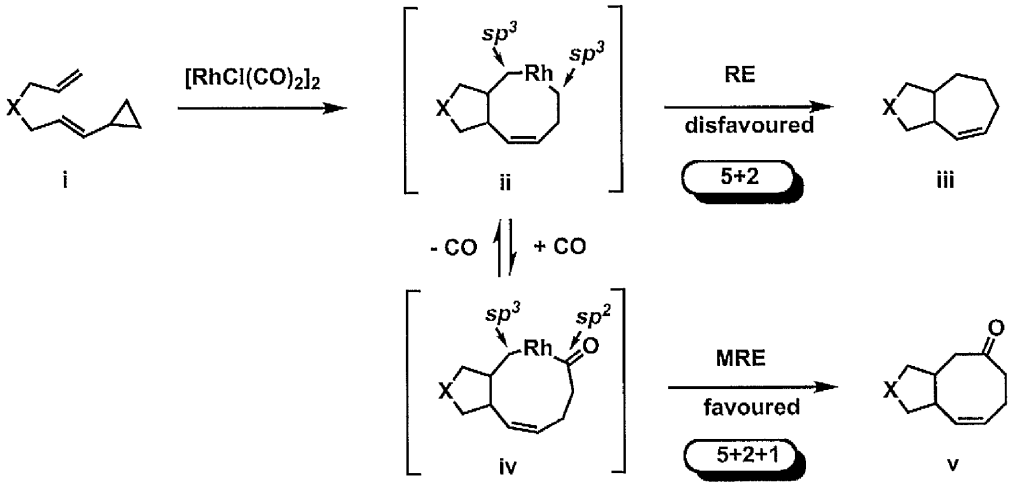

Hence, the theoretical findings provided the impetus to develop a new method for the construction of bicyclooctenone derivatives (Eq. 1.28).[72]

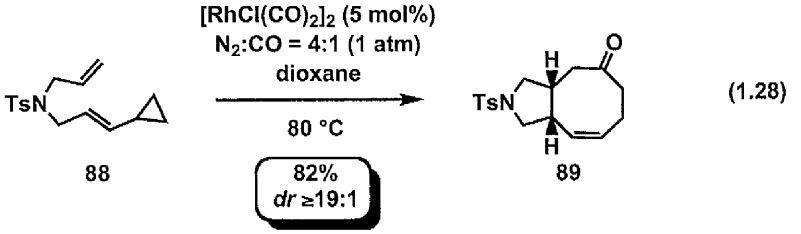

Further studies by the Yu group broadened the scope of this methodology with the highly stereoselective assembly of complex tricyclic scaffolds (Eq. 1.29).[73]

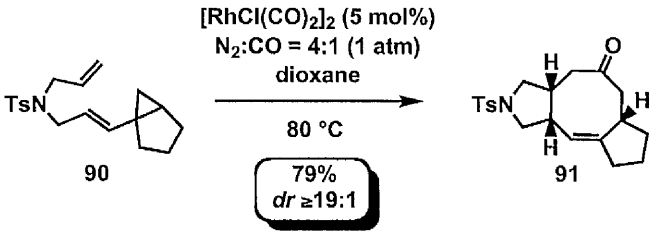

(1.29)

1.3.6. [6+1] and [7+1] Cycloadditions.

The role of the vinylcyclopentane moieties as a 5C synthon, prompted the Wender group to evaluate the reactivity of the homologous vinylcyclobutane group as a 6C component in the context of a Rh-catalysed carbonylative cycloaddition.[74a,b] Preliminary studies on a [6+1]-type process of vinylcyclobutanes under carbonylative conditions demonstrated an overall lack of reactivity. In light of this result, it was envisioned that the allene moiety would promote an effective coordination and enhance the rate of the oxidative addition step. The Rh-catalysed [6+1] cycloaddition of allenylcyclobutanes enabled the desired ring expansion, thereby providing an efficient approach to cycloheptenone derivatives (Eq. 1.30).[74b]

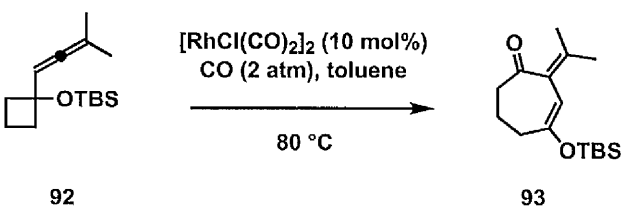

(1.30)

A putative mechanism involved initial 2π coordination of the allene moiety, oxidative addition of the cyclobutane ring and formation of metallacycle **ii** (**Scheme 1.32**). Subsequent CO insertion and reductive elimination afforded the desired cycloheptenone adduct **vi**.

Scheme 1.32. Mechanistic pathway of the Rh-catalysed [6+2+1] cycloaddition reaction.

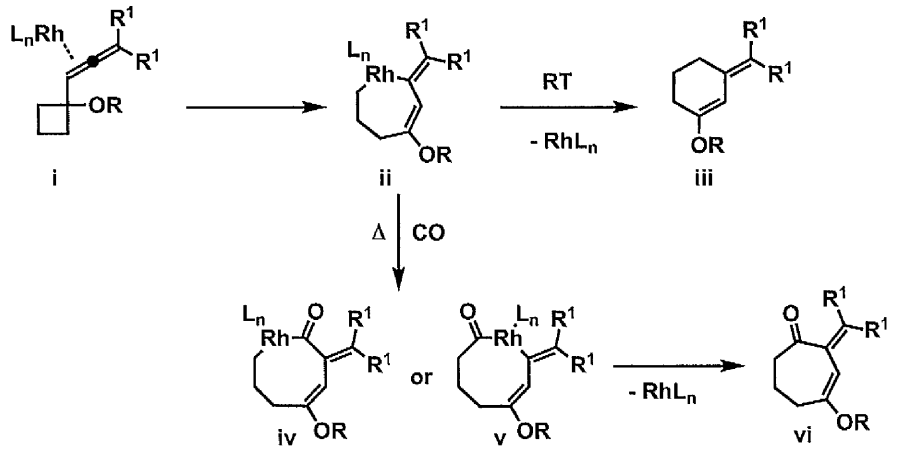

Additional studies by the Yu group envisaged that an additional alkene moiety in the vinylcyclopropane building block, namely dienylcyclopropanes, would permit a novel Rh-catalysed [7+1] cycloaddition process.[75] In this context, they provided the synthetically challenging construction of cyclooctenone rings (Eq. 1.31), which effectively overcame the inability of the intermolecular Rh-catalysed [5+2+1] cycloaddition to deliver eight-membered rings. Although high catalyst loading was required to promote useful rates and the reaction provides an isomeric mixture of **95a** and **95b**, the isolated adduct **95b** readily undergoes Rh-catalysed isomerisation to provide enone **95a** as the exclusive product.[75]

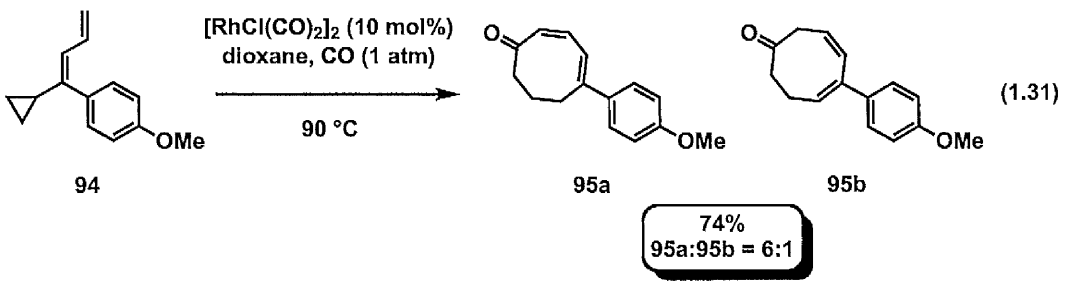

1.3.7. [m+n+o+1] Carbocyclisations.

The development of Rh-catalysed carbocyclisations has clearly estabilished the merit of the metal to coordinate a wide array of π-components and thereby promote the convergent

synthesis of complex polycyclic scaffolds. From a conceptual standpoint, the synthetic utility of this strategy could be further broadened to many multiple components, to increase the structural complexity of the carbocyclisation adducts. A major breakthrough in the application of the strategy was achieved by Ojima who developed a remarkable multicomponent Rh-catalysed [2+2+2+1] carbocyclisation reaction (Eq. 1.32).[76a]

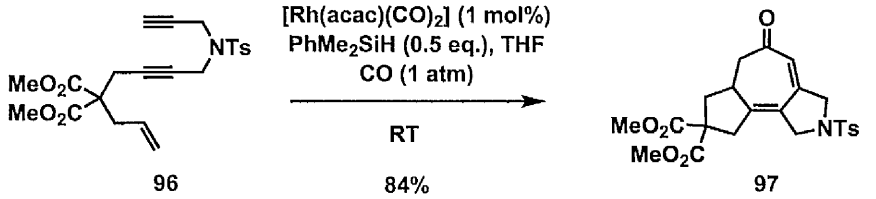

(1.32)

Scheme 1.33. Postulated mechanism of the silicon-initiated Rh-catalysed [2+2+2+1] cycloaddition reaction of ene-diynes and CO.

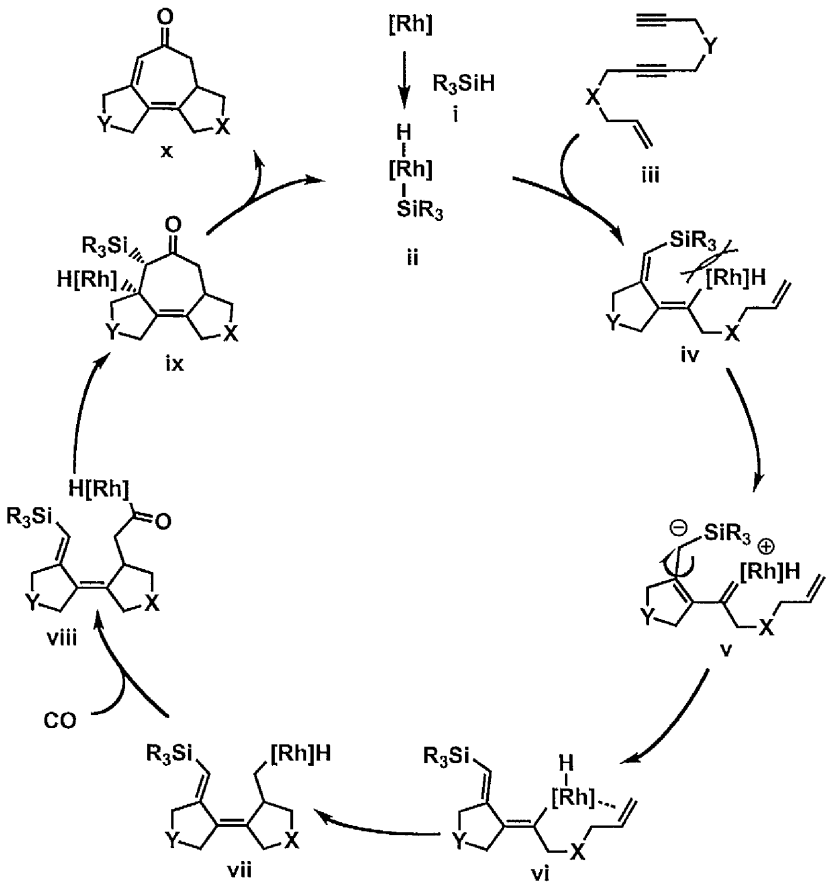

The proposed mechanism for the novel silicon-initiated carbotricyclisation is outlined in **Scheme 1.33**.[76a,b] Oxidative addition of the silane into the $[Rh(acac)(CO)_2]$ catalyst provides reactive complex **ii**. Further alkene insertion into the Rh-Si bond and an ene-type cycloisomerisation process afforded intermediate **iv**. Steric hindrance in **iv** between the vinylsilane and vinylrhodium moiety promoted isomerisation to **vi** through an Ojima-Crabtree mechanism. Cyclisation and CO insertion provided acylrhodium intermediate **viii**. The carbometallation and β-silyl elimination of intermediate **ix** afforded the [5-7-5] tricyclic derivative **x**. Further optimisation of this intriguing strategy provided the opportunity to achieve analogue scaffolds in the absence of silane initiators (Eq. 1.33).[76c]

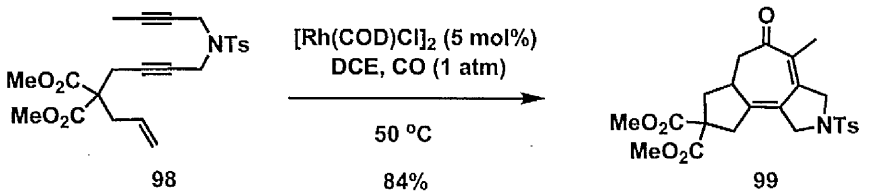

(1.33)

Scheme 1.34. Postulated mechanism of the Rh-catalysed [2+2+2+1] cycloaddition reaction of ene-diynes and CO.

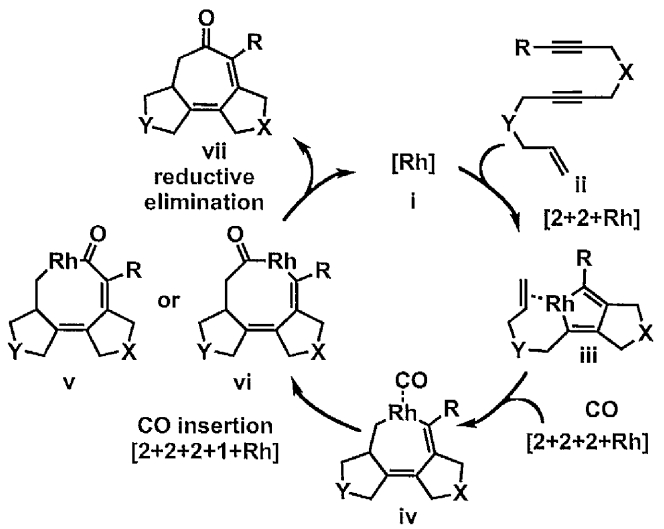

The alternative mechanistic pathway involved two consecutive migratory insertion steps *via* the formation of metallacycle **iv** (**Scheme 1.34**). Subsequent CO insertion and reductive elimination to provide the fused tricyclic adduct **vii**. The overall efficiency of both

methodologies relies on the exquisite reactivity of rhodium catalysts under mild conditions and the regioselective C-C bond formation between multiple π components. The demonstration of the synthetic potential of the method was further highlighted in the highly stereoselective assembly of complex tetracyclic scaffolds (Eq. 1.34).[76d]

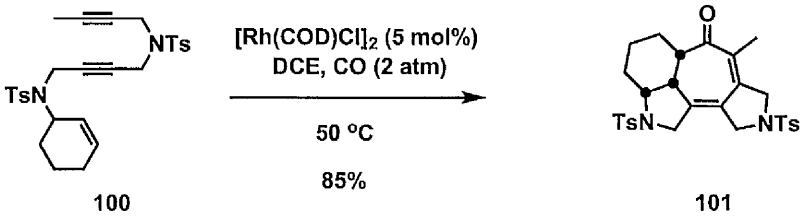

(1.34)

Optimisation studies on the intermolecular Rh-catalysed [5+2+1] of vinylcyclopropanes, alkynes and CO revealed that a different substitution pattern on the alkyne counterpart leads to divergent mechanistic pathway (**Scheme 1.35**).

Scheme 1.35. Mechanistic pathway of the Rh-catalysed [5+1+2+1] cycloaddition reaction.

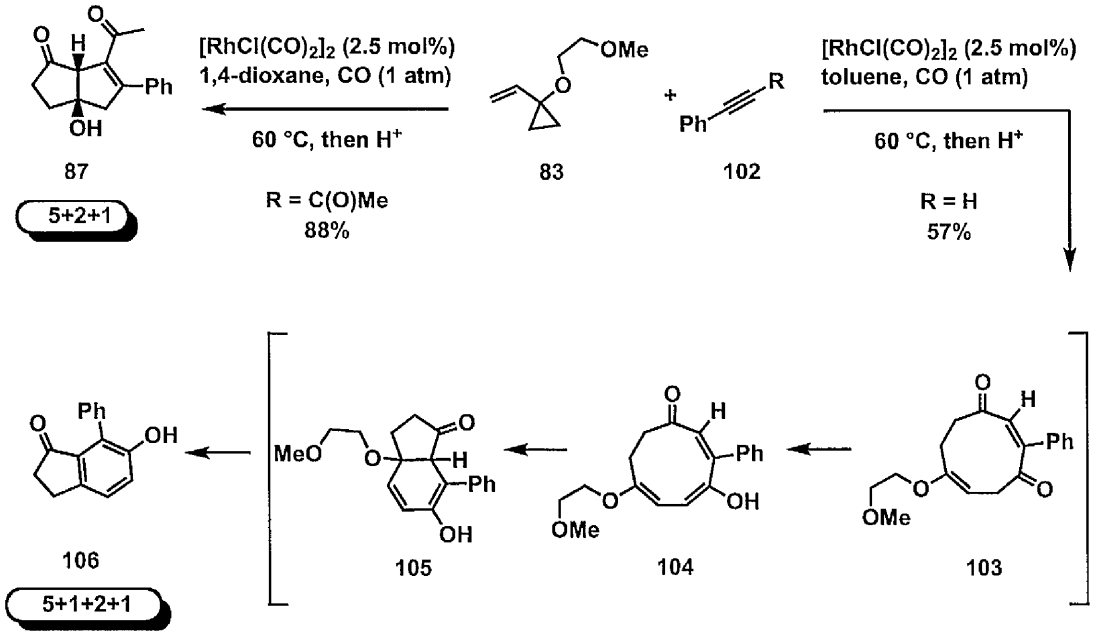

Employment of phenylacetylene substrates promotes a dicarbonylative process with the formation of the unstable dienone **103**. Subsequent tautomerisation to triene **104** and electrocyclic ring closure provided unstable diene **105**. Hence, the final elimination delivers the aromatic adduct **106** in excellent yield.[77] Despite the moderate synthetic utility and lack of stereogenic centres in the hydroxyindanone derivative, this methodology provided a rare example of *bis*-carbonylative multi-component process.

1.4 Diastereoselective Pauson-Khand Reactions.

1.4.1. Introduction.

The discovery of the Pauson-Khand cyclocarbonylation methodology highlighted the ability of transition metals to facilitate the simultaneous formation of multiple C-C bonds in a single operation step from readily available materials. Nonetheless, the impact of the original methodology was dramatically affected by the necessity to employ strained alkenes and the limited synthetic value of the cycloadducts. The introduction of tethered enynes for the intramolecular Pauson-Khand provided a new paradigm for the rapid construction of polycyclic structures. In this context, the ability to understand the stereochemical outcome of these reactions provided a formidable challenge for the exploitation of its synthetic utility.

1.4.2. Cobalt-catalysed Diastereoselective Pauson-Khand Reaction.

As a part of a program directed towards the synthesis of triquinanes, studies by Magnus explored the stereochemical outcome of the cobalt-mediated PK reaction and rationalisation of the experimental findings provided the current model for the stereocontrol in this process.[6] The cobalt-mediated thermal PK reaction of substituted 1,6-enynes provided complete diastereocontrol and resulted in the preferential formation of *cis*-fused bicyclopentenone adducts (Eq. 1.35-1.36). The observed 1,2- and 1,3-stereoselectivity could be explained in

terms of steric interactions in the alkene insertion step and corresponding formation of the cobalt metallacycle (Eq. 1.37-1.38).[6] Metallacycle **111a** can effectively minimise the interactions between the bulky C-3 substituent and TMS moiety on the alkyne terminus, whereas formation of metallacycle **111b** is disfavoured due to 1,3-*pseudo*-axial interaction on the *endo*-face.

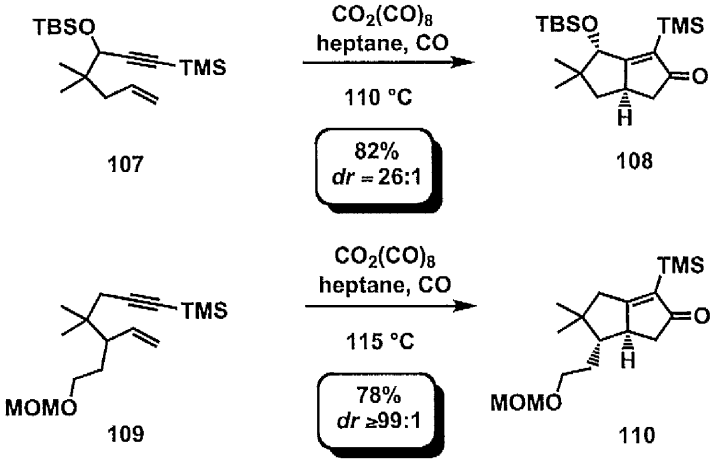

Analogous steric implications can rationalise the preferential formation of metallacycle **112a** in order to minimise 1,4-pseudoaxial interactions between the TMS group and the C2 allylic substituent (Eq. 1.38). Additional studies demonstrated that the bulky alkyne dramatically enhances the stereocontrol in process, thereby supporting the validity of the mechanistic hypothesis.

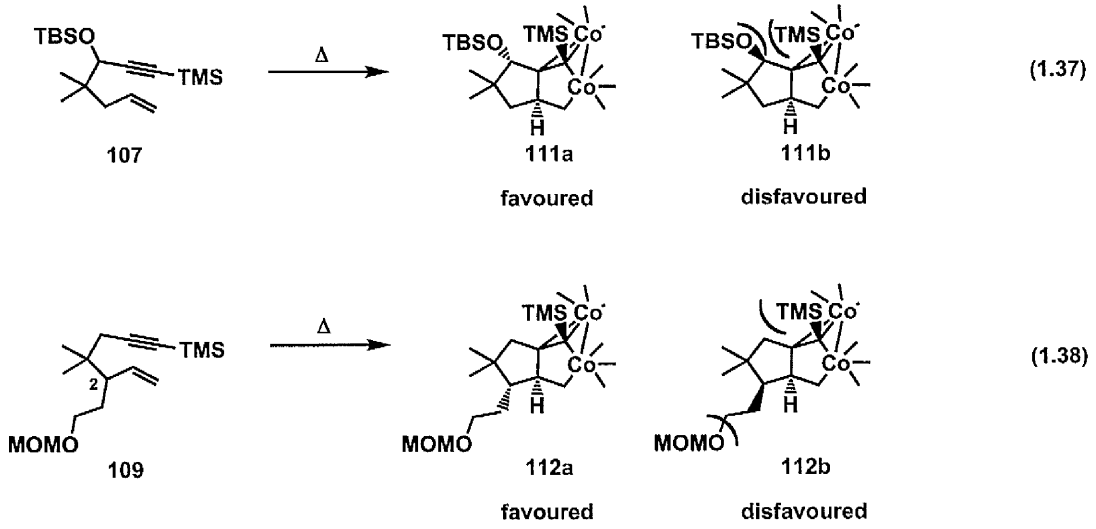

Nonetheless, additional investigations revealed how the stereochemical outcome of the process was dramatically affected by the nature of the tethering group and substituents on the enyne. In a program directed towards the total synthesis of picrotoxanes, Mukai and Hanaoka explored the feasibility of tartrate-derived 1,7-enyne in the PK reaction and to provide the highly functionalised bicyclo[4.3.0]nonanes (Eq. 1.39-1.40).[78] Previously invoked 1,3-pseudoaxial steric interactions between the protected hydroxyl group and phenyl substituent provided a rationale for the stereoselective formation of adduct **114**, albeit with the unexpected stereocomplementary formation of the corresponding dihydroxy derivative **116**, which prompted additional investigation into the nature of the reactive conformers.

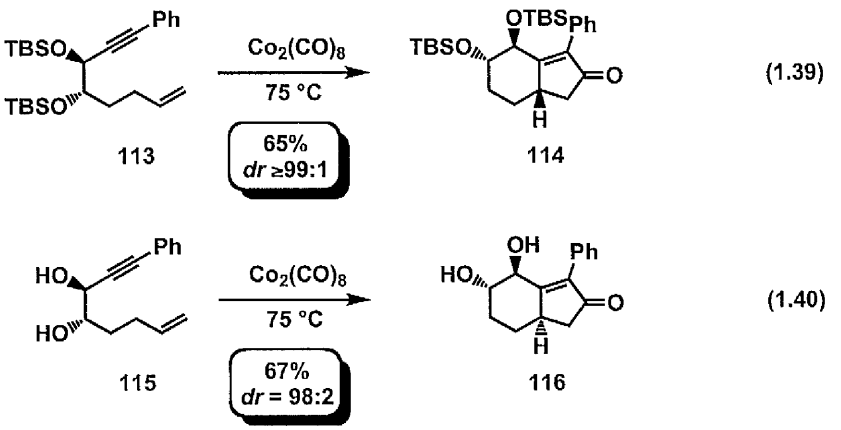

Scheme 1.36. Reactive conformers in the PK reaction of tartrate-derived 1,7-enynes.

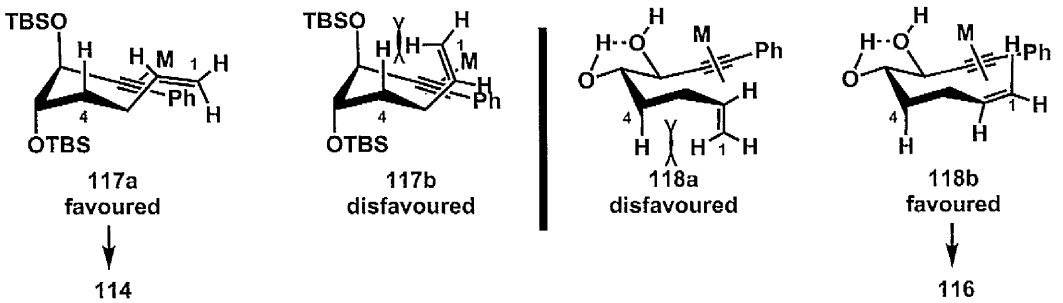

Analysis of conformers of both reactions rationalised the observed diastereocontrol on the basis of reduced steric interactions between the axial H4 and the olefinic proton H1 in **117a**

and **118b**. This revealed that the orientation of the hydroxyl groups was responsible for the stereocomplementary formation of **114** and **116** (**Scheme 1.36**).[78] For instance, hydrogen-bonding interactions in **115** generate a five-membered transient ring, wherein the vicinal hydroxyl groups are diequatorial, which contrasts the axial orientation of TBS ethers in **117** (**Scheme 1.36**). Additional studies revealed the key role of conformational restriction in the enyne substrates for the enhancement and control of the stereoselectivity.[78] Nonetheless, the application of this methodology towards to the synthesis of polycyclic alkaloid-type scaffolds provided poor diastereocontrol in the cobalt-mediated PK reaction of C2-substituted nitrogen-tethered enynes (Eq. 1.41).[79]

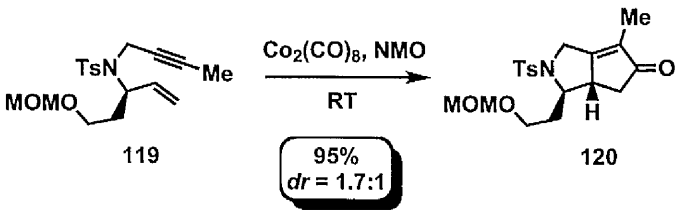

(1.41)

In contrast, incorporation of a C2 substituent and nitrogen tether inside a rigid cyclic structure drastically reduced the conformational mobility of the enyne substrate and provided a high level of diastereocontrol in the cycloaddition process (Eq. 1.42).[80]

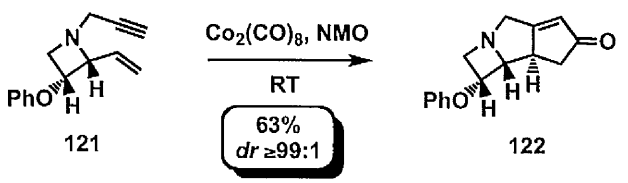

(1.42)

The aforementioned studies by Magnus confirmed the crucial role of bulky functional groups in the reaction with respect to diastereocontrol. In light of these observations, Carretero envisioned that incorporation of a bulky group on the alkene counterpart would provide additional steric interactions and enhance the level of stereoinduction in the metallacycle formation, thereby providing stereoselectivity in the process. The vinylsulfone moiety proved

to be optimal in this regard (Eq. 1.43), in which the 1,2-*cis* diastereoselectivity could be switched to facilitate the synthesis of 1,2-*trans*-substituted bicyclopentenone rings.

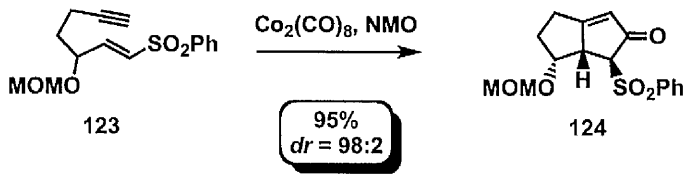

(1.43)

The observed *trans*-1,2 diastereoselectivity was explained in terms of 1,3-steric interactions in the alkene insertion step between the C2-substituent and bulky sulfone moiety in the formation of the cobalt metallacycle **125a** (Eq. 1.44).[81]

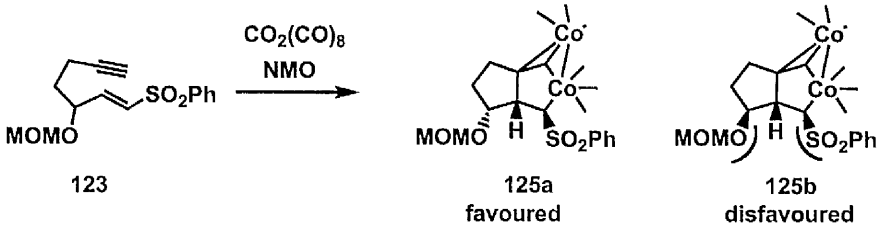

(1.44)

Additionally, the sulfone moiety provides a removable stereodirecting group in order to circumvent the poor diastereocontrol in the nitrogen-tethered PK reaction of 1,6-enynes (**Scheme 1.37**).[82]

Scheme 1.37. Sulfone group as a removable stereodirecting group in the PK reaction.

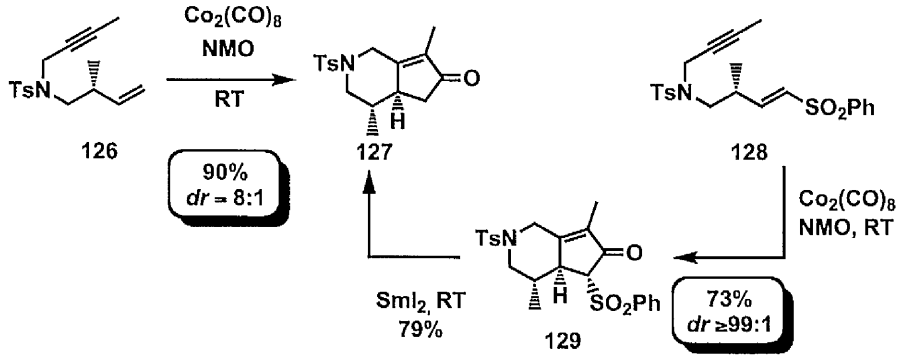

The high level of diastereocontrol in the cycloaddition was rationalised in terms of increased steric *pseudo*-axial interactions between the C2 methyl substituent and olefin group in **130a**, which enhanced the formation of **130b** and the stereoselective formation of adduct **129** (Eq. 1.45).[82]

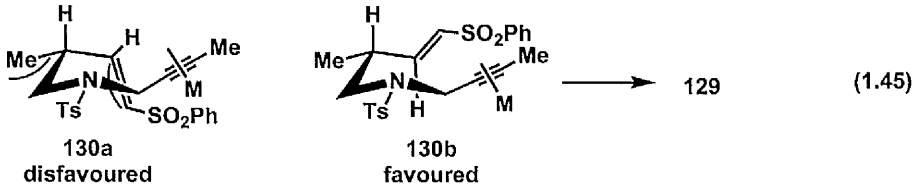

1.5. Diastereoselective PK and Related Cyclocarbonylation Reactions in Total Synthesis.

1.5.1. Introduction.

Since its inception in 1971, the PK reaction has undergone extensive development as highlighted by the persistent exploitation of the methodology in the context of the total synthesis of complex natural products. The employment of a wide variety of transition metals broadened the substrate scope using mild operating conditions. Moreover, elegant theoretical and mechanistic studies provided additional insights into the reaction, thus enhancing understanding and the factors that control the stereochemical outcome. Finally, these investigations have provided a wide range of π-components to assemble distinctive molecular architectures, as outlined in **Figure 1.1**. The outstanding synthetic value of the PK reaction is clearly epitomised by the number of total synthesis involving that utilise this methodology. The structural complexity of the cycloadducts has prompted the employment of this strategy in the total synthesis of terpene and terpinoid-type natural products. Moreover, the ability to incorporate nitrogen tethers permits the construction of nitrogen-containing polycyclic scaffolds, relevant to the synthesis of biologically active alkaloids. Additionally, the ability of the intermolecular manifold provides cyclopentane rings, which were utilised in the synthesis of natural prostaglandins. The present section will highlight the application of the PK reaction

and related metal-catalysed cyclocarbonylations in the total synthesis of challenging bioactive natural products.

Figure 1.1. Synthetic utility of the PK reaction in the construction of polycyclic scaffolds.

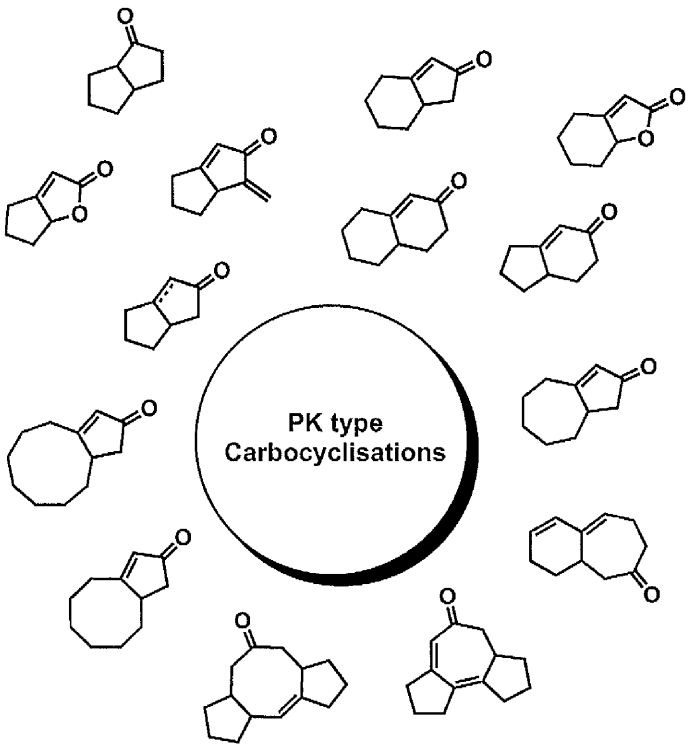

1.5.2. Terpenes.

1.5.2.1 Monoterpenes.

Pauson and Kerr outlined the problems[83] with the intermolecular PK reaction in the total synthesis of Japanese hop ether[84], which resulted in low regioselectivity and preferential formation of undesired butenolides. Nevertheless, the intramolecular manifold to overcame the abovementioned issues and resulted in an efficient synthesis of the monoterpene.[85] Other key issues with the methodology include enhanced reactivity of brucine *N*-oxide as a promoter in the cobalt-catalysed PK reaction (**Scheme 1.38**).

Scheme 1.38. Kerr's total synthesis of (±)-Japanese hop ether.

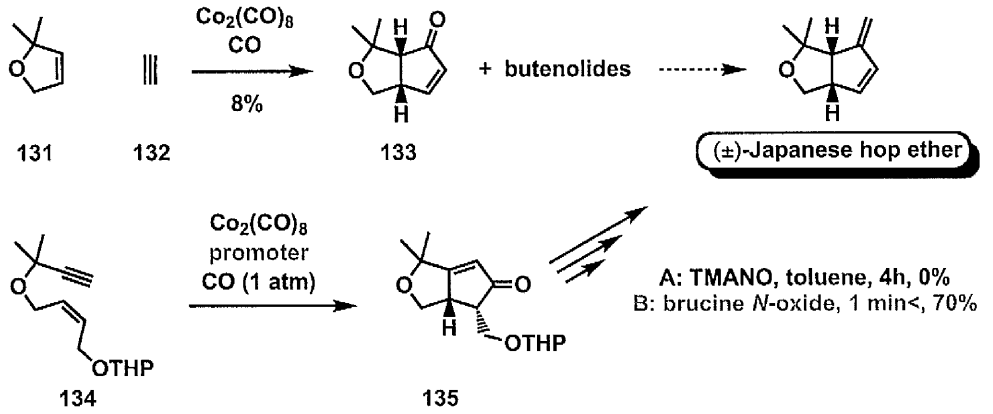

The development of the first Mo-catalysed hetero-PK reaction by Carretero[36] (*vide* section **1.2.4.1.2**) provided an optimal approach for the construction of butenolide-containing natural products. A straightforward five-step synthesis of epi-dihydrocanadensolide demonstrated the synthetic potential of this methodology (**Scheme 1.39**).[36] An analogue approach was applied by Gao in the construction of (−)-mintlactone A.[86]

Scheme 1.39. Hetero-PK reaction-mediated total synthesis of epi-dihydrocanadensolide.

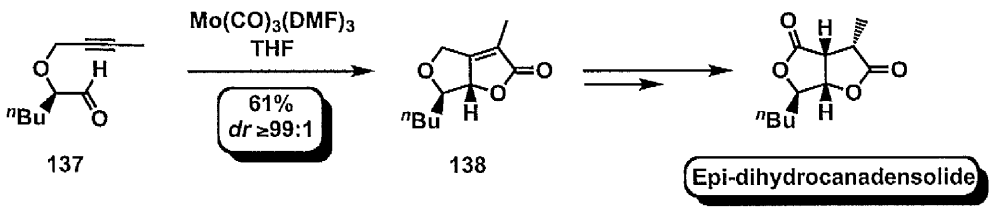

1.5.2.2. Sesquiterpenes.

1.5.2.2.1. Diquinanes.

Additional studies by Kerr and Pauson[87a] described the ability of vinyl esters to behave as a 2π component in the intermolecular PK reaction, followed by the reductive loss of the ester

moiety, to provide an ethylene surrogate. A key advantage of this strategy is the ability to avoid the utilisation of an autoclave apparatus for the, previously required, high pressure of ethylene. This was successfully demonstrated in the total synthesis of (+)-taylorione and (+)-nortaylorione (**Scheme 1.40**).[87b]

Scheme 1.40. Kerr's total synthesis of (+)-taylorione and (+)-nortaylorione.

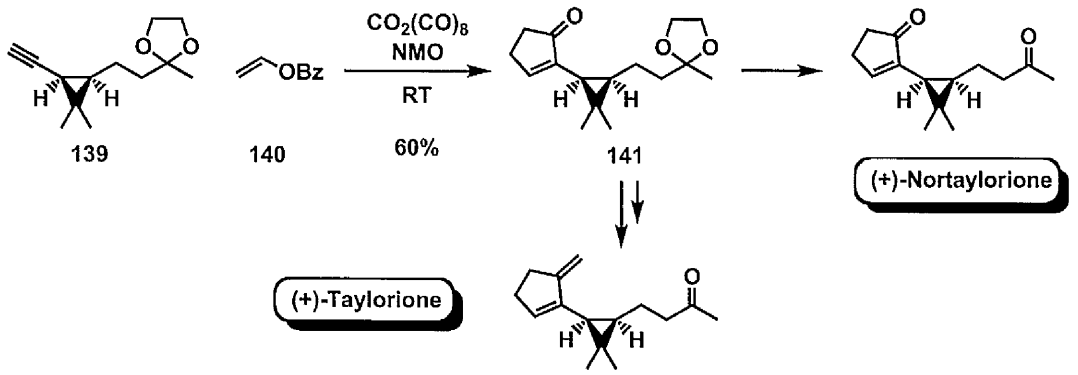

1.5.2.2.2 Linear Triquinanes.

Development of the intramolecular PK reaction[9] in 1981 delivered a versatile platform for the total synthesis of cyclopentenone derivatives. In this regard, Magnus recognised the opportunity to utilise this approach for total synthesis of coriolin.[88]

Scheme 1.41. Magnus' PK reaction-mediated total synthesis of the sesquiterpene coriolin.

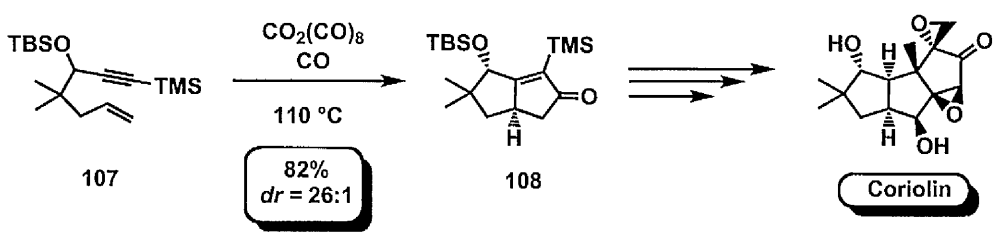

The associated high antitumor activity and the structural complexity of this sesquiterpene generated a wide interest in its construction, which is evident from the six completed total syntheses between 1980 and 1982.[88b,89] The development of a PKR-mediated total synthesis of coriolin demonstrated the synthetic potential of this carbocyclisation and provided preliminary support for the Magnus-type mechanism of Co-catalysed PK reaction (**Scheme 1.41**).[90] The validity of the approach prompted additional investigations into the construction of analogous linear triquinanes. Greene et al. described a mild coupling of chiral alcohols with terminal alkynes to afford chiral acetylenic ethers,[91] which provided the opportunity to utilise this functionality as a 2π component in the PK reaction and thereby provide asymmetric induction in the carbocyclisation. This resulted in the first asymmetric approach to the sesquiterpene hirsutene (**Scheme 1.42**).[92,93] The remarkable key advantage of this approach included the separation of the diastereoisomers and recover the chiral auxiliary, albeit the stereochemical outcome of the process was moderate.

Scheme 1.42. Greene's asymmetric synthesis of hirsutene.

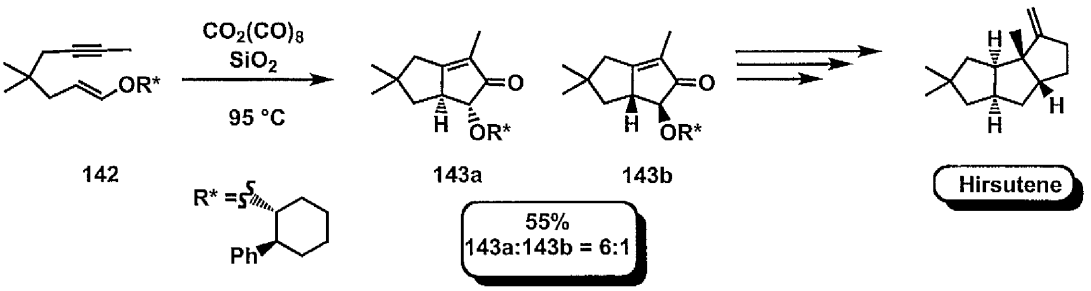

The development of Mo-mediated allenyne PK reactions[31] (*vide* section **1.2.4.1.1**) to provide bicyclo[4.3.0]nonane scaffolds was also utilised in the total synthesis of sesquiterpene natural products. Biological studies by MacDonald and Kelner[94] demonstrated that HMAF (hydroxymethylacylfulvene) sesquiterpene has outstanding antitumoral activity and concomitant low toxicity. Hence, the development of an asymmetric process was desirable since natural (*S*)-enantiomer has two-fold increase in activity.[94]

Scheme 1.43. Total synthesis of HMAF by Mo-mediated allenynes PK reaction.

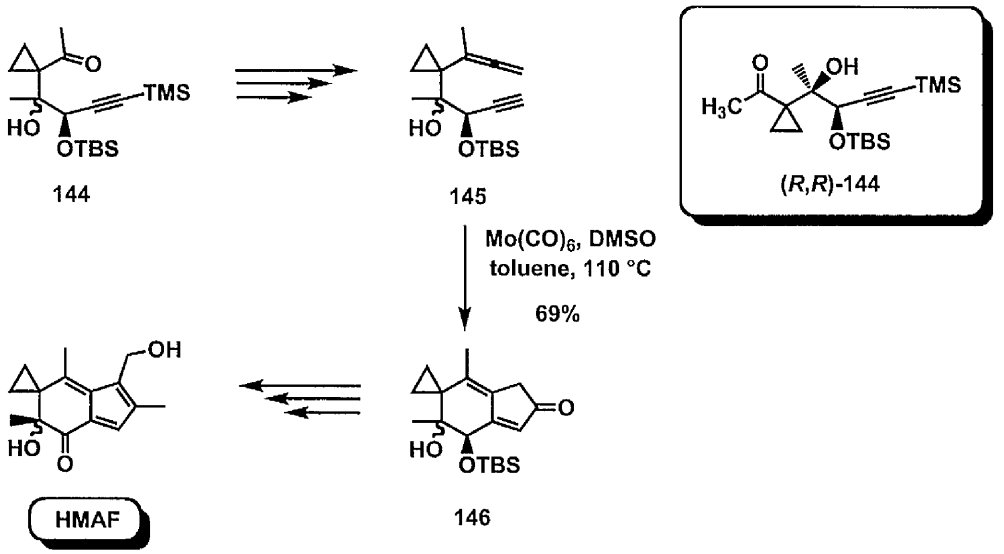

In this context, Brummond utilised a Mo-mediated PK reaction of allenynes in the racemic total synthesis of HMAF (**Scheme 1.43**) and additionally developed a synthetic route to enantiopure intermediate **(*R*,*R*)-144**, thus providing the first enantioselective route to HMAF.[32] The excellent antileukemial activity and the highly functionalised bicyclo[4.3.0]nonane architecture of *Jatropha neopauciflora*[95] sesquiterpenes prompted the Mukai group to investigate the Rh-catalysed PKR of allenyne **147** to assemble the complex scaffold **148** in a stereoselective fashion (**Scheme 1.44**).

Scheme 1.44. Total synthesis of *Jatropha neopauciflora sp.* by Rh-catalysed allenenes PK reaction.

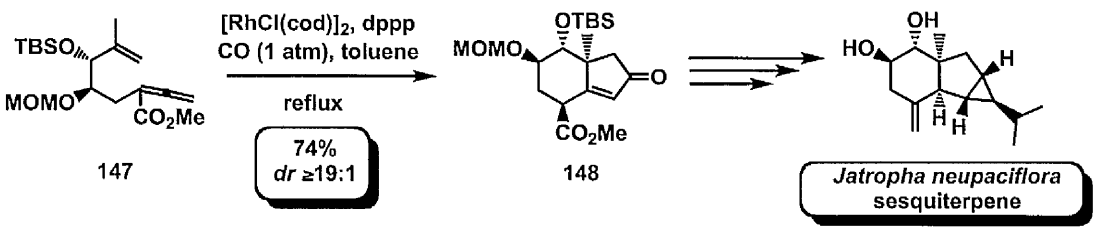

This approach provided an elegant strategy for the construction of the bicyclic scaffold with concomitant formation of two stereogenic centres (**Scheme 1.44**).[96]

Scheme 1.45. Total synthesis of achalensolide by Rh-catalysed allenynes PK reaction.

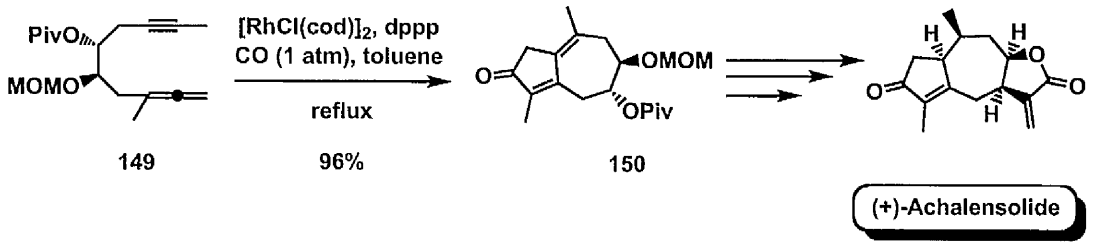

Mukai also examined the homologous allenyne to provide the bicyclo[5.3.0]nonane scaffolds[53a,b] in the enantioselective synthesis of guaianolide (+)-achalensolide (**Scheme 1.45**).[97,98] Interestingly, the employment of dppp ligand is critical for the Rh-catalysed cycloaddition, in the context of yield.

Scheme 1.46. Total synthesis of (±)-hirsutene and (±)-1-desoxhypnophylin.

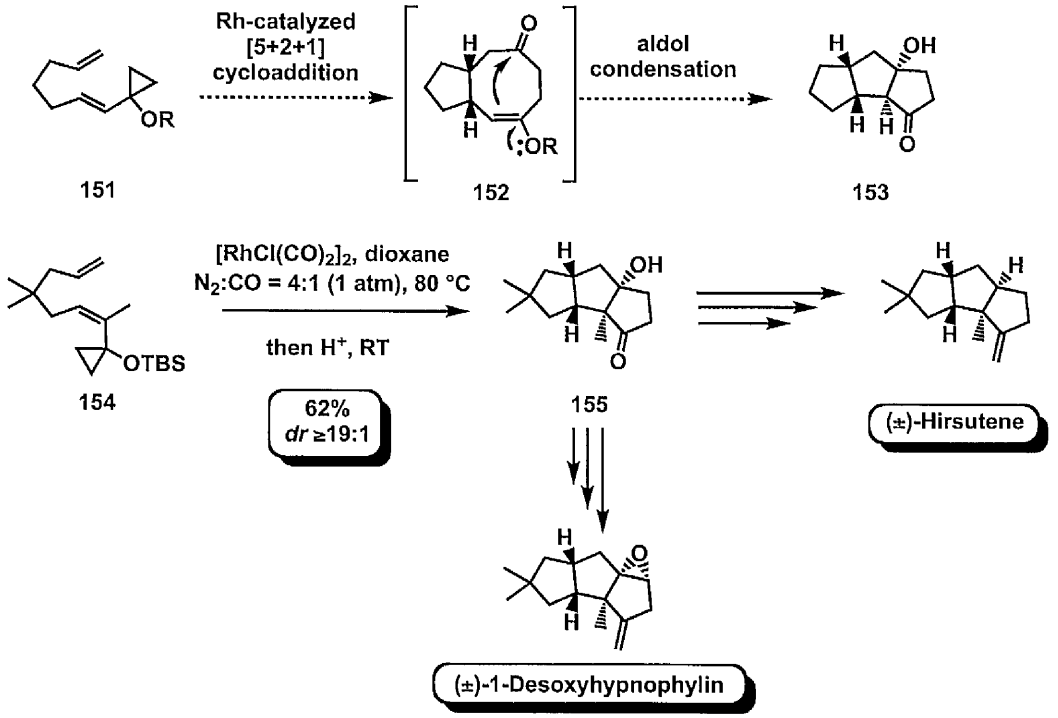

Recently developed Rh-catalysed [m+n+1] cycloadditions reactions have emerged as a powerful tool for the expeditious construction of a wide variety of polycyclic scaffolds. In this context, the Yu group developed a highly convergent synthesis of triquinane scaffolds using a tandem Rh-catalysed [5+2+1] cycloaddition/aldol reaction (**Scheme 1.46**).[99] A key feature of the strategy involved the ability to generate three rings and four stereogenic centres in a single operational step. Concise and stereoselective syntheses of (±)-hirsutene and (±)-1-desoxhypnophylin highlighted the synthetic utility of this approach (**Scheme 1.46**).[99] The strategy was also applied in the total synthesis of (±)-hirsutic acid, albeit the quaternary stereocentre on the carbon tether was too remote to induce effective diastereocontrol in the cycloaddition reaction (**Scheme 1.47**).[100,101]

Scheme 1.47. Yu's total synthesis of (±)-hirsutic acid.

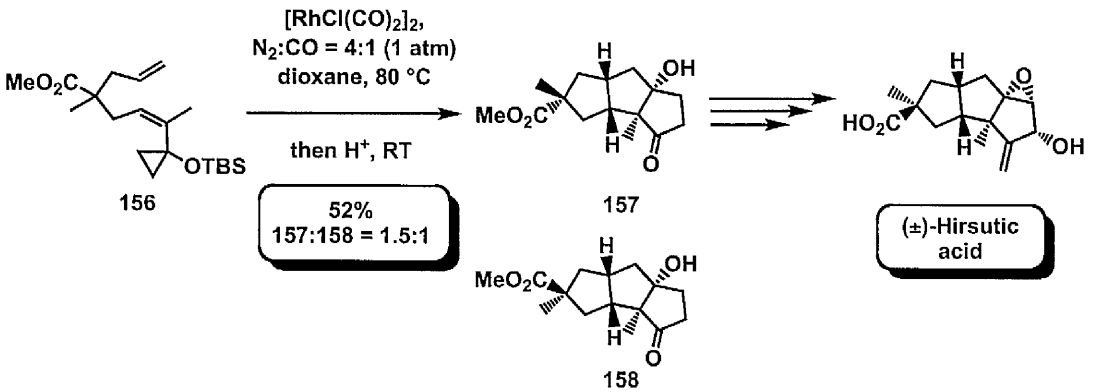

1.5.2.2.3 Angular Triquinanes.

The exploitation of the intramolecular PK reaction in the total synthesis of linear triquinane involved an obvious extension of the strategy for the construction of angular analogues. The recent isolation of several pentalenoids, which have marked antibiotical activity, provided an optimal scaffold for probing the synthetic potential of the carbocyclisation. Extensive studies by Schore led to the development of useful approaches to the (±)-pentalenene, (±)-pentalenic acid and (±)-silphinene angular triquinanes (Eq. 1.45).[102,103] The construction of the tricyclic

scaffold involved a Co-catalysed PK reaction of a 1,6-enyne bearing a cyclopentene moiety as a 2π component. Nevertheless, a major drawback with the approach was the inability of the remote methyl substituent to direct the stereochemical outcome of the process.[103]

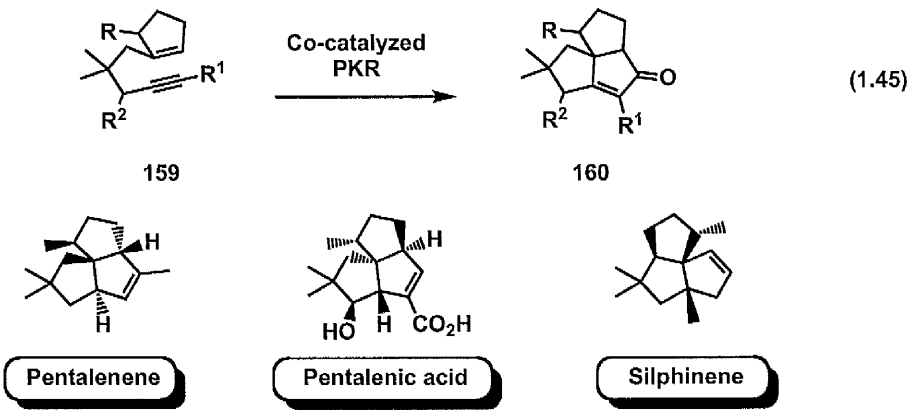

(1.45)

Additional investigations by Pericas and Moyano on the PKR-mediated construction of pentalenoid derivatives provided the first enantioselective synthesis of (+)-15-norpentalenene.[104] The bulky camphor-derived chiral auxiliary confers enhanced stereocontrol in the alkene insertion step and thereby promote a diastereoselective cyclisation (**Scheme 1.48**).

Scheme 1.48. PK reaction-mediated asymmetric synthesis of (+)-15-norpentalenene.

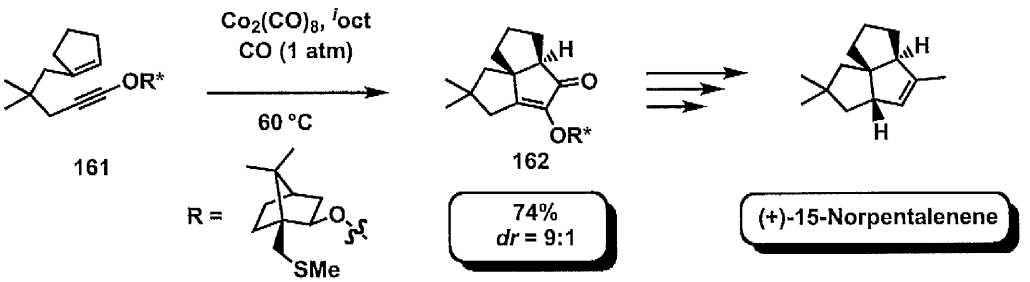

Recent studies by Fox employed cyclopropenes to act as a reactive 2π component in the cobalt-catalysed PK reaction.[105a] The methodology was successfully applied in the enantioselective synthesis of (–)-pentalenene (**Scheme 1.49**).[105b] As previously observed in

Schore's pentalenoid synthesis,[103] substituents on the cyclic ring do not effectively direct the stereochemical outcome of the Pauson-Khand reaction. Hence, the poor diastereocontrol in the total synthesis of angular triquinanes provided the impetus to explore alternative methodologies.

Scheme 1.49. Fox's asymetric total synthesis of (–)-pentalenene.

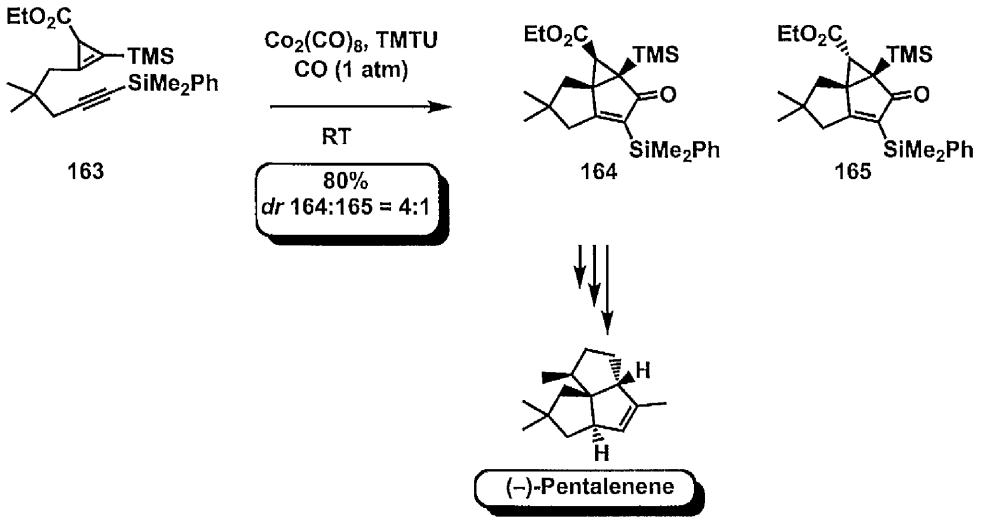

An early total synthesis of (±)-pentalenene by Pattenden revealed that final BF_3-catalysed ring closure of bicyclooctadiene derivative **166** promoted a highly stereoselective formation of the angular triquinane (**Scheme 1.50**).[106] The disclosed ability of Rh-catalysed [5+2+1] cycloaddition to generate bicyclooctenone scaffolds[72] was promptly exploited by Yu group in the synthesis of intermediate **166**, thereby providing a stereoselective formal synthesis of (±)-pentalenene (**Scheme 1.51**).[107]

Scheme 1.50. Pattenden's total synthesis of (±)-pentalenene.

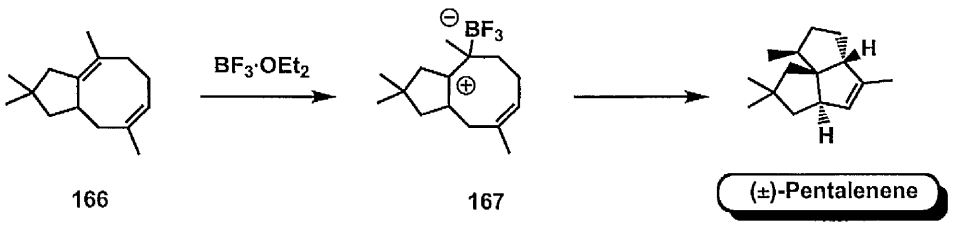

Scheme 1.51. Yu's formal total synthesis of (±)-pentalenene.

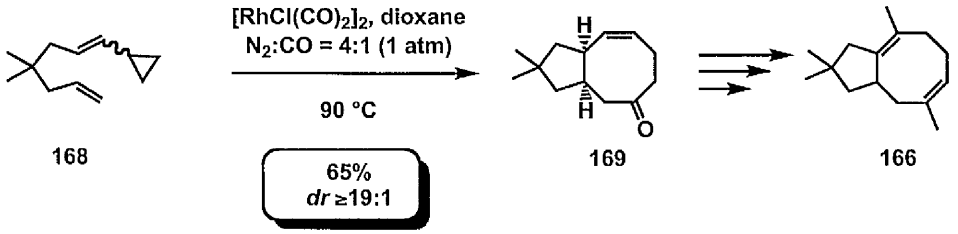

Cedrene sesquiterpenes[108] gained particular interest among the synthetic organic community in light of the unusual tricyclic structural core and wide utilisation as deodorant components. In this context, Kerr and Pauson reported an intramolecular PK reaction for the synthetically challenging construction of the fused tricyclic scaffold and thereby provide an efficient synthesis of (±)-α and β-cedrene (**Scheme 1.52**).[109] The acknowledged ability of sulfides to act as promoters[15] conferred optimal reactivity to the Co-catalysed carbocyclisation reaction.

Scheme 1.52. Kerr and Pauson formal total synthesis of (±)-α and β-cedrene.

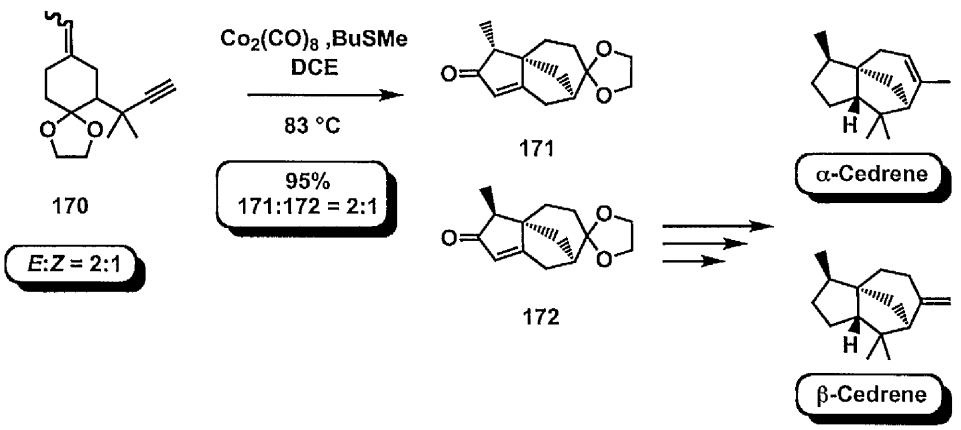

The isolation and characterisation of asteriscanolide by the San Feliciano group[110] provided a novel sesquiterpene architecture, which consists of a bicyclo[6.3.0]undecane scaffold bearing a bridged lactone and five stereocentres. An intriguing stereoselective total synthesis by Krafft involved an initial regioselective intermolecular PK reaction to provide a highly

functionalised cyclopentenone **174a (Scheme 1.53)**.[111] The appropriate choice of the alkyne substituents facilitates a lactonisation/ring opening sequence and then the construction of the eight-membered ring by a RCM reaction.

Scheme 1.53. Krafft's PKR-mediated total synthesis of (±)-asteriscanolide.

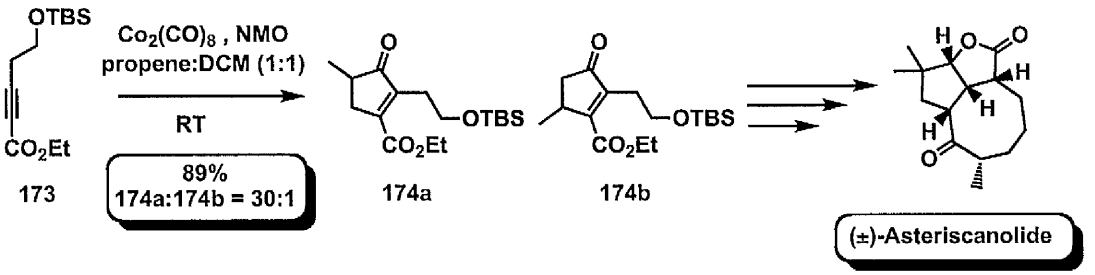

In an alternative enantioselective total synthesis of (+)-asteriscanolide by the Yu group the Rh-catalysed [5+2+1] cycloaddition of chiral ene/VCP **175** provided the corresponding bicyclooctenone **176 (Scheme 1.54)** as route to the natural product.[112] The radical annulation then provided the requisite bridging butyrolactone ring. Nevertheless, the efficiency of both strategies was partially diminished by the requirement of additional synthetic steps, in order to achieve optimal stereoselectivity for the bridging C3 centre.[111,112]

Scheme 1.54. Yu's PKR-mediated total synthesis of (+)-asteriscanolide.

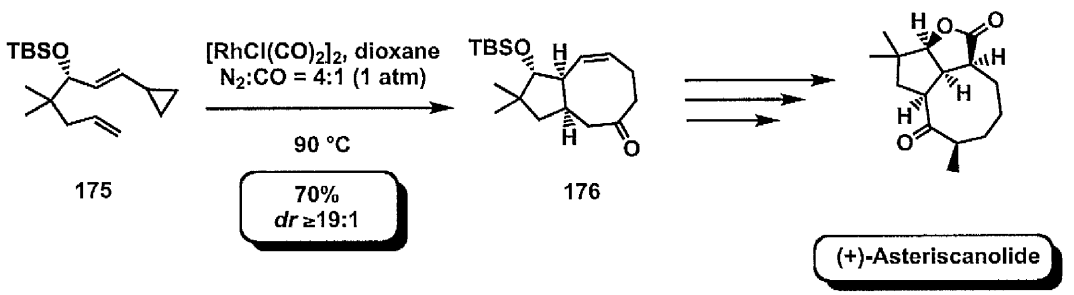

The development of the Rh-catalysed [3+2+1] cycloaddition of VCP-ynes provided a new approach for the construction of 6-6 bicyclic scaffolds. The exploitation of this strategy provided an efficient synthesis of antifeedant sesquiterpene (±)-α-agarofuran (**Scheme**

1.55).[60] The excellent stereocontrol was rationalised by favourable *trans*-equatorial configuration of the ester and vinyl substituents in the alkyne insertion transition state **177-TS**.

Scheme 1.55 Rh-catalysed [3+2+1] cycloaddition-mediated total synthesis of (±)-α-agarofuran.

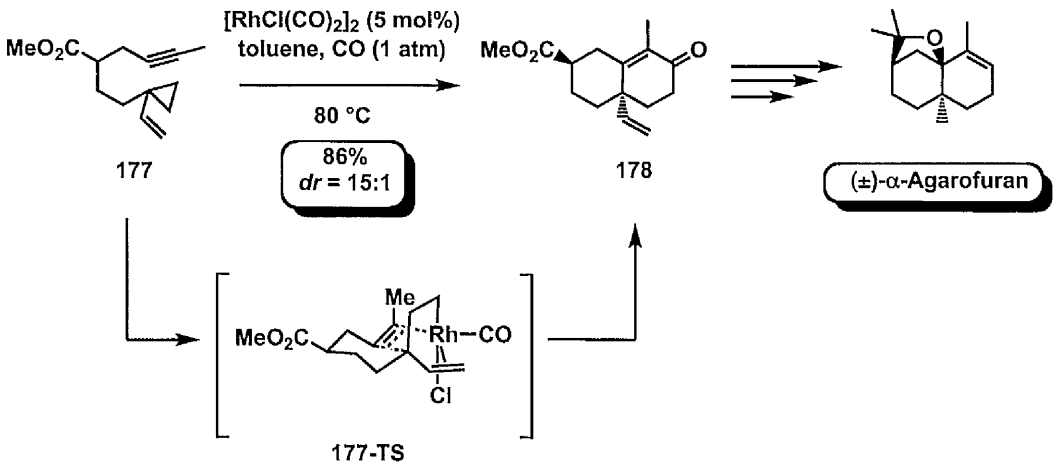

1.5.2.2.4. Tetracyclic Sesquiterpenes.

Terashima et al. reported the first total synthesis of enantiopure natural (–)-tricycloillicinone,[113] using a diastereoselective Co-catalysed PK reaction of enyne **179** (**Scheme 1.56**).[114] A remarkable feature of the carbocyclisation included the ability to exploit a generally unreactive bulky enones as a 2π component.

Scheme 1.56. Terashima's PK reaction-mediated approach to (–)-tricycloillicinone.

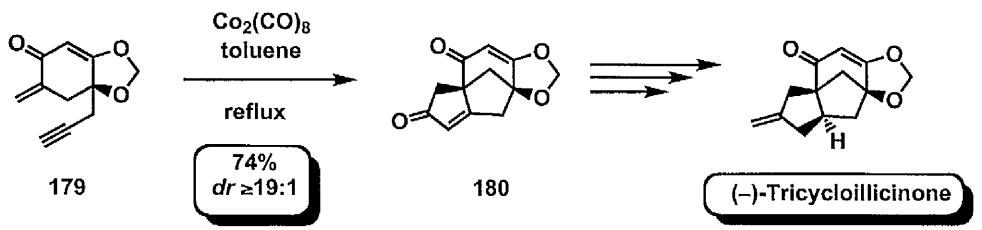

Paecilomycine A[115] has an unusual trichotechane-type architecture, which is characterised by a fused tetracyclic core and three contiguous quaternary stereogenic centres. Supplemental biological studies[115] revealed astonishing neurotrophic activity and, thus, identified this sesquiterpene as a candidate for the treatment of neurodegenerative diseases.

Scheme 1.57. Danishefsky's total synthesis of paecilomycine A.

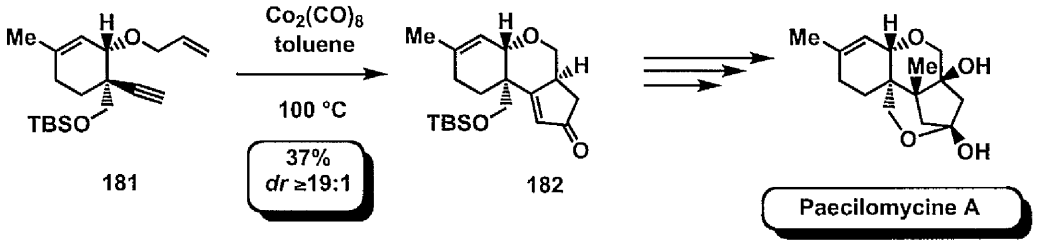

The structural complexity and intrinsic biological activity inspired the development of an efficient synthetic strategy. Elegant studies by Danishefsky led to the development of the first total synthesis of paecilomycine A (**Scheme 1.57**).[116] In this context, the utilisation of an intramolecular PK reaction afforded the desired tricyclic scaffold **182** in a stereoselective fashion.

1.5.2.3. Diterpenes.

The discovery of the beneficial effect of amine *N*-oxides as promoters[11,12] in the Co-catalysed PK reaction provided an opportunity to employ this process in the total synthesis of diterpene (+)-epoxydictymene[117] by Schreiber et *al.* (**Scheme 1.58**).[118] The initial Nicholas reaction of alkyne **183**, followed by Lewis acid-catalysed Sakurai cyclisation delivered a stereoselective construction of bicyclooctane derivative **184**, which prompted the Co-mediated PK reaction to afford the tetracyclic core. The NMO additive proved to be essential in order to enhance the stereochemical outcome of the cyclisation.[118] Hence, the sequential cobalt-mediated

process provided the direct assembly of three fused rings and two stereogenic centres in a single operation.

Scheme 1.58. Schreiber's total synthesis of (+)-epoxydictymine.

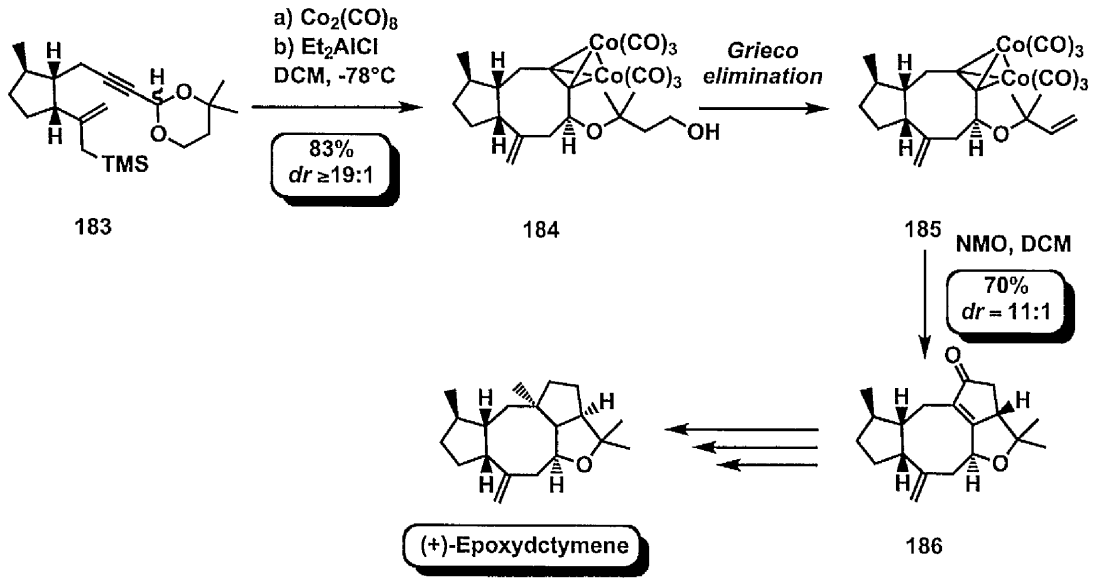

1.5.2.4 Nortriterpenes.

A recent total synthesis of the nortriterpinoid (±)-schindilactone A[119] embodies the enabling role of PK methodology for the expeditious construction of complex molecular architectures (**Scheme 1.59**).[120] The synthetic challenge associated with the cyclisation of enyne **187** is highlighted by the cycloaddition of the cyclooctene with an alkynoate moieties, which required the TMTU additive to facilitate the Co-mediated reaction to afford the bicyclopentenone **188** with *cis*-stereochemistry of the bicyclo[6.3.0]undecanone bridge. A key advantage of the strategy included the possibility to employ the ester moiety as a temporary tether, which, upon reduction, unveiled the functionalised cyclopentenone **189**, thereby serving as a "masked" stereo- and regioselective directing group.[120]

Scheme 1.59. PK reaction-mediated total synthesis of nortriterpinoid (±)-schindilactone A.

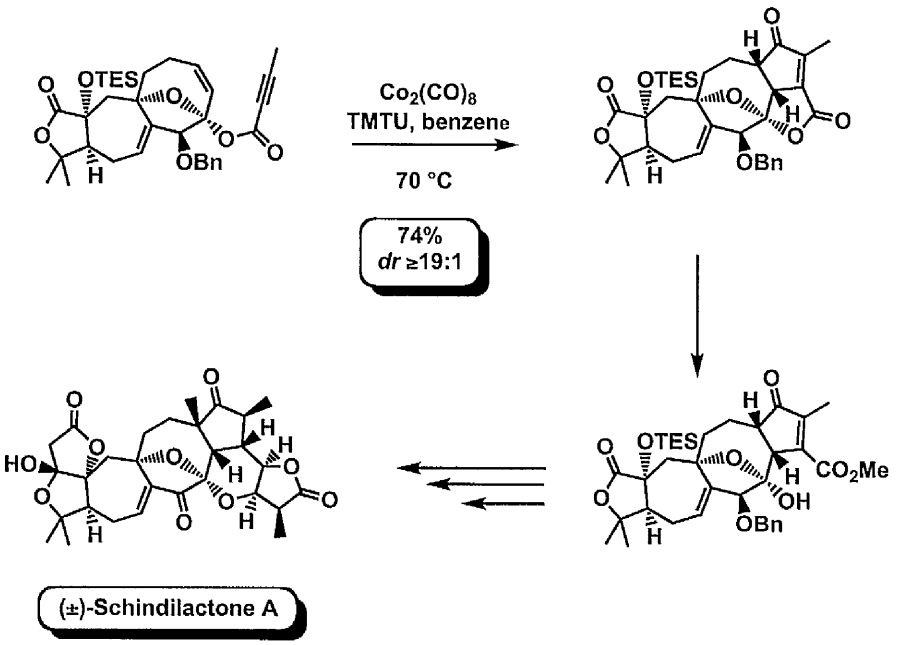

1.5.3 Alkaloids.

1.5.3.1 Monocyclic Alkaloids.

The important medicinal role of (–)-α-kainic acid[121] due to its anthelmintic and neurotrasmitting activity make it an important synthetic target.[122] The problem with supply and the excessive price has prompted renewed interest in the synthesis of this bioactive monocyclic alkaloid. Yoo and coworkers envisioned the opportunity to install all the three contiguous stereogenic centres through a diastereoselective PK reaction/hydrogenation sequence.[79] Further functionalisation of the cyclopentanone and ring opening would facilitate the introduction of the required methallyl and carboxylic side-chains. Interestingly, the cobalt-mediated PK reaction proceeds with poor diastereocontrol (**Scheme 1.60**). Moreover, alternative nitrogen protecting groups did not improve the selectivity of the process.[79] The examination of the crystal structure of hydrogenated bicyclopentenone offered an explanation for the neglegible stereochemical outcome (Eq. 1.46).[123]

Scheme 1.60. Yoo's PK reaction-mediated total synthesis of (–)-α-kainic acid.

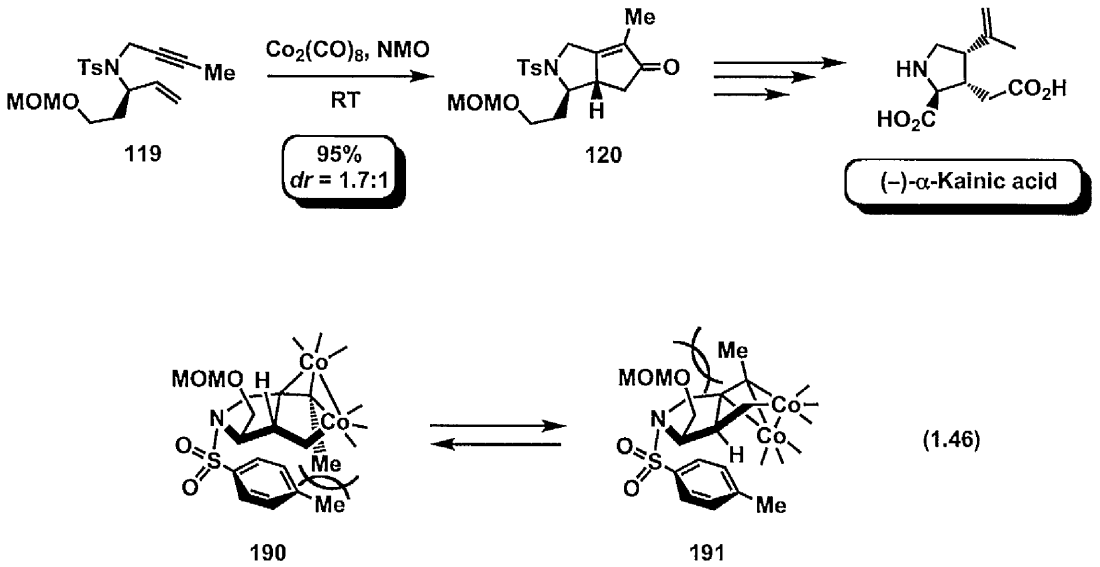

The spatial disposition of tosyl group under the bicyclic core leads to unfavourable steric interactions with methyl group on the alkyne terminus in **190**, while, in contrast, the stereocomplementary intermediate model **191** has a steric clash between the methyl group and MOM group on the C2-side chain. Hence, the comparable steric interactions in both intermediate configurations account for the poor stereochemical outcome of the process (Eq. 1.46). As previously discussed in section **1.4.2**, conformational locking by formation of a rigid oxazolidinone ring enhanced facial discrimination, thus providing excellent diastereoselectivity (**Scheme 1.61**).[123]

Scheme 1.61. Yoo's optimised PK reaction-mediated total synthesis of (–)-α-kainic acid.

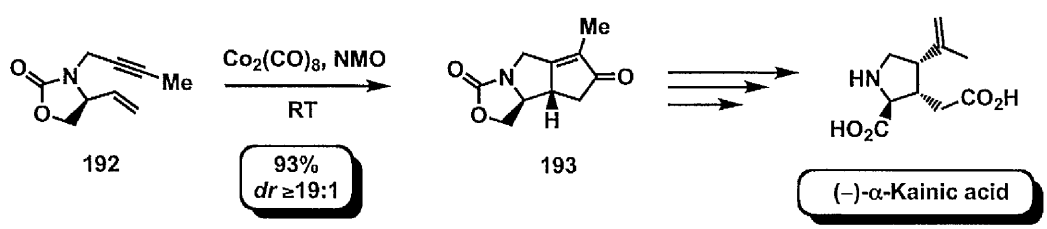

In a related process, Helmchen outlined that stereocontrol of the process could be otherwise improved by utilisation of a bulky C2 side-chain in conjunction with a Boc protecting group (**Scheme 1.62**).[124]

Scheme 1.62. Helmchen's PK reaction-mediated approach to (–)-α-kainic acid.

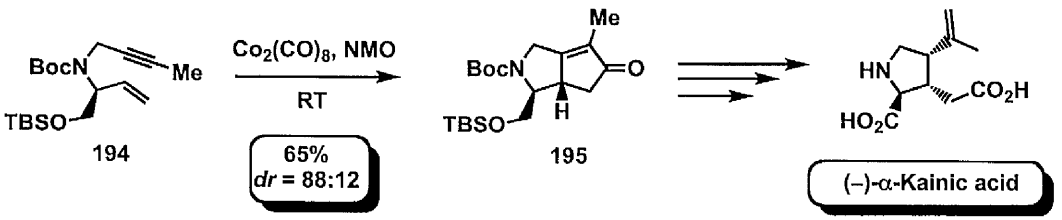

1.5.3.2. Bicyclic Alkaloids.

Despite the modest structural complexity, natural monoterpene alkaloids exhibit a wide range of biological and pharmacological activities such as analgesic, hypoglycaemic and anti-inflammatory (**Figure 1.2**).[125]

Figure 1.2. Bicyclic monoterpene alkaloids.

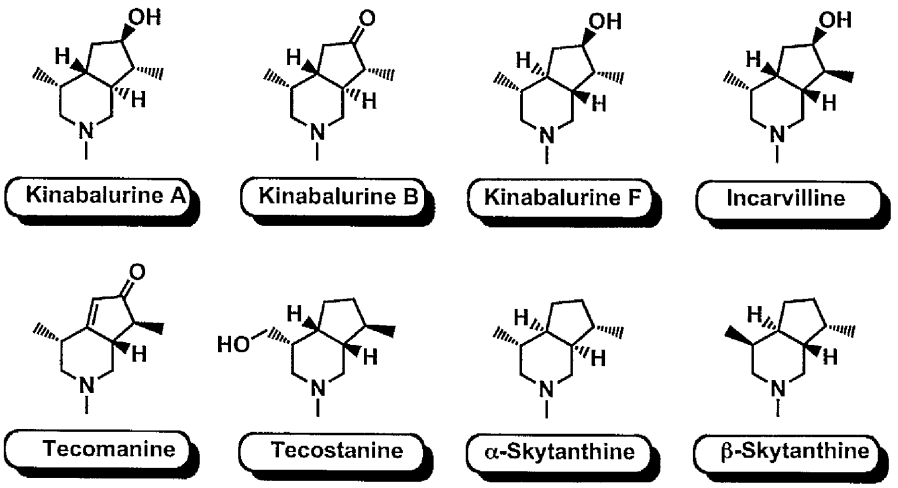

Although optimal reaction conditions required stoichiometric cobalt with sulfides as additives, high reactivity and diastereoselectivity could be accomplished in this process. From a conceptual standpoint, the PK reaction of nitrogen-tethered 1,7-enynes provided an optimal manifold for the straightforward construction of bicyclic piperidine units. Nonetheless, experimental studies towards the total synthesis of (±)-tecomanine[126] delineated several drawbacks with this strategy. As reported by Schore, the Co-mediated carbonylative cyclisation of 1,7-enynes afforded poor yields of the tecomanine precursor. Employment of alternative nitrogen protecting groups afforded comparable yields.[127] Additional studies by Honda demonstrated the possibility of applying a PK strategy for an efficient assembly of the bicyclopiperidine ring as outlined in the total synthesis of bicyclic alkaloid (–)-incarvilline (**Scheme 1.63**).[128a] The extension of the methodology to the total synthesis of the deoxygenated congener (+)-α-skytanthine served to illustrate the generality of this strategy (**Scheme 1.64**)[128b]

Scheme 1.63. PK reaction-mediated total synthesis of bicyclic alkaloid (–)-incarvilline.

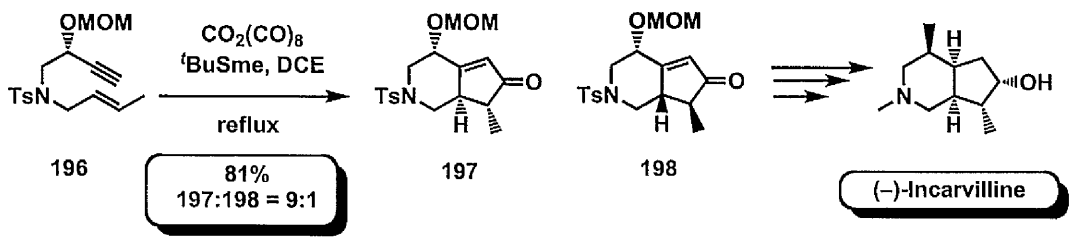

Scheme 1.64. PK reaction-mediated total synthesis of (+)-α-skytanthine.

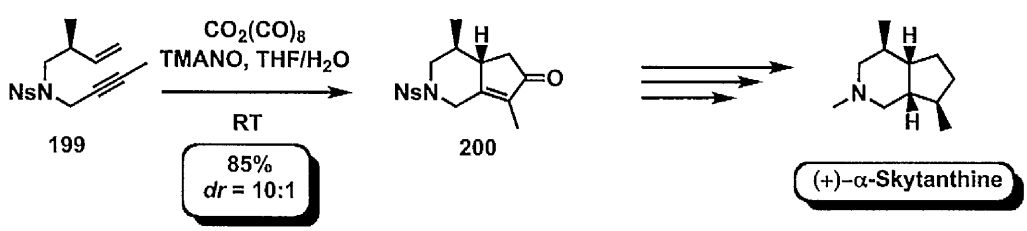

Although the utilisation of promoters provided a beneficial influence on the reaction rate, the efficacy of the strategy was lowered by poor stereoselectivity. In this context, the recent synthesis of kinabalurine derivatives[82] demonstrated the synthetic utility of the sulfone (*vide* section **1.4.2**) as a removable stereodirecting group (**Scheme 1.65**).[82]

Scheme 1.65. PK reaction-mediated total synthesis of kinabalurine derivatives.

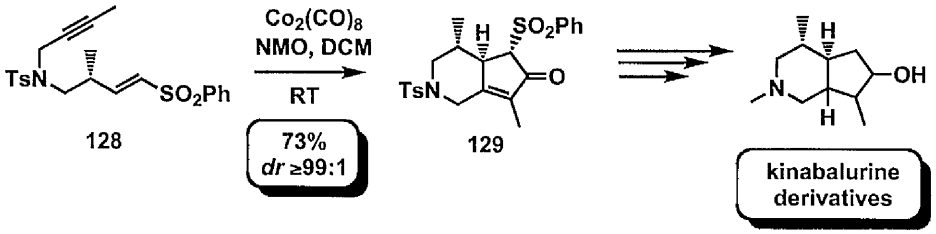

1.5.3.3. Tricyclic alkaloids.

Extensive studies by Mukai demonstrated the formidable reactivity of the allene moiety in the context of metal-catalysed [2+2+1] carbocyclisations.[53] From a theoretical perspective, Mukai envisaged that the allene moiety could be exchanged with an equally reactive heteroallene moiety and thereby enable a hetero-PK-type process. In this regard, the utilisation of the carbodiimide moiety as reactive 2π component provided the first example of cobalt-catalysed hetero-PK reaction.[129] This methodology is particularly significant in light of the abundance of pyrrolo[2,3-*b*]indole scaffolds in bioactive natural alkaloids (**Figure 1.3**).

Figure 1.3. Pyrrolo[2,3-*b*]indole scaffolds in complex natural products.

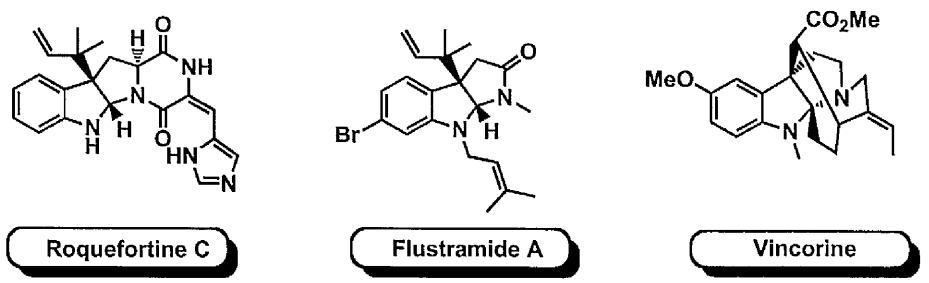

Mukai sought to exploit this enabling methodology in the total synthesis of (±)-physostigmine (**Scheme 1.66**).[130,131] The cobalt-catalysed hetero-PK reaction of the carbodiimide **201** provided the tricyclic core **202** of the parasympathomimetic alkaloid. Reductive aldol reaction generated the *cis*-configuration on the ring junction, which ultimately resulted in an eight-step total synthesis of the alkaloid.[129]

Scheme 1.66. Hetero-PK reaction-mediated total synthesis of the tricyclic core of (±)-physostigmine.

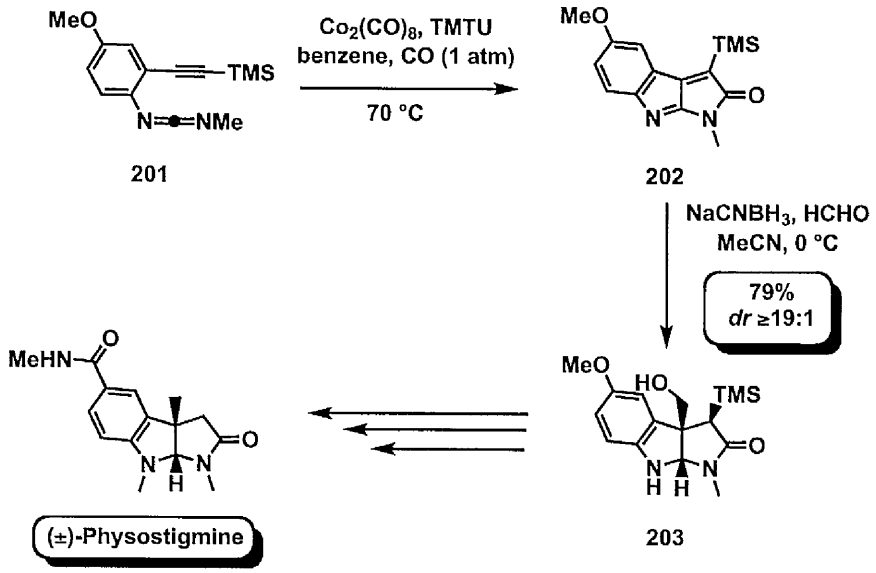

1.5.3.4. Polycyclic alkaloids.

Ogawasara reported the first application of a PKR-based approach for the assembly of polycyclic alkaloid scaffolds. Co-mediated carbonylative cyclisation of an enyne afforded a tricyclic intermediate, which was converted in a straightforward manner in the (–)-dendrobine core.[132] Remarkably, this approach allowed the diastereoselective formation of three contiguous stereogenic centres with the appropriate *cis* relationship. A decade later, the Zard group successfully exploited the original strategy for the total synthesis of (–)-dendrobine

(**Scheme 1.67**).[133a] Notably, coordinating solvent acetonitrile, was necessary in order to achieve high reactivity in the cycloaddition process.

Scheme 1.67. PK reaction-mediated total synthesis of (–)-dendrobine.

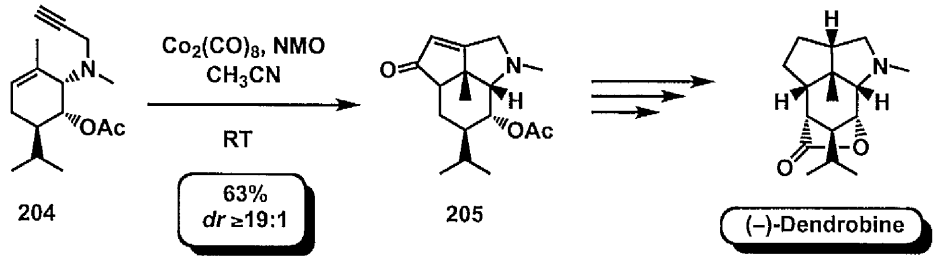

The Zard group also applied the Co-mediated carbocyclisations for the construction of bicyclo[4.3.0]nonane scaffold **207** , which was then converted to the tetracyclic alkaloid (±)-13-deoxyserratine (**Scheme 1.68**)[133b] by radical cyclisation and silyl group removal.

Scheme 1.68. PK reaction-mediated total synthesis of (±)-13-deoxyserratine.

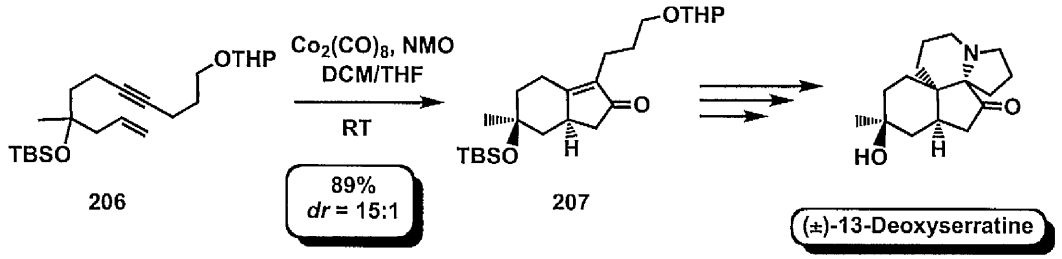

The enabling role of this methodology was further highlighted by several synthetic approaches towards related *Lycopodium* alkaloids. For example, the magellanines skeleton[134] provided an ideal system to demonstrate the versatility of the PK cyclisation towards for different bicyclic and tricyclic sections of the alkaloid core. The first total synthesis of (±)-magellanine by Ishizaki applied the Co-mediated process to the diastereoselective assembly of rings B and C,[135] wherein 1,3-pseudoaxial interaction between a hydroxyl group and the alkyne side chain accounted for the lower reactivity of **208** (**Scheme 1.69**). Nonetheless,

epimerisation at C3 by a Mitsunobu/hydrolysis sequence provided the required intermediate **213**.

Scheme 1.69. PK reaction-mediated formation of ring B and C of magellanine.

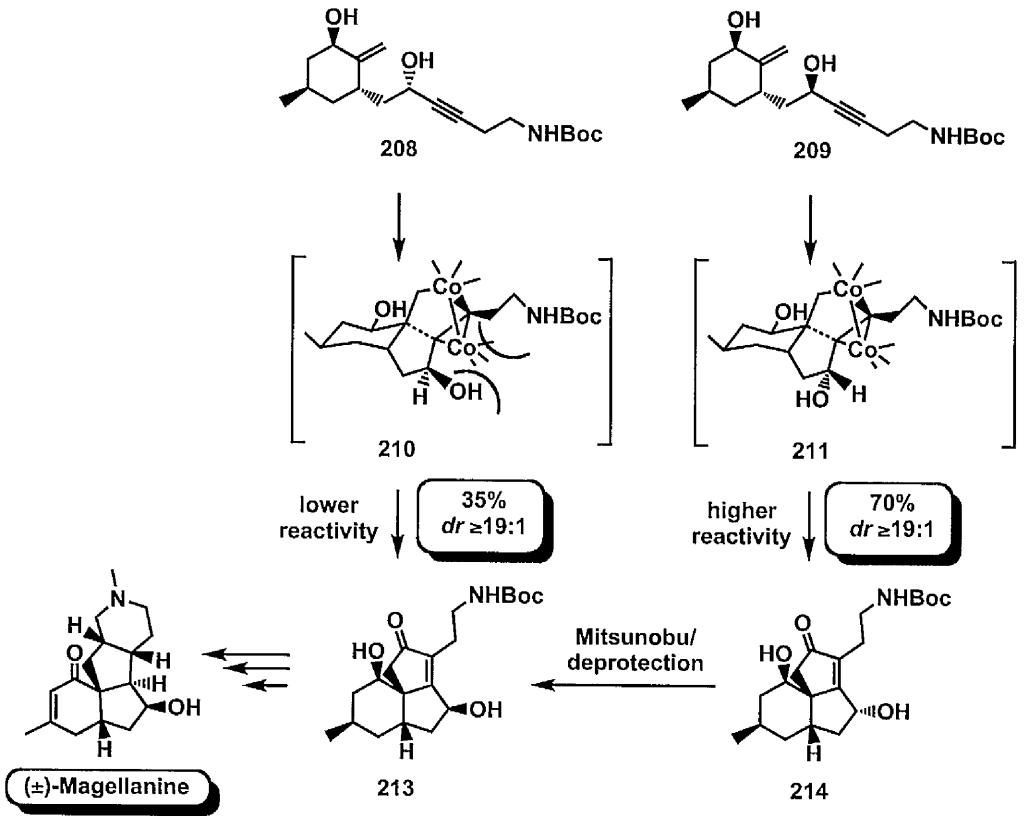

Comprehensive studies by Mukai provided an elegant approach to alkaloids (–)-magellanine, (+)-magellaninone and (+)-paniculatine (**Scheme 1.70**).[136] The synthetic strategy involved a Co-mediated PK reaction to construct the AB ring portion of the tetracyclic core and an additional Co-mediated cyclocarbonylation of a subsequent intermediate to efficiently assemble the remaining CD rings. This approach highlighted the key role of bulky enyne substituents to generate steric interactions and maximise the facial discrimination in the cobaltacycle formation step, thus conferring a high degree of stereoinduction in the carbocyclisation.[136]

Scheme 1.70. PK reaction-mediated total synthesis of magellanine-type natural alkaloids.

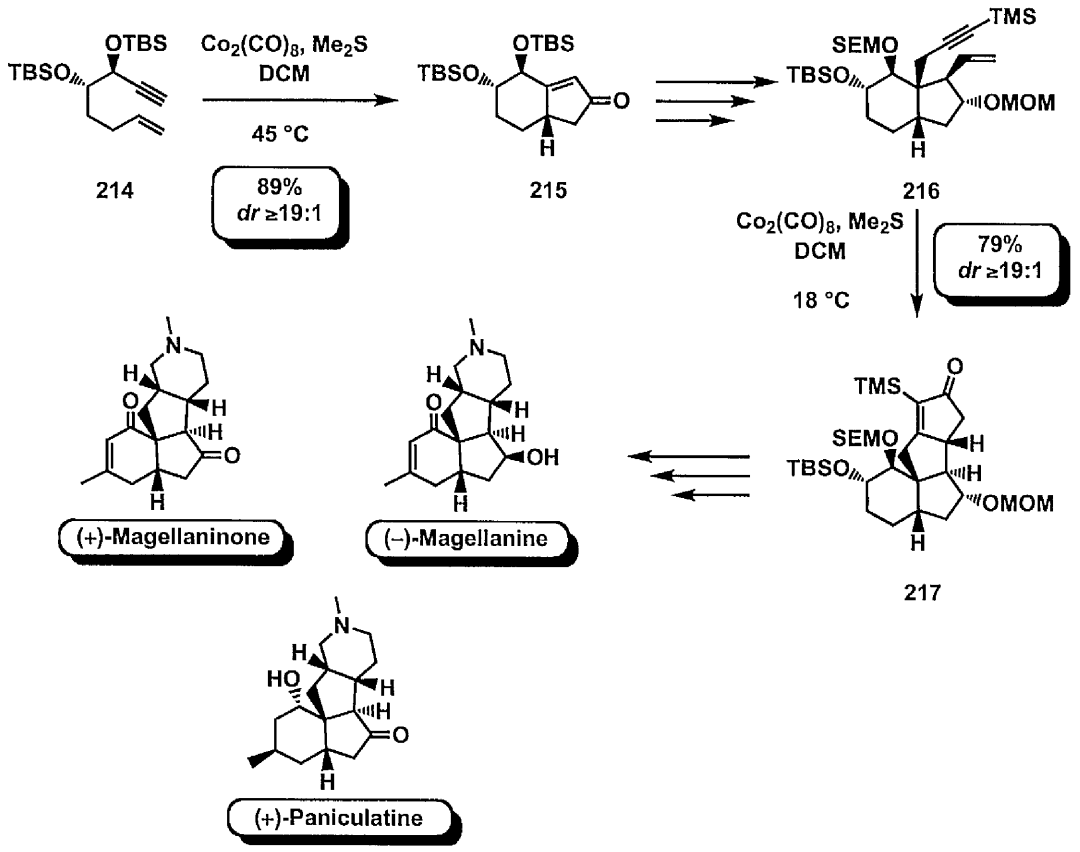

Prominent bioactivity[137] and unique complex structural features, such as adjacent quaternary stereocentres and spirominal moieties prompted wide interest towards the total synthesis of lycopodine alkaloids.[138] In this context, Takayama reported the first asymmetric total synthesis of related alkaloids lycoposerramine A and phlegmariurine A (**Scheme 1.71**).[139]

Scheme 1.71. Employment of PKR in the total synthesis of lycopodium alkaloids.

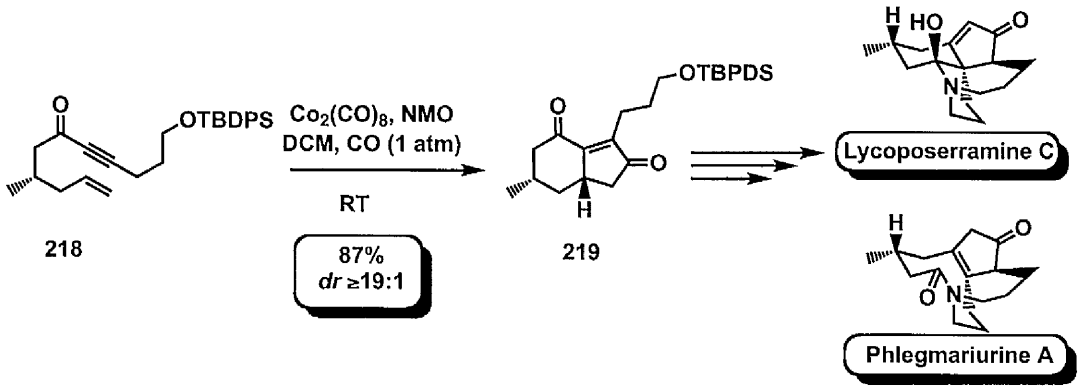

A diastereoselective Co-mediated PK reaction delivered a highly functionalised bicyclo[4.3.0]nonane framework in excellent yield,[140] thereby enabling the strategy to be profitably reiterated in the asymmetric total synthesis of the related alkaloid, huperzine Q (**Scheme 1.72**).[141]

Scheme 1.72. Effect of the conformational restriction in the enyne substrates in the stereochemical outcome of the PKR.

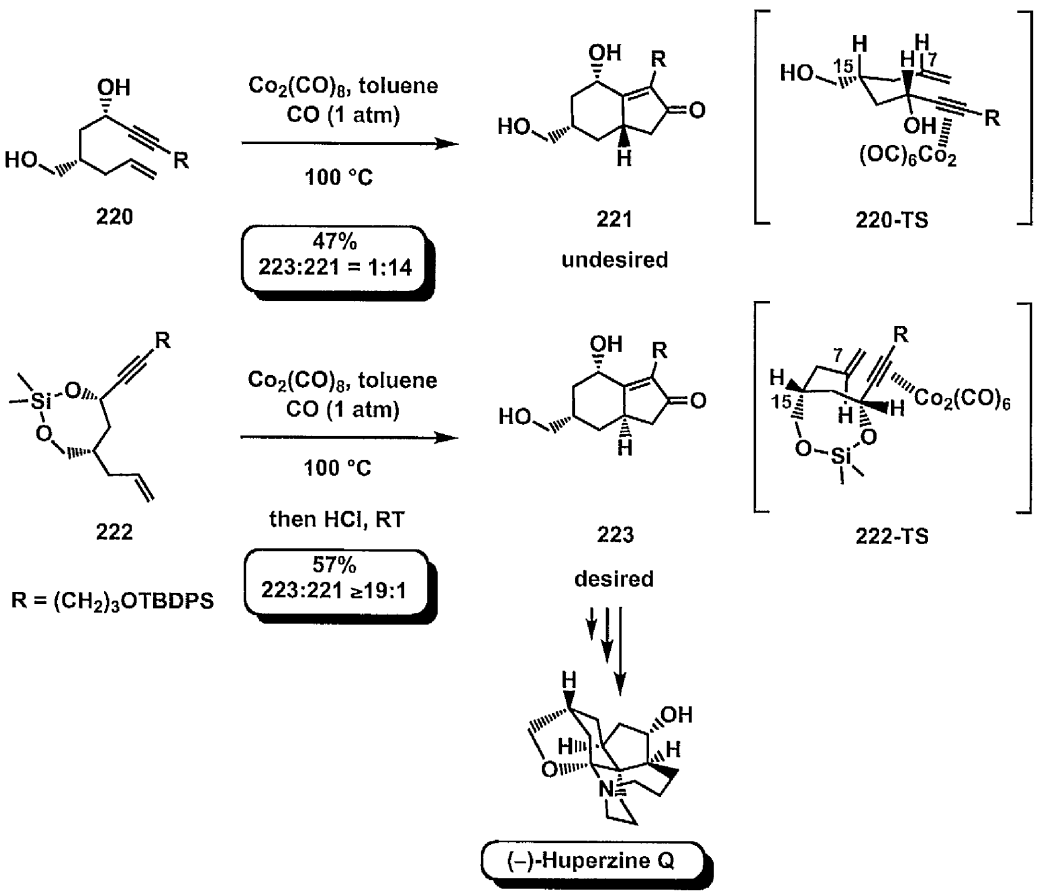

Nevertheless, the ability to achieve optimal stereocontrol in the carbocyclisation process provided an intriguing synthetic challenge. Preliminary experimental investigation on enyne **220** demonstrated the preferential formation of the undesired adduct **221** (**Scheme 1.72**). Mechanistic considerations postulated a chair-like conformation in the intermediate **220-TS** and that the side-chain at C15 controlled the stereochemistry in the alkene insertion step, thus providing **221** as the major diastereoisomer. Based on the previous works by Mukai using

tartrate-derived 1,7-enynes[78] (*vide* section **1.4.2**), Takayama postulated that conversion of the diol moiety into a silicon-tethered cyclic silaketal could alter the conformation of the related cobaltacycle **222-TS**, and thereby reverse the stereochemistry in the alkene insertion step. This aforementioned structural modification effectively reversed the stereochemical outcome of the reaction and, after silyl deprotection, allowed the exclusive formation of the desired adduct **223** (**Scheme 1.72**).[141]

Scheme 1.73. PKR-mediated construction of (–)-alstonerine core.

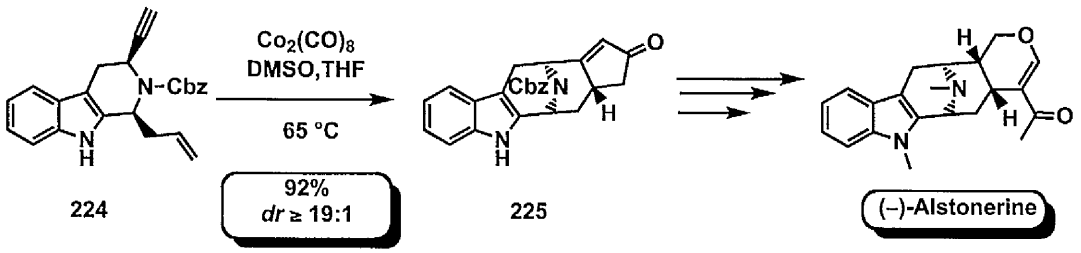

The synthetic potential of the PK carbocyclisation also has additional applicability within the unprecedented formation of azabridged bicyclic motifs. A synthetic approach to the macrolide alkaloid (–)-alstonerine[142] by Martin described an efficient assembly of the tetracyclic core using a challenging Co-mediated carbocyclisation of tryptophane-derived 1,7-enynes.[143] Derivatisation of the pentenone ring then permitted the completion of the total synthesis (**Scheme 1.73**). Despite the wide substrate scope and the ability of the PK reaction to generate a wide variety of polycyclic motifs, the utilization of activated alkenes and alkynes as 2π components has remained unexplored. The PKR-mediated total synthesis of (±)-meloscine[144] provided a formidable synthetic challenge, which addressed this issue by exploiting ynamine, enamine and propiolamide moieties. A recent total synthesis of (±)-meloscine by Mukai successfully accomplished this goal with a remarkable Co-mediated cyclocarbonylation reaction of propiolamide and enamine 2π components, thereby allowing the expeditious formation of the fused tetracyclic core in a single operation step (**Scheme 1.74**).[145]

Scheme 1.74. Mukai's PK reaction-mediated approach to (±)-meloscine.

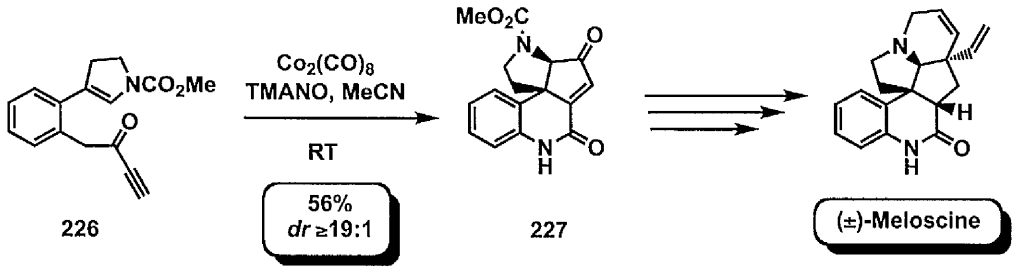

1.5.4. Prostanoids.

1.5.4.1. Prostaglandins.

The examination of prostaglandin lipids[146] highlights an opportunity to assemble the cyclopentanone motif with an intermolecular PK cycloaddition (**Figure 1.4**).

Figure 1.4. Natural prostaglandines.

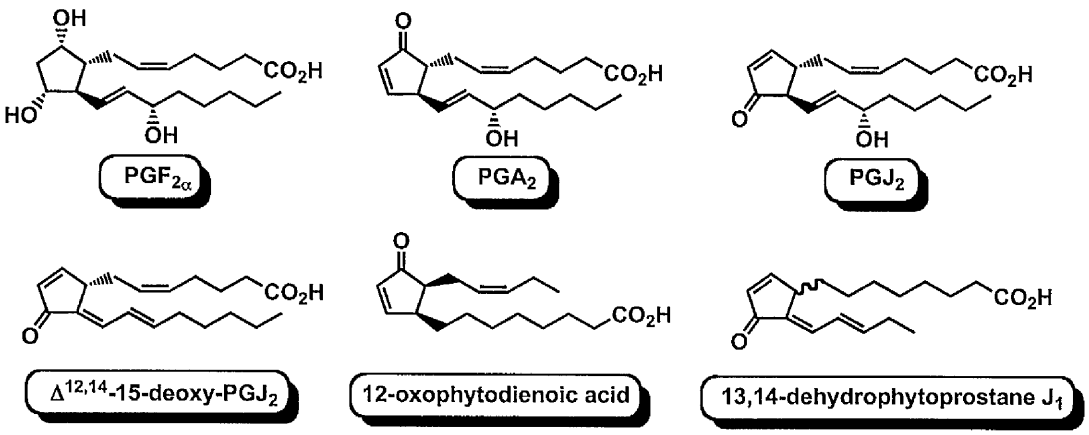

The feasibility of this approach relies on the intrinsic control of the regioselectivity and challenging exploitation of the reactivity of unstrained alkenes. In view of these issues, the development of the directed PK reaction by the Krafft group provided a major breakthrough

and therefore enhanced the synthetic potential of the intermolecular manifold (**Scheme 1.75**).[14]

Scheme 1.75. Directed intermolecular PK reaction.

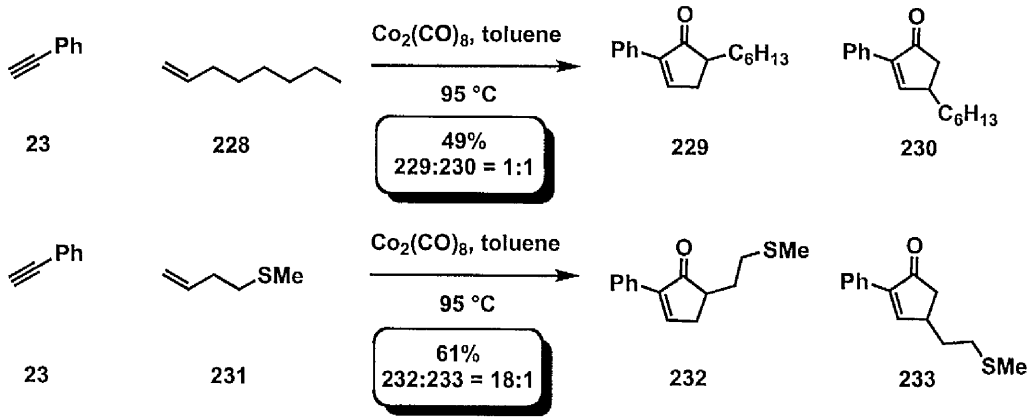

As outlined in **Scheme 1.75**, heteroatom substituted alkenes coordinate the cobalt metal centre and thereby provide a dual role for enhancing the metal reagent 's reactivity and direct the regiochemical outcome of the process.

Scheme 1.76. Utilisation of the directed PK reaction in the total synthesis of PGA_2.

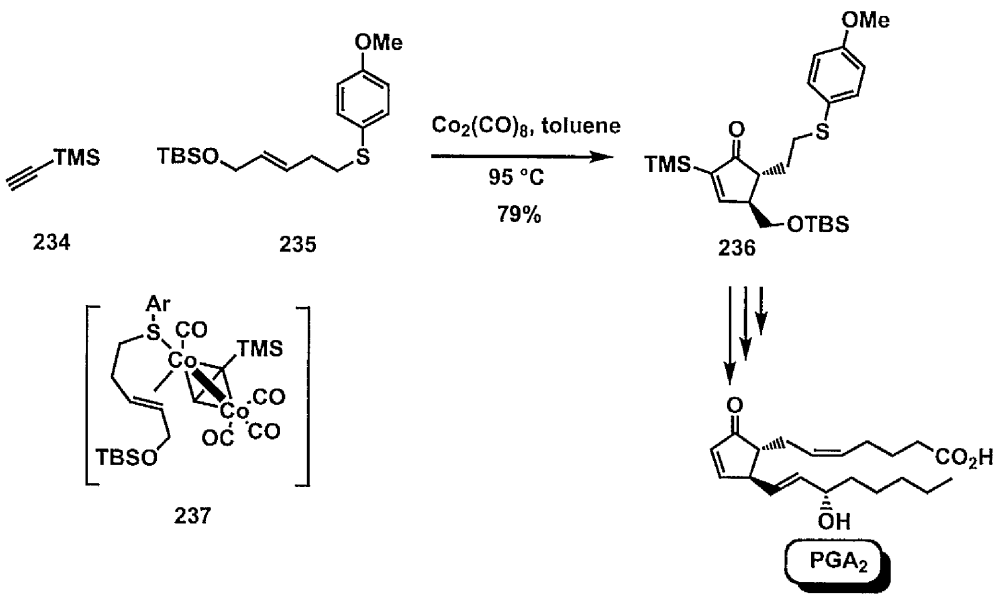

This enabling methodology was successfully exploited in the formal total synthesis of prostaglandine PGA_2 and outlined the ability of homoallylic sulfides to enhance regio- and diastereoselective formation of cyclopentenone derivatives (**Scheme 1.76**).[147]

Greene and Pericas capitalised on the ability of chiral acetylenic ethers[91] to exert high levels of stereocontrol, thereby providing a key step in an elegant asymmetric total synthesis of natural Brefeldin A.[148]

Scheme 1.77. Asymmetric total synthesis of brefeldin A.

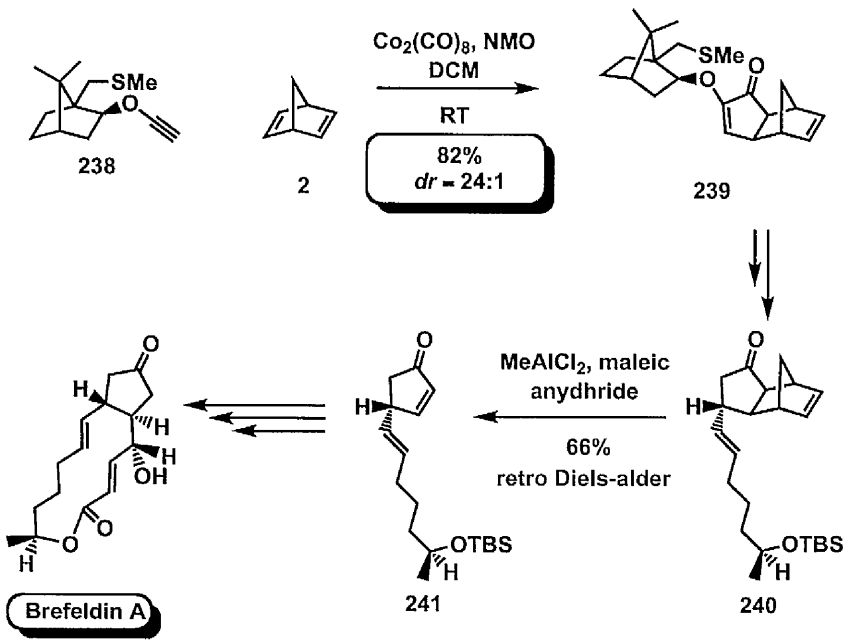

The employment of the bulky mercaptoisoborneol auxiliary proved essential to promote a highly diastereoselective transformation (**Scheme 1.77**). The subsequent retro-Diels-Alder cleavage of norbornene ring[149] then allowed further derivatisation of the cyclopentanone scaffold and completion of the synthesis. The use of norbornadiene as removable strained alkene was further exploited by the Riera group in the PK-mediated total synthesis of anti-HIV carbonucleosides, (–)-carbovir and (–)-abacavir (**Scheme 1.78**).[150] For example, chiral PNSO ligands facilitated the formation of the PK adduct **242** with high enantioselectivity.

Scheme 1.78. Enantioselective total synthesis of (–)-carbovir and (–)-abacavir.

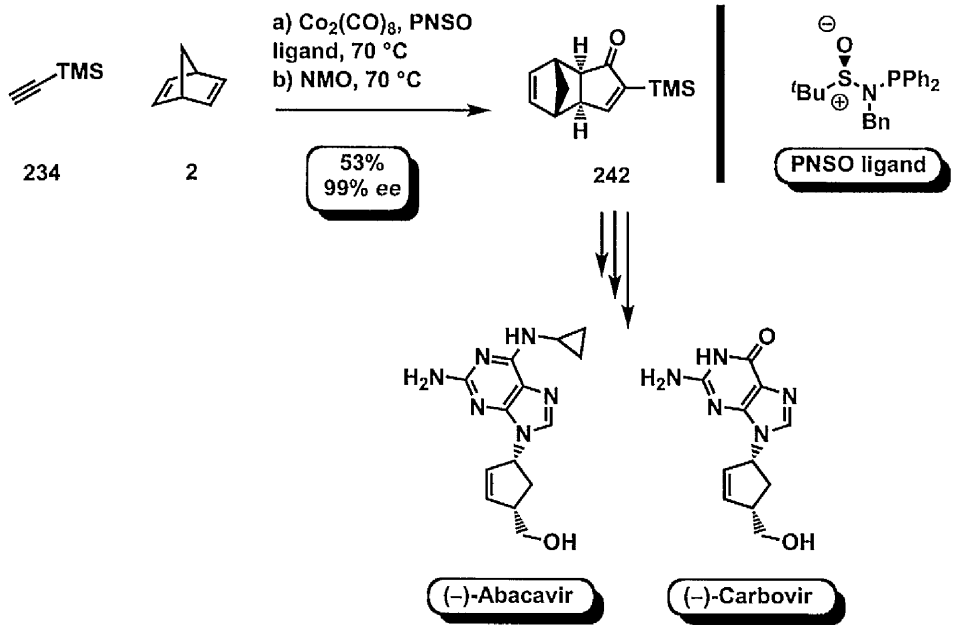

In contrast to the above approaches, a structural examination of 15-Deoxy-D^{12,14}-prostaglandin J_2 (**Figure 1.4**) indicated the difficulty in applying an intermolecular cyclocarbonylation between alkene and alkyne units, in light of the exocyclic olefin moiety on the cyclopentenone ring. From a conceptual standpoint, the substitution of the alkene for an allene would furnish the required exocyclic olefin functionality (**Scheme 1.79**).

Scheme 1.79. Intermolecular PKR of allenes and alkynes.

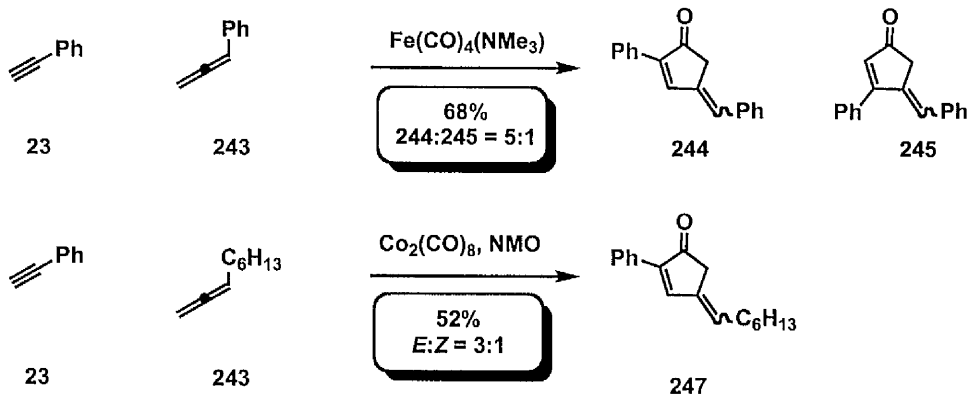

Nonetheless, the intermolecular cyclocarbonylation of alkynes and allenes is very synthetic challenging. Early reports by Narasaka[151] and Cazes[152] revealed on overall lack of regioselectivity in the process and the inability to control *E/Z* selectivity of the resulting exocyclic alkene (**Scheme 1.79**). The inherent reactivity of allenynes in the intramolecular manifold[30] inspired Brummond to connect the reactive 2π components by the means of a temporary silicon tether.[153] This strategy favourably overcame regioselectivity issues and, additionally, the increased coordinative aptitude of the 2π components to the metal centre enhanced the overall reactivity of the process (**Scheme 1.80**).

Scheme 1.80. Employment of temporary tethers in the Mo-catalysed PKR.

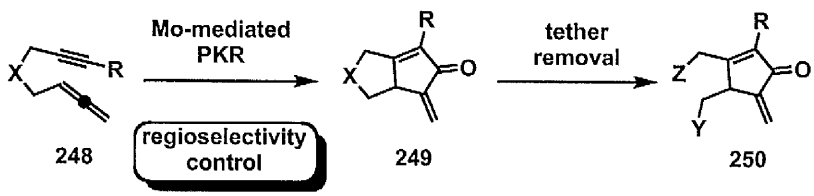

The examination (*vide* section **1.2.4.1.1**)) of the intramolecular PK reaction with allenynes highlighted the unique ability of molybdenum catalysts to promote an exclusive formation of bicyclopentenones derivatives bearing an exocyclic alkene.[30] Hence, Brummond postulated that a Mo-catalysed PKR of temporary-tethered allenynes could promote an optimal cycloaddition process and further provide the desired α-methylene cyclopentenone, upon removal of the tether. The testing of the aforementioned hypothesis resulted in the first total synthesis of 15-Deoxy-$\Delta^{12,14}$-prostaglandin J_2 (**Scheme 1.81**).[154] Mo-mediated cyclocarbonylation of silicon-tethered allenyne provided the desired bicyclic adduct in moderate yield and with low *E/Z* selectivity, albeit the yield of desired *E*-adduct could be improved *via* a Lewis acid-catalysed isomerisation. The removal of the silicon tether and side chain derivatisation completed the synthesis of the natural prostaglandin.

Scheme 1.81. Utilisation of Si-tethered enynes PKR for the total synthesis of 15-Deoxy-$D^{12,14}$-prostaglandin J_2.

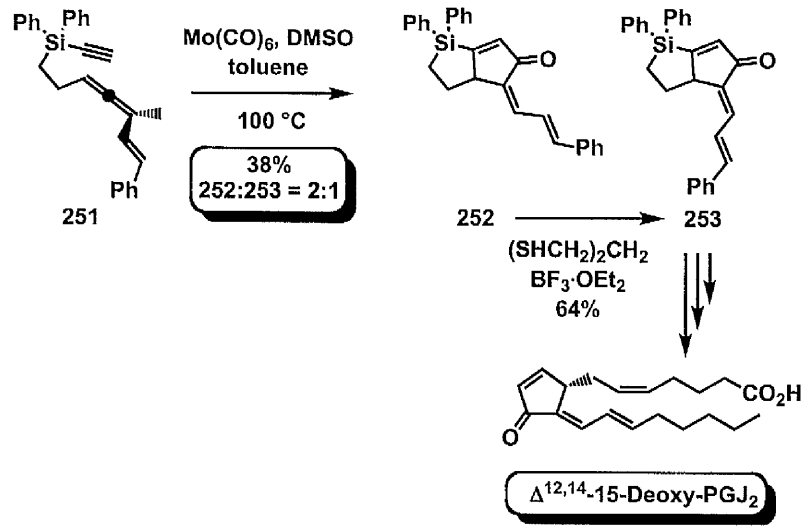

1.5.4.2. Prostacyclins.

The key role of the intramolecular PK process for the construction of sesquiterpene-type natural products revealed the possibility to extend the valuable methodology towards the total synthesis of carbacyclins and isocarbacyclins (**Figure 1.5**).[155]

Figure 1.5. Natural prostacyclins.

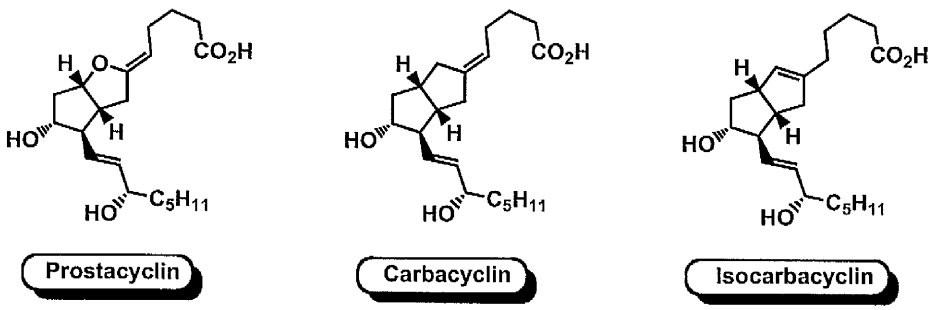

Moreover, this synthetic approach could install the required 1,2-*cis* diastereoselectivity in the corresponding bicyclic adducts, as previously observed in the total synthesis of coriolin. Seminal studies by Magnus explored the feasibility of the strategy towards the construction of carbacyclin analogues (**Scheme 1.82**).[156] Preliminary mechanistic studies hypothesised that

incorporation of the secondary hydroxyl group and C2 substituent into a rigid lactone structure could enhance steric interactions between the ring and acetylenic TMS, thus enhancing 1,2-*cis* diastereoselectivity of the cyclisation adduct. Unfortunately, PK reaction of enyne **254** showed and overall lack of reactivity due to the strained nature of the lactone and the inability for the alkene to insert. In contrast, the unstrained acetonide ring provided optimal reactivity for **255** and the desired 1,2-*cis* diastereoselectivity in the bicyclic adduct **256** (**Scheme 1.82**).

Scheme 1.82. Magnus's synthesis of carbacyclin derivatives.

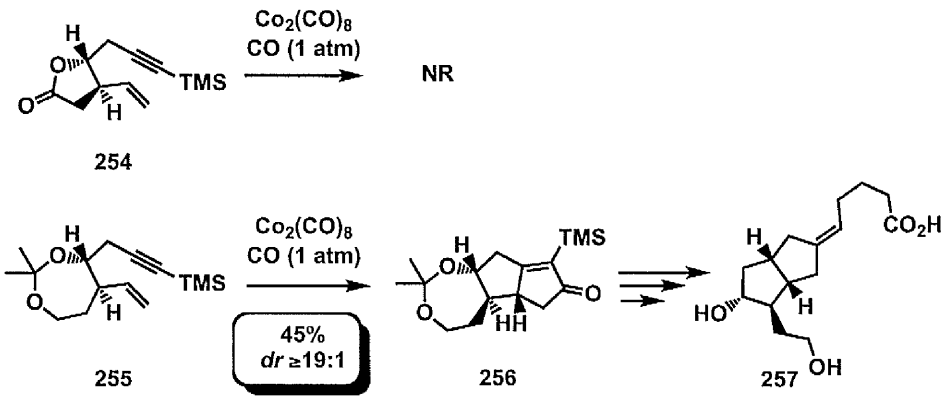

Medicinal studies on stable prostacyclin surrogates revealed prominent antithrombotic activity of isocarbacyclin and relative synthetic analogues.[157] Hence, in view of their widespread therapeutic utility, Saito and coworkers examined the viability of a synthetically valuable PK-mediated approach (**Scheme 1.83**).[158]

Scheme 1.83. PK reaction-mediated construction of isocarbacyclin.

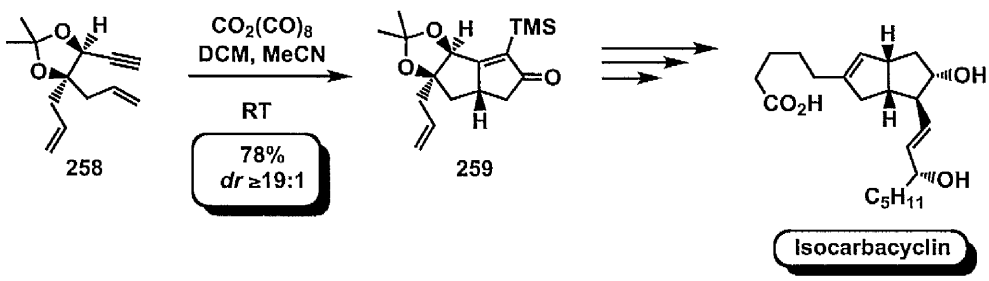

Treatment of L-ascorbic acid-derived enyne **258** under Co-mediated carbonylative conditions furnished the desired bicyclic core **259** as a single stereoisomer (**Scheme 1.83**). Further introduction of aliphatic side chains enabled the total synthesis of isocarbacyclin and provided a potential route for related bioactive analogues. For example, prostacyclins are used for the treatment of pulmonary hypertension. The aqueous sodium salt solution (Flolan®) provided the most effective therapy for the disease. Nonetheless, the moderate biological half-life and degradation upon transit through lungs[159a] prompted an examination of potential bioactive surrogates. In this context, treprostinil displayed improved *in vitro* and *in vivo* stability and subsequently marketed under the trade name Tremodulin® and Tivaso®.[159b-159c] The increasing demand for an efficient and scalable synthetic approach, prompted the Moriarty group to employ the PK methodology in an expeditious synthesis of the tricyclic core, which was converted to treprostinil in a concise manner (**Scheme 1.84**).[160]

Scheme 1.84. PK reaction-mediated construction of the tetracyclic core of treprostinil.

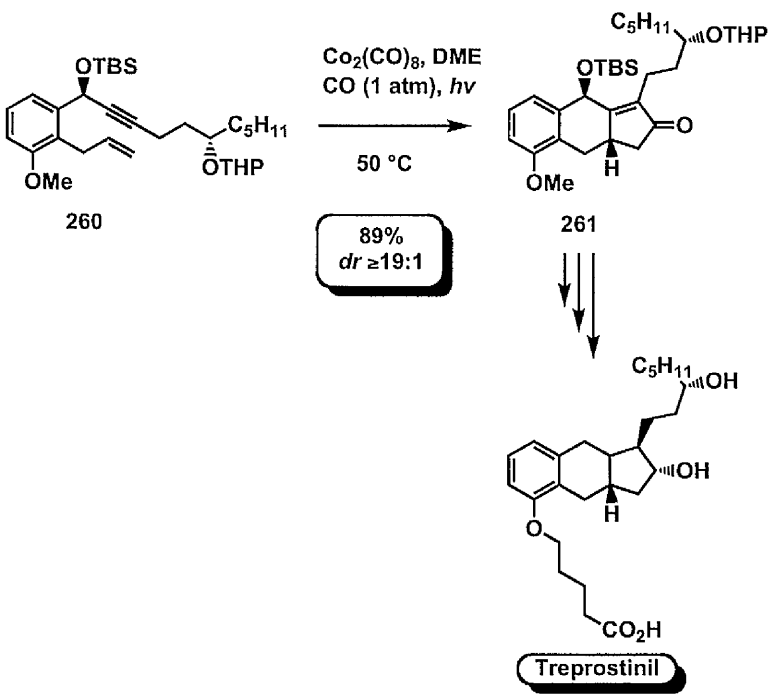

Co-mediated cyclocarbonylation of enyne **260** delivered the tricyclic core in high yield and with excellent diastereocontrol. Enone reduction and side chains derivatisation delivered a

concise 15-step synthesis of the prostacyclin analogue from inexpensive 3-methoxybenzyl alcohol.[160]

1.6. Investigation of the Rhodium-catalysed Diastereoselective PK Reaction.

1.6.1. Introduction.

The development of the Rh-catalysed PK reaction by Narasaka[49] provided initial insight into the diastereoselectivity for this process. In this context, the reaction is stereospecific for the formation of the *cis*- and *trans*- bicyclopentenone derivatives **263** and **264**, depending on which geometrical isomer is employed (Eq. 1.47).

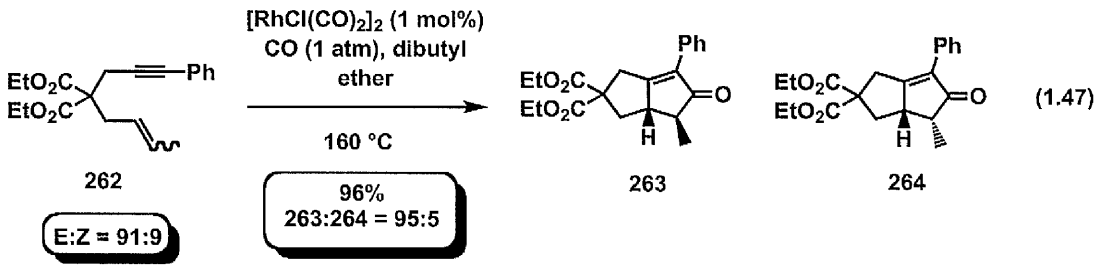

(1.47)

Low concentration of carbon monoxide and high substrate molarity was necessary for optimal reactivity in the process and thereby avoid the competitive ene-type cycloisomerisation reaction.

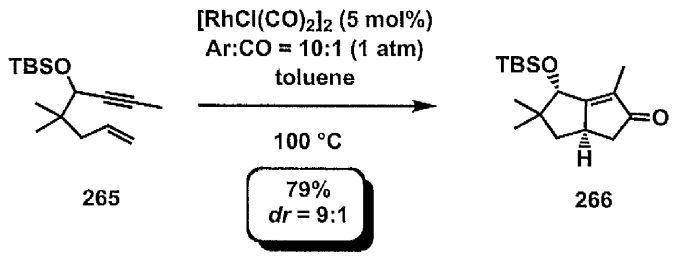

In light of Magnus' observations on the diastereoselective Co-catalysed PK reaction in the total synthesis of coriolin (*vide* section **1.5.2.2.2**), analogous studies on the Rh-catalysed manifold demonstrated that the reaction proceeds with high 1,3-*cis*-stereoselectivity, despite

the moderate 1,3-*pseudo*-axial interactions between C3-substituent and methyl group on the alkyne terminus (Eq. 1.48).[6] In contrast, the examination of 1,2-diastereoselectivity in this process was surprisingly unexplored. In this context, an unprecedented sequential Rh-catalysed allylic alkylation/PK reaction[161] process, developed by Evans and Robinson, estabilished the opportunity to conduct a highly diastereoselective Rh-catalysed PK reaction using C2-substituted 1,6-enynes. Moreover, this study provided the basis for additional mechanistic investigations to rationalise the stereochemical outcome of these reactions.[162] The enabling role of the metal-catalysed allylic alkylation[163] process to promote the formation 1,6-enynes coupled with the exquisite reactivity of these substrates in the PK carbocyclisation reactions provided the ability to merge these two strategies in a metal-catalysed domino-type process. Hence, this could either be accomplished using two metal catalysts or a single catalyst that is capable of catalysing both reactions.

Scheme 1.85. Jeong's sequential allylic alkylation/PK annulation strategy.

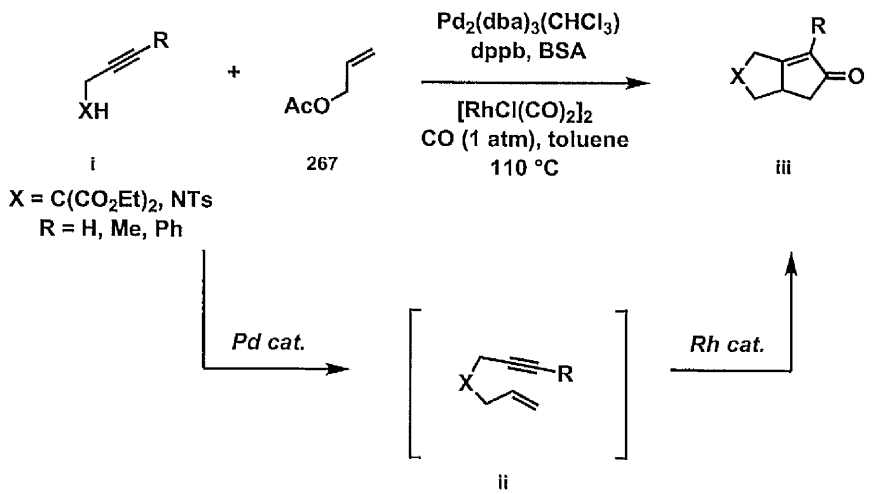

In this context, Jeong disclosed the first sequential allylic alkylations/PK carbocyclisation (**Scheme 1.85**).[164] Detailed optimisation studies revealed that a combination $Pd_2(dba)_3(CHCl_3)$ and $[RhCl(CO)(dppp)]_2$ promotes the domino process without any modification of the solvent system and temperature. Nonetheless, the synthetic value of this strategy was reduced by the inability to conduct the transformation in presence of a single

metal catalyst. Additionally, oxygen nucleophiles as propargyl alcohols displayed no reactivity in the process and regioselectivity issues in the Pd-catalysed alkylation step required the simple unsubstituted allyl acetate (**Scheme 1.85**). In contrast, Evans and Robinson reported a sequential Rh-catalysed allylic alkylation/PK reaction, which utilises a single precatalyst and deals with regio- and diastereocontrol (**Scheme 1.86**).[161]

Scheme 1.86. Evans' tandem allylic alkylation/PK annulation strategy.

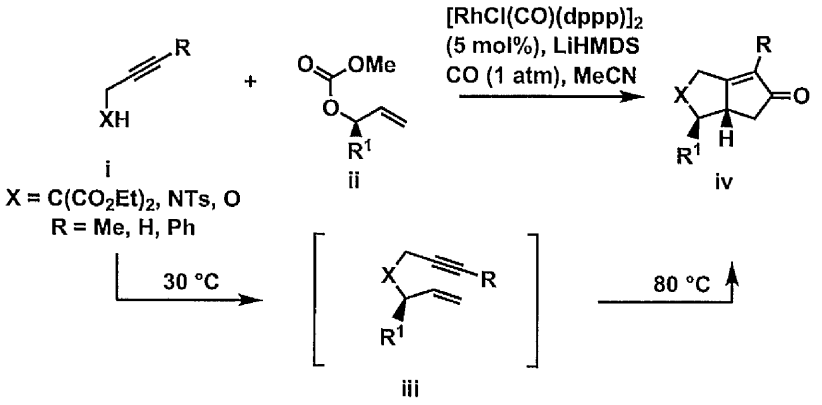

The observed *cis*-diastereoselectivity in the PK process was initially rationalised through reversible metal binding which results in the preferential formation of **iv**, due to the steric interactions between C2-substituent and bulky rhodium catalyst (**Scheme 1.87**).[161] Evans and coworkers group developed a highly regioselective Rh-catalysed alkylation reaction[166] and the ability of rhodium catalysts to promote regioselective formation of C2-substituted enynes outlined the opportunity to conduct a novel diastereoselective tandem reaction. Hence, optimisation studies showed that the utilisation of $[RhCl(CO)(dppp)]_2$ in acetonitrile efficiently promoted both the allylic alkylation and PK reaction with high levels of regio- and diastereoselectivity, thus leaving temperature as the sole parameter to be modulated for the optimal reactivity of the domino process (**Scheme 1.86**).[161] Remarkable features of the strategy included the ability to employ propargyl alcohols as nucleophiles and a wide range of substituents on the alkyne terminus.

Scheme 1.87. Proposed origin of diastereoselectivity in the Rh-catalysed PK reaction.

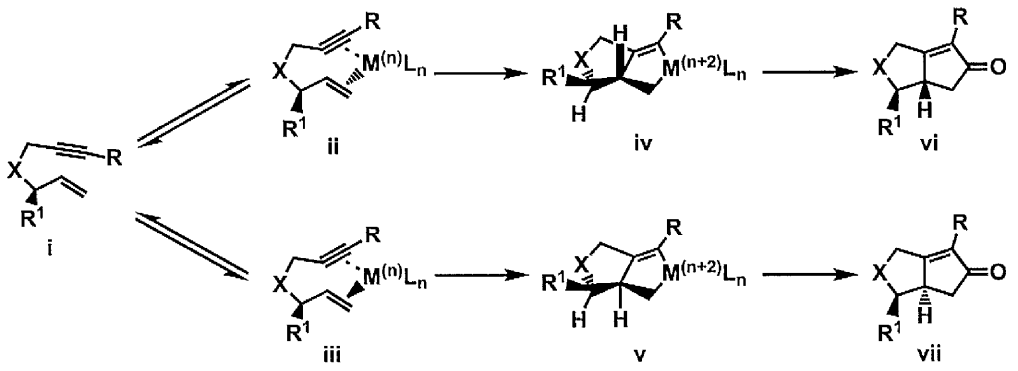

Moreover, the level of diastereoselectivity in this process was dramatically influenced by the nature of the enyne tether (**Table 1.1**).[161]

Table 1.1. Influence of the tether nature on the diastereoselectivity of the Rh-catalysed tandem allylic alkylation/PK reaction.

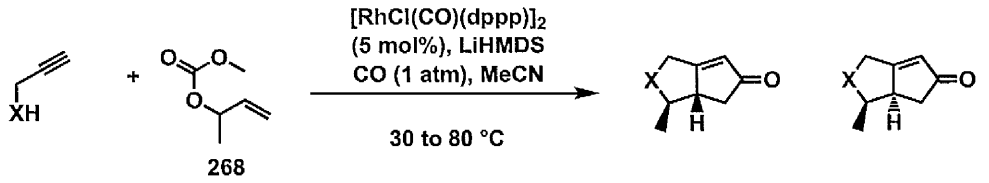

entry	X	Alkyne	Yield (%)	cis	trans	*dr* (*cis*:*trans*)
1	O	269	63	272	273	≥19:1
2	NTs	270	79	274	275	3:1
3	$C(CO_2Me)_2$	271	82	276	277	5:1

Supplementary studies revealed that the employment of high CO pressure in the tandem reaction could reverse the stereochemical outcome of the process, thus favouring the preferential formation of *trans*-bicyclopentenone adducts (**Scheme 1.88**).[165]

Scheme 1.88. Effect of the CO pressure on the diastereoselectivity of the Rh-catalysed tandem allylic alkylation/PK reaction.

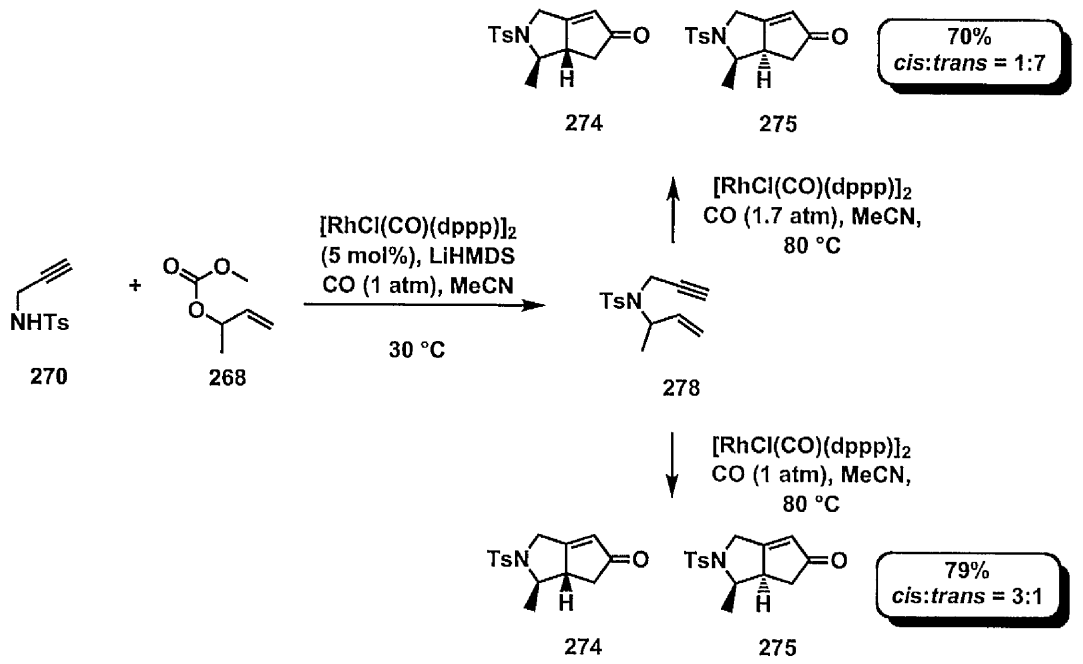

In light of the prominent influence of the tether and carbon monoxide pressure, steric arguments could not account for the stereochemical outcome of the reaction. Additional mechanistic investigations were therefore required in order to gain an optimal understanding into the origin of selectivity. This prompted the Evans and Baik groups to employ a synergic combination of computational and experimental studies in order to garner further insights into the diastereochemical outcome of the Rh-catalysed PK reaction.[162]

1.6.2. Effect of the CO Concentration on the Diastereoselective Rh-catalysed PK Reaction.

Initial computational studies focused on the analysis of the Rh-catalysed PK reaction of 1,6-enyne **279** and related formation of bicyclopentenone adducts **280** and **281** (Eq. 1.49).

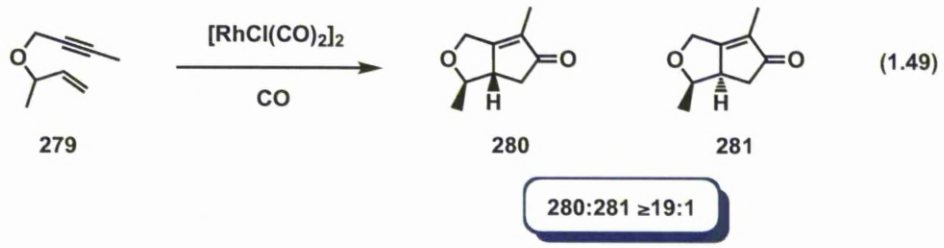

(1.49)

The objective of the computational study was the identification of the active catalytic species and the formulation of a mechanistic pathway that could explain the observed stereochemical outcome. [162] Additionally, the study allowed further insights to be gained into the role of the CO ligand in the carbocyclisation.

Scheme 1.89. Putative mechanistic pathways of the diastereoselective Rh-catalysed PK reaction under carbon monoxide atmosphere.

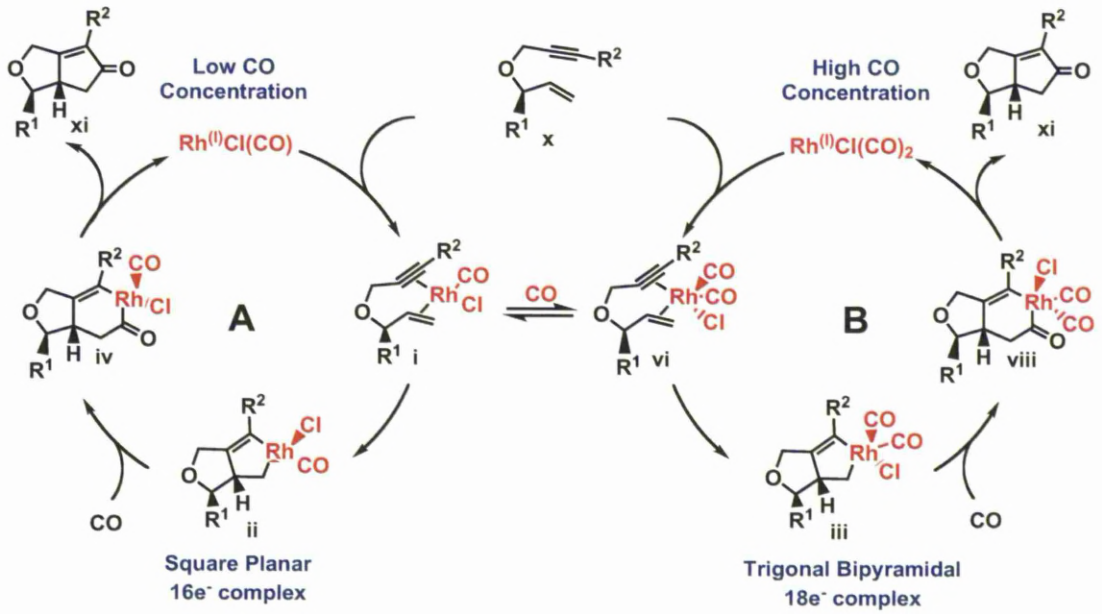

The generally accepted mechanism for the Rh-catalysed PKR involves initial π coordination of the alkene and alkyne to the rhodium metal centre, followed by the oxidative addition and formation of a five-membered rhodium metallacycle. Subsequent CO insertion and final reductive elimination provides desired bicyclopentenone adduct with regeneration of the

rhodium catalyst. Although the formulation of a detailed reaction mechanism was partially precluded by their limited knowledge of the catalytically active rhodium species, the authors envisaged two plausible mechanistic pathways for catalysts [Rh^{I}Cl(CO)] (**Scheme 1.89**, pathway A) and [Rh^{I}Cl(CO)$_2$] (**Scheme 1.89**, pathway B).[162] Hence, depending on the nature of the catalytic active species, π coordination of 1,6-enyne **x** would provide either the 16-electron square planar complex **ii** or 18-electron trigonal bipyramidal analogue **iii**. Computational analysis examined the relative reaction energy profiles for each complex, in the context of the aforementioned mechanistic pathway.[167]

Scheme 1.90. Energy profile for mechanistic pathway A.

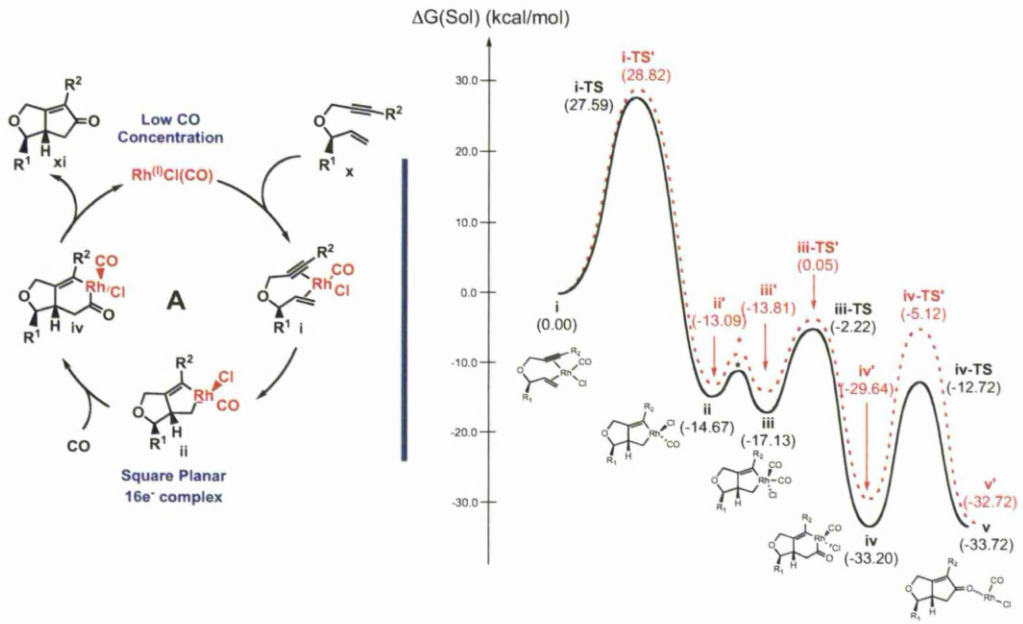

Scheme 1.90 outlines the computed solution-phase free-energy reaction profile employing [Rh^{I}Cl(CO)] as the catalytically active species (pathway A). Upon initial π coordination of the enyne to the rhodium centre and formation of the square planar complex **i**, subsequent oxidative addition could generate two possible diastereoisomeric rhodium metallacycles, in which the C3 hydrogen atom is either *anti* (**Scheme 1.90**, complex **ii'**) or *syn* to the C2-substituent R^{1} (**Scheme 1.90**, complex **ii**). Examination of the solution-phase activation free

energies of related transition states **i-TS'** (28.82 Kcal mol^{-1}) and **i-TS** (27.59 Kcal mol^{-1}) indicated a difference of 1.2 Kcal mol^{-1}, which can be equated of an approximate diastereomeric ratio (*dr*) of 10:1 in favour of *cis* adduct **280**. Hence, the computed energetic difference between transition states **i-TS'** and **i-TS** could not efficiently rationalise the experimentally high diastereoselectivity in the carbocyclisation process (Eq. 1.49).

Scheme 1.91. Energy profile for mechanistic pathway B.

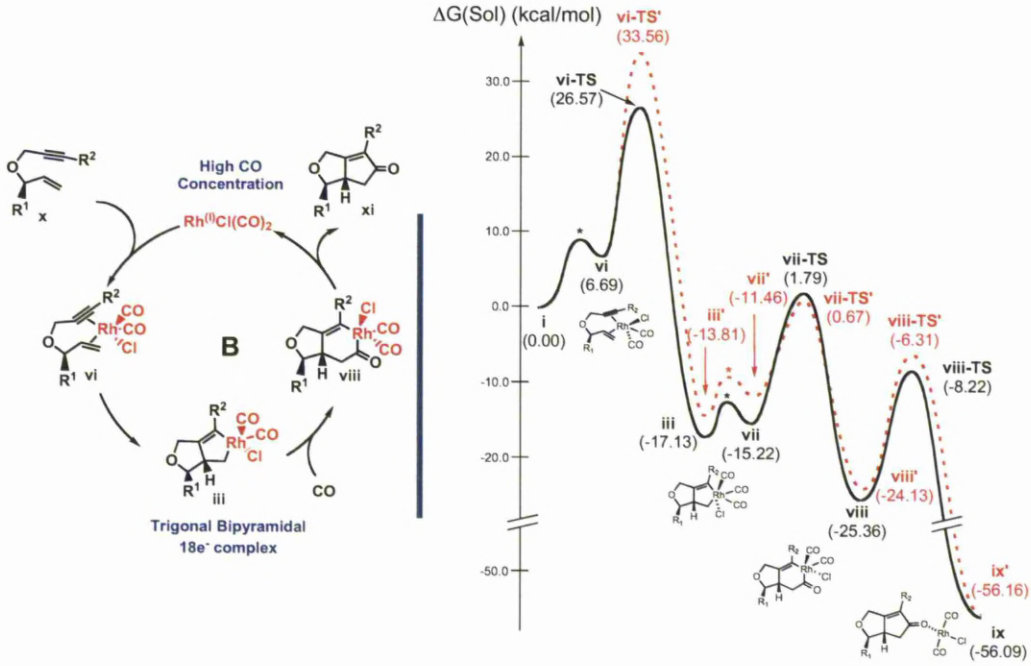

As the rhodium centre accepts σ electron density from the additional CO ligand, the antibonding interaction of the trigonal-bipyramidal complex with the original enyne becomes more prominent. Thus, axial coordination of an additional CO ligand to the *pseudo*-square-planar rhodium centre forces the chlorine ligand to adopt a *trans* axial spatial disposition into trigonal-bipyramidal complex **vi**. Coordination of an additional CO ligand and the resulting formation of a five-coordinate rhodium complex did not provide a substantial variation in activation energy for the formation of the *syn* metallacycle (27.59 Kcal mol^{-1} for **i-TS**, **Scheme 1.90** *vs* 26.57 Kcal mol^{-1} for **vi-TS**, **Scheme 1.91**). On the contrary, activation energy

for the formation of *anti* metallacycle was dramatically influenced by the geometry of the catalytically active rhodium complex (28.82 Kcal mol^{-1} for **i'-TS**, **Scheme 1.90** *vs* 33.56 Kcal mol^{-1} for **vi'-TS**, **Scheme 1.91**). Examination of the solution-phase activation free energies of transition states **vi-TS'** (33.56 Kcal mol^{-1}) and **vi-TS** (26.57 Kcal mol^{-1}) in pathway B indicated a difference of 7.0 Kcal mol^{-1}, thereby predicting an approximate diastereomeric ratio (*dr*) of ≥99:1 in favour of the *cis* PKR adduct **280**. Hence, formation of the trigonal-bipyramidal complex **vi** (pathway B, **Scheme 1.88**) as the prevalent catalytically active species accounted for the experimentally observed *cis* diastereoselectivity in the PK reaction (Eq. 1.49). The equilibrium between square-planar complex **i** and trigonal bipyramidal **vi** is clearly dependent on CO concentration in the system, whereas complex **vi** will be prevalent at relatively high CO concentration and complex **i** will be the predominant species at lower CO concentration. Therefore, the computational investigations predicted a relative loss of diastereoselectivity in the Rh-catalysed PK reaction at low CO concentration, in view of the shift in equilibrium towards the formation of the square planar complex **i**.

Table 1.2. Influence of the CO concentration in the Rh-catalysed PK reaction of enyne **279**.

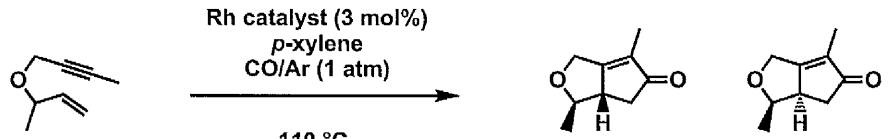

279 280 281

entry	Pressure		Catalyst	Yield (%)	*dr*
	CO	Ar			280:281
1	1.00	0.00	$[RhCl(CO)_2]_2$	81	22:1
2	0.10	0.90	$[RhCl(CO)_2]_2$	64	10:1
3	0.05	0.95	$[RhCl(CO)_2]_2$	57	6:1
4	1.00	0.00	$[RhCl(CO)(dppp)]_2$	88	≥99:1
5	0.10	0.90	$[RhCl(CO)(dppp)]_2$	51	58:1
6	0.05	0.95	$[RhCl(CO)(dppp)]_2$	44	57:1

Exploitation of the theoretical findings prompted the experimental correlation study between CO concentration and related diastereochemical outcome of the Rh-catalysed PK reaction system (**Table 1.2**, entries 1-3).[162] As outlined in **Table 1.2** (entry 2 and 3) the employment of low CO concentration resulted in a significant reduction in the diastereoselectivity of the process, thus endorsing the validity of the aforementioned computational predictions. Additionally, Baik and Evans envisaged that utilisation of metal-binding phosphine ligands could enforce the aptitude of Rh complexes to adopt trigonal bipyramidal geometry, thus providing enhanced diastereoselectivity in the reaction. Ligand optimisation studies estabilished that [RhCl(CO)(dppp)] imparts a high degree of diastereoselectivity, regardless of the CO concentration in the reaction (entries 4-6).

In summary, a combination of high-level density functional theory calculations and experimental studies disclosed fundamental mechanistic insights into the rhodium-catalysed Pauson-Khand reaction. Additionally, this work highlighted the powerful influence of CO concentration to promote the formation of trigonal bipyramidal catalytic species and enhance the diastereoselectivity of the process, thus disproving the original hypothesis of a purely sterically driven model for stereocontrol.

Table 1.3. Diastereoselective Rh-catalysed PK reaction of nitrogen and carbon-tethered enynes **282** and **283**.

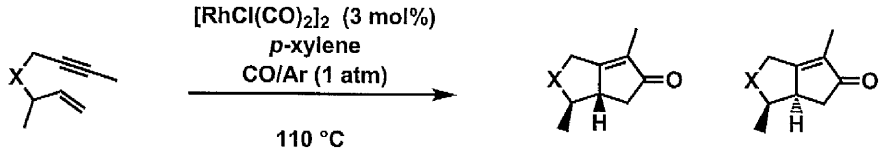

entry	Pressure		X	Enyne	Yield (%)	cis	trans	*dr*
	CO	Ar						cis:trans
1	1.00	0.00	NTs	282	77	284	285	3:1
2	0.10	0.90	"	"	69	"	"	1:1
3	1.00	0.00	$C(CO_2Me)_2$	283	80	286	287	5:1
4	0.10	0.90	"	"	64	"	"	2:1

Nevertheless, low degree of diastereoselectivity in the Rh-catalysed PK carbocyclisation of nitrogen and carbon-tethered enynes **282** and **283** remained a barrier for a highly general and selective carbocyclisation strategy (**Table 1.3**).[168] In light of the success with high-level density functional theory (DFT)[56,72,169.170] to predict and rationalise the stereochemical outcome of metal-catalysed carbocyclisation reactions, we decided to undertake additional computational and experimental studies and provide a new hypothesis to attain high diastereoselectivity in the rhodium(I)-catalysed PK reaction,[169] irrespectively from the nature of the tether.

1.6.3. Computational and Experimental Investigation of the Substitution Pattern on the Alkyne Terminus.

The computed solution-phase free-energy reaction profile for the rhodium trigonal bipyramidal species (**Scheme 1.89**) revealed a notable activation energy difference (7 Kcal mol^{-1}) for the formation of *syn* (complex **iii**) and *anti* (complex **iii'**) metallacycles and consequent high diastereoselectivity in the process.[162] Hence, in collaboration with the Baik group, we aimed to investigate the origin of the high diastereoselectivity in the oxidative addition step by computational analysis of transition states **1a-TS-1** and **1a-TS-2** which further furnish the *cis*- and *trans*- PK adducts, respectively (**Scheme 1.92**).[171] Examination of the partial charges[172] of the carbon atoms forming the C-C bond revealed an intriguing electronic feature. Although, both transition states are highly charge polarised, they displayed opposite direction of polarisation at the distal carbon atoms in the metallacyclic intermediates, as outlined by the partial charges in the transition states (**Scheme 1.92**). The computed partial charge for the C3-position is positive for **1a-TS-1** (+0.34) and negative for **1a-TS-2** (–0.34). Furthermore, the C3' in **1a-TS-1** and **1a-TS-2** is polarised with opposite sign (–0.10 and +0.11 respectively), which suggests that the oxidative addition is best conceptualised as a heterolytic cleavage of the π-bonds followed by an electronic reorganisation (**Scheme 1.92**).

Scheme 1.92. Computational analysis of partial charges of transition states **1a-TS-1** and **1a-TS-2**.

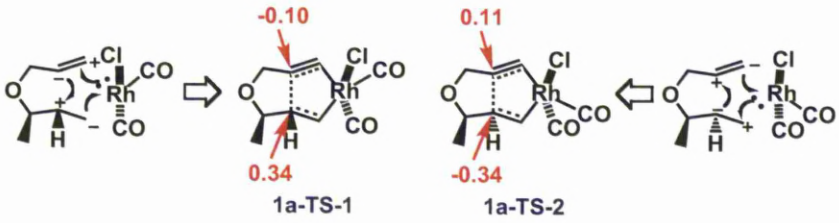

Conformational analysis of **1a-TS-1** and **1a-TS-2** provides a rationale for the observed charge polarisation pattern and the origin of stereocontrol in this process. As illustrated by the Newman projections (**Figure 1.6**), the methyl group at the C2-position is in a *trans*-disposition relative to the sp^2-hybridised orbital on C3, which will form a new δ-bond with the C3'-carbon in **1a-TS-1**.

Figure 1.6. Newman projections of **1a-TS-1** and **1a-TS-2**.

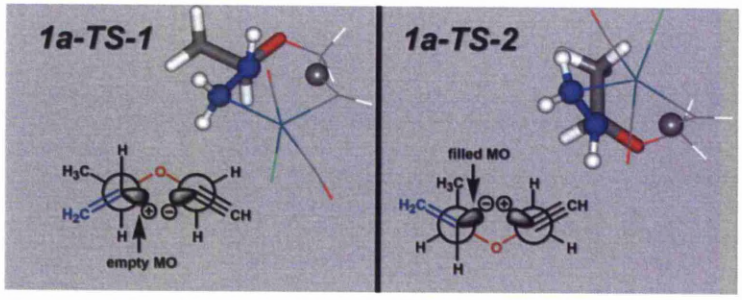

This orientation is necessary for obtaining the *cis*-adduct, since it provides the necessary *syn*-orientation of the C3-hydrogen relative to the C2-methyl group. Similarly, formation of the *trans*-PKR product results from the sp^2-hybridised orbital becoming *syn* to the C2-methyl in **1a-TS-2** (**Figure 1.6**). Considering the structural requirements in the transition state, the electronic consequences are evident. In **1a-TS-1** hyperconjugation amplifies the +I effect of the methyl group, which stabilises the developing positive charge on C3. Alternatively, in **1a-TS-2** the methyl group is orthogonal to the sp^2-orbital on C3, which reduces the electronic communication between the methyl group and the C3 sp^2-orbital. With the charge directing

effect of the methyl group reduced by this structural arrangement, the –I effect of the methylene moiety (blue in **Figure 1.6**) stabilises the developing negative charge on the sp^2-orbital on C3. This in turn causes a reversal of the charge polarisation in the metallacycle **1a-TS-2** compared to **1a-TS-1** (**Scheme 1.92**).

As previously discussed, the employment of [RhCl(CO)] as catalytically active species displayed moderate activation energy difference (1.2 Kcal mol^{-1}) for the formation of *syn* (complex **ii**) and *anti* (complex **ii'**) metallacycles, thereby predicting low diastereocontrol in the process (**Scheme 1.89**).[162] Hence, we were prompted to perform computational analysis of the partial charges of **2a-TS-1 and 2a-Ts-2** in order to assess the origin of the lower diastereoselectivity provided by square-planar rhodium species (**Scheme 1.93**).

Scheme 1.93. Computational analysis of partial charges of transition states **2a-TS-1** and **2a-TS-2**.

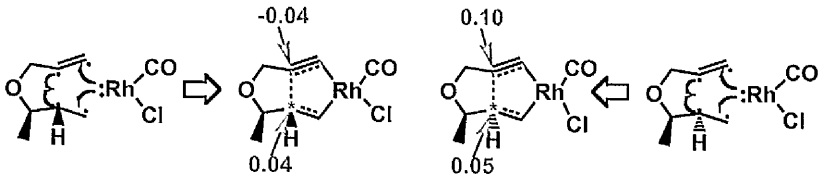

Examination of the partial charges of the relevant carbon atoms forming the C-C bond exhibited a divergent polarisation pattern, in which both transition states showed moderate charge and displayed a similar direction of polarisation at the distal carbon atoms in the metallacyclic intermediates, as outlined by the partial charges in the transition states (**Scheme 1.93**). The computed partial charge for the C3-position is both positive and similar for **2a-TS-1** (+0.04) and **2a-TS-2** (+0.05). Furthermore, the C3' in **2a-TS-1** and **2a-TS-2** is only slightly polarised with the opposite sign (–0.04 and +0.10, respectively), which suggests that the oxidative addition is best conceptualised as a radical recombination-type mechanism (**Scheme 1.92**).

Figure 1.7. MO of square planar Rh-fragment (**A**), trigonal-bipyramidal Rh fragment (**B**) and oxidative addition process for trigonal-bypiramidal Rh species (**B1**).

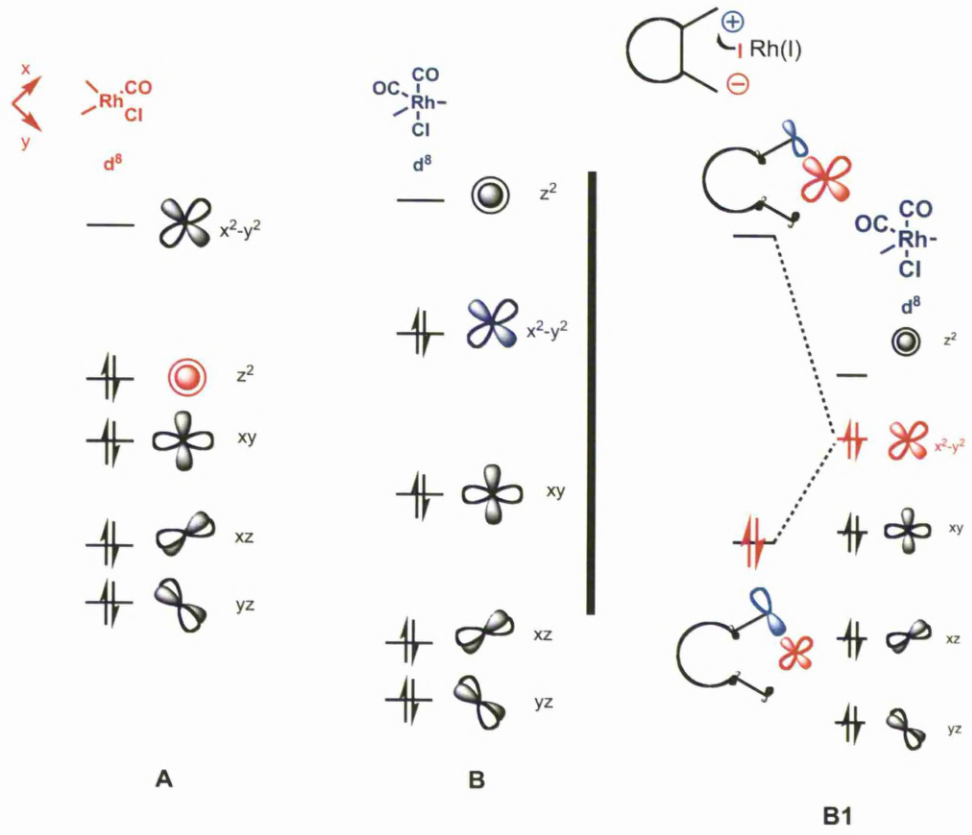

In summary, the oxidative addition process for square planar and trigonal bipyramidal involves different mechanisms, namely a closed-shell electron-pair polarisation-type (**Scheme 1.92**) and a radical recombination-type mechanism, respectively (**Scheme 1.93**). Analysis of molecular fragments of rhodium trigonal bipyramidal and square planar coordination complexes clarifies the varying nature of their subsequent oxidative addition process. As outlined in **Figure 1.7**, the HOMO of the rhodium atom in square planar (A) and trigonal bipyramidal (B) have different shapes, respectively d(z^2) and d(x^2-y^2). Therefore, in the subsequent oxidative addition step, orbital d(x^2-y^2) of trigonal bipyramidal rhodium complex is occupied and points directly towards the direction where the two new Rh-C bonds will be formed (**Figure 1.7, B1**). This orbital promotes a "push-pull" type of reaction that leads to the oxidative addition of the closed-shell electron-pair polarisation type. Hence, the distorted trigonal-bipyramidal complex promotes a stereoselective oxidative addition process in view

of the ability of the Rh centre to direct the charge polarisation as to match the heterolytic charge redistribution of the reactant. In contrast, the $d(x^2-y^2)$ orbital is empty in the corresponding square-planar rhodium system, thus the complex can not efficiently control the diastereoselectivity in the following oxidative addition step. A summary of the divergent mechanistic pathways is outlined in **Figure 1.8.**

Figure 1.8. Oxidative addition mechanism for trigonal-bipyramidal and square-planar Rh complexes.

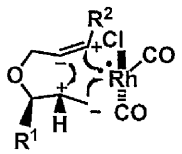

high CO concentration

trigonal bipyramidal

closed-shell electron-pair polarization

high diastereoselectivity

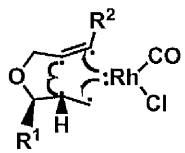

low CO concentration

square planar

radical recombination

low diastereoselectivity

The discussed computational analysis of the charges of distal carbon atoms of intermediate rhodium metallacycles provided an intriguing paradigm for the augmentation of reactivity and diastereocontrol in the Rh-catalysed PK reaction. From a conceptual standpoint, mimicking of the theoretical charges in transition state **1a-TS-1** (**Scheme 1.92**) by means of an enyne prepolarisation could efficiently serve this purpose (**Scheme 1.94**).

Scheme 1.94. Prepolarisation of 1,6-enynes by modification of the alkyne terminus.

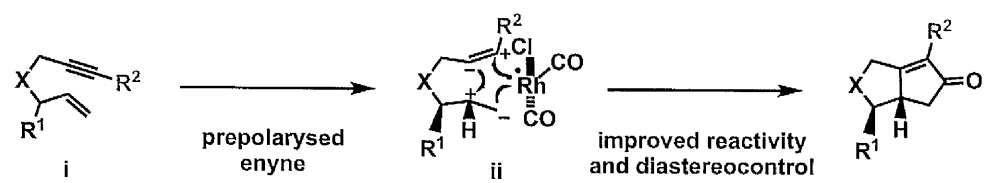

Theoretical analysis of several electron withdrawing groups (R^2 = aryl, ester and halide groups) indicated that the addition of a halogen to the alkyne terminus[173] should induce a positive partial charge at the C4'-position (**Table 1.4**), and thereby decrease the energy barrier for the rate-determining step to provide the conditions for a spontaneous room temperature reaction.[174]

Table 1.4. Effect of the C4' substituent on the computed barrier for the metallacycle formation (**Scheme 1.91**, R^1 = Me).[a]

entry	R^2	enyne	$\Delta G_{calc.}$*syn*[b]	$\Delta G_{calc.}$*anti*[b]
1	H	288	28.4	31.1
2	Cl	289	24.5	29.3
3	Br	290	24.5	29.5
4	I	291	25.7	30.3

[a] Jaguar 7.0, Schrodinger, LLC, New York, NY, 2007. [b] Kcal mol^{-1}.

Hence, we elected to examine the predicted reactivity of halogenated 1,6-enynes by means of a challenging room temperature diastereoselective PK reaction. As predicted by the computed activation energy barriers, the unsubstituted enyne **296** did not display any reactivity in the PK process at room temperature (entry 1, **Table 1.5**). Replacement of the alkyne moiety with a bromine unit (entry 3) provided moderate reactivity in the carbocyclisation, albeit the resulting adduct **298** was prone to undergo decomposition after isolation. Gratifyingly, the chloride substituted alkyne conferred optimal reactivity at room temperature and allowed for the formation of bicyclopentenone derivative **305** in good yield (entry 2, **Table 1.5**). Similar investigation on nitrogen-tethered enynes confirmed the outstanding ability of chlorinated 1,6-enynes to promote Rh-catalysed PK reaction under extremely mild operating conditions (entry 7), while analogous bromine and iodine derivative displayed an overall lack of reactivity. Finally, the carbon-tethered bicyclopentenone adduct could also be obtained in good yield at room temperature (entry 10). In light of these promising results, we decided to

investigate the reactivity and stereochemical outcome of a wide variety of C2-substituted 1,6-enynes under carbonylative conditions.

Table 1.5. Effect of the C4' halogen substituent on the Rh-catalysed PK reaction.[a]

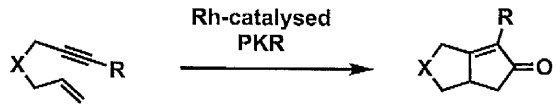

entry	X	R	Enyne	Yield (%)[b]	Product
1	O	H	296	NR	305
2	"	Cl	297	74	306
3	"	Br	298	39	307
5	"	I	299	NR	308
6	NTs	H	300	NR	309
7	"	Cl	301	81	310
8	"	Br	302	NR	311
9	"	I	303	NR	312
10	$C(CO_2Me)_2$	Cl	304	74	313

[a] All reactions were carried out on a 0.2 mmol scale utilizing 5 mol% $[RhCl(CO)_2]_2$ in *p*-xylene (0.1 M) at 25 °C under CO atmosphere (1 atm). [b] Isolated yields.

1.6.4. Scope of the Room Temperature Diastereoselective PK Reaction of 1,6-Chloro Enynes.

An initial optimization study on the reactivity of C2-substituted halogenated enynes confirmed the ability of the chloride moiety to confer excellent reactivity for this process (entry 1, **Table 1.6**). Moreover, the observed excellent reactivity and stereoselectivity for enyne **314** is particularly significant in view of the poor diastereoselectivity displayed by nitrogen-tethered enynes in previous rhodium [161] and cobalt-catalysed[11] PK reactions.

Table 1.6. Room temperature Rh-catalysed diastereoselective PK reaction of C2-methyl-substituted halogenated 1,6-enynes.[a]

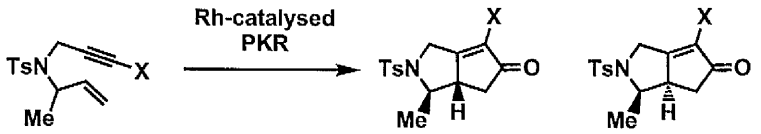

entry	X	Enyne	Yield (%)[b]	*cis*	*trans*	*cis*:*trans*[c]
1	Cl	314	80	317	318	97:3
2	Br	315	NR	319	320	"
3	I	316	NR	321	322	"

[a] All reactions were carried out on a 0.2 mmol scale utilizing 5 mol% $[RhCl(CO)_2]_2$ in *p*-xylene (0.1 M) at 25 °C under CO atmosphere (1 atm). [b] Isolated yields. [c] Ratios of diastereoisomers were determined by HPLC or GC analysis of the crude products.

Table 1.7 illustrates the scope of the diastereoselective room temperature PK methodology. Treatment of nitrogen and oxygen-tethered enynes under the actual conditions provided the corresponding bicyclopentenone adducts in good overall yield. Remarkably, the nature of the tether and the employment of benzyl, alkyl and hydroxymethyl C2 substituent provided a highly diastereoselective Rh-catalysed carbocyclisation. In this context, a benzyl substituent (entry 3 and 7, **Table 1.7**) proved to exert a beneficial effect in the process, thus allowing complete diastereocontrol and excellent yield. An additional key feature of the methodology included the exceptionally mild operating conditions and the ability to conduct the process at ambient temperature with a low catalyst loading. The aforementioned computational studies highlighted the ability of a trigonal bypiramidal rhodium species to exert a dramatic influence on the activation energy for the formation of *syn*- and *anti*- metallacycles, thereby conferring enhanced diastereoselectivity in the overall carbocyclization process. Hence, the employment of a high concentration of carbon monoxide proved to be of fundamental to enable the coordination of an additional CO ligand and achieve the required geometry.

Table 1.7. Scope of the RT diastereoselective Rh-catalysed PK reaction of chlorinated 1,6-enynes.[a]

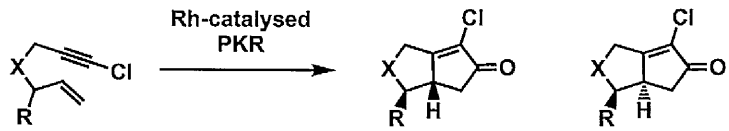

entry	X	R	Enyne	Yield (%)[b]	*cis*	*trans*	*cis*:*trans*[c]
1	NTs	Me	314	80	317	318	97:3
2	"	CH_2OBn	319	73	323	324	≥99:1
3	"	Bn	320	84	325	326	≥99:1
4	O	Me	289	82	327	328	98:2
5	"	CH_2OBn	321	84	329	330	≥99:1
6	"	Bn	322	87	331	332	≥99:1

[a] All reactions were carried out on a 0.2 mmol scale utilizing 5 mol% $[RhCl(CO)_2]_2$ in *p*-xylene (0.1 M) at 25 °C under CO atmosphere (1 atm). [b] Isolated yields. [c] Ratios of diastereoisomers were determined by HPLC or GC analysis of the crude products.

In view of the computationally predicted and experimentally confirmed role of the CO concentration, we elected to examine the influence of the carbon monoxide concentration in the room temperature PK reaction of chlorinated 1,6-enynes and thereby examine its influence on the diastereoselectivity of the process. **Table 1.8** outlines the reactivity and stereochemical outcome of the carbocyclization under reduced CO concentration (Ar:CO = 10:1). As predicted, oxygen-tethered enynes furnish the corresponding bicyclopentenones derivatives with a high level of stereoselectivity, albeit with a slight reduction in the overall yield (entries 4-6, **Table 1.8** and, entries 4-6, **Table 1.7**). In contrast, the variation of the CO atmosphere provided diminished reactivity and diastereocontrol for the analogous nitrogen-tethered substrates (entries 1-3, **Table 1.8** and entries 1-3, **Table 1.7**). Hence, the reduction in diastereoselectivity supports the hypothesis that square-planar rhodium complexes, prevalent species under reduced CO concentration, proceed through a different TS which is suboptimal for obtaining high level of diastereoselectivity in the oxidative addition step.[162]

Table 1.8. Room temperature Rh-catalysed diastereoselective PK reaction of chlorinated 1,6-enynes at low CO concentration (Ar:CO = 10:1).

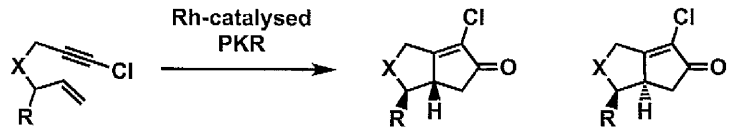

entry	X	R	Enyne	Yield (%)[b]	cis	trans	cis:trans[c]
1	NTs	Me	314	69	317	318	85:15
2	"	CH_2OBn	319	59	323	324	87:13
3	"	Bn	320	63	325	326	76:23
4	O	Me	289	76	327	328	96:4
5	"	CH_2OBn	321	64	329	330	99:1
6	"	Bn	322	65	331	332	≥99:1

[a] All reactions were carried out on a 0.2 mmol scale utilizing 5 mol% $[RhCl(CO)_2]_2$ in *p*-xylene (0.1 M) at 25 °C under Ar:CO atmosphere (10:1, 1 atm). [b] Isolated yields.[c] Ratios of diastereoisomers were determined by HPLC or GC analysis of the crude products.

1.6.5. Limitations of the Reaction.

As discussed, the installation of a chloride unit on the alkyne terminus reduces the activation energy in the oxidative addition step and confers enhanced reactivity in the process, thus enabling the accomplishment of a mild and stereoselective PK reaction. Nonetheless, additional experimental investigations revealed that prominent reactivity of chlorinated 1,6-enynes was largely affected by the size of substituent on the C2 position. In this context, substrates containing cyclic C2 substituents whether aliphatic or aromatic, display no reactivity in the Rh-catalysed carbocyclisation (Eq. 1.50). A plausible rationale for the observed behaviour could involve the steric effect exerted by the cyclic C2 moiety and the inability of the enyne substrate to efficiently coordinate to the metal centre. Hence, as described in previous studies on the diastereoselective Rh-catalysed PKR with enynes bearing cyclic C2 substituents require harsh thermal conditions in the process (T = 110 °C).[168]

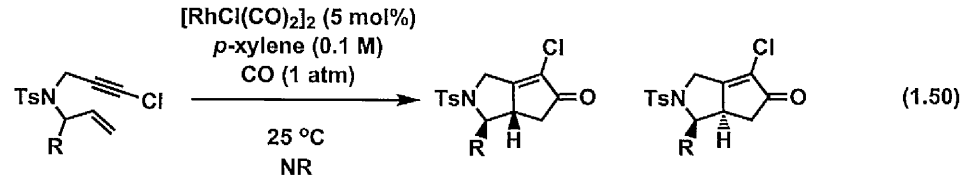

(1.50)

R	enyne
Cy	333
2-furyl	334
p-F-C_6H_4	335

The sequential Rh-catalysed tandem allylic alkylation/PK reaction developed by Evans and Robinson highlighted the effect of the tether nature on the diastereoselectivity of the reaction. Nonetheless, the employment of thermal conditions (80 °C) provided excellent reactivity rates for nitrogen, oxygen and carbon-tethered enynes.[162] In contrast, the development of the Rh-catalysed methodology with chlorinated 1,6-enynes demonstrates a remarkable influence of the tether on the reactivity at ambient temperature. As highlighted in **Table 1.9**, oxygen and nitrogen-tethered enynes **289** and **314** displayed high reactivity towards the carbocyclisation reaction whereas the analogous carbon-tethered substrate **336** displayed on overall lack of reactivity even after prolonged reaction time (48 h).

Table 1.9. Effect of tether nature on the reactivity of the RT Rh-catalysed diastereoselective PK reaction of chlorinated 1,6-enynes.[a]

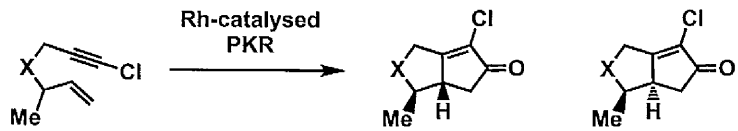

entry	X	Enyne	Time (h)	Yield (%)[b]	cis	trans	cis:trans[c]
1	O	289	20	82	327	328	98:2
2	NTs	314	27	80	317	318	97:3
3	$C(CO_2Me)_2$	336	48	NR	337	338	"

[a] All reactions were carried out on a 0.2 mmol scale utilizing 5 mol% $[RhCl(CO)_2]_2$ in *p*-xylene (0.1 M) at 25 °C under CO atmosphere (1 atm). [b] Isolated yields. [c] Ratios of diastereoisomers were determined by HPLC or GC analysis of the crude products.

Interestingly, in a related development in the group, the novel [2+2+2] Rh-catalysed carbocyclisation of diene-ynes[175] also suffers from low reactivity with carbon-tethered precursors in the formation of bicyclic and tricyclic scaffolds under mild thermal conditions (**Table 1.10**).

Table 1.10. Effect of tether nature on the Rh-catalysed [2+2+2] cycloaddition reaction of diene-ynes.

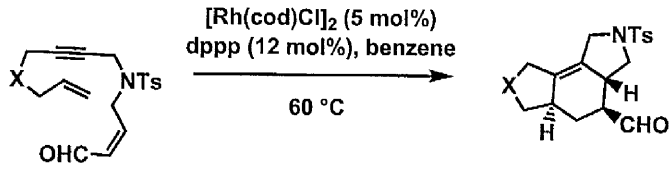

entry	X	Enal	Yield (%)	Product	*dr*
1	O	339	76	342	≥19:1
2	NTs	340	73	343	≥19:1
3	$C(CO_2Me)_2$	341	NR	344	—

Scheme 1.95. Oxidative addition process for enynes and diene-ynes.

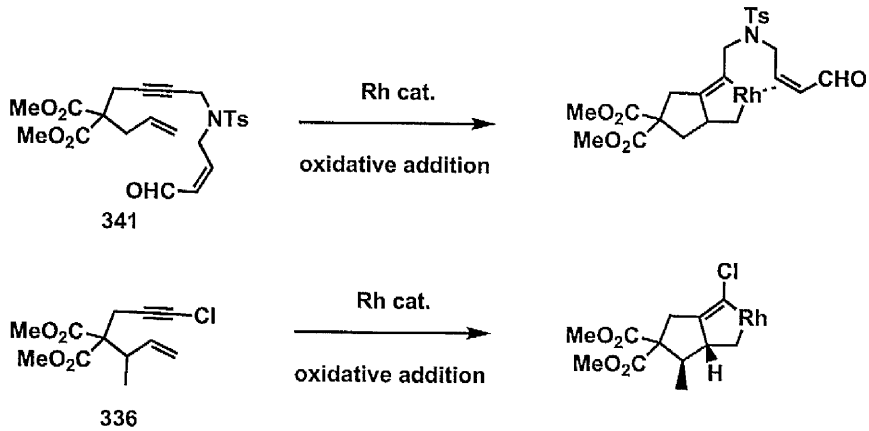

A common feature in the Rh-catalysed carbocyclisation of enynes **336** and **341** is the attempted construction of a malonate-containing five-membered rings (**Scheme 1.95**). The oxidative addition step involves a distortion of the enyne substrate in order to achieve an optimal coordination to the metal centre to undergo C-C bond formation. Hence, we

envisioned that the employment of malonate tethered enynes **336** and **341** might provide an energetically disfavoured distortion of the enyne substrate, thus lowering the aptitude of the alkene and alkyne counterparts to coordinate to the metal centre and undergo further oxidative addition (**Scheme 1.95**). In order to gain additional insights into the aforementioned theoretical hypothesis we performed a computational analysis of the C-X-C (X = NTs, O, $C(CO_2Me)_2$ bond angle variation in both initial substrates and related PK adducts (**Figure 1.9**).[176] Initial computational examination of oxygen-tethered enynes and their related PK adduct predicted an overall angle variation of 4.42 °, whereas investigation of the nitrogen- and carbon-tethered enynes indicated a larger angle variation, respectively 6.27 ° and 7.27 °. In light of the higher reactivity of oxygen-tethered enyne **289** with respect to the nitrogen- and carbon-tethered enynes **314** and **304** we envisioned that a wide angle variation could result in a higher energy for the enyne coordination step and the following oxidative addition step, with consequent lower reactivity in the PK reaction.

Figure 1.9. Examination of C-X-C (X = O, NTs, $C(CO_2Me)_2$) in 1,6-enynes and related PK adducts.

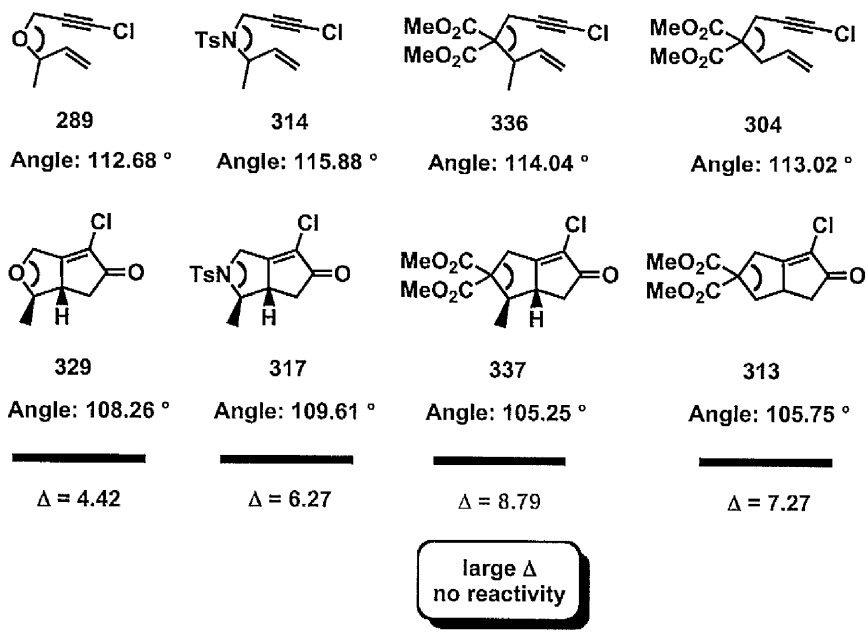

Analysis of malonate-tethered substrate **336** corroborated the hypothesised relationship and predicted a wide angle variation between enyne and related PK adduct (8.79 °). Hence, we believe that to the energy required for the distortion of the initial enyne geometry during the corresponding π-coordination Rh complex is too high for enyne **336** and this is indicated by the wide angle variation between starting material **336** and PK adduct **337** (**Figure 1.9**).

1.6.6. Proof of Stereochemistry in the Rh-catalysed Diastereoselective PK Reaction.

NOE analysis of the PK reaction adducts **317** and **327** confirmed the predicted *cis* stereochemistry of the bicyclopentenone derivatives (**Figure 1.10**).

Figure 1.10. NOE analysis of PK reaction adducts **327** and **317**.

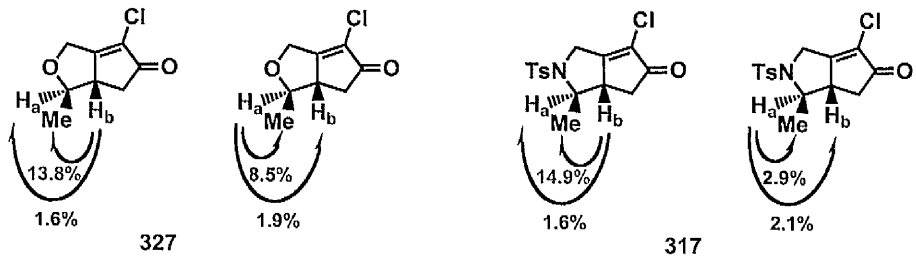

Figure 1.11. Homodecoupling experiments on C2-substituted PK reaction adducts.

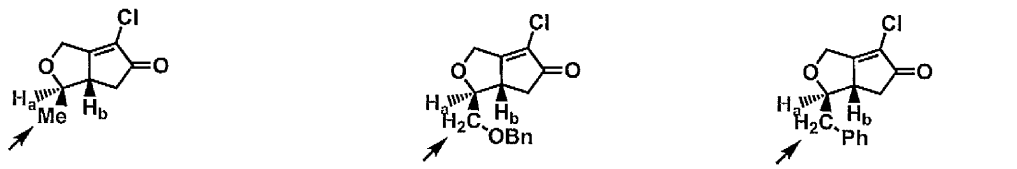

(CDCl$_3$) H_a: 3.56 (d, J = 10.2 Hz) (CDCl$_3$) H_a: 3.07 (d, J = 10.3 Hz) (CDCl$_3$) H_a: 3.56 (dt, J = 10.3, 6.3 Hz)

(DMSO-d_6) H_a: 4.24 (d, J = 8.2 Hz) (CDCl$_3$) H_a: 4.27 (d, J = 8.2 Hz) (CDCl$_3$) H_a: 4.62 (d, J = 7.9 Hz)

Further homodecoupling experiments on the related nitrogen and oxygen-tethered PK adducts confirmed the overall *cis* diastereoselectivity in the carbocyclisation process. Irradiation of the NMR signal corresponding to the methyl or methylene moiety adjacent to the C2 position demonstrated similar coupling constants between vicinal protons H_a and H_b, thereby denoting uniform *cis* stereochemistry in the bicyclopentenone adducts **(Figure 1.11)**.

We envisaged that further functionalisation of the chlorine moiety could enhance the synthetic utility of the diastereoselective methodology and, moreover, provide additional proof of stereochemistry by correlation to previously characterised compounds in the literature. In this context, we elected to derivatise the chlorine moiety by means of a dechlorination process or Suzuki coupling (**Scheme 1.96**).

Scheme 1.96. Derivatisation of PK reaction adducts.

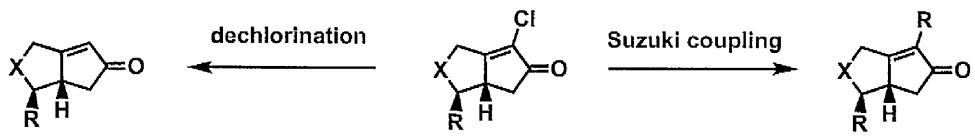

Experimental investigation of a challenging and relatively unexplored dechlorination of α-chloro-enones revealed the challenges of this process. Dechlorination under reductive (A-B, Eq. 1.51) and radical (C-F, Eq. 1.51) conditions provided recovered starting material and decomposition of enone **317**.

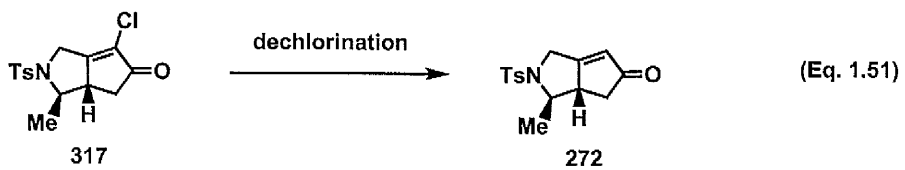

Conditions

A) Zn, MeOH, NH_4Cl, RT: no reaction
B) Zn, MeOH, NH_4Cl, reflux : decomposition

C) TTMSS, TEB, benzene (0.1 M): decomposition
D) TTMSS, TEB, benzene (0.02 M): no reaction
E) Bu_3SnH, ABCN, benzene, reflux: decomposition
F) Bu_3SnH, ABCN, benzene, 65 °C : decomposition

These disappointing results prompted us to investigate functionalisation of the vinyl chloride moiety by Pd-catalysed Suzuki coupling of α-chloro-enones with boronic acids, thereby installing an aliphatic and aromatic substituent at the α position of the enone moiety (Eq. 1.52).[177] Initial Pd-mediated coupling of bicyclopentenone **317** with methyl boronic acid revealed the inability of tetrakis(triphenylphosphine)palladium (0) catalyst to promote the desired transformation. However, a literature survey highlighted the opportunity to conduct the desired transformations under conditions developed by Buchwald and coworkers.[178]

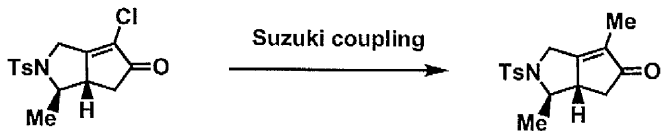

317 284 (Eq. 1.52)

Conditions

A) $MeB(OH)_2$, $Pd(PPh_3)_4$, Na_2CO_3, benzene, reflux: no reaction
B) $MeB(OH)_2$, $Pd(PPh_3)_4$, Na_2CO_3, toluene, 100 °C: no reaction
C) $MeB(OH)_2$, $Pd(OAc)_2$, dpdb, K_3PO_4, H_2O, THF, 100 °C: decomposition
D) $MeB(OH)_2$, $Pd(OAc)_2$, dpdb, K_3PO_4, H_2O, Toluene, 100 °C: decomposition
E) $MeB(OH)_2$, $Pd(OAc)_2$, dpdb, K_3PO_4, H_2O, Toluene, 65 °C: 62% yield

Gratifyingly, the employment of palladium acetate as catalyst with the monophosphine dpdb allowed the desired Suzuki-type coupling in good yield and with complete retention of stereochemistry (Eq. 1.52).[178] An essential requirement for the optimal exploitation of the transformation involved elimination of moisture and air from the reaction solvent by freeze-thaw degassing. Enone **284,** obtained by a PK reaction/Suzuki coupling sequence was further correlated with the compound prepared by carbocyclisation of enyne **282**. As predicted, the two synthetic pathways led to the formation of *cis*-enone **284** as the major diastereoisomer (**Scheme 1.97**). Additionally, the low diastereoselectivity obtained in the PK carbocyclisation of enyne **282** provided additional evidence for the ability of chlorinated 1,6-enynes to enhance the reactivity of the PK reaction and allow a highly diastereoselective annulation process.

Scheme 1.97. Diasteroeselective syntheses of enone **284**.

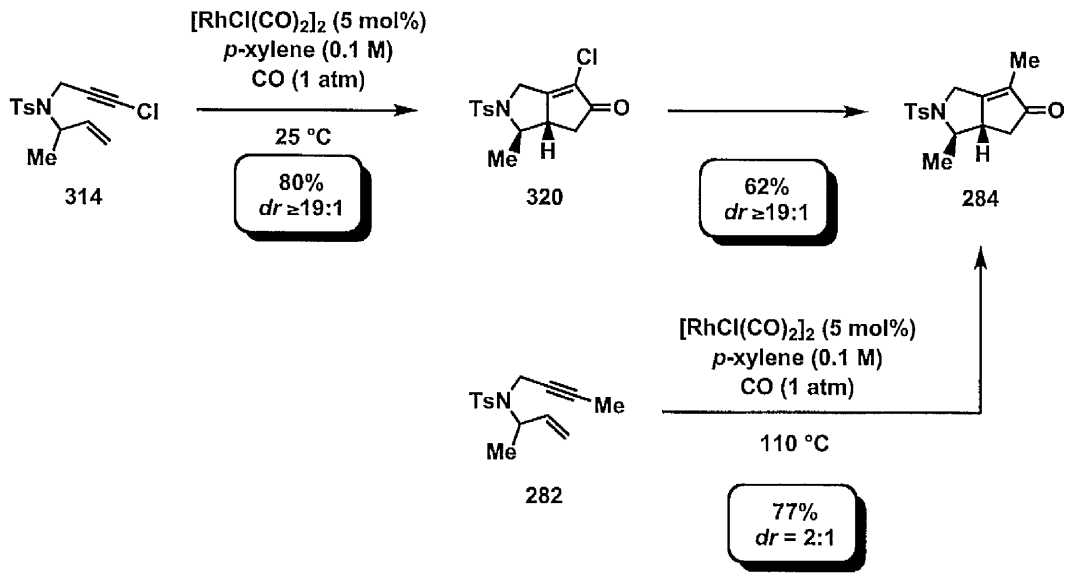

1.6.7. Conclusions.

As discussed in section **1.6**, initial computational and experimental studies on the diastereoselective Rh-catalysed Pauson-Khand reaction highlighted the ability of trigonal bipyramidal rhodium species to promote the stereoselective formation of *syn* rhodium metallacycles and the subsequent highly diastereoselective synthesis of *cis* bicyclopentenone derivatives.[162] In this context, a high concentration of carbon monoxide proved to be of fundamental importance in order to achieve the requisite trigonal-bypiramidal geometry in the metal catalyst. In order to garner additional insights into the carbocyclisation process, we performed detailed computational examination of the partial charges of the transition states intermediates of *syn*- and *anti*- rhodium metallacycles.[169] This study revealed a highly charge polarised metallacycle intermediate and the opposite direction of polarisation at the distal carbon atoms in the these species. Those theoretical findings prompted the investigation of substituted 1,6-enynes by mimicking the charge pattern on the *syn* metallacycle intermediate. Hence, theoretical predictions highlighted that favourable prepolarisation could be achieved by replacement of the alkyne terminus with a halogen moiety, thereby conferring enhanced

reactivity to the enyne substrate in the oxidative addition step. Consequent experimental investigations validated the outstanding reactivity of chlorinated 1,6-enynes and thereby facilitate a highly diastereoselective Rh-catalysed PK reaction under exceptionally mild operating conditions.[169] Remarkably, the methodology could deliver an unprecedented stereoselective carbocyclization of nitrogen-tethered enynes. Finally, the possibility to functionalise α-chloro-enone adducts by means of Pd-catalysed coupling reactions showcase the synthetic potential of this strategy. In this context, Chapter 2 will describe the additional exploitation of chlorinated enynes in the development of a unique room temperature enantioselective Pauson-Khand carbocyclisation process.

1.7. Experimental

1.7.1 General.

Unless otherwise indicated, all reactions were carried out in flame-dried glassware under an atmosphere of carbon monoxide (CO balloon, 1 atm). Xylene and toluene were distilled from CaH_2 and kept over sieves, under an Ar atmosphere, and THF was distilled from benzophenone ketyl. All other starting materials and solvents were purchased from Acros, Aldrich, Alfa Aesar, Fluorochem or Strem and used without further purification. Catalyst $[RhCl(CO)_2]_2$ was purchased by Strem, kept in the glove box at –35 °C and entirely utilized in the glove box. Carbon monoxide gas and mixture of Ar:CO (10:1) gas were purchased by CK Gas (CO purity = 99.97%). High purity of CO (≥99.95) proved to be essential for the optimal exploitation of the PK reaction.

Thin layer chromatography (TLC) was performed on Whatman F_{254} precoated silica gel plates. Visualisation was accomplished with a UV light and/or $KMnO_4$ solution. Flash chromatography (FC) was performed using either Merck Silica Gel 60 (230-400 mesh) or Whatman Silica Gel Purasil® 60 (230-400 mesh). Solvents for extraction and FC were analytical grade. Reported solvent mixtures for TLC and FC are volume/volume mixtures. Infrared spectra were obtained on a Perkin-Elmer spectrum 100 series FTIR spectrometer. Peaks are reported in cm^{-1} with the following relative intensities: vs (very strong), s (strong), m (medium) and w (weak). Mass spectra were performed at either the University of Liverpool Mass Spectrometry Center or the EPSRC National Mass Spectrometry Service Centre, Swansea. High resolution electron-impact (EI, ionization voltages of 70 eV), chemical ionization (CI, reagent gas CH_4 or NH_3) were obtained on either an Autospec ZAB 2SE, Kratos MS-80, VG 7070E double focusing magnetic sector mass spectrometer equipped with a solid probe inlet, a QUATRO II, MAT 95, or MAT 900. The electrospray ionization (ESI) and mass spectra were obtained on a Waters micromass and LCT mass spectrometer. ^1H and

^{13}C NMR were recorded on a Bruker AV 500 MHz NMR spectrometer in the indicated deuterated solvent, which were obtained from Cambridge Isotope Labs. For ^{1}H NMR, $CDCl_3$ was set to 7.26 ppm ($CDCl_3$, singlet). For ^{13}C NMR, $CDCl_3$ was set to 77.16 ppm ($CDCl_3$, centre of triplet). ^{1}H data are reported in the following order: chemical shift in ppm (δ) (multiplicity, which are indicated by br (broadened), s (singlet), d (doublet), t (triplet), q (quartet), m (multiplet)); assignment of 2nd order pattern, if applicable; coupling constant (*J*, Hz); integration values for all ^{13}C NMR spectra data using the descriptor *o* and *e* refer to whether the peak is odd or even, respectively, and correlate to an attached proton test (APT) experiments. All liquid chromatograms were obtained on a HPLC Agilent 1200 machine with a variable UV detector. The instrument was fitted with a ZORBAX RX-SIL analytical column (4.6 mm x 250 mm, 5 μ) or semipreparative column (9.4 x 250 mm, 5 μ). All the gas chromatograms were obtained on GC Agilent 7890A machine. The instrument was fitted with a HP-1 19091Z-433 analytical column (length = 30 m, I.D. = 0.25 mm, film = 0.25 μm).

1.7.2. Experimental Procedures.

General Procedure for the Preparation of Tethered 1-Chloro-1,6-enynes (Method A): Cesium carbonate (4 mmol) and tetra-*n*-butylammonium fluoride trihydrate (1 mmol) were added to a solution of the requisite 1,6-enyne (2 mmol) in CCl_4 (3 mL) and the reaction mixture stirred for *ca.* 20-40 minutes at room temperature. The resulting mixture was then diluted by the addition of dichloromethane (25 mL), filtered through a short pad of celite and the filtrate concentrated *in vacuo* to afford a crude oil. Purification by flash chromatography (silica gel, eluting with diethyl ether/hexanes) afforded the desired 1-chloro-1,6-enyne.

General Procedure for the Preparation of Tethered 1-Chloro-1,6-enynes (Method B): a solution of the requisite 1,6-enyne (2 mmol) in THF (4 mL) was cooled to -78 °C under an argon atmosphere. LiHMDS (2.2 mL, 2.2 mmol, 1M solution in hexane) was added dropwise and the resulting suspension stirred for 20 minutes at -78 °C. Then, a solution of *p*-

toluenesulfonyl chloride (2.2 mmol) in THF (2 mL) was added dropwise and reaction stirred for 4 hours at -78 °C. The resulting suspension was allowed to warm at RT and quenched with brine (10 mL) and diethyl ether (10 mL) and extracted with diethyl ether (3 x 15 mL). The organic layer was dried over $MgSO_4$, filtered and concentrate *in vacuo* to afford a crude oil. Purification by flash chromatography (silica gel, eluting with diethyl ether/hexanes) afforded the desired 1-chloro-1,6-enyne

General Procedure for the Preparation of Tethered 1-Bromo-1,6-enynes: *N*-bromosuccinimide (1.3 eq.) and silver nitrate (0.13 mmol) were added to a solution of the requisite 1,6-enyne (1 mmol) in acetone (3 mL) and the reaction mixture stirred for *ca.* 3 hours minutes at room temperature. The resulting white suspension was filtered through a short pad of celite and the filtrate concentrated *in vacuo* to afford a crude oil. Purification by flash chromatography (silica gel, eluting with diethyl ether/hexanes) afforded the desired 1-bromo-1,6-enyne.

General Procedure for the Preparation of Tethered 1-Iodo-1,6-enynes: *N*-iodosuccinimide (1.2 eq.) and silver nitrate (0.12 mmol) were added to a solution of the requisite 1,6-enyne (1 mmol) in acetone (7 mL) and the reaction mixture stirred for *ca.* 2 hours at room temperature. The resulting white suspension was filtered through a short pad of celite and the filtrate concentrated *in vacuo* to afford a crude oil. Purification by flash chromatography (silica gel, eluting with diethyl ether/hexanes) afforded the 1-iodo-1,6-enyne.

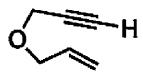

296

3-(Prop-2-ynyloxy)prop-1-ene.[179]

Colour and State: Pale yellow liquid.

^{1}H NMR (500 MHz, $CDCl_3$) δ 5.89 (ddt, *J* = 17.2, 10.4, 5.8 Hz, 1H), 5.30 (*app.* dq, *J* = 17.3, 1.6 Hz, 1H), 5.21 (*app.* dq, *J* = 10.4, 1.4 Hz, 1H), 4.14 (d, *J* = 2.4 Hz, 2H), 4.06 (*app.* dt, *J* = 5.8, 1.3 Hz, 2H), 2.42 (t, *J* = 2.4 Hz, 1H).

^{13}C NMR (125 MHz, $CDCl_3$) δ 133.94 (o), 118.10 (e), 79.75 (e), 74.52 (e), 70.68 (e), 57.16 (e).

IR (Neat) 3298 (w), 2856 (w), 2118 (w), 1648 (w), 1443 (w), 1075 (s), 925 (m) cm^{-1}.

HRMS (CI, $[M+NH_4]^+$) calcd for $C_6H_{12}NO$ 114.0913, found 114.0912.

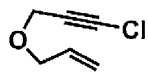

297

3-(3-Chloroprop-2-ynyloxy)prop-1-ene.

Synthesised by the general procedure for the preparation of tethered 1-chloro-1,6-enynes (Method A, yield = 53%).

Colour and State: Pale yellow liquid.

^{1}H NMR (500 MHz, $CDCl_3$) δ 5.90 (ddt, *J* = 16.5, 10.8, 5.5 Hz, 1H), 5.32 (d, *J* = 17.2 Hz, 1H), 5.23 (d, *J* = 10.4 Hz, 1H), 4.16 (s, 2H), 4.05 (d, *J* = 5.7 Hz, 2H).

^{13}C NMR (125 MHz, $CDCl_3$) δ 133.87 (o), 118.19 (e), 70.84 (e), 65.55 (e), 64.56 (e), 57.60 (e).

IR (Neat) 2854 (w), 2239 (w), 1648 (w), 1353 (m), 1096 (s), 924 (s) cm^{-1}.

HRMS (CI, $[M+NH_4]^+$) calcd for $C_6H_{11}{}^{35}ClNO$ 148.0524, found 148.0524.

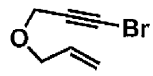

298

3-(3-Bromoprop-2-ynyloxy)prop-1-ene.[180]

Synthesised by the general procedure for the preparation of tethered 1-bromo-1,6-enynes (yield = 74%).

Colour and State: Pale yellow liquid.

^{1}H NMR (500 MHz, $CDCl_3$) δ 5.90 (ddt, J = 17.2, 10.5, 5.8 Hz, 1H), 5.32 (*app.* dq, J = 17.2, 1.6 Hz, 1H), 5.23 (*app.* dq, J = 10.4, 1.3 Hz, 1H), 4.18 (s, 2H), 4.06 (*app.* dt, J = 5.8, 1.3 Hz, 2H).

^{13}C NMR (125 MHz, $CDCl_3$) δ 133.86 (o), 118.23 (e), 76.30 (e), 70.87 (e), 58.20 (e), 46.12 (e).

IR (Neat) 2852 (w), 2214 (w), 1648 (w), 1351 (m), 1090 (vs), 926 (s) cm^{-1}.

HRMS (CI, $[M+NH_4]^+$) calcd for $C_6H_{11}{}^{79}BrNO$ 129.0019, found 129.0020.

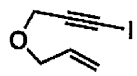

299

3-(3-Iodoprop-2-ynyloxy)prop-1-ene.

Synthesised by the general procedure for the preparation of tethered 1-iodo-1,6-enynes (yield = 82%).

Colour and State: yellow liquid.

^{1}H NMR (500 MHz, $CDCl_3$) δ 5.87 (ddt, J = 17.2, 10.6, 5.7 Hz, 1H), 5.29 (*app.* dq, J = 17.2, 1.4 Hz, 1H), 5.20 (*app.* dq, J = 10.4, 1.1 Hz, 1H), 4.27 (s, 2H), 4.03 (d, J = 5.8 Hz, 2H).

^{13}C NMR (125 MHz, $CDCl_3$) δ 133.77 (o), 118.13 (e), 90.48 (e), 70.74 (e), 58.73 (e), 3.14 (e).

IR (Neat) 3081 (w), 2850 (w), 2185 (w), 1711 (w), 1647 (w), 1349 (m), 1071 (s), 924 (m) cm^{-1}.

HRMS (CI, $[M+NH_4]^+$) calcd for $C_6H_{11}{}^{127}INO$ 239.9880, found 239.9881.

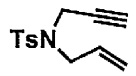

300

***N*-Allyl-4-methyl-*N*-(prop-2-ynyl)benzenesulfonamide.**[181]

Colour and State: White crystalline solid; mp = 60-62 °C.

^{1}H NMR (500 MHz, $CDCl_3$) δ 7.73 (d, *J* = 8.3 Hz, 2H), 7.29 (d, *J* = 8.2 Hz, 2H), 5.70 (ddt, *J* = 16.9, 10.3, 6.6 Hz, 1H), 5.29 (dd, *J* = 17.1, 1.4 Hz, 1H), 5.24 (dd, *J* = 10.1, 1.1 Hz, 1H), 4.09 (d, *J* = 2.5 Hz, 2H), 3.82 (d, *J* = 6.5 Hz, 2H), 2.42 (s, 3H), 2.00 (t, *J* = 2.5 Hz, 1H).

^{13}C NMR (125 MHz, $CDCl_3$) δ 143.70 (e), 136.14 (e), 132.00 (o), 129.61 (o), 127.88 (o), 120.13 (e), 76.62 (e), 73.84 (e), 49.11 (e), 35.88 (e), 21.67 (o).

IR (Neat) 3269 (m), 2908 (w), 2118.85 (w), 1644 (w), 1599 (w), 1325 (m), 1157 (s), 929 (s) cm^{-1}.

HRMS (ESI, $[M+Na]^+$) calcd for $C_{13}H_{15}NNaO_2S$ 272.0721, found 272.0721.

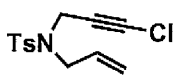

301

***N*-Allyl-*N*-(3-chloroprop-2-ynyl)-4-methylbenzenesulfonamide.**

Synthesised by the general procedure for the preparation of tethered 1-chloro-1,6-enynes (Method A, yield = 84%).

Colour and State: White crystalline solid; mp = 39-41 °C.

^{1}H NMR (500 MHz, $CDCl_3$) δ 7.71 (d, *J* = 8.1 Hz, 2H), 7.31 (d, *J* = 8.0 Hz, 2H), 5.70 (ddt, *J* = 17.0, 10.2, 6.5 Hz, 1H), 5.26 (*app.* dq, *J* = 17.1, 1.5 Hz, 1H), 5.22 (*app.* dq, *J* = 10.1, 1.3 Hz, 1H), 4.05 (s, 2H), 3.76 (d, *J* = 6.5 Hz, 2H), 2.41 (s, 3H).

^{13}C NMR (125 MHz, $CDCl_3$) δ 143.81 (e), 135.63 (e), 131.90 (o), 129.57 (o), 127.76 (o), 120.10 (e), 63.46 (e), 62.34 (e), 49.39 (e), 36.25 (e), 21.58 (o).

IR (Neat) 2907 (w), 2856 (w), 2244 (w), 1645 (w), 1598 (w), 1334 (s), 1163 (s), 933 (s) cm^{-1}.

HRMS (ESI, $[M+Na]^+$) calcd for $C_{13}H_{14}{}^{35}ClNNaO_2S$ 306.0331, found 306.0320.

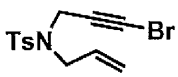

302

***N*-Allyl-*N*-(3-bromoprop-2-ynyl)-4-methylbenzenesulfonamide.**

Synthesised by the general procedure for the preparation of tethered 1-bromo-1,6-enynes (yield = 89%).

Colour and State: Yellow crystalline solid; mp = 63-65 °C.

^{1}H NMR (500 MHz, $CDCl_3$) δ 7.68 (d, *J* = 8.3 Hz, 2H), 7.28 (d, *J* = 8.2 Hz, 2H), 5.67 (ddt, *J* = 16.9, 10.2, 6.6 Hz, 1H), 5.24 (dd, *J* = 17.0, 1.2 Hz, 1H), 5.20 (d, *J* = 10.0 Hz, 1H), 4.04 (s, 2H), 3.74 (d, *J* = 6.5 Hz, 2H), 2.39 (s, 3H).

^{13}C NMR (125 MHz, $CDCl_3$) δ 143.71 (e), 135.47 (e), 131.78 (o), 129.49 (o), 127.66 (o), 119.99 (e), 72.76 (e), 49.30 (e), 45.01 (e), 36.87 (e), 21.48 (o).

IR (Neat) 2907 (w), 2856 (w), 2220 (w), 1645 (w), 1597 (w), 1423 (m), 1331 (s), 1161 (s), 891 (s) cm^{-1}.

HRMS (ESI, $[M+Na]^+$) calcd for $C_{13}H_{14}{}^{79}BrNNaO_2S$ 349.9826, found 349.9828.

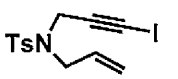

303

***N*-Allyl-*N*-(3-iodoprop-2-ynyl)-4-methylbenzenesulfonamide.**

Synthesised by the general procedure for the preparation of tethered 1-bromo-1,6-enynes (yield = 88%).

Colour and State: White crystalline solid; mp = 73-75 °C.

^{1}H NMR (500 MHz, $CDCl_3$) δ 7.71 (d, J = 8.1 Hz, 2H), 7.31 (d, J = 8.0 Hz, 2H), 5.70 (ddt, J = 17.0, 10.2, 6.5 Hz, 1H), 5.26 (*app.* dq, J = 17.1, 1.5 Hz, 1H), 5.22 (*app.* dq, J = 10.1, 1.3 Hz, 1H), 4.05 (s, 2H), 3.76 (d, J = 6.5 Hz, 2H), 2.41 (s, 3H).

^{13}C NMR (125 MHz, $CDCl_3$) δ 143.76 (e), 135.42 (e), 131.80 (o), 129.60 (o), 127.77 (o), 120.15 (e), 86.60 (e), 49.37 (e), 37.71 (e), 21.64 (o), 2.04 (e).

IR (Neat) 2912 (w), 2860 (w), 2184 (w), 1645 (w), 1648 (w), 1429 (m), 1318 (s), 1151 (s), 898 (s) cm^{-1}.

HRMS (ESI, $[M+Na]^+$) calcd for $C_{13}H_{14}INNaO_2S$ 397.9688, found 397.9688.

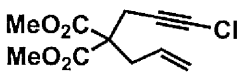

304

Dimethyl 2-allyl-2-(3-chloroprop-2-ynyl)malonate.

Synthesised by the general procedure for the preparation of tethered 1-chloro-1,6-enynes (Method B, yield = 91%).

Colour and State: Colourless oil.

^{1}H NMR (500 MHz, $CDCl_3$) δ 5.58 (ddt, J = 17.2, 10.0, 7.5 Hz, 1H), 5.15 (*app.* dq, J = 17.0, 1.3 Hz, 1H), 5.11 (*app.* dq, J = 10.1, 1.0 Hz, 1H), 3.72 (s, 6H), 2.77 (s, 2H), 2.75 (d, J = 7.5 Hz, 2H).

^{13}C NMR (125 MHz, $CDCl_3$) δ 170.14 (e), 131.63 (o), 120.10 (e), 64.26 (e), 60.65 (e), 56.94 (e), 52.91 (o), 36.79 (e), 23.13 (e).

IR (Neat) 2955 (w), 2247 (w), 1735 (vs), 1642 (w), 1436 (m), 1200 (s) cm^{-1}.

HRMS (ESI, $[M+Na]^+$) calcd for $C_{11}H_{13}{}^{35}ClNaO_4$ 267.0400, found 267.0397.

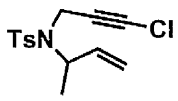

314

***N*-(But-3-en-2-yl)-*N*-(3-chloroprop-2-ynyl)-4-methylbenzenesulfonamide.**

Synthesised by the general procedure for the preparation of tethered 1-chloro-1,6-enynes (Method A, yield = 79%).

Colour and State: colourless oil.

^{1}H NMR (500 MHz, $CDCl_3$) δ 7.76 (d, J = 8.1 Hz, 2H), 7.28 (d, J = 7.9 Hz, 2H), 5.70 (ddd, J = 17.3, 10.6, 4.6 Hz, 1H), 5.15 (d, J = 10.5 Hz, 1H), 5.12 (d, J = 17.3 Hz, 1H), 4.58-4.54 (m, 1H), 4.11 (d, A of AB, J_{AB} = 18.4 Hz, 1H), 3.85 (d, B of AB, J_{AB} = 18.4 Hz, 1H), 2.41 (s, 3H), 1.21 (d, J = 7.0 Hz, 3H).

^{13}C NMR (125 MHz, $CDCl_3$) δ 143.48 (e), 137.72 (e), 137.35 (o), 129.53 (o), 127.50 (o), 117.18 (e), 65.67 (e), 62.31 (e), 54.68 (o), 32.66 (e), 21.61 (o), 16.91 (o).

IR (Neat) 2983 (w), 2243 (w), 1639 (w), 1597 (w), 1351 (m), 1331 (s), 1145 (s) cm^{-1}.

HRMS (CI, $[M+H]^+$) calcd for $C_{14}H_{17}{}^{35}ClNO_2S$ 298.0669, found 298.0659.

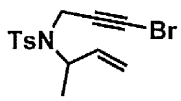

315

***N*-(But-3-en-2-yl)-*N*-(3-bromoprop-2-ynyl)-4-methylbenzenesulfonamide.**

Synthesised by the general procedure for the preparation of tethered 1-bromo-1,6-enynes (yield = 89%).

Colour and State: off-white solid. mp = 54-56 °C.

^{1}H NMR (500 MHz, $CDCl_3$) δ 7.76 (d, J = 8.0 Hz, 2H), 7.29 (d, J = 8.0 Hz, 2H), 5.70 (ddd, J = 17.2, 10.8, 4.7 Hz, 1H), 5.15 (d, J = 10.1 Hz, 1H), 5.13 (d, J = 17.1 Hz, 1H), 4.59-4.52 (m, 1H), 4.13 (d, A of AB, J_{AB} = 18.5 Hz, 1H), 3.87 (d, B of AB, J_{AB} = 18.5 Hz, 1H), 2.41 (s, 3H), 1.21 (d, J = 7.0 Hz, 3H).

^{13}C NMR (125 MHz, $CDCl_3$) δ 143.45 (e), 137.73 (e), 137.38 (o), 129.52 (o), 127.55 (o), 117.17 (e), 76.20 (e), 54.73 (o), 44.06 (e), 33.38 (e), 21.62 (o), 16.92 (o).

IR (Neat) 2981 (w), 2926 (w), 2218 (w), 1639 (w), 1597 (w), 1351 (m), 1330 (s), 1143 (s) cm^{-1}.

HRMS (ESI, $[M+Na]^+$) calcd for $C_{14}H_{16}{}^{79}BrNNaO_2S$ 363.9983, found 363.9988.

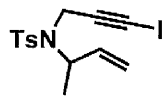

316

***N*-(But-3-en-2-yl)-*N*-(3-iodoprop-2-ynyl)-4-methylbenzenesulfonamide.**

Synthesised by the general procedure for the preparation of tethered 1-iodo-1,6-enynes (yield = 83%).

Colour and State: white solid. mp = 69-71 °C.

^{1}H NMR (500 MHz, $CDCl_3$) δ 7.75 (d, J = 8.4 Hz, 2H), 7.29 (d, J = 8.1 Hz, 2H), 5.70 (ddd, J = 17.3, 10.6, 4.6 Hz, 1H), 5.16-5.09 (m, 2H), 4.59-4.52 (m, 1H), 4.24 (d, A of AB, J_{AB} = 18.6 Hz, 1H), 3.98 (d, B of AB, J_{AB} = 18.6 Hz, 1H), 2.41 (s, 3H), 1.20 (d, J = 7.0 Hz, 3H).

^{13}C NMR (125 MHz, $CDCl_3$) δ 143.39 (e), 137.65 (e), 137.36 (o), 129.52 (o), 127.57 (o), 117.13 (e), 90.03 (e), 54.73 (o), 34.13 (e), 21.63 (o), 16.90 (o), 1.26 (e).

IR (Neat) 2980 (w), 2929 (w), 2188 (w), 1598 (w), 1351 (m), 1324 (s), 1154 (s), 893 (s) cm^{-1}.

HRMS (ESI, $[M+Na]^+$) calcd for $C_{14}H_{16}INNaO_2S$ 411.9844, found 411.9846.

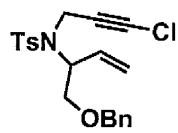

319

***N*-(1-(Benzyloxy)but-3-en-2-yl)-*N*-(3-chloroprop-2-ynyl)-4-methylbenzenesulfonamide.**

Synthesised by the general procedure for the preparation of tethered 1-chloro-1,6-enynes (Method A, yield = 75%).

Colour and State: Pale yellow oil.

^{1}H NMR (500 MHz, $CDCl_3$) δ 7.78 (d, J = 8.3 Hz, 2H), 7.38-7.25 (m, 5H), 7.22 (d, J = 8.1 Hz, 2H), 5.81 (ddd, J = 17.4, 10.6, 5.4 Hz, 1H), 5.26 (*app.* dt, J = 10.3, 1.2 Hz, 1H), 5.23 (*app.* dt, J = 17.2, 1.3 Hz, 1H), 4.72-4.68 (m, 1H), 4.48 (d, A of AB, J_{AB} = 11.8 Hz, 1H), 4.43 (d, B of AB, J_{AB} = 11.8 Hz, 1H), 4.24 (d, A of AB, J_{AB} = 18.5 Hz, 1H), 4.06 (d, B of AB, J_{AB} = 18.5 Hz, 1H), 3.69-3.64 (m, 2H), 2.42 (s, 3H).

^{13}C NMR (125 MHz, $CDCl_3$) δ 143.39 (e), 137.78 (e), 137.50 (e), 133.16 (o), 129.34 (o), 128.45 (o), 127.83 (o), 127.79 (o), 127.74 (o), 119.00 (e), 73.25 (e), 70.45 (e), 65.44 (e), 62.19 (e), 58.98 (o), 34.04 (e), 21.67 (o).

IR (Neat) 3028 (w), 2862 (w), 2244 (w), 1598 (w), 1336 (s), 1157 (s), 1092 (s) cm^{-1}.

HRMS (ESI, $[M+Na]^+$) calcd for $C_{21}H_{22}{}^{35}ClNNaO_3S$ 426.0907, found 426.0914.

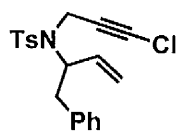

320

***N*-(3-Chloroprop-2-ynyl)-4-methyl-*N*-(1-phenylbut-3-en-2-yl)benzenesulfonamide.**

Synthesised by the general procedure for the preparation of tethered 1-chloro-1,6-enynes (Method A, yield = 86%).

Colour and State: Pale yellow oil.

^{1}H NMR (500 MHz, $CDCl_3$) δ 7.64 (d, J = 8.2 Hz, 2H), 7.28-7.14 (m, 5H), 7.22 (d, J = 8.1 Hz, 2H), 5.77 (ddd, J = 17.3, 10.5, 5.8 Hz, 1H), 5.15 (d, J = 10.5 Hz, 1H), 5.10 (d, J = 17.3 Hz, 1H), 4.71 (*app.* q, J = 7.4 Hz, 1H), 4.17 (d, A of AB, J_{AB} = 18.5 Hz, 1H), 3.95 (d, B of AB, J_{AB} = 18.5 Hz, 1H), 2.96 (d, A of AB, J_{AB} = 14.3 Hz, 1H), 2.92 (d, B of AB, J_{AB} = 14.0 Hz, 1H), 2.40 (s, 3H).

^{13}C NMR (125 MHz, $CDCl_3$) δ 143.47 (e), 137.68 (e), 137.53 (e), 134.81 (o), 129.49 (o), 129.42 (o), 128.57 (o), 127.66 (o), 126.67 (o), 118.72 (e), 65.48 (e), 62.80 (e), 61.31 (o), 38.98 (e), 33.60 (e), 21.65 (o).

IR (Neat) 3028 (w), 2925 (w), 2245 (w), 1598 (w), 1496 (w), 1337 (s), 1164 (s), 1093 (s), 700 (m) cm^{-1}.

HRMS (ESI, $[M+Na]^+$) calcd for $C_{20}H_{20}{}^{35}ClNNaO_2S$ 396.0801, found 396.0815.

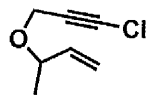

289

3-(3-Chloroprop-2-ynyloxy)but-1-ene.

Synthesised by the general procedure for the preparation of tethered 1-chloro-1,6-enynes (Method A, yield = 61%).

Colour and State: Pale yellow liquid.

^{1}H NMR (500 MHz, $CDCl_3$) δ 5.68 (ddd, J = 17.5, 10.1, 7.6 Hz, 1H), 5.23 (d, J = 17.3 Hz, 1H), 5.19 (d, J = 10.4 Hz, 1H), 4.16 (d, A of AB, J_{AB} = 15.5 Hz, 1H), 4.04 (d, B of AB, J_{AB} = 15.6 Hz, 1H), 4.03-4.00 (m, 1H), 1.27 (d, J = 6.4 Hz, 3H).

^{13}C NMR (125 MHz, $CDCl_3$) δ 139.06 (o), 117.47 (e), 76.18 (o), 65.96 (e), 63.93 (e), 55.62 (e), 21.30 (o).

IR (Neat) 2980 (w), 2857 (w), 2239 (w), 1372 (w), 1085 (s), 928 (m) cm^{-1}.

HRMS (CI, $[M+NH_4]^+$) calcd for $C_7H_{13}{}^{35}ClNO$ 162.0680, found 162.0679

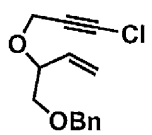

321

((2-(3-Chloroprop-2-ynyloxy)but-3-enyloxy)methyl)benzene.

Synthesised by the general procedure for the preparation of tethered 1-chloro-1,6-enynes (Method A, yield = 81%).

Colour and State: Pale yellow oil.

^{1}H NMR (500 MHz, $CDCl_3$) δ 7.36-7.26 (m, 5H), 5.74 (ddd, J = 17.5, 10.3, 7.5 Hz, 1H), 5.36 (*app.* dt, J = 17.3, 1.4 Hz, 1H), 5.32 (d, J = 10.5 Hz, 1H), 4.61 (d, A of AB, J_{AB} = 12.2 Hz, 1H), 4.57 (d, B of AB, J_{AB} = 12.1 Hz, 1H), 4.27 (d, A of AB, J_{AB} = 15.6 Hz, 1H), 4.14 (d, B of AB, J_{AB} = 15.6 Hz, 1H), 4.18-4.12 (m, 1H), 3.57 (dd, A of ABX, J_{AB} = 10.4 Hz, J_{AX} = 6.3 Hz, 1H), 3.53 (dd, B of ABX, J_{AB} = 10.4 Hz, J_{BX} = 4.2 Hz, 1H).

^{13}C NMR (125 MHz, $CDCl_3$) δ 138.21 (e), 134.68 (o), 128.48 (o), 127.82 (o), 127.73 (o), 119.58 (e), 79.11 (o), 73.51 (e), 72.75 (e), 65.79 (e), 64.28 (e), 56.30 (e).

IR (Neat) 3030 (w), 2857 (w), 2238 (w), 1496 (w), 1362 (w), 1087 (s), 930 (m), 736 (m) cm^{-1}.

HRMS (ESI, $[M+Na]^+$) calcd for $C_{14}H_{15}{}^{35}ClNaO_2$ 273.0658, found 273.0656.

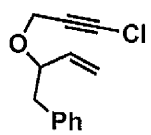

322

(2-(3-Chloroprop-2-ynyloxy)but-3-enyl)benzene.

Synthesised by the general procedure for the preparation of tethered 1-chloro-1,6-enynes (Method A, yield = 87%).

Colour and State: Yellow liquid.

^{1}H NMR (500 MHz, $CDCl_3$) δ 7.30-7.20 (m, 5H), 5.67 (ddd, J = 17.3, 10.0, 7.5 Hz, 1H), 5.21 (dd, J = 10.4, 1.0 Hz, 1H), 5.17 (dd, J = 17.3, 0.8 Hz, 1H), 4.16 (d, A of AB, J_{AB} = 15.7 Hz, 1H), 4.10 (*app.* q, J = 6.9 Hz, 1H), 4.02 (d, B of AB, J_{AB} = 15.6 Hz, 1H), 2.96 (dd, A of ABX, J_{AB} = 13.8 Hz, J_{AX} = 6.8 Hz, 1H), 2.80 (dd, B of ABX, J_{AB} = 13.8 Hz, J_{BX} = 6.4 Hz, 1H).

^{13}C NMR (125 MHz, $CDCl_3$) δ 137.86 (e), 137.10 (o), 129.68 (o), 128.27 (o), 126.38 (o), 118.68 (e), 81.08 (o), 65.85 (e), 63.95 (e), 55.94 (e), 42.02 (e).

IR (Neat) 3029 (w), 2855 (w), 2238 (w), 1605 (w), 1496 (w), 1081 (s), 699 (s) cm^{-1}.

HRMS (ESI, $[M+Na]^+$) calcd for $C_{13}H_{13}{}^{35}ClNaO$ 243.0553, found 243.0564.

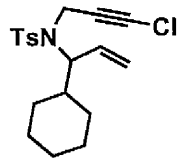

333

***N*-(3-Chloroprop-2-ynyl)-*N*-(1-cyclohexylallyl)-4-methylbenzenesulfonamide.**

Synthesised by the general procedure for the preparation of tethered 1-chloro-1,6-enynes (Method A, yield = 80%).

Colour and State: colourless oil.

^{1}H NMR (500 MHz, $CDCl_3$) δ 7.71 (d, J = 8.3 Hz, 2H), 7.25 (d, J = 8.2 Hz, 2H), 5.66 (ddd, J = 17.2, 10.2, 8.7 Hz, 1H), 5.05 (dd, J = 10.4, 0.5 Hz, 1H), 4.94 (d, J = 17.1 Hz, 1H), 4.05 (d, A of AB, J_{AB} = 18.5 Hz, 1H), 3.99 (*app* t, J = 9.5 Hz, 1H), 3.93 (d, B of AB, J_{AB} = 18.5 Hz, 1H), 2.40 (s, 3H), 1.92-1.48 (m, 6H), 1.28-0.77 (m, 5H).

^{13}C NMR (125 MHz, $CDCl_3$) δ 143.26 (e), 137.76 (e), 134.00 (o), 129.30 (o), 127.75 (o), 119.33 (e), 66.40 (o), 65.26 (e), 62.36 (o), 38.86 (o), 33.45 (e), 30.65 (e), 30.39 (e), 26.35 (e), 26.17 (e), 25.99 (e), 21.61 (o).

IR (Neat) 2924 (w), 2852 (w), 2245 (w), 1598 (w), 1336 (m), 1333 (s), 1092 (s) cm^{-1}.

HRMS (ESI, $[M+Na]^+$) calcd for $C_{19}H_{24}{}^{35}ClNNaO_2S$ 390.1084, found 390.1092.

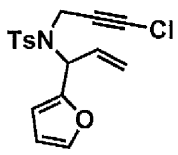

334

***N*-(3-Chloroprop-2-ynyl)-*N*-(1-(furan-2-yl)allyl)-4-methylbenzenesulfonamide.**

Synthesised by the general procedure for the preparation of tethered 1-chloro-1,6-enynes (Method A, yield = 86%).

Colour and State: off-white solid. mp = 60-62 °C.

^{1}H NMR (500 MHz, $CDCl_3$) δ 7.77 (d, J = 8.3 Hz, 2H), 7.30-7.22 (m, 3H), 6.26 (dd, J = 3.2, 2.0 Hz, 1H), 6.17 (d, J = 3.4 Hz, 1H), 6.04 (ddd, J = 16.6, 10.9, 5.5 Hz, 1H), 5.73 (d, J = 5.3

Hz, 1H), 5.36-5.30 (m, 2H), 3.99 (d, A of AB, J_{AB} = 18.5 Hz, 1H), 3.94 (d, B of AB, J_{AB} = 18.4 Hz, 1H), 2.40 (s, 3H).

^{13}C NMR (125 MHz, $CDCl_3$) δ 150.46 (e), 143.49 (e), 142.84 (o), 137.24 (o), 132.35 (o), 129.25 (o), 127.82 (o), 119.24 (o), 110.39 (o), 109.90 (o), 64.29 (e), 61.82 (e), 56.99 (o), 34.05 (e), 21.55 (o).

IR (Neat) 2925 (w), 2246 (w), 1598 (w), 1498 (w), 1334 (m), 1157 (s), 1091 (m) cm^{-1}.

HRMS (ESI, $[M+Na]^+$) calcd for $C_{17}H_{16}{}^{35}ClNNaO_3S$ 372.0437, found 372.0430.

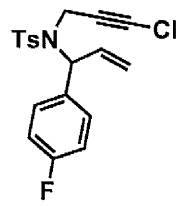

335

***N*-(3-chloroprop-2-ynyl)-*N*-(1-(4-fluorophenyl)allyl)-4-methylbenzenesulfonamide.**

Synthesised by the general procedure for the preparation of tethered 1-chloro-1,6-enynes (Method A, yield = 72%).

Colour and State: pale yellow oil.

^{1}H NMR (500 MHz, $CDCl_3$) δ 7.77 (d, J = 8.3 Hz, 2H), 7.28-7.20 (m, 4H), 6.99-6.96 (m, 2H), 6.04 (ddd, J = 17.2, 10.2, 7.0 Hz, 1H), 5.58 (d, J = 7.1 Hz, 1H), 5.24 (d, J = 10.4 Hz, 1H), 5.12 (d, J = 17.1 Hz, 1H), 4.04 (d, A of AB, J_{AB} = 18.5 Hz, 1H), 3.81 (d, B of AB, J_{AB} = 18.4 Hz, 1H), 2.39 (s, 3H).

^{13}C NMR (125 MHz, $CDCl_3$) δ 162.32 (e, d, J_{CF} = 252.8 Hz), 143.53 (e), 137.25 (e), 133.55 (e, d, J_{CF} = 3.2 Hz), 133.42 (o), 132.35 (o), 129.86 (o, d, J_{CF} = 8.1 Hz), 127.64 (o), 119.45 (e), 115.27 (o, d, J_{CF} = 21.4 Hz), 64.77 (e), 62.67 (e), 62.55 (o), 34.04 (e), 21.40 (o).

IR (Neat) 2925 (w), 2245 (w), 1601 (w), 1508 (w), 1349 (m), 1157 (s), 1092 (m), 906.75 cm^{-1}.

HRMS (ESI, $[M+Na]^+$) calcd for $C_{19}H_{17}{}^{35}ClFNNaO_3S$ 400.0550, found 400.0544.

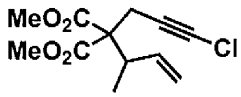

336

Dimethyl 2-(but-3-en-2-yl)-2-(3-chloroprop-2-ynyl)malonate.

Synthesised by the general procedure for the preparation of tethered 1-chloro-1,6-enynes (Method B, yield = 92%).

Colour and State: pale yellow oil.

^{1}H NMR (500 MHz, $CDCl_3$) δ 5.67 (ddd, J = 17.0, 10.2, 8.7 Hz, 1H), 5.12-5.06 (m, 1H), 5.02 (dd, J = 10.3, 1.5 Hz, 1H), (3.70, s, 3H), (3.69, s, 3H), 3.04-2.97 (m, 1H), 2.75 (d, A of AB, J_{AB} = 17.1 Hz, 1H), 2.71 (d, B of AB, J_{AB} = 16.9 Hz, 1H), 1.09 (d, J = 7.0 Hz, 3H).

^{13}C NMR (125 MHz, $CDCl_3$) δ 169.95 (e), 169.82 (e), 138.24 (o), 116.85 (e), 64.89 (e), 60.32 (e), 60.24 (e), 52.42 (o), 41.40 (o), 24.05 (e), 16.36 (o).

IR (Neat) 2954 (w), 2247 (w), 1731(s), 1435 (m), 1270 (s), 1226 (s), 1202 (m), 1055 (m), 922 (m) cm^{-1}.

HRMS (CI, $[M+H]^+$) calcd for $C_{12}H_{16}{}^{35}ClO_4$ 259.0670, found 259.0664.

General Procedure for the Room Temperature Rhodium(I)-Catalysed Pauson-Khand Reaction (Method A, CO:Ar = 100:0, 1 atm): $[Rh(CO)_2Cl]_2$ (3.9 mg, 0.01 mmol) was weighed into a 10 mL round bottom flask under an atmosphere of argon and the flask was evacuated and backfilled three times with carbon monoxide. Freshly distilled *p*-xylene (2 mL) was added to the flask fitted with a carbon monoxide balloon (1 atm.) and the resulting solution stirred in a preheated 25 °C bath for *ca.* 10 minutes. The requisite 1-halo-1,6-enyne was added in one portion *via* a tared syringe and the mixture was allowed to stir at 25 °C until the reaction was complete (t.l.c. control). The reaction mixture was concentrated *in vacuo* and purified by flash chromatography (silica gel, eluting *via* a gradient 15-40% diethyl ether/hexane) to furnish the desired PK adduct.

General Procedure for the Room Temperature Rhodium(I)-Catalysed Pauson-Khand Reaction (Method B, CO:Ar = 10:90, 1 atm): $[Rh(CO)_2Cl]_2$ (3.9 mg, 0.01 mmol) was weighed into a 10 mL round bottom flask under an atmosphere of argon and the flask was evacuated and backfilled three times with a balloon containing a mixture of CO:Ar = 10:90. Freshly distilled *p*-xylene (2 mL) was added to the flask fitted with a balloon containing a mixture of CO:Ar = 10:90 (1 atm) and the resulting solution stirred in a preheated 25 °C bath for *ca.* 10 minutes. The requisite 1-halo-1,6-enyne was added in one portion *via* a tared syringe and the mixture was allowed to stir at 25 °C until the reaction was complete (t.l.c. control). The reaction mixture was concentrated *in vacuo* and purified by flash chromatography (silica gel, eluting *via* a gradient 15-40% diethyl ether/hexane) to furnish the desired PK adduct.

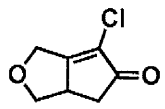

306

6-Chloro-3a,4-dihydro-1*H*-cyclopenta[*c*]furan-5(3*H*)-one.

Synthesised by the general procedure for the room temperature rhodium(I)-catalysed Pauson-Khand reaction (Method A, CO:Ar = 100:0, 1 atm, t = 22 h, yield = 74%).

Colour and State: pale yellow oil.

^{1}H NMR (500 MHz, $CDCl_3$) δ 4.67 (d, A of AB, J_{AB} = 16.6 Hz, 1H), 4.57 (d, B of AB, J_{AB} = 16.5 Hz, 1H), 4.36-4.34 (m, 1H), 3.35-3.26 (m, 2H), 2.82 (dd, A of ABX, J_{AB} = 18.1 Hz, J_{AX} = 5.7 Hz, 1H), 2.28 (dd, B of ABX, J_{AB} = 18.2 Hz, J_{BX} = 1.8 Hz, 1H).

^{13}C NMR (125 MHz, $CDCl_3$) δ 200.45 (e), 175.60 (e), 127.26 (e), 71.99 (e), 65.22 (e). 43.44 (o), 37.96 (e).

IR (Neat) 2919 (w), 2251 (w), 1729 (s), 1662 (m), 1024 (s), 952 (s) cm^{-1}.

HRMS (CI, $[M+H]^+$) calcd for $C_7H_8{}^{35}ClO_2$ 159.0207, found 159.0203.

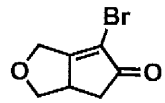

307

6-Bromo-3a,4-dihydro-1*H*-cyclopenta[*c*]furan-5(3*H*)-one.

Synthesised by the general procedure for the room temperature rhodium(I)-catalysed Pauson-Khand reaction (Method A, CO:Ar = 100:0, 1 atm, t = 24 h, yield = 39%).

Colour and State: Yellow oil.

^{1}H NMR (500 MHz, $CDCl_3$) δ 4.66 (d, A of AB, J_{AB} = 16.7 Hz, 1H), 4.50 (d, B of AB, J_{AB} = 16.6 Hz, 1H), 4.40-4.35 (m, 1H), 3.33-3.29 (m, 2H), 2.85 (dd, A of ABX, J_{AB} = 18.2 Hz, J_{AX} = 5.3 Hz, 1H), 2.29 (dd, B of ABX, J_{AB} = 17.8 Hz, J_{AX} = 1.8 Hz, 1H).

^{13}C NMR (125 MHz, $CDCl_3$) δ 201.10 (e), 180.00 (e), 117.01 (e), 72.03 (e), 66.04 (e). 45.33 (o), 37.90 (e).

IR (Neat) 2911 (w), 2852 (w), 1723 (s), 1655 (s), 1407 (w), 1122 (m), 1025 (s), 904 (m) cm^{-1}.

HRMS (ESI, $[M+Na]^+$) calcd for $C_7H_7{}^{79}BrNaO_2$ 224.9527, found 224.9528.

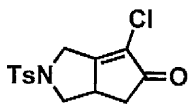

310

6-Chloro-2-tosyl-2,3,3a,4-tetrahydrocyclopenta[*c*]pyrrol-5(1*H*)-one.

Synthesised by the general procedure for the room temperature rhodium(I)-catalysed Pauson-Khand reaction (Method A, CO:Ar = 100:0, 1 atm, t = 27 h, yield = 81%).

Colour and State: pale yellow oil.

^{1}H NMR (500 MHz, $CDCl_3$) δ 7.72 (d, J = 8.2 Hz, 2H), 7.35 (d, J = 8.1 Hz, 2H), 4.34 (d, A of AB, J_{AB} = 17.2 Hz, 1H), 4.06-4.03 (m, 1H), 4.03 (d, B of AB, J_{AB} = 17.4 Hz, 1H), 3.21-3.15 (m, 1H), 2.76 (dd, A of ABX, J_{AB} = 18.2 Hz, J_{AX} = 6.4 Hz, 1H), 2.62 (dd, B of ABX, J_{AB} = 11.0 Hz, J_{BX} = 9.6 Hz, 1H), 2.44 (s, 3H), 2.18 (dd, B of ABX, J_{AB} = 18.2 Hz, J_{BX} = 2.9 Hz, 1H).

^{13}C NMR (125 MHz, $CDCl_3$) δ 199.09 (e), 170.70 (e), 144.53 (e), 133.26 (e), 130.25 (o), 128.69 (e), 127.59 (o), 52.69 (e), 47.17 (e), 41.60 (o), 38.50 (e), 21.71 (o).

IR (Neat) 2923 (w), 1732 (vs), 1667 (s), 1597 (m), 1345 (vs), 1161 (vs) cm^{-1}.

HRMS (CI, $[M+H]^+$) calcd for $C_{14}H_{15}{}^{35}ClNO_3S$ 312.0456, found 312.0461.

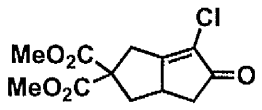

313

Dimethyl 6-chloro-5-oxo-3,3a,4,5-tetrahydropentalene-2,2(1*H*)-dicarboxylate.

Synthesised by the general procedure for the room temperature rhodium(I)-catalysed Pauson-Khand reaction (Method A, CO:Ar = 100:0, 1 atm, t = 44 h, yield = 74%).

Colour and State: yellow oil.

^{1}H NMR (500 MHz, $CDCl_3$) δ 3.80 (s, 3H), 3.77 (s, 3H), 3.38 (d, A of AB, J_{AB} = 19.7 Hz, 1H), 3.31 (d, B of AB, J_{AB} = 19.6 Hz, 1H), 3.16-3.10 (m, 1H), 2.84 (dd, A of ABX, J_{AB} = 12.9 Hz, J_{AX} = 7.3 Hz, 1H), 2.81 (ddd, A of ABMX, J_{AB} = 18.2 Hz, J_{AM} = 6.3 Hz, J_{AX} = 0.8 Hz, 1H), 2.25 (dd, B of ABX, J_{AB} = 18.2 Hz, J_{AX} = 2.9 Hz, 1H), 1.78 (*app.* t, J = 12.8 Hz, 1H).

^{13}C NMR (125 MHz, $CDCl_3$) δ 200.78 (e), 176.93 (e), 171.68 (e), 170.86 (e), 127.81 (e), 60.60 (e), 53.61 (o), 53.46 (o), 42.59 (o), 40.55 (e), 39.36 (e), 34.56 (e).

IR (Neat) 2956 (m), 2925 (w), 1733 (vs), 1655 (s), 1262 (s), 955 (m) cm^{-1}.

HRMS (CI, $[M+H]^+$) calcd for $C_{12}H_{14}{}^{35}ClO_5$ 273.0524, found 273.0531.

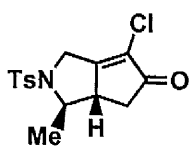

317

(3*R,3a*S**)-6-Chloro-3-methyl-2-tosyl-2,3,3a,4-tetrahydrocyclopenta[*c*]pyrrol-5(1*H*)-one.**

Synthesised by the general procedure for the room temperature rhodium(I)-catalysed Pauson-Khand reaction (Method A, CO:Ar = 100:0, 1 atm, t = 27 h, yield = 80%). *Selectivity:* **317/318** = 97:3.

Synthesised by the general procedure for the room temperature rhodium(I)-catalysed Pauson-Khand reaction (Method B, CO:Ar = 10:90, 1 atm, t = 27 h, yield = 69%). *Selectivity:* **317/318** = 85:15.

Colour and State: pale yellow oil.

HPLC analysis (25 cm x 9.4 mm ZORBAX RX-SIL), 7% isopropanol/hexane at 1.5 mL/min, 230 nm, T = 20 °C; t_R (*major*) 29.5 min, t_R (*minor*) 30.5 min.

^{1}H NMR (500 MHz, $CDCl_3$) δ 7.74 (d, J = 8.3 Hz, 2H), 7.32 (d, J = 8.2 Hz, 2H), 4.33-4.27 (m, 1H), 4.28 (d, A of AB, J_{AB} = 17.6 Hz, 1H), 4.20 (d, B of AB, J_{AB} = 17.5 Hz, 1H), 2.90 (dddd, J = 9.6, 6.5, 3.3, 1.6 Hz, 1H), 2.54 (dd, A of ABX, J_{AB} = 18.6 Hz, J_{AX} = 6.6 Hz, 1H), 2.41 (s, 3H), 2.20 (dd, B of ABX, J_{AB} = 18.6 Hz, J_{BX} = 3.0 Hz, 1H), 1.01 (d, J = 6.8 Hz, 3H).

^{13}C NMR (125 MHz, $CDCl_3$) δ 199.95 (e), 170.82 (e), 144.22 (e), 135.52 (e), 130.20 (o), 128.11 (e), 127.12 (o), 56.85 (o), 45.76 (e), 45.01 (o), 36.02 (e), 21.62 (o), 16.05 (o).

IR (Neat) 2978 (w), 2929 (w), 1731 (vs), 1669 (m), 1598 (m), 1346 (s), 1162 (s), 1094 (s) cm^{-1}.

HRMS (CI, $[M+NH_4]^+$) calcd for $C_{15}H_{20}{}^{35}ClN_2O_3S$ 343.0883, found 343.0876.

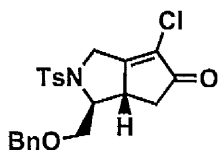

323

(3*S,3a*S**)-3-(Benzyloxymethyl)-6-chloro-3a,4-dihydro-1*H*-cyclopenta[*c*]furan-5(3*H*)-one.**

Synthesised by the general procedure for the room temperature rhodium(I)-catalysed Pauson-Khand reaction (Method A, CO:Ar = 100:0, 1 atm, t = 27 h, yield = 73%). *Selectivity:* **323/324** = ≥99:1.

Synthesised by the general procedure for the room temperature rhodium(I)-catalysed Pauson-Khand reaction (Method B, CO:Ar = 10:90, 1 atm, t = 27 h, yield = 59%). *Selectivity:* **323/324** = 87:13.

Colour and State: Yellow oil.

HPLC analysis (25 cm x 4.9 mm ZORBAX RX-SIL), 2% isopropanol/hexane at 1 mL/min, 230 nm, T = 22 °C; t_R (*major*) 37.5 min, t_R (*minor*) 13.5 min.

^{1}H NMR (500 MHz, $CDCl_3$) δ 7.75 (d, J = 8.3 Hz, 2H), 7.34-7.27 (m, 5H), 7.12-7.11 (m, 2H), 4.35 (d, A of AB, J_{AB} = 17.4 Hz, 1H), 4.34 (d, A of AB, J_{AB} = 11.5 Hz, 1H), 4.30 (d, B of AB, J_{AB} = 11.6 Hz, 1H), 4.25-4.22 (m, 1H), 4.21 (d, B of AB, J_{AB} = 17.7 Hz, 1H), 3.60 (dd, A of ABX, J_{AB} = 10.3 Hz, J_{AX} = 2.5 Hz, 1H) 3.56 (dd, B of ABX, J_{AB} = 10.3 Hz, J_{BX} = 5.3 Hz, 1H), 2.91 (dddd, J = 10.0, 6.7, 3.4, 1.7 Hz, 1H), 2.58 (dd, A of ABX, J_{AB} = 18.3 Hz, J_{AX} = 6.4 Hz, 1H), 2.49 (dd, B of ABX, J_{AB} = 18.3 Hz, J_{BX} = 3.4 Hz, 1H), 2.43 (s, 3H).

^{13}C NMR (125 MHz, $CDCl_3$) δ 200.10 (e), 171.66 (e), 144.39 (e), 137.18 (e), 135.40 (e), 135.37 (e), 130.28 (o), 128.65 (o), 128.07 (o), 127.64 (o), 127.24 (o), 73.74 (e), 70.13 (e), 60.09 (o), 47.67 (e), 44.11 (o), 36.70 (e), 21.72 (o).

IR (Neat) 2862 (w), 1726 (s), 1670 (m), 1598 (w), 1346 (m), 1161 (s), 1093 (s), 679 (m) cm^{-1}.

HRMS (ESI, $[M+Na]^+$) calcd for $C_{22}H_{22}{}^{35}ClNNaO_4S$ 454.0856, found 454.0848.

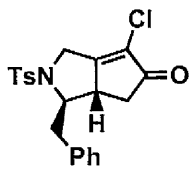

325

(3*R,3a*S**)-3-Benzyl-6-chloro-3a,4-dihydro-1*H*-cyclopenta[*c*]furan-5(3*H*)-one 2ai.**

Synthesised by the general procedure for the room temperature rhodium(I)-catalysed Pauson-Khand reaction (Method A, CO:Ar = 100:0, 1 atm, t = 27 h, yield = 84%). *Selectivity:* **325/326** = ≥99:1.

Synthesised by the general procedure for the room temperature rhodium(I)-catalysed Pauson-Khand reaction (Method B, CO:Ar = 10:90, 1 atm, t = 27 h, yield = 63%). *Selectivity:* **325/326** = 76:23.

Colour and State: Yellow oil.

HPLC analysis (25 cm x 4.9 mm ZORBAX RX-SIL), 2% isopropanol/hexane at 0.8 mL/min, 230 nm, T = 22 °C; t_R (*major*) 21.9 min, t_R (*minor*) 19.4 min.

^{1}H NMR (500 MHz, $CDCl_3$) δ 7.67 (d, J = 8.3 Hz, 2H), 7.38-7.17 (m, 5H), 7.32 (d, J = 8.1 Hz, 2H), 4.62 (*app.* q, J = 7.4 Hz, 1H), 4.33 (d, A of AB, J_{AB} = 17.7 Hz, 1H), 4.22 (d, B of AB, J_{AB} = 17.7 Hz, 1H), 3.02 (dddd, J = 9.7, 7.9, 3.7, 2.0 Hz, 1H), 2.81-2.72 (m, 2H), 2.56-2.50 (m, 2H), 2.45 (s, 3H).

^{13}C NMR (125 MHz, $CDCl_3$) δ 199.85 (e), 171.44 (e), 144.30 (e), 136.53 (e), 135.53 (e), 130.23 (o), 129.36 (o), 128.87 (o), 128.37 (e), 127.34 (o), 127.13 (o), 61.54 (o), 46.33 (e), 45.57 (o), 36.86 (e), 36.26 (e), 21.72 (o).

IR (Neat) 3029 (w), 2925 (w), 1728 (s), 1668 (m), 1598 (w), 1347 (m), 1160 (s), 1093 (m), 671 (m) cm^{-1}.

HRMS (ESI, $[M+Na]^+$) calcd for $C_{21}H_{20}ClNNaO_3S$ 424.0750, found 424.0741.

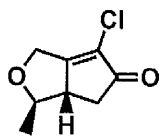

327

(3*R,3a*S**)-6-Chloro-3-methyl-3a,4-dihydro-1*H*-cyclopenta[*c*]furan-5(3*H*)-one.**

Synthesised by the general procedure for the room temperature rhodium(I)-catalysed Pauson-Khand reaction (Method A, CO:Ar = 100:0, 1 atm, t = 24 h, yield = 82%). *Selectivity:* **327/328** = 98:2.

Synthesised by the general procedure for the room temperature rhodium(I)-catalysed Pauson-Khand reaction (Method B, CO:Ar = 10:90, 1 atm, t = 24 h, yield = 76%). *Selectivity:* **327/328** = 96:4.

Colour and State: Yellow oil.

GC analysis (HP-1 19091Z-433 analytical column), 4 °C/min, 50 to 200 °C; t_R (*major*) 18.1 min, t_R (*minor*) 18.9 min.

^{1}H NMR (500 MHz, $CDCl_3$) δ 4.74 (d, A of AB, J_{AB} = 16.8 Hz, 1H), 4.58 (d, B of AB, J_{AB} = 16.8 Hz, 1H), 3.55 (*app* dq, J = 11.1, 5.9 Hz, 1H), 2.86-2.81 (m, 1H), 2.76 (dd, A of ABX, J_{AB} = 17.9 Hz, J_{AX} = 6.3 Hz, 1H), 2.21 (dd, B of ABX, J_{AB} = 17.9 Hz, J_{BX} = 2.5 Hz, 1H), 1.40 (d, J = 6.0 Hz, 3H).

^{13}C NMR (125 MHz, $CDCl_3$) δ 200.32 (e), 176.67 (e), 126.88 (e), 79.96 (o), 65.64 (e). 49.78 (o), 37.25 (e), 18.98 (o).

IR (Neat) 2974 (m), 2928 (w), 2854 (w), 1732 (s), 1661 (s), 1389 (w), 1067 (m), 965 (s) cm^{-1}.

HRMS (CI, $[M+H]^+$) calcd for $C_8H_{10}{}^{35}ClO_2$ 173.0364, found 173.0369.

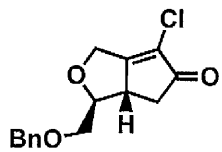

329

(3*S,3a*S**)-3-(Benzyloxymethyl)-6-chloro-3a,4-dihydro-1*H*-cyclopenta[*c*]furan-5(3*H*)-one.**

Synthesised by the general procedure for the room temperature rhodium(I)-catalysed Pauson-Khand reaction (Method A, CO:Ar = 100:0, 1 atm, t = 24 h, yield = 84%). *Selectivity:* **329/330** = ≥99:1.

Synthesised by the general procedure for the room temperature rhodium(I)-catalysed Pauson-Khand reaction (Method B, CO:Ar = 10:90, 1 atm, t = 24 h, yield = 64%). *Selectivity:* **329/330** = 99:1.

Colour and State: Yellow oil.

HPLC analysis (25 cm x 4.9 mm ZORBAX RX-SIL), 2% isopropanol/hexane at 0.3 mL/min, 230 nm, T = 22 °C; t_R (*major*) 28.7 min, t_R (*minor*) 31.0 min.

^{1}H NMR (500 MHz, $CDCl_3$) δ 7.38-7.29 (m, 5H), 4.77 (d, A of AB, J_{AB} = 16.5 Hz, 1H), 4.65 (d, B of AB, J_{AB} = 16.5 Hz, 1H), 4.63 (d, A of AB, J_{AB} = 11.8 Hz, 1H), 4.59 (d, B of AB, J_{AB} = 12.1 Hz, 1H), 3.75-3.66 (m, 3H), 3.17 (dddd, J = 11.6, 6.5, 3.3, 1.7 Hz, 1H), 2.76 (dd, A of ABX, J_{AB} = 18.2 Hz, J_{AX} = 6.4 Hz, 1H), 2.29 (dd, B of ABX, J_{AB} = 18.2 Hz, J_{BX} = 3.1 Hz, 1H).

^{13}C NMR (125 MHz, $CDCl_3$) δ 200.46 (e), 175.49 (e), 137.73 (e), 128.64 (o), 128.04 (o), 127.83 (o), 127.19 (e), 82.28 (o), 73.79 (e), 70.18 (e), 65.74 (e), 45.36 (o), 37.84 (e).

IR (Neat) 2857 (m), 1730 (s), 1661 (m), 1453 (w), 1100 (m), 958 (m) cm^{-1}.

HRMS (ESI, $[M+Na]^+$) calcd for $C_{15}H_{15}{}^{35}ClNaO_3$ 301.0607, found 301.0609.

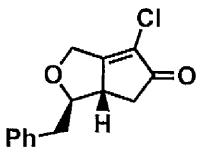

331

(3*R,3a*S**)-3-Benzyl-6-chloro-3a,4-dihydro-1*H*-cyclopenta[*c*]furan-5(3*H*)-one.**

Synthesised by the general procedure for the room temperature rhodium(I)-catalysed Pauson-Khand reaction (Method A, CO:Ar = 100:0, 1 atm, t = 24 h, yield = 87%). *Selectivity:* **331/332** = ≥99:1.

Synthesised by the general procedure for the room temperature rhodium(I)-catalysed Pauson-Khand reaction (Method B, CO:Ar = 10:90, 1 atm, t = 24 h, yield = 65%). *Selectivity:* **331/332** = ≥99:1.

Colour and State: Yellow oil; *Selectivity:* **331/332** ≥99:1

HPLC analysis (25 cm x 4.9 mm ZORBAX RX-SIL), 2% isopropanol/hexane at 0.3 mL/min, 230 nm, T = 22 °C; t_R (*major*) 34.7 min, t_R (*minor*) 22.8 min.

^{1}H NMR (500 MHz, $CDCl_3$) δ 7.35-7.23 (m, 5H), 4.78 (d, A of AB, J_{AB} = 16.7 Hz, 1H), 4.64 (d, B of AB, J_{AB} = 16.7 Hz, 1H), 3.71 (dt, J = 10.4, 6.6 Hz, 1H), 3.21 (dd, A of ABX, J_{AB} = 13.5 Hz, J_{AX} = 6.0 Hz, 1H), 2.97-2.92 (m, 1H), 2.94 (dd, B of ABX, J_{AB} = 13.4 Hz, J_{BX} = 7.3

Hz, 1H), 2.44 (dd, A of ABX, J_{AB} = 18.4 Hz, J_{AX} = 6.3 Hz, 1H), 1.84 (dd, B of ABX, J_{AB} = 18.3 Hz, J_{BX} = 2.9 Hz, 1H).

^{13}C NMR (125 MHz, $CDCl_3$) δ 200.41 (e), 175.93 (e), 136.49 (e), 129.30 (o), 128.78 (o), 127.13 (o), 127.02 (e), 84.31 (o), 65.67 (e), 48.09 (o), 40.26 (e), 37.92 (e).

IR (Neat) 3027 (w), 2920 (w), 2853 (w), 1729 (s), 1660 (m), 1603 (w), 1497 (w), 1454 (w), 1011 (m), 959 (s) cm^{-1}.

HRMS (ESI, $[M+Na]^+$) calcd for $C_{14}H_{13}{}^{35}ClNaO_2$ 271.0502, found 271.0506.

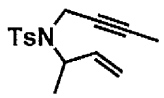

282

***N*-(but-2-ynyl)-*N*-(but-3-en-2-yl)-4-methylbenzenesulfonamide.**

A flame-dried 100 mL flask was charged with triphenylphosphine (1.18 g, 4.5 mmol) and *N*-(but-2-ynyl)-4-methylbenzenesulfonamide (0.670 g, 3 mmol), evacuated and backfilled with argon. Anhydrous THF (12 mL) and 3-buten-2-ol (0.325 g, 4.5 mmol) were added and the resulting solution was placed in a ice bath for *ca* 15 minutes. Diisopropyldiazodicarboxylate (DIAD) (0.88 mL, 4.5 mmol) then was added drop-wise over 5 minutes *via* syringe. The resultant reaction mixture was stirred for 18 hours, slowly warming to room temperature, then a TLC (20% diethyl ether/ petroleum ether) showed complete consumption of the secondary amine. The reaction mixture was concentrated *in vacuo* onto silica gel. Purification *via* FCC on silica gel (petroleum ether-diethyl ether, 95:5) provided the sulfonamide product **282** (0.706 g, 82%).

Colour and State: Yellow oil.

^{1}H NMR (500 MHz, $CDCl_3$) δ 7.80 (d, J = 8.3 Hz, 2H), 7.28 (d, J = 8.2 Hz, 2H), 5.77 (ddd, J = 17.2, 10.8, 4.8 Hz, 1H), 5.14 (s, 1H), 5.12 (dd, J = 7.9, 1.4 Hz, 1H), 4.59-4.51 (m, 1H), 4.08

(dq, A of ABX, J_{AB} =18.2 Hz, J_{AX}= 2.3 Hz, 1H), 3.83 (dq, B of ABX, J_{AB} =18.2 Hz, J_{BX} = 2.3 Hz, 1H), 2.42 (s, 3H), 1.67 (t, J = 2.4 Hz, 3H), 1.25 (d, J = 7.0 Hz, 3H).

^{13}C NMR (125 MHz, $CDCl_3$) δ 143.08 (e), 138.12 (e), 137.72 (o), 129.26 (o), 127.56 (o), 116.69 (e), 80.18 (e), 75.28 (e), 54.84 (o), 32.87 (e), 21.51 (o), 17.15 (o), 3.43 (o).

IR (Neat) 2979 (w), 2921 (w), 1598 (w), 1332 (m), 1155 (s), 1093 (s), 1093 (s), 896 (m) cm^{-1}.

HRMS (ESI, $[M+Na]^+$) calcd for $C_{15}H_{19}NNaO_2S$ 300.1034, found 300.1037.

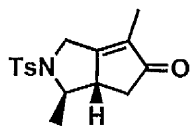

284

(3*R,3a*S**)-6-Methyl-3-methyl-2-tosyl-2,3,3a,4-tetrahydrocyclopenta[*c*]pyrrol-5(1*H*)-one.**[168]

*Method A (Suzuki-Coupling reaction of α-chloroenone **317**)*: methyl boronic acid (18 mg, 0.3 mmol), K_3PO_4 (43 mg, 0.2 mmol), $Pd(OAc)_2$ (4.5 mg, 0.02 mmol) and dpdb (2-dicyclohexylphosphino-2'-6'-dimethoxybiphenyl) (16.5 mg, 0.04 mmol) were placed in a 15 mL flame-dried reaction tube under argon atmosphere. The reaction tube was then evacuated and backfilled three times with argon. A solution of enone **317** (32 mg, 0.1 mmol) in anhydrous toluene (1 mL) was added by tared syringe in the reaction tube, followed by addition of water (3 μL). The resulting suspension was placed in a 65 °C bath and allowed to stir for 24 h. After completion of the reaction (TLC control), mixture was allowed to cool at RT, directly placed on silica gel column and purified (petroleum ether-diethyl ether, 50:50), to afford enone **284** as a pale yellow oil (62% yield, *dr* ≥19:1 by NMR analysis).

*Method B (Rh-catalysed PK reaction of enyne **317**)*: $[Rh(CO)_2Cl]_2$ (3.9 mg, 0.01 mmol) was weighed into a 15 mL flame-dried reaction tube under an atmosphere of argon. After the flask was evacuated and backfilled three times with CO gas, a solution of enyne **282** (55 mg, 0.2

mmol) in *p*-xylene (2 mL) was added by tared syringe. The reaction was stirred at room temperature for *ca.* 10 minutes and then heated at 110 °C until the reaction was complete (TLC control, t = 20 h). The reaction mixture was allowed to cool down at RT, directly placed on silica gel column and purified (petroleum ether-diethyl ether, 50:50), to afford enone **284** as a pale yellow oil (77% yield, *dr* = 2:1).

Colour and State: Pale yellow oil.

^{1}H NMR (500 MHz, $CDCl_3$) δ 7.77 (d, *J* = 8.3 Hz, 2H), 7.33 (d, *J* = 8.1 Hz, 2H), 4.28- 4.16 (m, 2H), 4.09 (d, *J* = 16.3 Hz, 1H), 2.80-2.72 (m, 1H), 2.43 (s, 3H), 2.42-2.37 (m, 1H), 2.08 (dd, *J* = 18.4, 3.3 Hz, 1H), 1.73 (s, 3H), 1.00 (d, *J* = 6.7 Hz, 3H).

IR (Neat) 2978 (w), 2928 (w), 1717 (vs), 1669 (m), 1598 (m), 1346 (s), 1158 (s), 1089 (s) cm^{-1}.

1.8. References.

1. For reviews on metal-catalysed cycloaddition reaction, see: a) Lautens, M.; Klute, W.; Tam, W. *Chem. Rev.* **1996**, *96*, 49; b) Aubert, C.; Buisine, O.; Malacria, M. *Chem. Rev.* **2002**, *102*, 813; c) Nakamura, I.; Yamamoto, Y. *Chem. Rev.* **2004**, *104*, 2127; d) *Modern Rhodium-Catalysed Organic Reactions* (Ed.: Evans, P. A.), Wiley-VCH: Weinheim, **2005**; e) Inglesby, P. A.; Evans, P. A. *Chem. Soc. Rev.* **2010**, *39*, 2791.
2. For recent reviews of PK reactions, see: a) Jeong, N. in *Modern Rhodium-Catalysed Organic Reactions*; (Ed.: Evans, P. A.) Wiley-VCH: Weinheim, **2005**, Ch. 11, 215; (b) Shibata, T. *Adv. Synth. Catal.* **2006**, *348*, 2328. (c) Perez-Castells, J. *Top. Organomet. Chem.* **2006**, *19*, 207. (d) Lee, H.-W.; Kwong, F.-Y. *Eur. J. Org. Chem.* **2010**, 789.
3. a) Khand, I. U.; Knox, G. R.; Pauson, P. L.; Watts, W. E. *J. Chem. Soc., Perkin Trans. I* **1973**, 975; b) Khand, I. U.; Knox, G. R.; Pauson, P. L.; Watts, W. E.; Foreman, M. I. *J. Chem. Soc., Perkin Trans. I* **1973**, 977.
4. Khand, I. U.; Knox, G. R.; Pauson, P. L.; Watts, W. E. *J. Chem. Soc. Chem. Comm.* **1971**, 36.

5. Dickson, R. S.; Fraser, P. J. *Adv. Organomet. Chem.* **1974**, *12*, 323.

6. (a) Magnus, P. C.; Exon, C.; Albaugh-Robertson P. *Tetrahedron* **1985**, *41*, 5861; (b) Magnus, P. C.; Principe, L. M. *Tetrahedron Lett.* **1985**, *26*, 4851.

7. La Belle, B. E.; Knudsen, M. J.; Olmstead, M. M.; Hope, H.; Yanuck, M. D.; Schore, N. E. *J. Org. Chem.* **1985**, *50*, 5215.

8. a) Yamanka, M.; Nakamura, E. *J. Am. Chem. Soc.* **2001**, *123*, 1703; b) Pericàs, M. A.; Balsells, J.; Castro, J.; Marchueta, I; Moyano, A.; Riera, A.; Vázquez, J.; Veraguer, X. *Pure Appl. Chem.* **2002**, *74*, 167; c) Gimbert, Y.; Lesage, D.; Milet, A.; Fournier, F.; Greene, A. E.; Tabet, J.-C. *Org. Lett.* **2003**, *5*, 4073.

9. Schore, N. E.; Croudace, M. C. *J. Org. Chem.* **1981**, *46*, 5346.

10. Jeong, N.; Chung, Y. K.; Lee, B. Y.; Lee, S. H.; Yoo, S.-E. *Synlett* **1991**, 204.

11. Shambayati, S.; Crowe, W. E.; Schreiber, S. L. *Tetrahedron Lett.* **1990**, *31*, 5289.

12. a) Dennenberg, R. J.; Darensbourg, D. J. *Inorg. Chem.* **1972**, *11*, 72; b) Atwood, J. D.; Brown, T. L. *J. Am. Chem. Soc.* **1976**, *98*, 3160; c) Darensbourg, D. J.; Kump, R. L. *Inorg. Chem.* **1978**, *17*, 2680.

13. a) Sugihara, T.; Yamad, M.; Ban, H.; Yamaguchi, M.; Kaneko, C. *Angew. Chem. Int. Ed.* **1997**, *36*, 2801; b) Sugihara, T.; Yamaguchi, M.; Nishizawa, M. *Chem. Eur. J.* **2001**, *8*, 2801.

14. Krafft, M. E.; Scott,I. L.; Romero, R. H.; Feibelmann, S.; Van Pelt, C. E. *J. Am. Chem. Soc.* **1993**, *115*, 7199.

15. Sugihara, T.; Yamada, M.; Yamaguchi, M.; Nishizawa, M. *Synlett* **1999**, 771.

16. Rautenstrauch, V.; Mégard, P.; Conesa, J.; Küster, W. *Angew. Chem. Int. Ed.* **1990**, *29*, 1413.

17. Jeong, N.; Hwang, S. H.; Lee, Y.; Chung, Y. K. *J. Am. Chem. Soc.* **1994**, *116*, 3159.

18. a) Pagenkopf, B. L.; Livinghouse, T. *J. Am. Chem. Soc.* **1996**, *118*, 2285.; b) Belanger, D. B.; O'Mahony, D. J. R.; Livinghouse, T. *Tetrahedron Lett.* **1998**, *39*, 7637.

19. Krafft, M. E.; Bonaga, L. V. R.; Hirosawa, S. *Tetrahedron Lett.* **1999**, *40*, 9171.

20. Belanger, D. B.; Livinghouse, T. *Tetrahedron Lett.* **1998**, *39*, 7641.

21. Krafft, M. E.; Hirosawa, C.; Bonaga, L. V. R. *Tetrahedron Lett.* **1998**, *39*, 9177.

22. a) Comely, A. C.; Gibson, S. E.; Stevenazzi, A.; Hales, N. J. *Tetrahedron Lett.* **2001**, *42*, 1183; b) Gibson, S. E.; Johnstone, C.; Stevenazzi, A. *Tetrahedron* **2002**, *58*, 4937.

23. Blanco-Urgoiti, J.; Abdi, D.; Domínguez, G.; Pérez-Castells, J. *Tetrahedron* **2008**, *64*, 67.

24. Beck, J. A.; Knox, S. A. R.; Stansfield, R. F. D; Stone, F. G. A.; Winter, M. J.; Woodward, P. *J. Chem. Soc., Dalton Trans.*, **1982**, 195.

25. Mukai, C.; Uchiyama, M.; Hanaoka, M. *J. Chem. Soc., Chem. Commun.* **1992**, 1014.

26. Jeong, N.; Lee, S. J.; Lee, B. Y.; Chung, Y. K. *Tetrahedron Lett.* **1993**, *34*, 4027.

27. Experimental studies by Jeong revealed the low reactivity of tungsten and chromium carbonyl complexes in the intramolecular PK reaction. However, Hoye and Moreto reported several studies on W and Cr-catalysed PKR: (a) Hoye, T. R.; Suriano, J. A. *Organometallics* **1992**, *11*, 2044; b) Hoye, T. R.; Suriano, J. A. *J. Am. Chem. Soc.* **1993**, *115*, 1154; c) Jordi, L.; Segundo, A.; Camps, F.; Ricart, S.; Moreto, J. M. *Organometallics* **1993**, *12*, 3795.

28. Adrio, J.; Rivero, M. R.; Carretero, J. C. *Org. Lett.* **2005**, *7*, 431.

29. *The Chemistry of Allenes, Vol. 2* (Ed.: Landor, S. R.), Academic Press: New York, **1982**, 321.

30. Kent, J. L.; Wan, H.; Brummond K. M. *Tetrahedron Lett.* **1995**, *36*, 2407.

31. a) Brummond, K. M.; Wan, H. *Tetrahedron Lett.* **1998**, *39*, 931; b) Brummond, K. M.; Kent, J. L.; Wan, H. *J. Org. Chem.* **1998**, *63*, 6535.

32. a) Brummond, K. M.; Lu, J. *J. Am. Chem. Soc.* **2000**, *122, 4915*; b) Brummond, K. M.; Sill, P. C.; Chen H. *Org. Lett.* **2004**, *6*, 149.

33. (a) Kablaoui, N. M.; Hicks, F. A.; Buchwald, S. L. *J. Am. Chem. Soc.* **1996**, *118*, 5818; (b) Kablaoui, N. M.; Hicks, F. A.; Buchwald, S. L. *J. Am. Chem. Soc.* **1997**, *119*, 4424.

34. Crowe, W. E.; Vu, A. T. *J. Am. Chem. Soc.* **1996**, *118*, 1557.

35. a) Chatani, N.; Morimoto, T.; Fukumoto, Y.; Murai, S. *J. Am. Chem. Soc.* **1998**, *120*, 5335; (b) Chatani, N.; Motimoto, T.; Kamitani, A.; Fukumoto, Y.; Murai, S. *J. Organomet. Chem.* **1999**, *579*, 177.

36. Adrio, J.; Carretero, J. C. *J. Am. Chem. Soc.* **2007**, *129*, 778.

37. Pearson, A. J.; Dubbert, R. A. *J. Chem. Soc., Chem. Commun.* **1991**, 202; b) Pearson, A. J.; Dubbert, R. A. *Organometallics* **1994**, *13*, 1656.

38. Chatani, N.; Fukumoto, Y.; Ida, T.; Murai, S. *J. Am. Chem. Soc.* **1993**, *115*, 11614.

39. Morimoto, T.; Chatani, N.; Fukumoto, Y.; Murai, S. *J. Org. Chem.* **1997**, *62*, 3762.

40. Kondo, T.; Suzuki, N.; Okada, T.; Mitsudo, T. *J. Am. Chem. Soc.* **1997**, *119*, 6187.

41. a) Itami, K.; Mitsudo, K.; Yoshida, J. *Angew. Chem. Int. Ed.* **2002**, *41*, 3481; b) Itami, K.; Mitsudo, K.; Fujita, Y.; Ohashi, J.; Yoshida, J. *J. Am. Chem. Soc.* **2004**, *126*, 11058.

42. Finnegan, D.; Snapper, M. L. *J. Org. Chem.* **2011**, *76*, 3644.

43. (a) Tamao, K.; Kobayashi, K.; Ito, Y. *J. Am. Chem. Soc.* **1988**, *110*, 1286; (b) Tamao, K.; Kobayashi, K.; Ito, Y. *Synlett* **1992**, 539.

44. Zhang, M.; Buchwald, S. L. *J. Org. Chem.* **1996**, *61*, 4498.

45. a) Y. Tang, L. Deng, Y. Zhang, G. Dong, J. Chen, Z. Yang, *Org. Lett.* **2005**, *7*, 1657; b) J. Liu, J.-Q. Huang, Y. Hu, M. Chen, Y. Lan, J.-H. Chen, A. Lei, Z. Yang, *Synthesis* **2007**, 2565. c) Y. Lan, L. Deng, J. Liu, C. Wang, O. Wiest, Z. Yang, Y.-D. Wu, *J. Org. Chem.* **2009**, 74, 5049.

46. Tang, Y.; Deng, L.; Zhang, Y.; Dong, G.; Chen, J.; Yang, Z. *Org. Lett.* **2005**, *7*, 593.

47. Jolly, R. S.; Luedtke, G.; Sheehan, D., Livinghouse, T. *J. Am. Chem. Soc.* **1990**, *112*, 4965.

48. Wender, P.; Takahashi, H.; Witulski, B. *J. Am. Chem. Soc.* **1995**, *117*, 4720.

49. a) Koga, Y.; Kobayashi, T.; Narasaka, K. *Chem. Lett.* **1998**, 249; b) Kobayashi, T.; Koga, Y.; Narasaka, K. *J. Organomet. Chem.* **2001**, *624*, 73.

50. Jeong, N.; Lee, S.; Sung, B. K. *Organometallics* **1998**, *17*, 3642.

51. Jeong, N.; Sung, B. K.; Choi, Y. K. *J. Am. Chem. Soc.* **2000**, *122*, 6771.

52. Brummond, K. M.; Chen, H.; Fisher, K. D.; Kerekes, A. D.; Rickards, B.; Sill, P. C.; Geib, S. J. *Org. Lett.* **2002**, *11*, 1931.

53. a) Mukai, C.; Nomura, I.; Yamanishi, K.; Hanaoka, M. *Org. Lett.* **2002**, *4*, 1755; b)

Mukai, C.; Nomura, I.; Kitagaki, S. *J. Org. Chem.* **2003**, *68*, 1376; c) Inagaki, F.; Mukai, C. *Org. Lett.* **2006**, *8*, 1217; d) Inagaki, F.; Narita, S.; Hasegawa, T.; Kitagaki, S.; Mukai, C. *Angew. Chem. Int. Ed.* **2009**, *48*. 2007.

54. Makino, T.; Itoh, K. *Tetrahedron Lett.* **2003**, *44*, 6335.

55. a) Wender, P.; Deschamps, N.; Gamber, G. *Angew. Chem. Int. Ed.* **2003**, *42*, 1853; b) Wender, P.; Deschamps, N.; Williams, T. *Angew. Chem. Int. Ed.* **2004**, *43*, 3076; c) Wender, P.; Croatt, M.; Deschamps, N. M. *J. Am. Chem. Soc.* **2004**, *126*, 5948.

56. Pitcock, W. H.; Lord R. L.; Baik M.-H. *J. Am. Chem. Soc.* **2008**, *130*, 5821.

57. a) Voigt, H. W.; Roth, J. A. *J. Catal.* **1975**, *39*, 198; b) Al-Essa, R. J.; Puddephatt, R. J.; Perkins, D. C. L.; Rendle, M. C.; Tipper, C. F. H. *J. Chem. Soc., Dalton Trans.* **1981**, 1738.

58. Koga, Y.; Narasaka, K. *Chem. Lett.* **1999**, *7*, 705.

59. a) Jiao, L.; Ye, S.; Yu, Z.-X. *J. Am. Chem. Soc.* **2008**, *130*, 7178; b) Jiao, L.; Lin, M.; Yu, Z.-X. *Chem. Commun.* **2010**, *46*, 1059; c) Li, Q.; Jiang, G.-J.; Jiao, L.; Yu, Z.-X. *Org. Lett.* **2010**, *12*, 1332.

60. Jiao, L.; Lin, M.; Zhuo, L.-G.; Yu, Z.-X. *Org.Lett.* **2010**, *12*, 2528.

61. Lin, M.; Li, F.; Jiao, L.; Yu, Z.-X. *J. Am. Chem. Soc.* **2010**, *133*, 1690.

62. Li, C.; Zhang, H.; Feng, J.; Zhang, Y.; Wang, J. *Org. Lett.* **2010**, *12*, 3082.

63. Kim, S. Y.; Lee, S. I.; Choi, S. Y.; Chung, Y. K. *Angew. Chem. Int. Ed.* **2008**, *47*, 4914.

64. Eaton, B. E.; Rollman B.; Kaduk, J. A. *J. Am. Chem. Soc.* **1992**, *114*, 6245.

65. Murakami, M.; Itami, K.; Ito, Y. *Angew. Chem. Int. Ed. Engl.* **1995**, *34*, 2691.

66. Murakami, M.; Itami, K.; Ito, Y. *J. Am. Chem. Soc.* **1997**, *119*, 2950.

67. Cho, S. H.; Liebeskind, L. S. *J. Org. Chem.* **1987**, *52*, 2631.

68. Kurahashi, T.; de Meijere, A. *Synlett*, **2005**, 2619.

69. Brancour, C.; Fukuyama, T.; Ohta, Y.; Ryu, I.; Dhimane, A.-L.; Fensterbank, L.; Malacria, M. *Chem. Commun.* **2010**, *46*, 5470.

70. Wender, P. A.; Gamber, G. G.; Hubbard, R. D.; Zhang, L. *J. Am. Chem. Soc.* **2002**, *124*, 2876.

71. Wender, P. A.; Husfeld, C. O.; Langkopf, E.; Love, J. A.; Pleuss, N. *Tetrahedron* **1998**, *54,* 7203.

72. Wang, Y.; Wang, J.; Su, J.; Huang, F.; Jiao, L.; Liang, Y.; Yang, D.; Zhang, S.; Wender, P. A.; Yu, Z.-X. *J. Am. Chem. Soc.* **2007**, *129*, 10060.

73. Huang, F.; Yao, Z.-K.; Wang, Y.; Wang, Y.; Zhang, J.; Yu, Z.-X. *Chem. Asian J.* **2010**, *5*, 1555.

74. a) Wender, P. A.; Corrrea, A. G.; Sato, Y.; Sun, R. *J. Am. Chem. Soc.* **2000**, *122*, 7815; b) Wender, P. A.; Deschamps, N. M.; Sun, R. *Angew. Chem. Int. Ed.* **2006**, *45*, 3957.

75. Yao, Z.-K.; Li, J.; Yu, Z.-X. *Org. Lett.* **2011**, 13, 134.

76. a) Ojima, I.; Lee, S.-Y. *J. Am. Chem. Soc.* **2000**, *122*, 2385; b) Bennacer, B.; Fujiwara, M.; Lee, S.-Y.; Ojima, I. *J. Am. Chem. Soc.* **2005**, *127*, 17756; c) Bennacer, B.; Fujiwara, M.; Ojima, I. *Org. Lett.* **2004**, *6*, 3589; d) Kaloko, J. J.; Teng, Y.-H. G.; Ojima, I. *Chem. Commun.* **2009**, 4569.

77. Wender, P. A.; Gamber, G. G.; Hubbard, R. D.; Pham, S. M.; Zhang, L. *J. Am. Chem. Soc.* **2005**, *127*, 2836.

78. a) Mukai, C.; Kim, J. S.; Uchiyama, M.; Hanaoka, M. *Tetrahedron Lett.* **1998**, *39*, 7909; b) Mukai, C.; Kim, J. S.; Sonobe, H.; Hanaoka, M. *J. Org. Chem.* **1999**, *64*, 6822.

79. Yoo, S.-E.; Lee, S. H.; Jeong, N.; Cho, I. *Tetrahedron Lett.* **1991**, *34*, 3435.

80. Alcaide, B.; Polanco, C.; Sierra, M. A. *J. Org. Chem.* **1998**, *63*, 6786.

81. a) Adrio, J.; Rodríguez Rivero, M.; Carretero, J. C. *Angew. Chem., Int. Ed.* **2000**, *39*, 2906; b) Adrio, J.; Rodríguez Rivero, M.; Carretero, J. C. *Synlett* **2005**, 26.

82. Kavanagh, Y.; O'Brien, M.; Evans, P. *Tetrahedron* **2009**, *65*, 8259.

83. Billington, D. C.; Kerr, W. J.; Pauson, P. L. *J. Organomet. Chem.* **1987**, *328*, 223.

84. Naya, Y.; Kotake, M. *Tetrahedron Lett.* **1968**, 1645.

85. Caldwell J. J.; Cameron I. D.; Christie S. D. R.; Hay A. M.; Johnstone C.; Kerr, W. J.; Murray, A. *Synthesis* **2005**, 3293.

86. Gao, P.; Xu, P. F.; Zhai, H. *J. Org. Chem.* **2009**, *74*, 2592.

87. a) Kerr, W. J.; McLaughlin, M.; Pauson, P. L.; Robertson, S. M. *Chem. Commun.* **1999**,

2171; b) Kerr, W. J.; McLaughlin, M.; Pauson, P. L.; Robertson, S. M. *J. Organomet. Chem.* **2001**, *630*, 104.

88. a) Takeuchi, T.; Linuma, H.; Iwanaga, J.; Takahashi, H.; Umezawa, H. *J. Antibiot.* **1969**, *22,* 215; b) Nishimura, Y.; Koyama, Y.; Umezawa, S.; Takeuchi, T.; Ishizuka, M.; Umezawa, H. J. *Antibiot.* **1980**, *33,* 404.

89. a) Tatsuta, K.; Akimota, K.; Kinoshita, M. *Tetrahedron* **1981**, *37*, 4365; b) Danishefsky, S.; Zamboni, R.; Kahn, H.; Etheredge, S. J. *J. Am. Chem. Soc.* **1981**, *103*, 3460; c) Shibasaki, M.; Iseki, K.; Ikegami, S. *Tetrahedron* **1981**, *37*, 4411; d) Trost, B. M.; Curran, D. P. *J. Am. Chem. Soc.* **1981**, *103*, 7380; e) Mehta, G.; Reddy, A. V.; Murty, A. N.; Reddy, D. S. K. *J. Chem. Soc., Chem. Commun.* **1982**, 540.

90. Exon, C.; Magnus, P. *J. Am. Chem. Soc.* **1983**, *105*, 2477.

91. Moyano, A.; Charbonnier, F.; Greene, A. E. *J. Org. Chem.* **1987**, *52*, 2919.

92. Isolation: Hashimoto, H.; Tsuzuki, K.; Sakan, F.; Shirahama, H.; Matsumoto, T. *Tetrahedron Lett.* **1974**, *15*, 3745.

93. Castro, J.; Sorensen, H.; Riera, A.; Morin, C.; Moyano, A.; Pericas M. A.; Greene A. E. *J. Am. Chem. Soc.* **1990**, *112*, 9388.

94. (a) MacDonald, J. R.; Muscoplat, C. C.; Dexter, D. L.; Mangold, G. L.; Chen, S.-F.; Kelner, M. J.; McMorris, T. C.; Von Hoff, D. D. *Cancer Res.* **1997**, *57*, 279; (b) Kelner, M. J.; McMorris, T. C.; Estes, L. A.; Wang, W.; Samson, K. M.; Taetle, R. *Investigational New Drugs* **1996**, *14*, 161.

95. Garcıa, A.; Delgado, G. *Helv. Chim. Acta* **2006**, *89*, 16.

96. Hayashi, Y.; Miyakoshi, N.; Kitagaki, S.; Mukai, C. *Org. Lett.* **2008**, *10*, 2385.

97. Isolation: Castro, V.; Ciccio, F.; Alvarado, S.; Bohlmann, F.; Schmeda - Hirschmann, G.; Jakupovic, J. *Liebigs Ann. Chem.* **1983**, 974-981.

98. Hirose, T.; Miyakoshi, N.; Mukai, C. *J. Org. Chem.* **2008**, 73, 1061.

99. Jiao, L.; Yuan, C.; Yu, Z.-X. *J. Am. Chem. Soc.* **2008**, *130*, 4421.

100. Isolation: Comer, F. W.; McCapra, F.; Qureshi, I. H.; Scott, A. I. *Tetrahedron*, **1967**, *23*, 4761.

101. Yuan, C.; Jiao, L.; Yu, Z.-X. *Tetrahedron Lett.* **2010**, *51*, 5674.

102. Isolation: Seto, H.; Sasaki, T.; Uzawa, J.; Takeuchi, S.; Yonehara, H. *Tetrahedron Lett.* **1978**, *19*, 4411.

103. a) Rowley, E. G.; Schore, N. E. *J. Org. Chem.* **1992**, *57*, 6853; b) Schore, N. E.; Rowley, E. G. *J. Am. Chem. Soc.* **1988**, *110*, 5224.

104. Tormo, J.; Moyano, A.; Pericas, M. A.; Riera, A. *J. Org. Chem.* **1997**, *62*, 4851.

105. a) Pallerla, M. K.; Fox, J. M. *Org. Lett.* **2005**, *7*, 3593; b) Pallerla, M. K.; Fox, J. M. *Org. Lett.* **2007**, *9*, 5625.

106. Pattenden, G.; Teague, S. J. *Tetrahedron* **1987**, *43*, 5637.

107. Fan, X.; Zhuo, L.-G.; Tu, Y. Q.; Yu, Z.-X. *Tetrahedron* **2009**, *65*, 4709.

108. a) Barrero, A. F.; del Moral, J. Q.; Lara, A. *Tetrahedron* **2000**, *56*, 3717 and references therein; b) Stork, G.; Breslow, R. *J. Am. Chem. Soc.* **1953**, *75*, 3291; c) Walter, P. *Ann. Chem.* **1841**, *39*, 247.

109. Kerr, W. J.; McLaughlin, M.; Morrison, A. J.; Pauson, P. L. *Org. Lett.* **2001**, *3*, 2945.

110. San Feliciano, A.; Barrero, A. F.; Medarde, M.; Del Corral, J. M. M.; Aramburu, A.; Perales, A.; Fayos, J. *Tetrahedron Lett.* **1985**, *26*, 2369.

111. a) Krafft, M. E.; Cheung, Y. Y.; Juliano-Capucao, C. A. *Synthesis* **2000**, 1020; b) Krafft, M. E.; Cheung, Y. Y.; Abboud, K. A. *J. Org. Chem.* **2001**, *66*, 7443.

112. Liang, Y.; Jiang, X.; Yu, Z.-X. *Chem. Commun.* **2011**, *47*, 6659.

113. Fukuyama, Y.; Shida, N.; Kodama, M.; Chaki, H.; Yugami, T. *Chem. Pharm. Bull.* **1995**, *43*, 2270.

114. Furuya, S.; Terashima, S. *Tetrahedron Lett.* **2003**, *44*, 6875.

115. Kikuchi, H.; Miyagawa, Y.; Sahashi, Y.; Inatomi, S.; Haganuma, A.; Nakahata, N.; Oshima, Y. *Tetrahedron Lett.* **2004**, *45*, 6225.

116. Min, S.-J.; Danishefsky, S. J.; *Angew. Chem. Int. Ed.* **2007**, *46*, 2199.

117. Isolation: Enoki, N.; Furusaki, A.; Suehiro, K.; Ishida, R.; Matsumoto, T. *Tetrahedron Lett.* **1983**, *24*, 4341

118. a) Jamison, T. F.; Shambayati, S.; Crowe, W. E.; Schreiber, S. L. *J. Am. Chem. Soc.* **1994**, *116*, 5505; b) Jamison, T. F.; Shambayati, S.; Crowe, W. E.; Schreiber, S. L. *J. Am. Chem. Soc.* **1997**, *119*, 4353.

119. Huang, S. X.; Li, R. T.; Liu, J. P.; Lu, Y.; Chang, Y.; Lei, C.; Xiao, W. L.; Yang, L. B.; Zheng, Q. T.; Sun, H. D. *Org. Lett.* **2007**, *9*, 2079.

120. Xiao, Q.; Ren, W.-W.; Chen, Z.-X; Sun, T.-W.; Li, Y.; Ye, Q.-D.; Gong, J.-X.; Meng, F.-M.; You, L.; Liu, Y.-F.; Zhao, M.-Z.; Xu, L.-M.; Shan, Z.-H.; Shi, Y.; Tang, Y.-F.; Chen, J.-H.; Yan, Z. *Angew. Chem. Int. Ed.* **2011**, *50*, 7373.

121. Isolation: a) Murakami, S.; Takemoto, T.; Shimizu, Z.; Daigo, K. *Jpn. J. Pharm. Chem.* **1963**, *25*, 571. (b) Murakami, S.; Takemoto, T.; Shimizu, Z. *J. Pharm.* Soc. *Jpn.* 1953, *73*, 1026; c) Morimoto, H.; *J. Pharm. Soc. Jpn.* **1955**, *75*, 901; d) Ueno, Y.; Nawa, H.; Ueyanagi, J.; Morimoto, H.; Nakamori, R.; Matsuoka, T. *J. Pharm. Soc. Jpn.* **1955**, *75*, 807; e) Murakami, S.; Takemoto, T.; Tei, Z.; Daigo, K. *J. Pharm. Soc. Jpn.* **1955**, *75*, 866.

122. Biological activity: a) Shinozaki, H.; Konishi, S. *Brain Res.* **1970**, *24*, 368; b) Johnston, G. A. R.; Curtis, D. R.; Davies, J.; McCulloch, R. M. *Nature* **1974**, *248*, 804.

123. Yoo, S.-E.; Lee, S. H. *J. Org. Chem.* **1994**, *59*, 6968.

124. a) Farwick, A.; Helmchen, G. *Org. Lett.* **2010**, *12*, 1108; b) Farwick, A.; Engelhart, J. U.; Tverskoy, O.; Welter, C.; UmLauf, Q. A.; Rominger, F.; Kerr, W. J.; Helmchen, G. *Adv. Synth. Catal.* **2011**, *353*, 349.

125. Cordell, G. A. in *The Alkaloids, Vol. 16* (Ed.: Manske, R. H. F.), Academic Press: New York, **1977**, 432.

126. Isolation: a) Hammouda, Y.; Motawi, M. M. *Egypt Pharm. Bull.* **1959**, *41*, 73, *Chem. Abstr.* **1960**, *54*, 113; b) Hammouda, Y.; Plat, M.; Le Men, J. *Ann. Pharm. Fr.* **1963**, *21*, 699; c) Hammouda, Y.; Plat, M.; Le Men, *J. Bull. Soc. Chim. Fr.* **1963**, 2802.

127. Ockey, D. A.; Lewis, M. A.; Schore, N. E. *Tetrahedron* **2003**, *59*, 5377.

128. a) Honda, T.; Kaneda, K. *J. Org. Chem.* **2007**, 72, 6541; b) Kaneda, K.; Honda, T. *Tetrahedron* **2008**, *64*, 11589.

129. Mukai, C.; Yoshida, T.; Sormachi, M.; Odani, A. *Org. Lett.* **2006**, *8*, 83.

130. Isolation: a) Jobst, J.; Hesse, O. *Justus Liebigs Ann. Chem.* **1864**, *129*, 115; b) Stedman, E.; Barger, G. *J. Chem. Soc.* **1925**, *127*, 247.

131. Biological activity: a) Triggle, D. J.; Mitchell, J. M.; Filler, R. *CNS Drug Rev.* **1998**, *4*, 87; b) Giacobini, E. *Neurochem. Int.* **1998**, *32*, 413; c) Brufani, M.; Castellano, C.; Marta, M.; Murroni, F.; Oliverio, A.; Pagella, P. G.; Pavone, F.; Pomponi, M.; Rugarli, P. L. *Curr. Res. Alzheimer Ther.: Cholinesterase Inhib.* **1988**, 343; d) Granacher, R. P.; Baldessarini, R. *J. Clin. Neuropharmacol.* **1976**, *1*, 63; e) Takano, S.; Ogasawara, K. *Yuki Gosei Kagaku Kyokaishi* **1982**, *40*, 1037; f) Sneader, W. *Drug News Perspect* **1999**, *12*, 433.

132. Takano, S.; Inomata, K.; Ogasawara, K. *Chem. Lett.* **1992**, 443.

133. a) Cassayre, J.; Zard, S. Z. *J. Am. Chem. Soc.* **1999**, *121*, 6072; b) Cassayre, J.; Gagosz, F.; Zard, S. Z. *Angew. Chem. Int. Ed. Eng.* **2002**, *41*, 1783.

134. Isolation: Castillo, M.; Loyola, L. A.; Morales, G.; Singh, I.; Calvo, C.; Holland, H. L.; MacLean, D. B. *Can. J. Chem.* **1976**, *54*, 2893.

135. a) Ishizaki, M.; Niimi, Y.; Hoshino, O. *Tetrahedron Lett.* **2003**, *44*, 6029; b) Ishizaki, M.; Niimi, Y.; Hoshino, O.; Hara, H.; Takahashi, Y. *Tetrahedron* **2005**, *61*, 4053.

136. Kozaka, T.; Miyakoshi, N.; Mukai, C. *J. Org. Chem.* **2007**, *72*, 10147.

137. a) Hirasawa, Y.; Kobayashi, J.; Morita, H. *Heterocycles* **2009**, *77*, 679; b) Kobayashi, J.; Morita, H. in *The Alkaloids, Vol. 61*; (Ed.: Cordell, G. A.) Academic Press: New York, **2005**, 1; c) Ayer, W. A.; Trifonov, L. S. in *The Alkaloids, Vol. 45*; (Ed.: Cordell, G. A.) Academic Press: New York, **1994**, 233; d) Ma, X.; Gang, D. R. *Nat. Prod. Rep.* **2004**, *21*, 752.

138. Isolation: Takayama, H.; Katakawa, K.; Kitajima, M.; Yamaguchi, K.; Aimi, N. *Tetrahedron Lett.* **2002**, *43*, 8307.

139. Nakayama, A.; Kogure, N.; Kitajima, M.; Takayama, H. *Org. Lett.* **2009**, *11*, 5554.

140. Otsuka, Y.; Inagaki, F.; Mukai, C. *J. Org. Chem.* **2010**, *75*, 3420.

141. Nakayama, A.; Kogure, N.; Kitajima, M.; Takayama, H. *Angew. Chem. Int. Ed. Eng.* **2011**, *50*, 8025.

142. a) Lounasmaa, M.; Hanhinen, P.; Westersund, M. in *The Sarpagine Group of Indole Alkaloids, Vol. 52*; (Ed.: Cordell, G. A.) Academic Press: San Diego, **1999**;. b) Hamaker, L. K.; Cook, J. M. in *Alkaloids: Chemical and Biological Perspectives, vol. 9*; (Ed.: Pelletier, S. V.) Elsevier Science: New York, **1995**; c) Keawpradub, N.; Kirby, G. C.; Steele, J. C. P.; Houghton, P. J. *Planta Med.* **1999**, *65*, 690.

143. Miller, K. A.; Martin, S. F. *Org. Lett.* **2007**, *9*, 1113.

144. a) Bernauer, K.; Englert, G.; Vetter, W. *Experientia* **1965**, *21*, 374; b) Plat, M.; Hachem-Mehri, M.; Koch, M.; Scheidegger, U.; Potier, P. *Tetrahedron Lett.* **1970**, *11*, 3395; c) Daudon, M.; Mehri, M. H.; Plat, M. M.; Hagaman, E. W.; Wenkert, E. *J. Org. Chem.* **1976**, *41*, 3275; d) Mehri, H.; Diallo, A. O.; Plat, M. *Phytochemistry* **1995**, *40*, 1005.

145. Hayashi, Y.; Inagaki, F.; Mukai, C. *Org. Lett.* **2011**, *13*, 1778.

146. For a recent review on prostaglandins, see: Das, S.; Chandrasekhar, S.; Yadav, J. S.; Gree, R. *Chem. Rev.* **2007**, *107*, 3286.

147. Krafft, M. E.; Wright, C. *Tetrahedron Lett.* **1992**, *33*, 151.

148. Bernardes, V.; Kann, N.; Riera, A.; Moyano, A.; Pericas, M. A.; Greene, A. E. *J. Org. Chem.* **1995**, *60*, 6670.

149. Grieco, P. A.; Abood, N. *J. Org. Chem.* **1989**, *54,* 6008.

150. Vazquez-Romero, A.; Rodriguez, J.; Lledo, A.; Verdaguer, X.; Riera, A. *Org. Lett.* **2008**, *10*, 4509.

151. a) Narasaka, K.; Shibata, T. *Chem. Lett.* **1994**, 315; b) Shibata, T.; Koga, Y.; Narasaka, K. *Bull. Chem. Soc. Jpn.* **1994**, *68*, 911.

152. Ahmar, M.; Antras, F.; Cazes, B. *Tetrahedron Lett.* **1995**, *36*, 4417.

153. For a recent review on silicon-tethered processes, see: Bracegirdle, S.; Anderson, E. A. *Chem. Soc. Rev.* **2010**, *39*, 4114.

154. Brummond, K. M.; Sill, P. C.; Chen, H. *Org. Lett.* **2004**, *6*, 149.

155. Collins, P. W.; Djuric, S. W. *Chem. Rev.* **1993**, *93*, 1533.

156. Magnus, P.; Becker, D. P. *J. Am. Chem. Soc.* **1987**, *109*, 7495.

157. Shibasaki, M.; Torisawa, Y.; Ikegami, S. *Tetrahedron Lett.*, **1983**, *24*, 3493; b) Suzuki, M., Koyano, H., Noyori, R. *J. Org. Chem.*, **1987**, *52*, 5583.

158. Ishikawa, T.; Ishii, H.; Shimizu, K.; Nakao, H.; Urano, J.; Kudo, T.; Saito, S. *J. Org. Chem.* **2004**, *69,* 8133.

159. (a) *Remodulins stable form of prostacyclin*; United Therapeutics Corp. Web Site March 23, 2001. b) Aristoff, P. A.; Harrison, A. W.; Aiken, J. W.; Gorman, R. R.; Pike, J. E. in *Advances in Prostaglandin Thromboxane and Leukotriene Research, Vol. 11*; (Eds.: Samuelsson, B., Paoletti, R., Ramwell, P. W.) Raven Press: New York, **1983**, 264. c) Sorbera, L. A.; Rabasseda, X.; Castaner, J. *Drugs Future* **2001**, *26*, 364.

160. Moriarty, R. M.; Rani, N.; Enache, L. A.; Rao, M. S.; Batra, H.; Guo, L.; Penmasta, R. A.; Staszewski, J. P.; Tuladhar, S. M.; Prakash, O.; Crich, D.; Hirtopeanu, A.; Gilardi, R. *J. Org. Chem.* **2004**, *69*, 1890.

161. Evans, P. A.; Robinson, J. E. *J. Am. Chem. Soc.* **2001**, *121*, 4609.

162. Wang, H.; Sawyer, J. R.; Evans, P. A.; Baik, M.-H. *Angew. Chem. Int. Ed.* **2008**, *47*, 342.

163. For a review on the transition metal-catalysed allylic alkylation reaction, see: (a) Trost, B. M.; Van Vracken, D. L. *Chem. Rev.* **1996**, *96*, 395. (b) Trost, B. M.; Crawley, M. L. *Chem. Rev.* **2003**, *103*, 2921.

164. Jeong, N.; Seo, S. D.; Shin, J. Y. *J. Am. Chem. Soc.* **2000**, *122*, 10220.

165. Evans, P. A.; Robinson, J. E. *unpublished results.*

166. For references on the rhodium-catalysed allylic alkylation see: (a) Evans, P. A.; Nelson, J. D. *J. Am. Chem. Soc.* **1998**, *120*, 5581. (b) Evans, P. A.; Robinson, J. E.; Nelson, J. D. *J. Am. Chem. Soc.* **1999**, *121*, 6761. (c) Evans, P. A.; Leahy, D. K. *J. Am. Chem. Soc.* **2000**, *122*, 5012. (d) Evans, P. A.; Kennedy, L. J. *J. Am. Chem. Soc.* **2001**, *123*, 1234.

167. Computational studies employed high-level density functional method B3LYP/cc-pVTZ(-f). Software: Jaguar 6.0. Schrodinger Inc., Portland, Oregon, **2003**.

168. Evans, P. A.; Sawyer, J. R. *Unpublished results.*

169. Baik, M.-H.; Mazumder, S.; Ricci, P.; Sawyer, J. R.; Song, Y.-G.; Wang, H.; Evans, P. A. *J. Am. Chem. Soc.* **2011**, *133*, 7621.

170. For recent examples of DFT calculations on the understanding of rhodium-catalysed [m+n] and [m+n+o] carbocyclization reactions, see: (a) [(5+2)]: Yu, Z.-X.; Wender, P. A.; Houk, K. N. *J. Am. Chem. Soc.* **2004**, *126*, 9154. (b) [4+(2+2)]: Baik, M.-H.; Baum, E. W.; Burland, M. C.; Evans, P. A. *J. Am. Chem. Soc.* **2005**, *127*, 1602. (c) [2+2+2+1]: Montero-Campillo, M. M.; Rodríguez-Otero, J.; Cabaleiro-Lago, E. *J. Phys. Chem.* **2008**, *112*, 2423.

171. Software: Jaguar 7.0, Schrödinger, LLC, New York, NY, **2007**. The computational studies on the room-temperature diastereoselective PK reaction of chlorinated 1,6-enynes have been performed by the following members of the Baik Group: Mazumder, S; Song, Y.-G.; Wang, H.

172. We used the CHELP charges, as defined in Breneman, C. M.; Wiberg, K. B. *J. Comp. Chem.* **1990**, *11*, 361.

173. For examples of metal-catalysed [m+n] and [m+n+o] carbocyclizations with alkynyl halides, see: (a) **Ru** *[(2+2)]:* Villenueve, K.; Riddell, N.; Jordan, R. W.; Tsui, G. C.; Tam, W. *Org. Lett.* **2004**, *6*, 4543. (b) **Rh** *[(4+2)]:* Yoo, W.-J.; Allen, A.; Villeneuve, K.; Tam, W. *Org. Lett.* **2005**, *7*, 5853. (c) **Ru** *[(2+2)+2]:* Nicolaou, K. C.; Tang, Y.; Wang, J. *Angew. Chem., Int. Ed.* **2009**, *48*, 3449.

174. For the challenges associated with conducting room temperature PK reactions, see: Schmid, T. M.; Consiglio, G. *Chem. Commun.* **2004**, 2318.

175. Evans, P. A.; Laidlaw, H.; Sawyer, J. R.; Atkinson, S. *manuscript in preparation.*

176. Geometry optimization were performed with a 3.21 G* method (equilibrium geometry, solvent: toluene) utilizing Spartan Software, Wavelenght Inc., **2008**.

177. *Metal-Catalyzed Cross-Coupling Reactions*, 2nd Ed.; de Meijere, A., Diederich, F., Eds.; Wiley-VCH: Weinheim, **2004**.

178. a) Walker, S. D.; Barder, T. E.; Martinelli, J. R.; Buchwald, S. L.; b) *Angew. Chem. Int. Ed.* **2004**, *43*, 1871; b) Carret, S.; Deprés, J.-P. *Angew. Chem. Int. Ed.* **2007**, *46*, 6870.

179. Gao, G. L.; Niu, Y. N.; Wang, H. L.; Wang, G. W.; Shaukat, A.; Liang, Y. M. *J. Org. Chem.* **2010**, *75*, 1305.

180. Yun, S. Y.; Kim, M.; Lee, D.; Wink, D. J. B. *J. Am. Chem. Soc.* **2009**, *131*, 24.

181. Sylvester, K. T.; Chirik, P. J. *J. Am. Chem. Soc.* **2009**, *131*, 8772.

CHAPTER 2

RHODIUM(I)-CATALYSED [2+2+1] ENANTIOSELECTIVE PAUSON-KHAND CARBOCYCLISATIONS OF CHLORINATED 1,6-ENYNES AT ROOM TEMPERATURE.

2.1. Enantioselective Pauson-Khand Reactions.

2.1.1. Introduction.

The development of the PK reaction in 1971 provided an innovative strategy for the construction of bicyclopentenone derivatives.[3,4] The synthetic potential of the process inspired the exploration of a wide variety of transition metals in order to enhance the substrate scope and the applicability of the process towards the total synthesis of biologically active targets. In this context, the enantioselective synthesis of bioactive natural compounds also prompted a the investigation of asymmetric PK reactions.[2]

The development of the Co-catalysed carbocyclisation by Pauson and Khand coincided with the concomitant accomplishment of the first asymmetric metal-catalysed hydrogenation process. Hence, pioneering studies by Knowles[182] and Horner[183] demonstrated that chiral monophosphine ligands exerted modest enantiocontrol in the hydrogenation of styrene (Eq. 2.1) and acrylic acid derivatives (Eq. 2.2). Despite the low enantioselectivity and the problems associated with the preparation of ligands with chirality on the phosphorous atom, these studies outlined the ability of chiral phosphine ligands[184] to promote asymmetric metal-catalysed reactions. The subsequent development of the C_2-symmetric chelating bisphosphine DIOP by Kagan outlined the importance of the backbone chirality in the ligand design (Eq. 2.3).[185] In this context, it was envisaged that a C_2-symmetric ligand with two equivalent P atoms reduced the number of possible isomeric metal complexes, as well as the number of

possible substrate–catalyst arrangements, thus enhancing the enantioselectivity of the reaction.

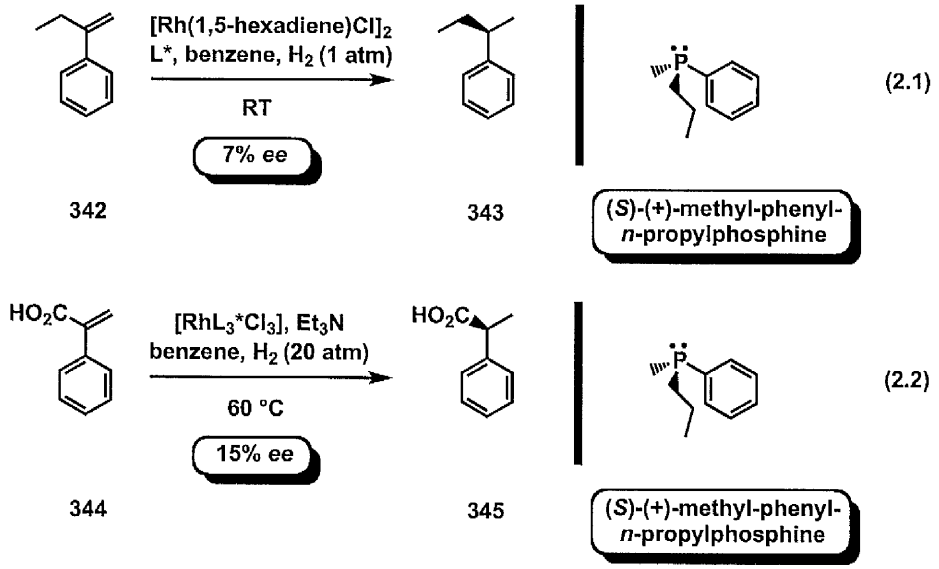

Further developments to the ligand for the Rh-catalysed hydrogenation of acrylic acids provided outstanding enantioselectivity, compared to the previous chiral phosphine ligands (Eq. 2.1-2.2).

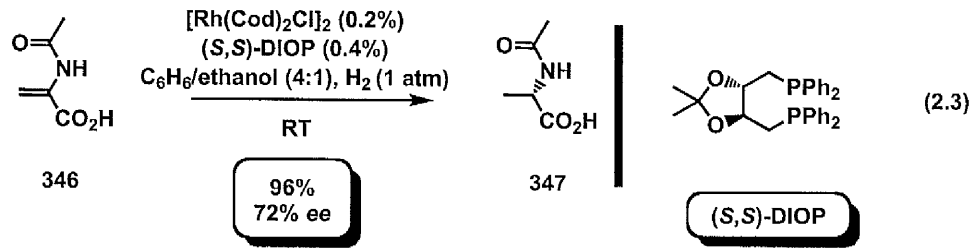

The acknowledged ability of a C2-symmetric bisphosphine to induce high level of enantioselectivity in the asymmetric metal-catalysed reactions, prompted Knowles to develop the P-chiral bisphosphine ligand DIPAMP (**Scheme 2.1**).[186] Application to the asymmetric hydrogenation highlighted the synthetic utility of the ligand in the context of excellent enantioselectivity in the reaction and the ability to conduct the reaction with an extremely low catalyst loading (**Scheme 2.1**). The ability of the ligand to provide access to enantiopure amino acids was further exploited in the first industrial-scale total synthesis of L-DOPA.[186]

Scheme 2.1. Total synthesis of L-DOPA.

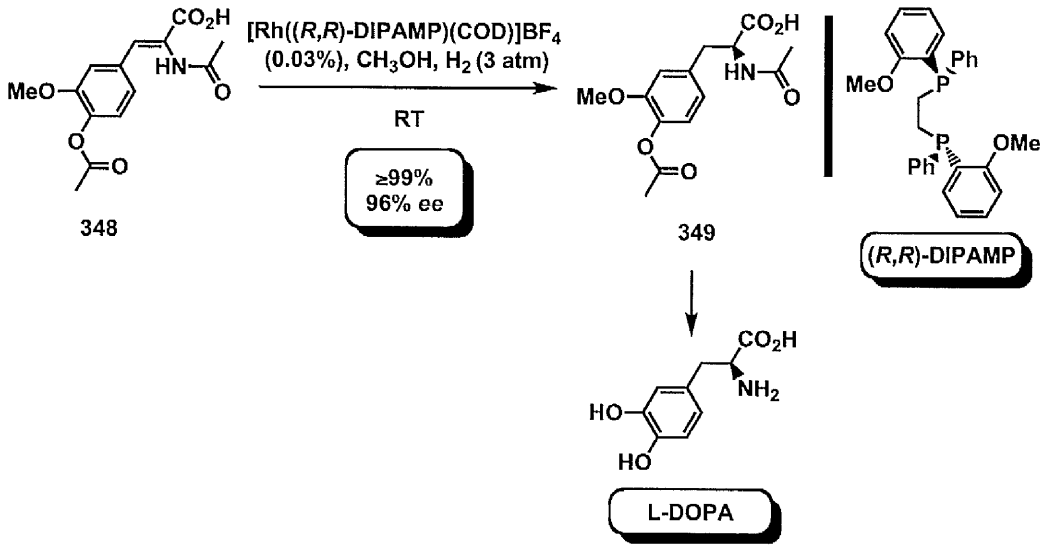

Despite the outstanding advancement in the design of bisphosphine ligands and the high level of enantioselectivity displayed in the asymmetric hydrogenation of various olefins, the major breakthrough in the field of chiral ligands came in 1980 with the development of the BINAP bisphosphine by Noyori.[187a] The synergic ability of the ligand and rhodium species to catalyse the asymmetric hydrogenation of α-(acylamino)acrylic acids with outstanding enantioselectivity, high yields and low catalyst loading provided analogous results, albeit the synthesis of biaryl chiral backbones was easily accessible compared to the previously employed chiral phosphines (Eq.2.4).[187b]

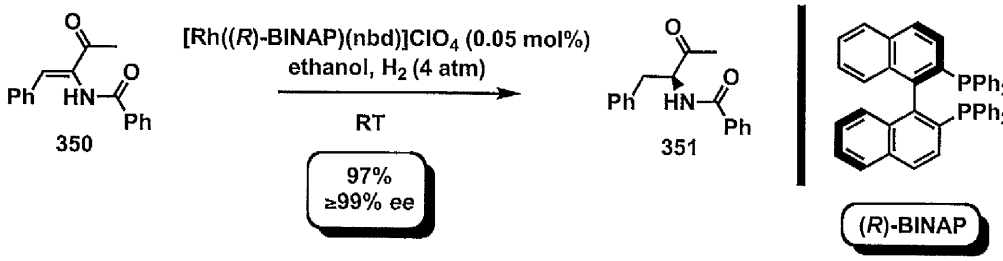

The outstanding ability of this ligand to provide high levels of enantioselectivity in metal-catalysed reactions was further demonstrated in the asymmetric reduction of carbonyl compounds with Ru/BINAP complexes (Eq. 2.5).[187c]

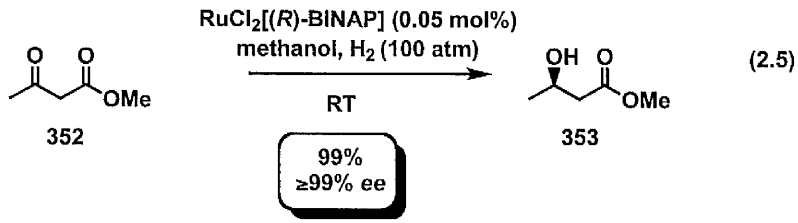

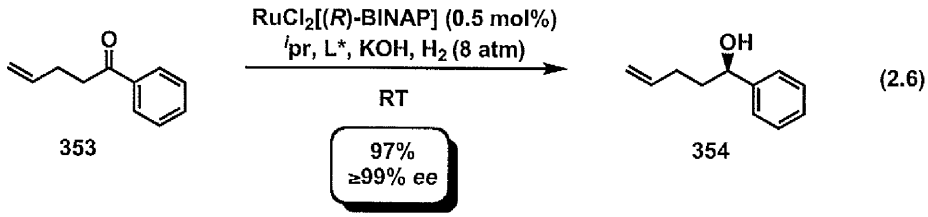

An additional feature with this process, is the ability to selectively reduce ketones in presence of other carbon-carbon double bonds, which is particularly useful in total synthesis (Eq. 2.6).[187d] The enantiofacial discrimination imparted by the BINAP ligand could be explained by the "quadrant diagram", originally developed by Knowles (**Figure 2.1**).[186b]

Figure 2.1. Knowles' quadrant diagram theory.[188]

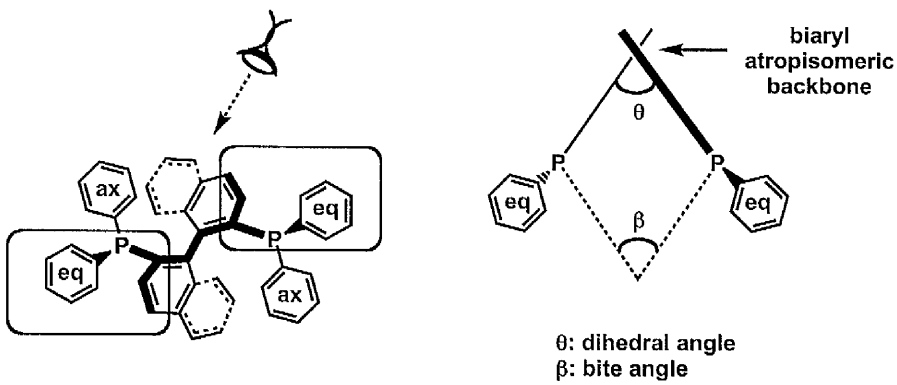

The model highlights the role of the aromatic substituents on the P atom as blocking groups and their ability to enhance the enantiofacial discrimination in the hydrogenation process.

Additionally, a remarkable feature of this atropisomeric ligand resides in the possibility to modify the biaryl-type backbone, which impacts the bite angle of the related metal-ligand complex, thereby enhancing the reactivity of the metal complex towards the hydrogenation of different unsaturated functional groups (**Figure 2.1**). As a result of this seminal contribution to the field of asymmetric catalysis, Noyori[187e] and Knowles[186c] were awarded the 2001 Nobel Prize. Hence, the outstanding advancements in the field of chiral ligands inspired the design and synthesis of many novel chiral bisphosphine ligands in order to improve the reactivity and enantioselectivity of asymmetric metal-catalysed reactions. A notable effort was devoted to the tuning of the chiral backbone of the atropisomeric ligands and the modification of the steric environment around the phosphorous atom. For instance, in 1991, Burk designed a series of strongly electron-donating bisphospholane ligands, namely Duphos and BPE, which have a rigid chiral backbone.[199] The novel ligands provided high enantioselectivity in the hydrogenation of a wide range of functionalised olefins (**Figure 2.2**). Togni and Splinder subsequently reported a series of non C2-symmetric ferrocene-based bisphosphines, named Josiphos ligands (**Figure 2.2**).[189] Key feature of this class of ligands was the ability to introduce a wide range of sterically and electronically different phosphines on the cyclopentadienyl moiety.

Figure 2.2. Chiral C2-simmetric bisphosphine ligands.

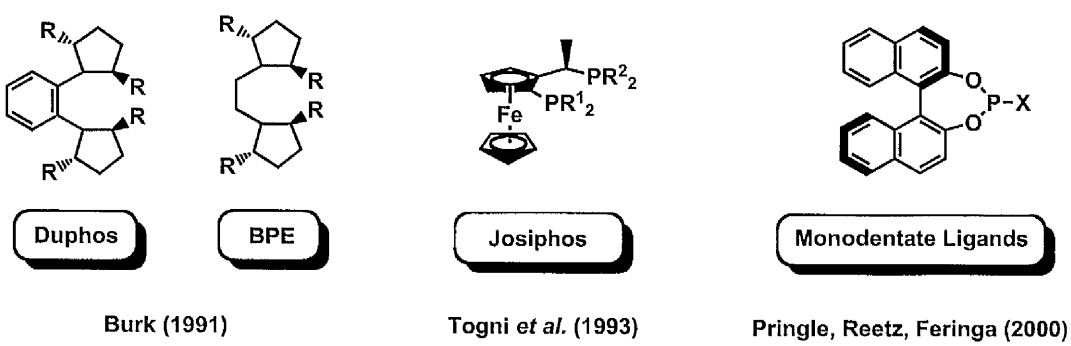

Additionally, these bisphosphine ligands were effective applicability in the commercial synthesis of (+)-biotin[191] and the herbicide (*S*)-metolachlor.[192] Recent work by Pringle,[193a] Reetz[193b] and Feringa[193c] had the merit to introduce monodentate phosphoramidates could function as ligands in the Rh-catalysed asymmetric hydrogenation of different olefins, providing similar reactivity and levels of enantioselectivity displayed by other bisphosphine derivatives (**Figure 2.2**).

This section provided a summary of the advancements in the design of chiral bisphosphine ligands and their application to metal-catalysed hydrogenation reactions. The high levels of enantioselectivity imparted by the these chiral ligands coupled with the high reactivity prompted the extension of these studies to other metal-catalysed reactions, including the Pauson-Khand reaction.

2.1.2. Titanium.

Despite the tremendous advancements in the development of the PK reaction and its widespread application in the context of total synthesis, the first asymmetric catalytic version was achieved 25 years after the pivotal work of Pauson and Khand. Surprisingly, the enantioselective variant involved a chiral titanium catalyst whereas the previous non-enantioselective protocols employed cobalt.

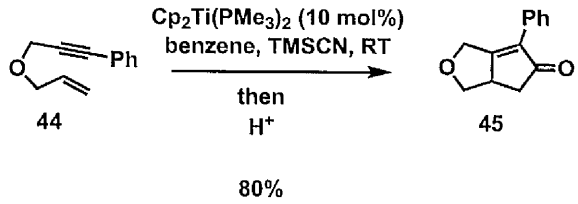

44 45 80% (2.7)

The first report by Buchwald and coworkers described the ability of cyclopentadienyl titanium complexes to catalyse the [2+2+1] carbocyclisation of enynes and isocyanides (Eq. 2.7).[194a] The corresponding iminocyclopentenes derivatives undergo *in situ* hydrolysis, to afford the corresponding bicyclopentenone adducts. Hence, this seminal study highlighted the

opportunity to achieve a direct Ti-catalysed formation of bicyclopentenone adducts under a carbon monoxide atmosphere. The employment of thermal conditions and a positive CO atmosphere (1.3 atm) allowed the desired transformation in good to excellent overall yield (Eq. 2.8).[194b,c]

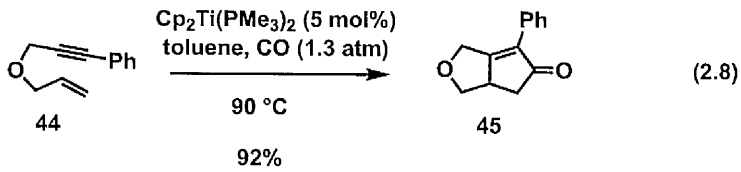

The development of the first Ti-catalysed asymmetric carbonylation was mainly hampered by the ability of carbon monoxide to easily dissociate the chiral ligand from the metal centre and thereby promote the racemic carbocyclisation. The Buchwald group could easily this problem by connecting the chiral ligand and the metal center by an alkyl chain, thereby avoiding the formation of an achiral Ti catalyst (Eq. 2.9). Hence, the chiral ligand EBTHI in conjunction with high CO pressure provided the desired enantiocontrol and reactivity in the process, albeit the catalyst is very sensitive to air and moisture, which required the reaction to be conducted in a glovebox.[195]

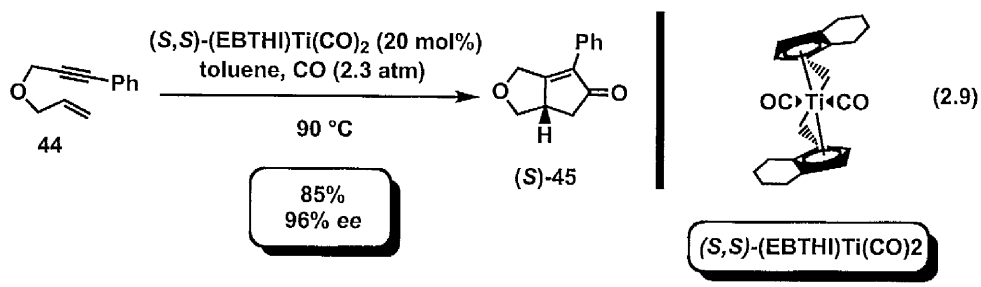

The proposed mechanism involved the initial formation of the active catalyst **ii**, followed by the displacement of a CO ligand and coordination of the alkyne moiety to provide metallacycle **iv** (**Scheme 2.2**). Coordination to the alkene and displacement of an additional CO ligand generates intermediate **v**, which undergoes reductive cyclisation and provides Ti-

metallacycle **vi**. The catalytic cycle is completed by CO insertion and reductive elimination, to afford the desired bicyclopentenone **viii**.

Scheme 2.2. Mechanism of the Ti-catalysed intramolecular enantioselective PK reaction.

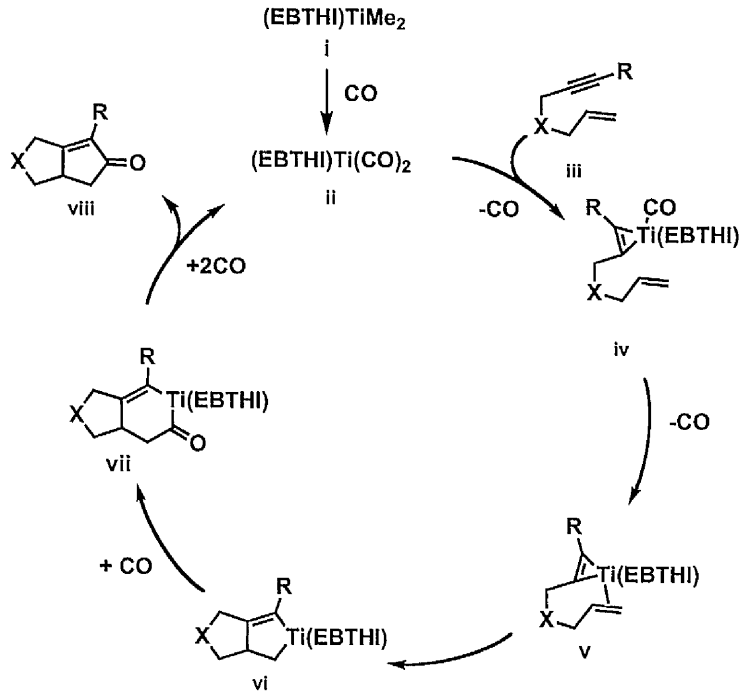

Scheme 2.3. Origin of enantioselectivity in the Ti-catalysed PK reaction.

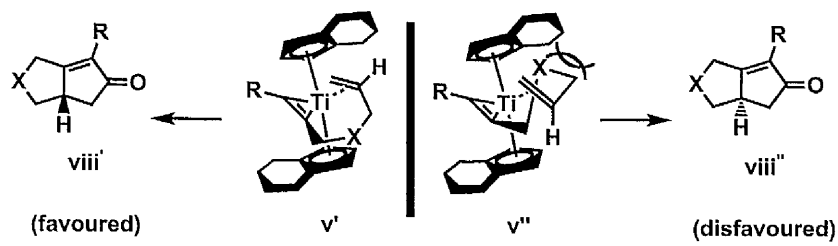

The reductive cyclisation of intermediate **v** into metallacycle **vi** is considered to be the enantioselective determining step in this process. Hence, unfavourable steric interactions between the enyne and the chiral ligand backbone promote the preferential formation of the intermediate **v'**, which explains the absolute configuration of the product (**Scheme 2.3**).

2.1.3. Cobalt.

The first example of a Co-catalysed catalytic asymmetric Pauson-Khand reaction was described by Hiroi in 2000 (Eq. 2.10).[196] The cobalt-catalyst with the atropisomeric bisphosphine ligand BINAP facilitated the formation of bicyclopentenone derivatives in moderate yield and good enantioselectivity, albeit the methodology was severely affected by the limited substrate scope.

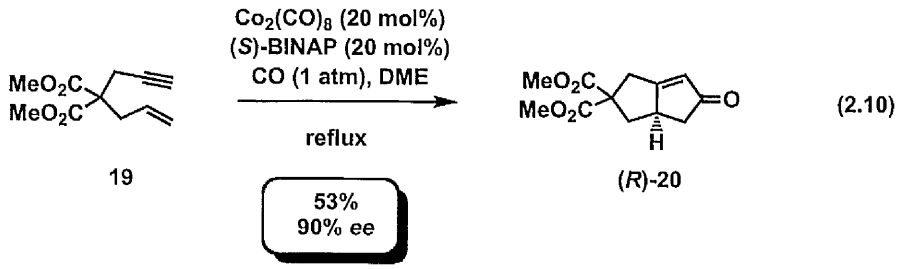

(2.10)

Additional experimental investigations highlighted that the enantioselectivity of the transformation was clearly influenced by the ligand loading, since a 1:0.5 and 1:1.5 metal:BINAP ratio decreased the enantioselectivity to 22 and 30%, respectively. An initial investigation into the stereoselectivity of the process postulated a hypothetical coordination of the BINAP to a single cobalt atom would be largely unfavoured by the bulky nature of the ligand and catalyst. Hence, each phosphorous of the BINAP ligand would coordinate to a different cobalt-atom, thereby promoting the formation of two possible conformers with a boat-like or chair-like conformation (**Figure 2.3**). In light of the pronounced steric interference between phenyl rings on the phosphorus atoms and the naphthyl rings of (*S*)-BINAP in the chair-like conformer, preferential alkene insertion in the boat-like intermediate was envisioned to determine a stereoselective cobaltacycle formation. Further mechanistic studies on the BINAP/Co complexes by the Gibson group confirmed the postulated origin of stereoinduction in the reaction.[197]

Figure 2.3. Origin of the enantioselectivity in the Co-catalysed PK reaction.

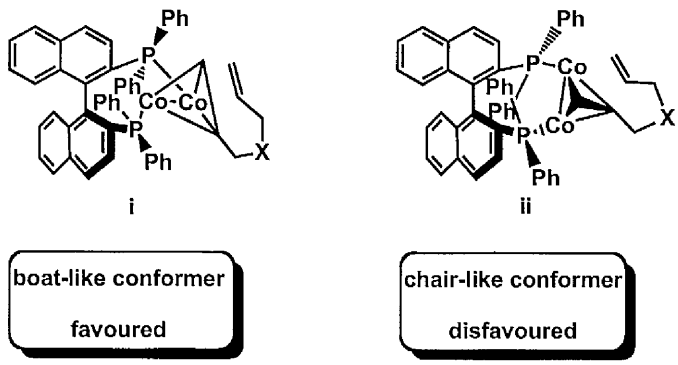

Buchwald and coworkers exploited triphenylphosphite[17] as coligand in the Co-catalysed PK reaction and further utilised chiral phosphite ligands in the context of the asymmetric Co-catalysed carbocyclisation.[198] Unfortunately, despite the good reactivity of the C2-symmetric binaphthyl-type phosphites, the observed enantioselectivity was poor, particularly with 1,6-enynes bearing no substitution on the alkyne terminus (Eq. 2.11).

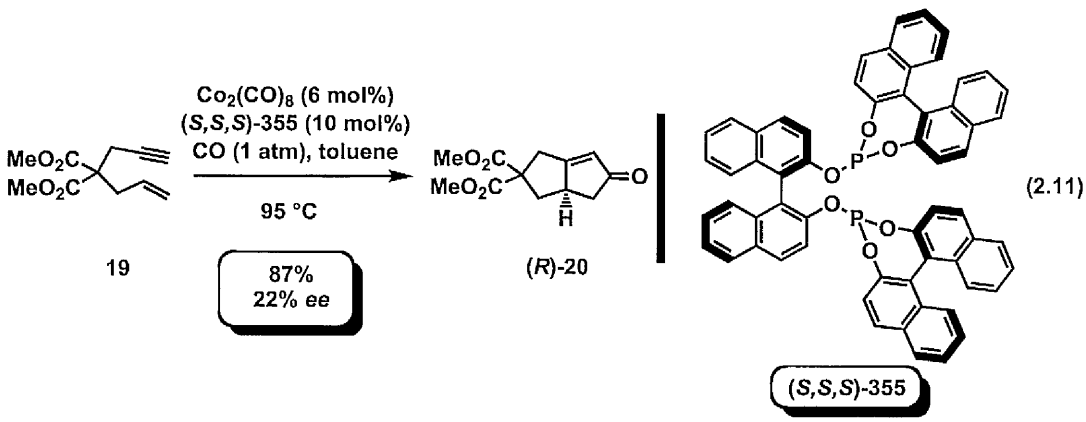

In contrast to the intramolecular manifold, the intermolecular Co-catalysed PK reaction required a stoichiometric metal complex on the alkyne unit to induce chirality in the process.[93,199] In this context, studies by Greene demonstrated that an intermolecular carbocyclisation of phenylacetylene and norbornene could be achieved in presence of a

catalytic amount of cobalt catalyst and chiral phosphoramidate ligand MONOPHOS (Eq. 2.12).[200]

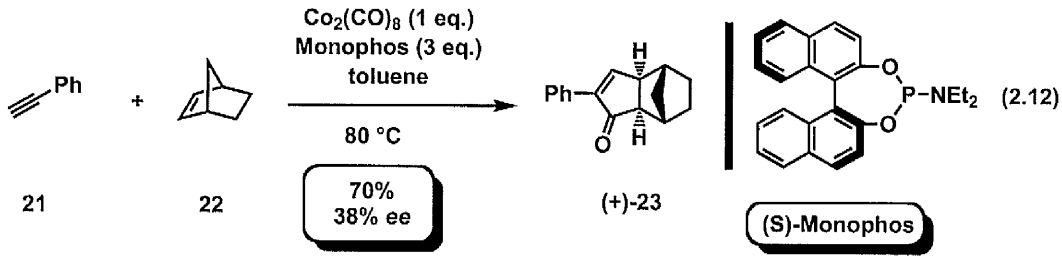

Despite the moderate enantioselectivity, this work provided the first example of a catalytic and asymmetric intermolecular Co-catalysed PK reaction. The discovery of the Co-catalysed directed PK reaction by the Krafft group revealed that a sulfur atom on the alkene unit efficiently coordinated to the cobalt centre, thereby directing the regiochemistry of the alkene insertion.[14] These findings inspired Pericas to design a new class of sulfur-containing bidentate ligands that could chelate the (alkynyl)-hexacarbonyldicobalt complexes, and thereby promote a stereospecific alkene insertion and facilitate the enantioselective intermolecular carbocyclisation. In this context, the PuPHOS ligands, which are readily accessible from natural (+)-pulegone, confer optimal reactivity and enantioselectivity in the intermolecular PK reaction of norbornene and monosubstituted alkynes (**Scheme 2.4**).[201] The outstanding efficacy of the PuPhos inspired an additional investigation into the design of alternative bidentate PS (phosphorous-sulfur) ligands, in order to enhance the substrate scope of the intermolecular Co-catalysed process. An intriguing opportunity for this goal resides in the ability to exploit ligands bearing chirality on the phosphorous or sulphur atom. Unlike phosphorous, the introduction of chirality on the sulphur atom has become relatively routine, as demonstrated by the efficient synthesis of chiral *tert*-butyl sulfinamides by Ellman.[202] The scalable synthesis of bidentate *N*-phosphino sulfinamides ligands (PNSO) bearing a sulfoxide moiety as the only source of chirality further exemplifies this idea (**Scheme 2.5**).[203]

Scheme 2.4. PuPhos ligands in the intermolecular Co-catalysed PK reaction.

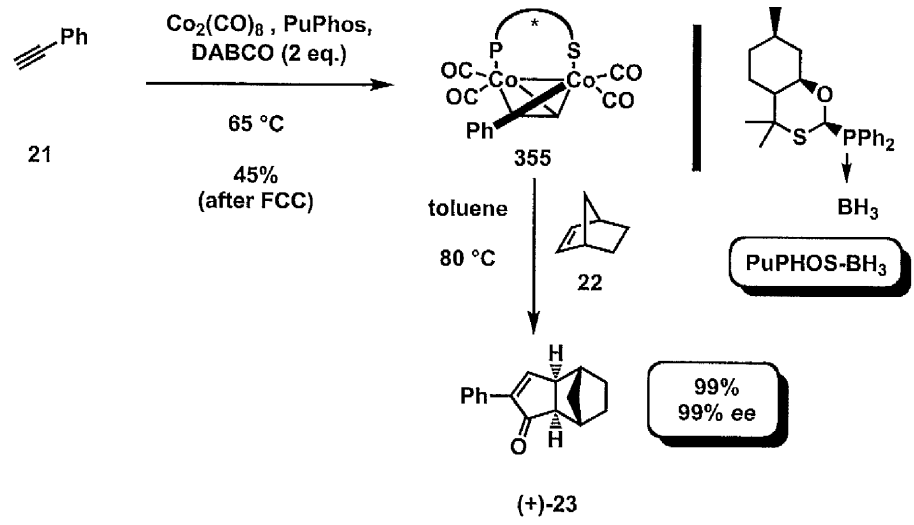

Scheme 2.5. PNSO ligands in the intermolecular Co-catalysed PK reaction.

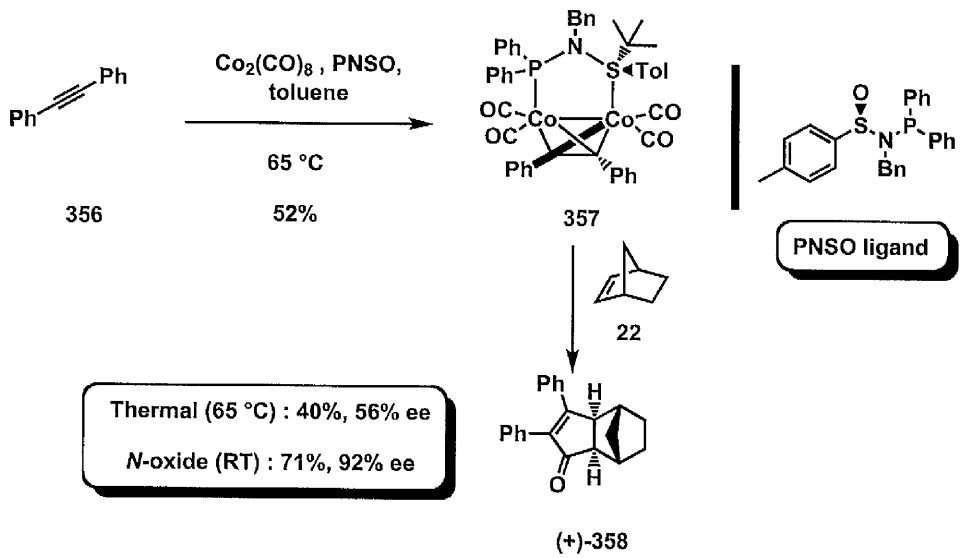

The extension of the Co-catalysed intermolecular PK reaction to the asymmetric intermolecular carbocyclisation of internal alkynes is an impressive demonstration of the synthetic utility of these ligands.[203c] The development of this methodology highlighted the key role of NMO for achieving highly enantioselective transformations. Employment, the role of the amine *N*-oxide is to generate a vacant coordination site on the cobalt centre and thereby allow the coordination of the sulfoxide moiety in a bidentate manner, which is

followed by stereoselective insertion of the alkene (**Figure 2.4**). In absence of additives, the inability to coordinate with a site on the cobalt centre forces the PNSO to behave as a monodentate ligand. Hence, the diminished enantiofacial discrimination in the subsequent alkene insertion step results in lower stereoselectivity in the carbocyclisation process.[203c]

Figure 2.4. Role of the NMO additive in the enantioselective Co-catalysed intermolecular PK reaction.

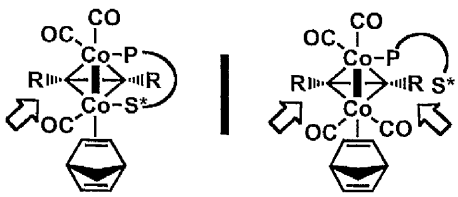

2.1.4. Iridium.

The development of the first Rh-catalysed PK reaction by the Jeong group employing $[RhCl(cod)]_2$ and bisphosphine ligand dppp,[50] inspired the Shibata group to examine the feasibility of a novel PK reaction in presence of the congener $[IrCl(Cod)]_2$. The beneficial effect of dppp ligand in the former process provided the intriguing opportunity to replace the achiral bisphosphine with chiral BINAP-type analogues and carry out an enantioselective transformation.

Although the synthetic value of the process was partly affected by the high catalyst loading and high temperature, the methodology demonstrated the synergistic role of iridium catalyst and chiral atropisomeric binaphthyl ligands to facilitate a highly enantioselective PK reaction (Eq. 2.13).[204a] A putative mechanism for the carbocyclisation involves the initial dissociation of $[Ir(Cod)Cl]_2$ complex, complexation with the phosphine ligand and formation of a monomeric square-planar iridium complex **ii** (**Scheme 2.6**).

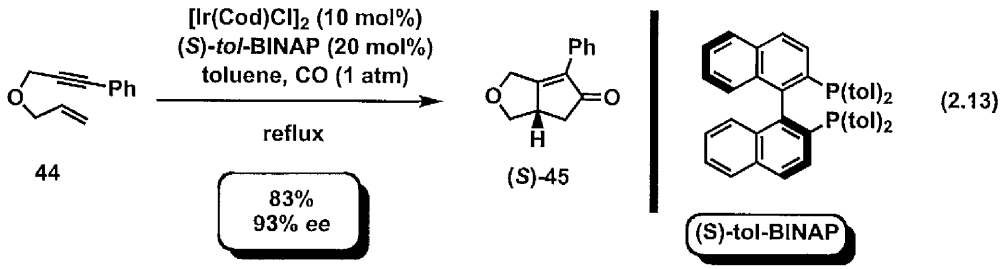

Scheme 2.6. Mechanism of the Ir-catalysed intramolecular enantioselective PK reaction.

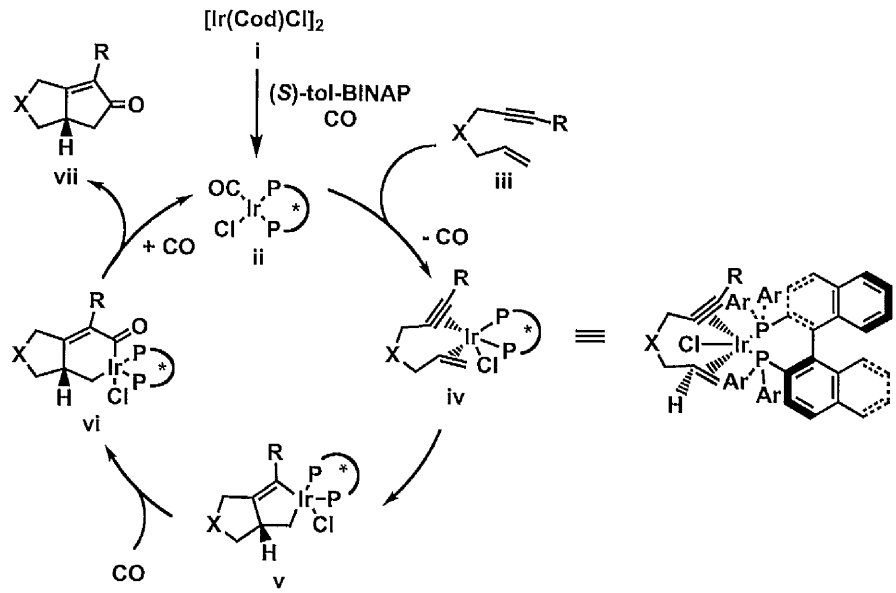

Coordination of the enyne **iii** to the active catalyst **ii**, followed by oxidative addition provided the iridium metallacycle **v**. The process is then completed by CO insertion and reductive elimination to afford the desired bicyclopentenone derivative **vii**. Shibata also identified the oxidative addition of intermediate **iv** as the enantioselectivity determining step.[204a] Coordination of the enyne **iii** to the chiral complex **ii** forces the alkyne substituent into the upper position, in order to prevent steric interactions with the tolyl substituents on the phosphorous atom. Thus, the alkene unit can exclusively approach from the lower side, to promote enantiospecific oxidative addition. The scope of the process was further extended to the corresponding intermolecular manifold, which was applied to a challenging catalytic

asymmetric cyclocarbonylation of norbornene and internal asymmetrical alkynes (Eq. 2.14). Despite the low reactivity, this result is very significant, since it provides a unique example of an intermolecular catalytic process with a high level of regio- and enantioselectivity.[204a]

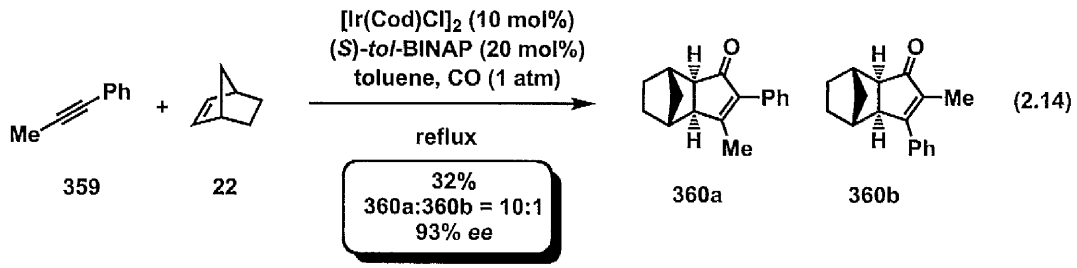

The ability of the iridium catalysts to promote an efficient cyclocarbonylation prompted the Shibata[204b] and Chan[215] groups to examine alternative catalysts and sources of CO, in order to avoid the high catalyst loading and the employment of poisonous carbon monoxide gas. Gratifiingly, aldehydes provide an excellent alternative, which also allow a reduction in catalyst loading from 10 to 5 mol% (**Scheme 2.7**).

Scheme 2.7. Aldehydes as a CO surrogate in the enantioselective Ir-catalysed PK reaction.

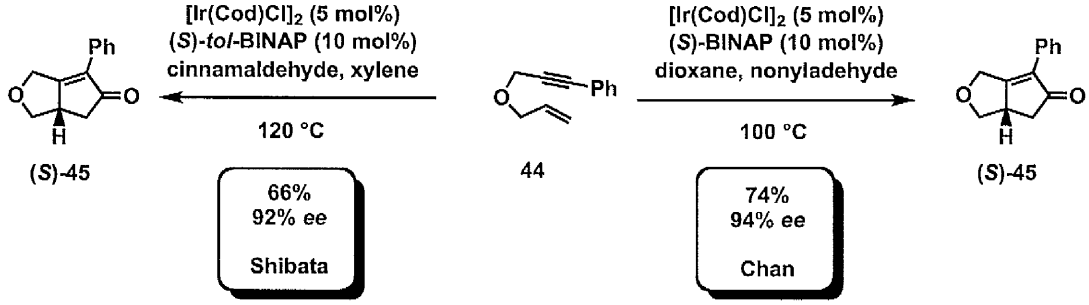

Pfaltz and coworkers demonstrated that Ir/Phox catalyst also promotes the enantioselective hydrogenation of a wide range of unsaturated systems, including imines and unfunctionalised olefins.[206] Hence, in light of the ability of iridium catalysts to promote the PK reaction, Pfaltz

examined the efficacy of the Ir/Phox system in the asymmetric cyclocarbonylation of 1,6-enynes (Eq. 2.15).[207]

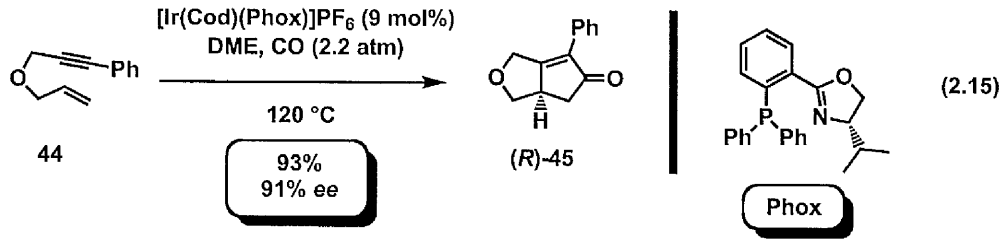

(2.15)

The utilisation of Phox ligands in metal-catalysed cycloaddition reactions was relatively unexplored. Additionally, this class of P,N (phosphorous-nitrogen) ligands has divergent geometrical and electronic properties compared to the classic BINAP-type ligands. Specifically, the PHOX ligands are characterised by a non C2-symmetric backbone, a soft P-ligand with π-acceptor properties and a ''hard'' N-ligand acting primarily as a σ-donor. Thus, their ability to affect an array of transformations in a highly enantioselective manner had a remarkable significance and provided a novel template for the design of ligands for many carbocyclisation reactions.

2.2. Rhodium-catalysed Enantioselective PK Reactions.

2.2.1. Historical Background.

The development of rhodium-catalysed reactions with chiral bisphosphine ligands demonstrated that rhodium was a privileged metal for a variety of transformations. Additionally, the demonstration of dppp ligand in the Rh-catalysed PK reaction[50] provided a further evidence of the synergic ability of rhodium catalysts and bisphosphine ligands. Hence, shortly after the discovery of the Rh-catalysed PK reaction,[50] the Jeong group reported the first asymmetric Rh-catalysed manifold.[208] The process relied in the outlined the ability of BINAP-type ligands to induce chirality, in an analogous manner to Hiroi[196a] and Shibata[204a] in

the development of the first Co- and Ir-catalysed PK reactions. Additionally, in contrast the cobalt and iridium manifolds, the Rh-catalysed reaction occurs with low catalyst loading.

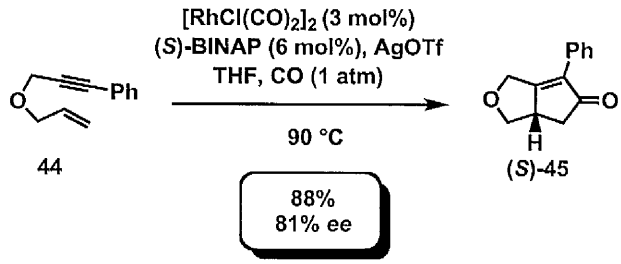

(2.16)

Jeong rationalised the carbocyclisation in the following manner. Treatment of the dimeric metal-catalyst **i** with a silver salt and the bisphosphine ligand lead to the formation of the cationic chiral rhodium active catalyst **ii**. Subsequent coordination of the enyne **iii** and oxidative addition provides the corresponding rhodium metallacycle **v**, which is the enantiodetermining step. CO insertion, followed by reductive elimination provides the desired enantiomerically enriched bicyclopentenone derivative **vii** (**Scheme 2.8**).[208]

Scheme 2.8. Mechanism of the Rh-catalysed enantioselective PK reaction.

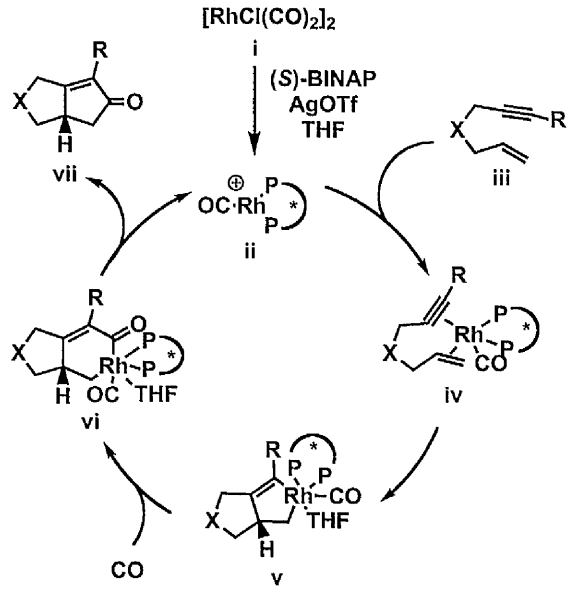

Similar to the Ir-catalysed methodology, coordination of the enyne **iii** to the chiral complex **ii** forces the alkyne substituent on the upper position, in order to prevent steric interactions with the phenyl substituents on the phosphorous atom. Thus, the alkene unit can exclusively approach from the lower side, thereby determining a subsequent enantioselective oxidative addition (**Figure 2.5**).[208]

Figure 2.5. Origin of the enantioselectivity in the Rh-catalysed PK reaction.

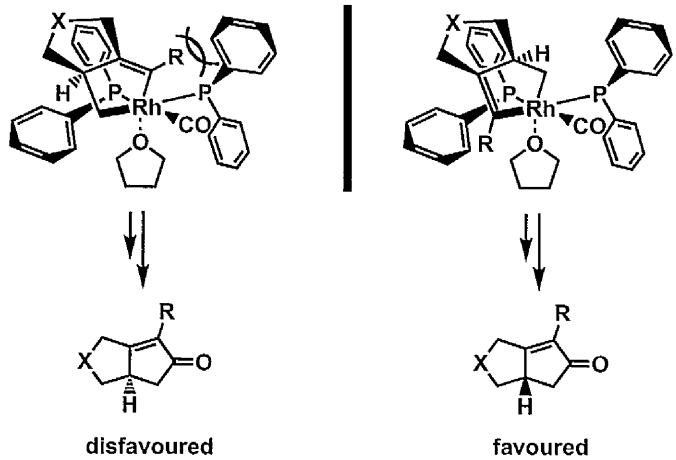

However, the manifolds involve divergent operating conditions, whereas the Ir-catalysed[204a] employed a neutral catalyst in a non-coordinating solvent (toluene) and the analogous Rh-catalysed process utilised a cationic catalyst in a coordinating solvent (THF). As postulated by Jeong, the coordination of the solvent could force the rhodium metallacycle to adopt an octahedral geometry in the oxidative addition (**Figure 2.5**).[208] Additional experimental investigations revealed that the use of THF was essential for the achievement of a high degree of enantioselectivity and thus confirmed that the coordinating solvent could provide the optimal geometry in the Rh-complex for an enantiospecific oxidative addition.

Following studies by the Consiglio group aimed at the identification of the active catalytic species in the asymmetric Rh-catalysed PK reaction (**Scheme 2.9**).[209] A series of detailed kinetic and mechanistic studies provided an alternative scenario, in which the active catalytic

Rh-species **ii** is a square-planar complex bearing two molecules of solvent on the metal centre. Hence, the carbon monoxide component is solely involved only the insertion step and does not coordinate on the rhodium centre in the oxidative addition step (**Scheme 2.9**).

Scheme 2.9. Experimentally confirmed mechanism of the Rh-catalysed enantioselective PK reaction.

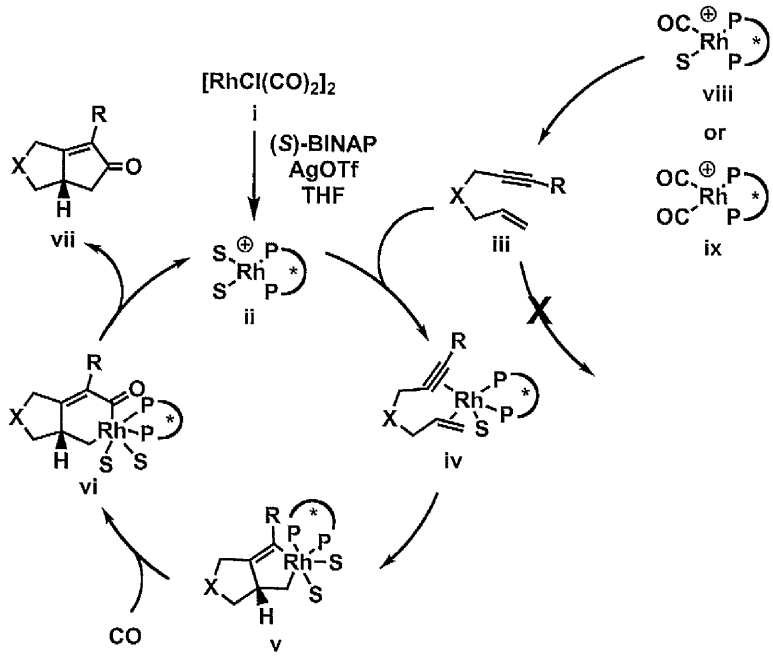

2.2.2. Effect of the Bisphosphine Ligands.

As highlighted in section **2.1.1**, the possibility to alter the backbone and the steric environment around the phosphorous atom of the atropisomeric bisphosphines inspired the design and optimisation of novel ligands in order to enhance the reactivity and enantioselectivity of metal-catalysed reactions. In this context, studies by Genet and Jeong examined the relationship between the structural properties of atropisomeric bisphosphines and the enantioselectivity conferred by these ligands in the Rh-catalysed PK reaction.[210]

Figure 2.6 outlines the electronic and structural profile of a series of atropisomeric bisphosphine ligands. Utilising BINAP as a ligand of reference, the electron density on the phosphorous can be tuned by the modification of the phenyl ring.

Figure 2.6. Electronic and structural properties of C2-symmetric atropisomeric bisphosphine ligands.

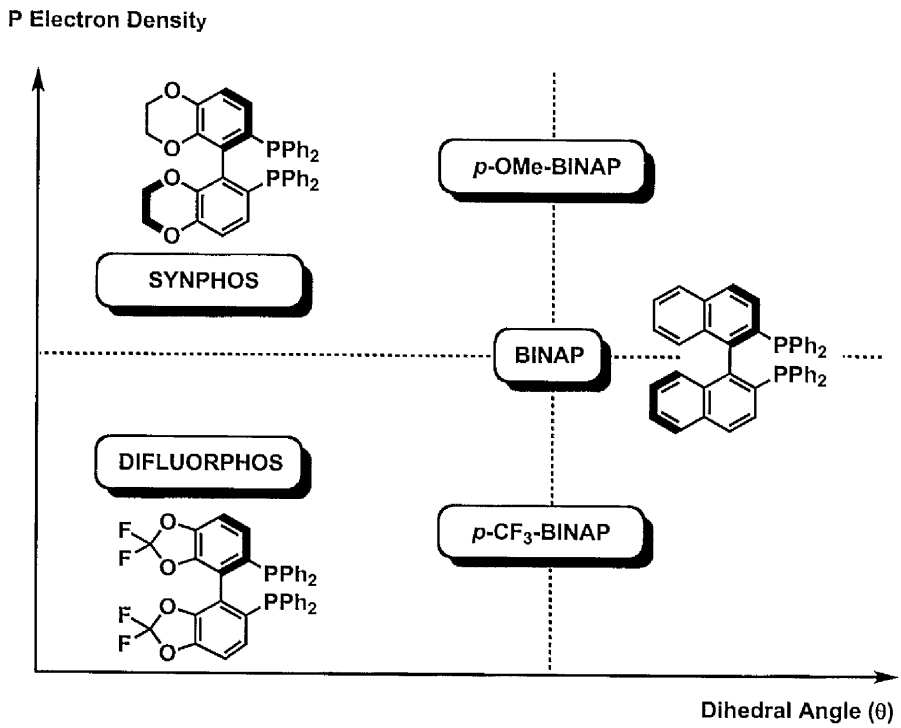

Similarly, the influence of different aromatic substituents on the phosphorous atom electron density is evident from the variation of the ^{31}P chemical shift (Parameter C, **Table 2.1**). Hence, the spectroscopic data demonstrate that *p*-MeO-BINAP (δ = -16.9) and DIFLUORPHOS (δ = -12.5) have the highest and lowest electron density on the phosphorous atom, respectively. Additionally, the electronic analysis included the examination of IR stretching frequency of the CO ligand in the [RhCl(CO)(L*)] complexes, thereby allowing a comparison of the π-acidic character of the chelating bisphosphines (Parameter D, **Table 2.1**). The high CO stretching in the *p*-CF_3-BINAP complex illustrates the high π-acidic character of

the bisphosphine whereas the low CO stretching frequency in *p*-OMe-BINAP complex is consistent with low π-acidic character.

Table 2.1. Structural and spectroscopic properties of C2-symmetric atropisomeric bisphosphine ligands.

Ligand	A (θ, °)	B (θ, °)	C (δ, ppm)	D (υ, cm^{-1})
p-OMe-BINAP	85.2	78.3	-16.9	1998
BINAP	86.2	78.3	-14.4	2003
p-CF_3-BINAP	83.8	78.0	-13.8	2022
SYNPHOS	70.7	73.0	-14.3	2000
DIFLUORPHOS	67.6	72.2	-12.5	2014

A = dihedral angle of the free ligand.

B = dihedral angle of ligand in the [RhCl(CO)L*] complex.

D = ^{31}P NMR chemical shift.

E = IR carbonyl stretching frequency in [RhCl(CO)L*] complex.

Table 2.2. Effect of the bisphosphine ligand on the enantioselectivity of the Rh-catalysed PK reaction.

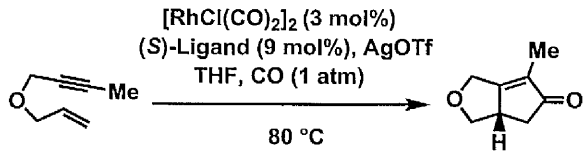

361 (*S*)-362

Ligand	yield (%)	ee (%)
p-OMe-BINAP	53	81
BINAP	70	83
p-CF_3-BINAP	65	84
SYNPHOS	57	93
DIFLUORPHOS	52	89

Subsequent experimental studies on the asymmetric Rh-catalysed PK reaction in presence of atropisomeric bisphosphine ligands provided divergent results in terms of reactivity and enantioselectivity. Hence, as illustrated in **Table 2.2** the bisphosphines with a reduced dihedral angle (SYNPHOS and FLUOROPHOS) provided the highest enantioselectivity in the reaction.[210] As previously outlined in **Figure 2.5**, the steric interactions between alkyne terminus and aryl substituents on the phosphorous atom account for the high stereoselectivity in the oxidative addition step. Additional experimental studies investigated the effect of the substitution on the alkyne moiety on the level of enantioselectivity (**Table 2.3**). The observed results demonstrate the dramatic influence of the alkyne substitution pattern and illustrated that the electronic nature of the terminus (Me or *p*-MeO-C_6H_4), more than the size impact the stereochemical outcome.[210] The outstanding stereoselectivity conferred by binaphthyl- and bisphospholane-type bisphophines in the Rh-catalysed PK reaction inspired the design of novel chiral scaffolds to analyse the effect of the different backbones on the level of enantioselectivity.

Table 2.3. Effect of the alkyne terminus on the Rh-catalysed enantioselective PK reaction.

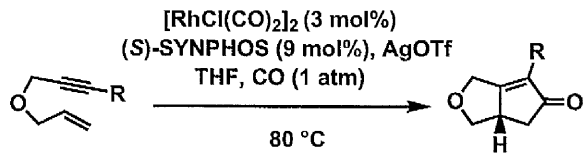

Enyne	R	Product	yield (%)	ee (%)
361	Me	(*S*)-362	57	93
363	*p*-OMe-C_6H_4	(*S*)-364	64	89
44	Ph	(*S*)-44	65	65
365	*p*-CF_3-C_6H_4	(*S*)-366	68	68

For instance, Zhou and coworkers described an efficient asymmetric Rh-catalysed Pauson-Khand reaction in presence of SDP ligands, based on the 1,1'-spirobiindane scaffold. Which has a wide dihedral angle (95 °) (Eq. 2.17).[211]

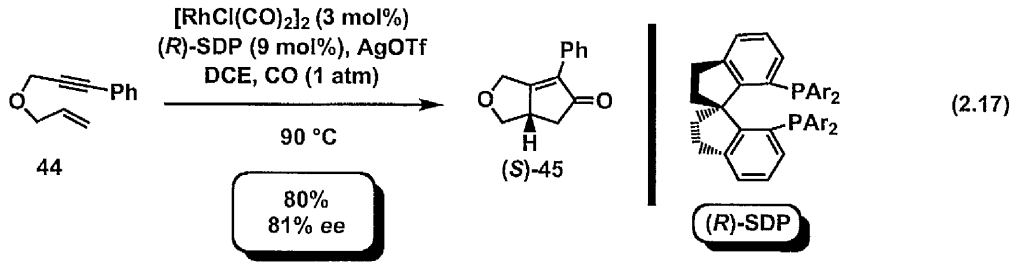

(2.17)

In view of this result, Zhou investigated the Rh-catalysed cyclocarbonylation of 1,6-enynes in presence of monodentate phosphoramidate SIPHOS (Eq. 2.18).[212] The resulting methodology provided the first example of Rh-catalysed PK reaction in presence of a monodentate phosphorous ligand.

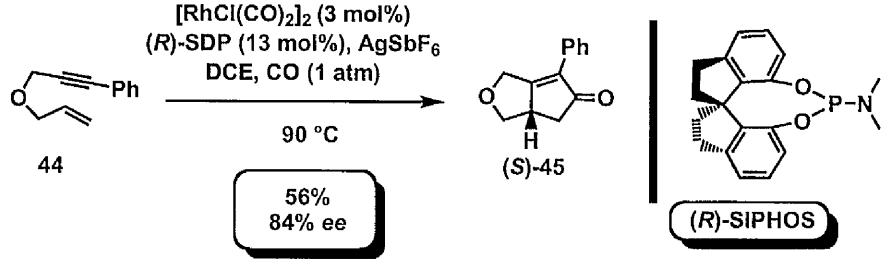

(2.18)

2.2.3. Alternative CO Sources.

The aforementioned developments highlight the wide range of different ligands that impart optimal reactivity and stereoselectivity in the Rh-catalysed asymmetric manifold. Therefore, additional studies focused on the ability to avoid gas CO and thereby provide environmentally benign conditions. In this context, three aromatic provide a CO surrogate (**Scheme 2.10**). The process involves a metal-catalysed decarbonylation to generate CO, which then undergoes cyclocarbonylation process. Independent studies by Morimoto[213] capitalised on two strategies and developed the first example of Rh-catalysed PK reactions employing aldehydes as a CO surrogate (**Scheme 2.11**).

Scheme 2.10. Utilisation of aldehydes as CO surrogate in the PK reaction.

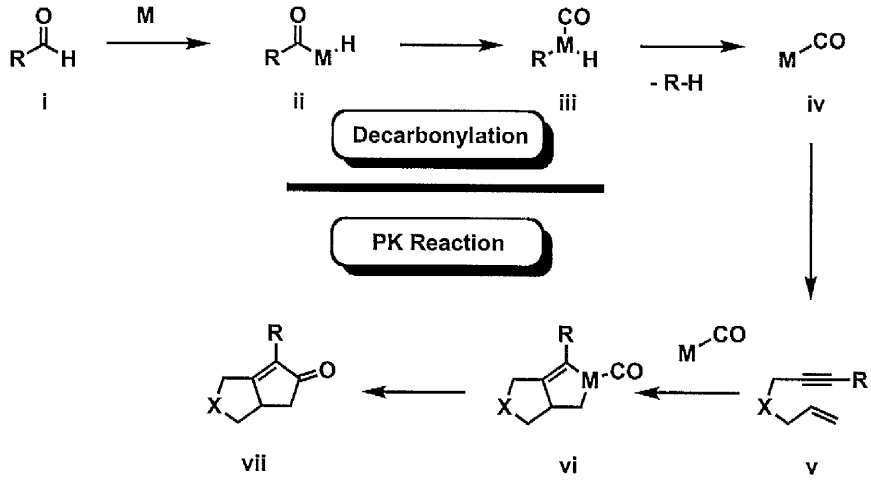

Scheme 2.11. Rh-catalysed PK reaction using aldehydes as a CO surrogate.

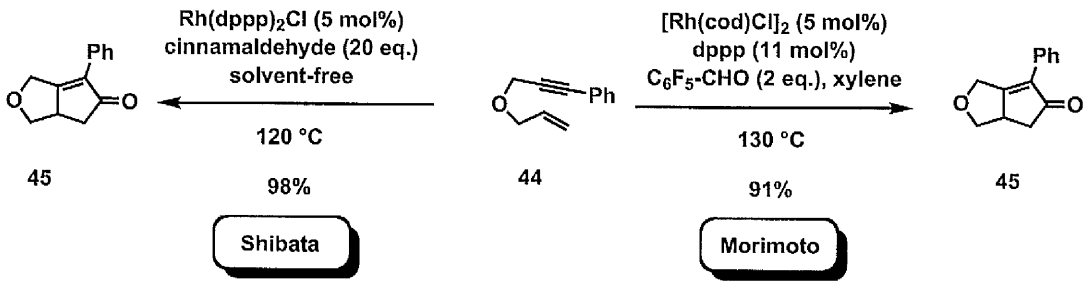

Additional studies by Shibata[215] described the corresponding enantioselective manifold by replacing the dppp with a BINAP-type catalyst using aldehydes or carbon monoxide, which provided similar results in terms of yields and stereoselectivity (**Scheme 2.12**). In this context, the Morimoto group envisioned the possibility of developing a novel asymmetric Rh-catalysed PK reaction by using aldehydes as a CO surrogate and water as the reaction solvent.[216a]

Scheme 2.12. Rh-catalysed enantioselective PK reaction using aldehydes as a CO surrogate.

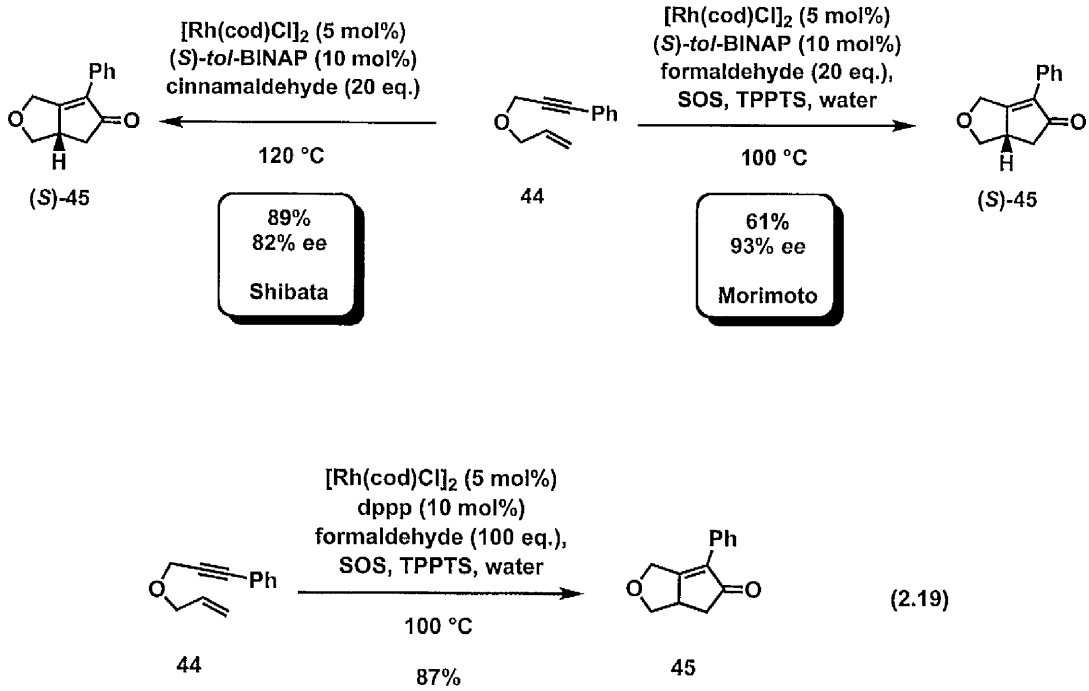

This accomplishment involved the employment of a Rh-complex with high stability and solubility under aqueous conditions.[216a] Initial studies on the reaction focused on the development of a non-enantioselective Rh-catalysed aqueous PK reaction employing formaldehyde as a CO surrogate (Eq. 2.19). Optimisation demonstrated that the dppp ligand, a water-soluble phosphine (TPPTS) and a surfactant (SOS) were essential to achieve an excellent yield. Hence, the mechanistic hypothesis in **Scheme 2.13** outlines the role of the reaction components. For instance, TPPTS and dppp phosphine provides the formation of two distinct rhodium complexes: a hydrophilic Rh-TPPTS complex and the hydrophobic Rh-dppp complex. The water-soluble catalyses the decarbonylation process, to generate the CO-containing complex. Employment of SOS surfactant allows the formation of a hydrophobic micellar phase, which contains the Rh-dppp complex and the enyne substrate. A CO transfer process from the aqueous to the micellar phase allows the CO insertion into metallacycle and subsequent formation of the bicyclopentenone derivative. The first Rh-catalysed aqueous PK reaction prompted the subsequent development of the related asymmetric manifold, by

substitution of dppp with the chiral *tol*-BINAP (**Scheme 2.12**), thus allowing the remarkable opportunity to perform a highly asymmetric carbocyclisation under environmentally friendly conditions.[216b]

Scheme 2.13. Mechanism of the Rh-catalysed aqueous PK reaction in presence of aldehydes as a CO surrogate.

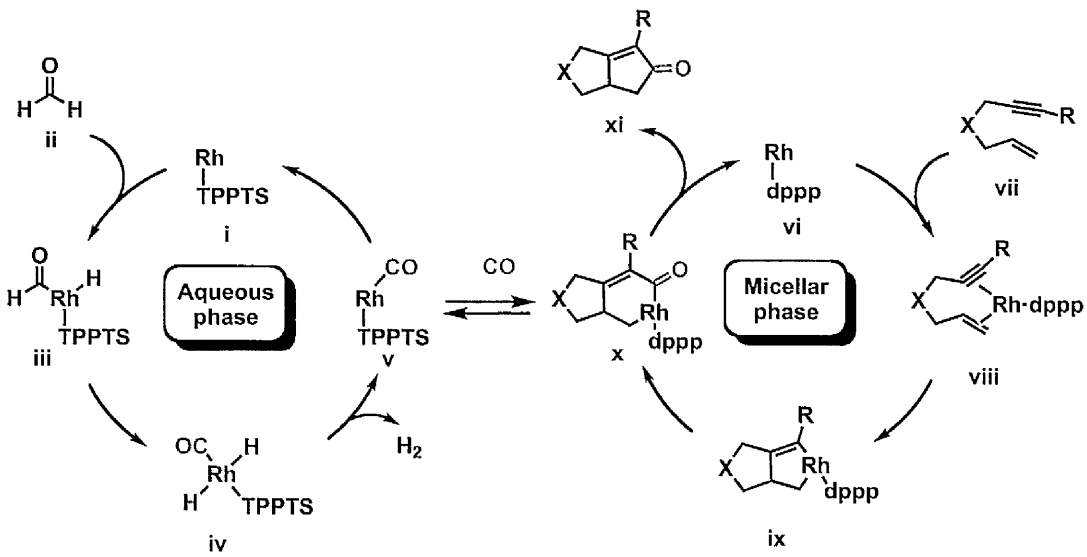

Nonetheless, the synthetic value of the methodology was partially affected by the necessity to employ a surfactant and two different bisphosphine ligands. Hence, these drawbacks prompted the development of more practical operating reaction conditions. Extensive studies by the Chan group revealed that employment of P-PHOS ligands and cinnamaldehyde as a CO surrogate facilitate the aqueous asymmetric Rh-catalysed aqueous Pauson-Khand reaction without any requirement of additive or surfactant (Eq. 2.20).[217] The low catalyst loading and the small excess of cinnamaldehyde enhanced the synthetic value of this protocol. In a similar process, Chan and coworkers described the Rh-catalysed PK reaction using SYNPHOS and alcoholic solvents to achieve a similar highly enantioselective synthesis of bicyclopentenone adducts (Eq. 2.21).[218]

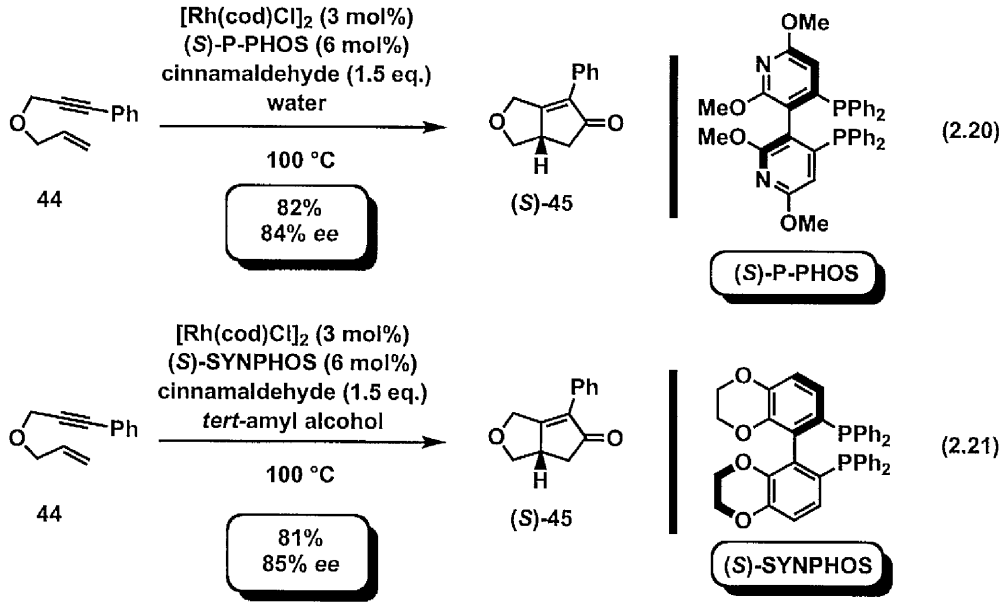

Figure 2.7. Effect of the alkyne terminus on the enantiocontrol of the Rh-catalysed PK reaction.

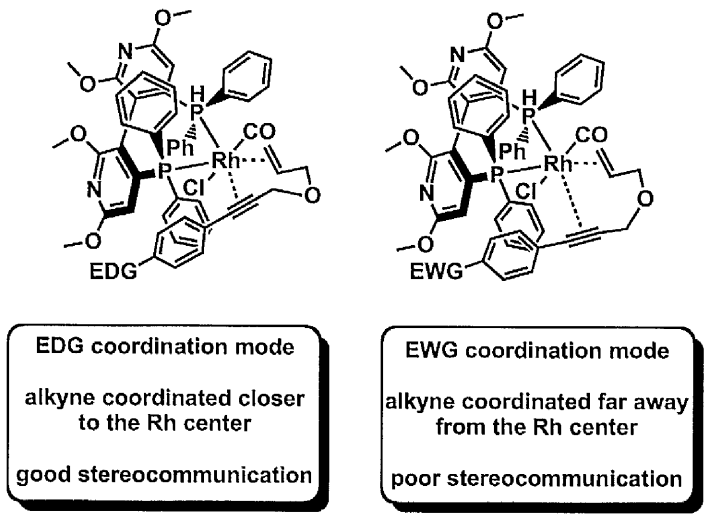

Moreover, they investigated the correlation between the electronic effects on the 1,6-enyne substrates and the enantioselectivity of the related Rh-catalysed PK reaction.[217] Hence, the linear free-energy relationship in the Hammett plot showed an unprecedented correlation of the enantiomeric excess with the electronic properties of the substrate. Experimental studies

outlined the beneficial effect of electron-donating substituents on the enantioselectivity of the reaction, from the more efficient stereocommunication between the alkyne moiety and the rhodium centre (**Figure 2.7**), which contrasts to the more electron withdrawing groups that have a much "loosen" transition state.

2.2.4. Desymmetrisation of Meso-dienynes.

The desymmetrisation of *meso*-dienynes by means of a PK reaction provided an attractive methodology in view of the possibility to generate two contiguous stereocenters from prochiral 1,6-enynes. Hence, following the successful achievement of the first Rh-catalysed asymmetric PK reaction,[208] Jeong investigated the feasibility of an asymmetric Rh-catalysed desymmetrisation of *meso*-dienynes. Subsequent studies confirmed the feasibility of the process in presence of rhodium and iridium catalyst using chiral BINAP-type ligands.[219] Nevertheless, iridium and rhodium congeners displayed a different reactivity in the process and a divergent stereochemical outcome (**Scheme 2.14**).

Scheme 2.14. Desymmetrisation of *meso*-dienynes by Rh-catalysed enantioselective PK reaction.

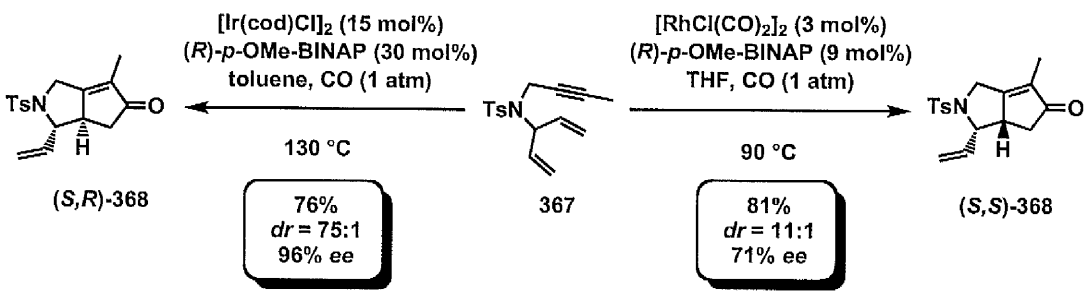

Although the $[Ir(Cod)Cl]_2$ catalysed process afforded bicyclopentenone **368** with excellent diastereo- and enantioselectivity, albeit with 30% metal loading and harsh temperature conditions (130 °C), whereas the $[RhCl(CO)_2]_2$ catalysed process provided the opposite

diastereoisomer with less selectivity but high catalytic activity (6 mol% of metal loading).[219] Surprisingly, further experimental studies revealed that the level of stereoinduction provided by the rhodium and iridium catalysts was dramatically influence by the alkyne substitution pattern (**Scheme 2.15**).[219]

Scheme 2.15. Influence of the alkyne substitution pattern on the asymmetric PK reaction of *meso*-dienynes.

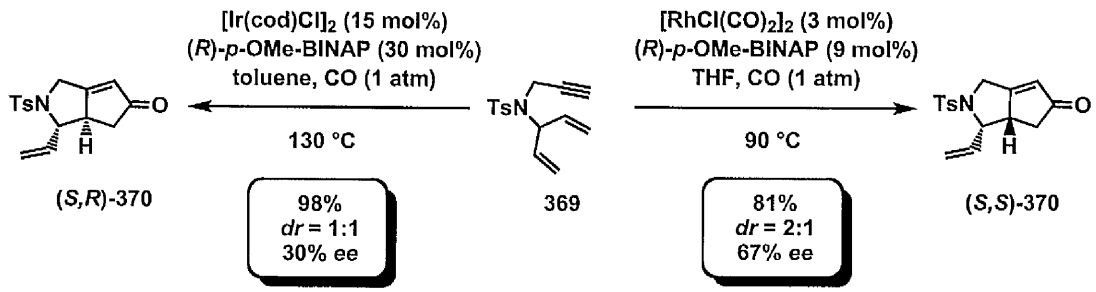

In a recent study, the Jeong group applied the Rh-catalysed desymmetrisation of *meso*-dienynes bearing an acetal moiety.[220] Unfortunately, these substrates undergo decomposition under a CO atmosphere, which required the use of aldehydes as CO surrogate (Eq. 2.21). Additionally, the synthetic value of the methodology was affected by poor diastereoselectivity.[220]

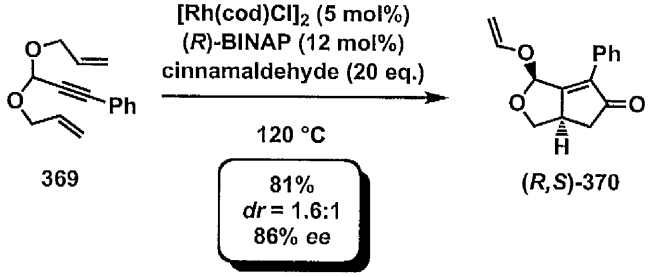

(2.21)

2.2.5. Effect of the CO Concentration.

As discussed in section **2.2.1** kinetic and mechanistic studies by the Consiglio group[209] revealed that the active catalytic species in the asymmetric Rh-catalysed PK coordinated two molecule of solvent (complex **ii, Scheme 2.9**, in which carbon monoxide is solely involved in the insertion step. From a conceptual point of view, a high concentration of carbon monoxide is not essential for optimal reactivity and stereoselectivity. Furthermore, a high level of CO could enhance the formation of Rh complexes **viii** and **ix,** which are inactive towards the coordination to the enyne substrate. Therefore, the employment of a low concentration could enhance the reactivity rate and additionally influence the stereochemical outcome of the carbocyclisation. In line with this hypotheses, Jeong envisioned the possibility to perform the originally developed Rh-catalysed PK reaction[208] under low CO concentration with the aim of improving the operating conditions and the level of enantioselectivity (**Scheme 2.16**).[232]

Scheme 2.16. Effect of the CO concentration on the Rh-catalysed enantioselective PK reaction.

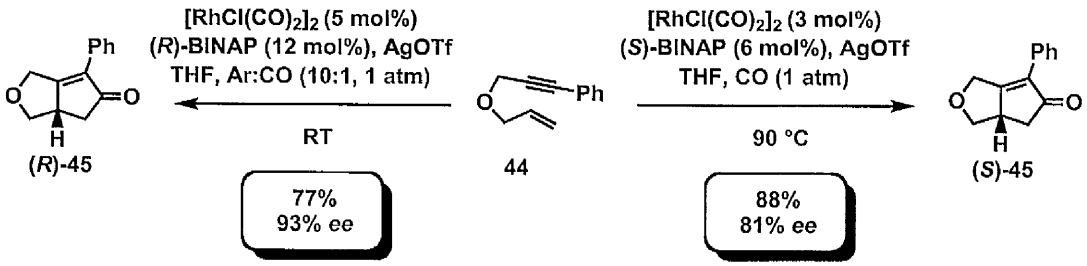

The discovery of the positive effect of a low CO concentration and the recent improvements in the design of bisphosphine ligands provided the basis for a reinvestigation of the Rh-catalysed desymmetrisation of *meso*-dienynes.[219] In this context, utilisation of DIFLUORPHOS ligand under low CO concentration allowed an ambient temperature reaction with improved yield and enantioselectivity (**Scheme 2.17**).[221]

Scheme 2.17. Effect of the CO concentration on the Rh-catalysed enantioselective PK reaction of *meso*-dienynes.

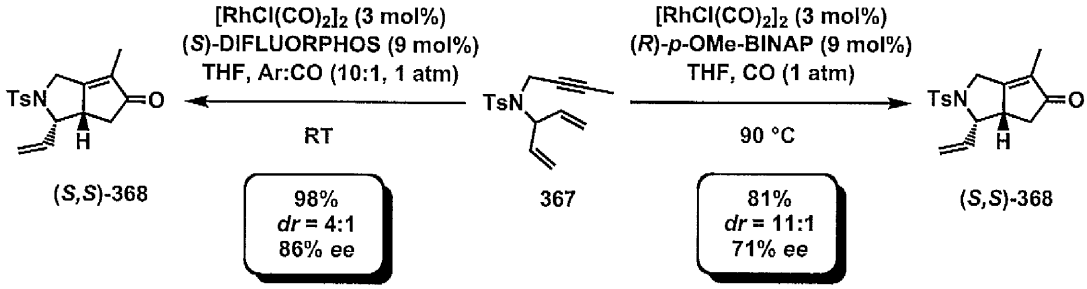

2.3. Rhodium-catalysed Enantioselective Reactions of Chlorinated 1,6-Enynes.

2.3.1. Introduction.

The synergic ability of the rhodium catalysts and bisphosphine ligands to promote a highly enantioselective PK reaction coupled with the improvement of the operating conditions, t allowed the development of a process that avoids poisonous CO, in environmentally friendly solvents or in absence of a thermal process. Despite these noteworthy achievements, the synthetic potential of the enantioselective manifold was largely affected by its limited substrate scope. As described in **Figure 2.8**, 1,6-enynes bearing an unsubstituted alkene moiety provided optimal reactivity in the asymmetric process. In contrast, substitution on the alkene position exerted a dramatic influence on the reactivity in the carbocyclisation. 1,6-Enynes bearing internal alkene substitution displays low or no reactivity in the enantioselective process. Therefore, the rare exploitation of these substrates involves harsh temperature conditions ($T \geq 100$ °C) and is limited to sterically unhindered substituents (R^1 = Me).[204a,207,217] Introduction of a terminal substituent on the alkene moiety provides low reactivity towards the enantioselective PK reaction and the undesired formation of undesired

ene-cycloisomerisation adducts.[222] Hence, the poor reactivity these substrates in the Rh-catalysed PK reaction is further supported by the absence of any enantioselective version. In a similar way, employment of 1,7-enynes provides complete unreactivity towards the asymmetric process. In our previous studies we demonstrated that the introduction of a chlorine moiety on the alkyne terminus provided enhanced reactivity in the Rh-catalysed diastereoselective PK reaction.[169] Hence, we decided to examine the enantioselective variant with 1,6-chlorinated enynes to examine the influence of the chlorine atom on the reactivity and selectivity of the carbocyclisation. Additionally, despite the fact that the first room temperature enantioselective Rh-catalysed PK reaction had been reported, it was limited to 1,6-enynes bearing terminal alkenes.[221]

Figure 2.8. Reactivity profile of 1,*n*-enynes towards the enantioselective PK reaction.

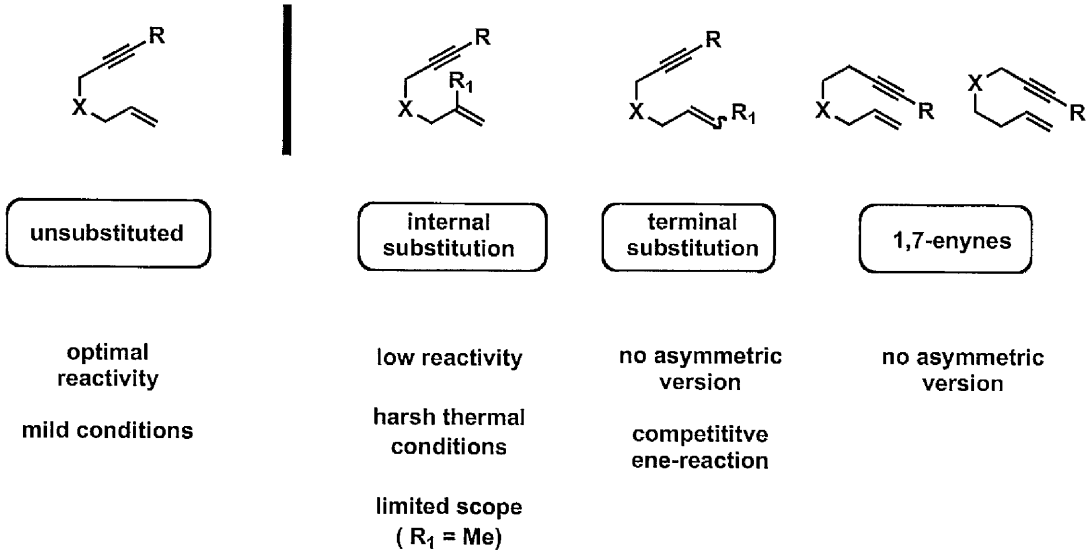

In light of this limitation, we envisioned that employment of the chlorine substituted alkyne would improve the reactivity and thereby, it should facilitate the enantioselective reaction of substituted alkenes at room temperature (**Scheme 2.18**).

Scheme 2.18. Rh-catalysed enantioselective PK reaction of chlorinated 1,6-enynes at room temperature.

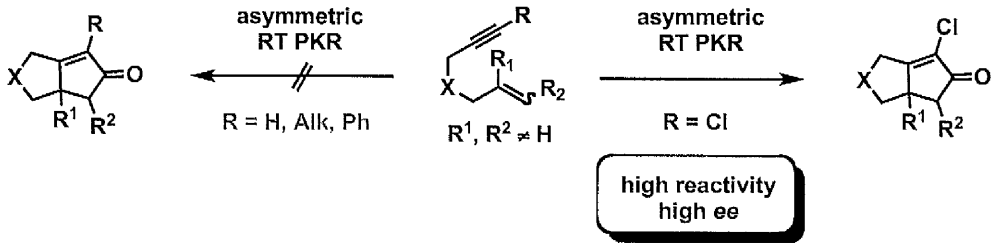

This study would further demonstrate the beneficial role of the halogen moiety and thereby expand the applicability of the methodology to the total synthesis of bioactive natural targets.

2.3.2. Investigation of the Reaction.

Previous works on the Rh-catalysed enantioselective Pauson-Khand process highlighted the remarkable influence of the alkyne terminus on the reactivity and enantioselectivity.[210,217] This inspired the examination the of the 1,6-chlorinated enyne **301** and to compare its reactivity with the previously employed aliphatic and aromatic substituents. Solvent screening demonstrated moderate reactivity and enantioselectivity[222] (**Table 2.4**). However, apolar and non-coordinating solvents provided no reactivity in the carbocyclisation (entry 1 and 2, **Table 2.4**), which was attrbiuted to the limited solubility of the cationic Rh-BINAP complex in benzene and xylene at room temperature. In contrast, strongly coordinating solvents, such as acetonitrile, were relatively unreactive, due to the solvent competing with the enyne for the metal centre (entry 4). Gratifiingly, acetone (entry 5) afforded the most promising yield and enantioselectivity[222] in the reaction and was thereby used in the ligand screening study (**Table 2.5**). Previous studies with BINAP-type ligands highlighted the ability to tune the dihedral angle of the chiral backbone and the electron density on the phosphorous atom in order to enhance the reactivity and the stereoselectivity of the PK reaction.[210]

Table 2.4. Effect of solvents in the Rh-catalysed enantioselective PK reaction.[a]

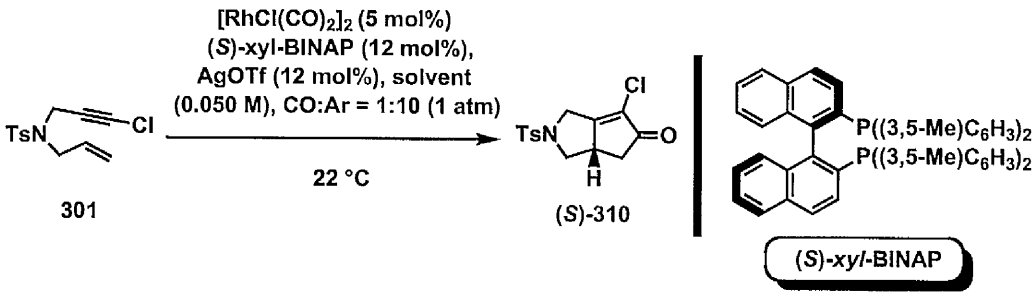

301 (*S*)-310 (*S*)-*xyl*-BINAP

Entry	Solvent	yield (%)[b]	ee (%)[c]
1	*p*-xylene	NR	--
2	benzene	NR	--
3	THF	32	27
4	CH_3CN	17	48
5	Acetone	65	60

[a] All reactions were carried out on a 0.1 mmol scale. [b] Isolated yields. [c] Ratios of enantiomers were determined by HPLC analysis of the crude products.

Table 2.5. Effect of bisphosphine ligands in the Rh-catalysed enantioselective PK reaction.[a]

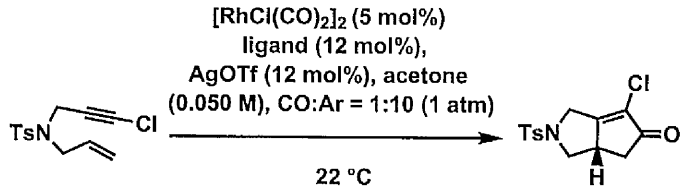

301 (*S*)-310

Entry	Ligand	Yield (%)[b]	ee (%)[c]
1	(*S*)-*xyl*-BINAP	65	60
2	(*S*)-*P*-Phos	54	48
3	(*S*)-*xyl*-*P*-Phos	86	73
4	(*S*)-Tunephos	58	72
5	(*S*)-SDP	12	49
6	(*S,S*)-Me-Duphos	NR	--

[a] All reactions were carried out on a 0.1 mmol scale. [b] Isolated yields. [c] Ratios of enantiomers were determined by HPLC analysis of the crude products.

We envisioned that screening structurally different chiral bisphosphines would provide the necessary insights to identify the optimal ligand for the carbocyclisation (**Table 2.5**). The examination of the results confirmed that the variation of the dihedral angle did indeed influence the reaction. Hence, using *xyl*-BINAP as a reference ligand, indicated that ligands with a larger dihedral angle were inferior in terms of overall reactivity and selectivity (Entry 5 and 6, **Table 2.5**), whereas the bisphosphines with a narrow dihedral angle were superior (Entry 3 and 4).The structural examination between *xyl*-BINAP and xyl-*P*-Phos corroborates the aforementioned importance of the dihedral angle. The two ligands show an equal steric environment (3,5-methyl) and similar electron density (δ (*xyl*-P-Phos) = -14.0 ppm, δ (*xyl*-BINAP) = -13.8 ppm) on the phosphorous atom. Hence, the narrower dihedral angle of the 2,2'-bipirydil backbone predominantly accounts for the enhanced yield and enantioselectivity.

Figure 2.9. Dihedral angle of bisphosphine ligands and corresponding reactivity in the Rh-catalysed enantioselective PK reaction.

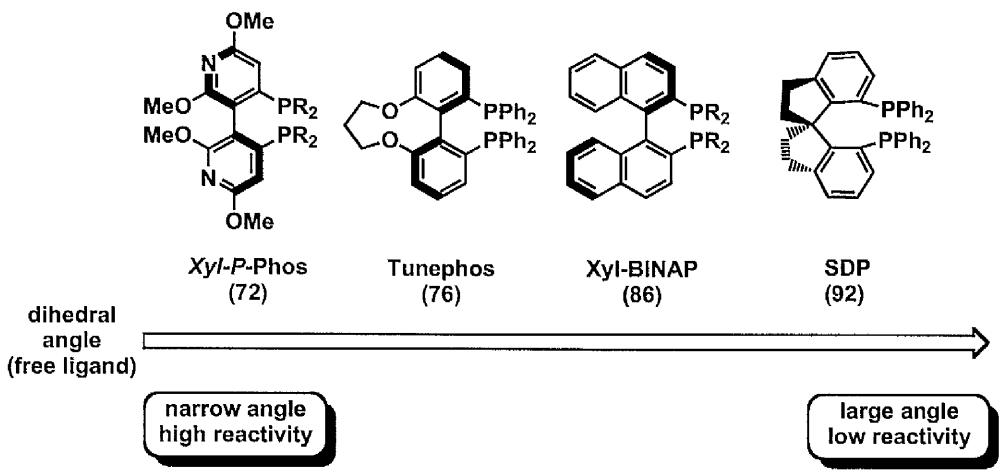

Figure 2.9 summarises the correlation between the dihedral angle of chiral bisphophines and the activity in the Rh-catalysed enantioselective PK reaction. Additionally, the correlation between P-Phos and *xyl-P*-Phos (Entry 2 and 3, **Table 2.5**) indicates that the steric bulkiness of the phosphorous atom increases the yield and stereoselectivity of the process. The observed

results prompted the utilisation of the *xyl-P*-Phos ligand and evaluate the effect of silver additives on the carbocyclisation.

As outlined in previous studies, the counter anion of the Rh-phosphine complex plays an important role in the PK reaction.[211,212] Although the abundance of silver salts provides the opportunity to introduce different counter anions on the metal center, previous Rh-catalysed PK reactions have demonstrated AgOTf or $AgSbF_6$ as optimal additives. Interestingly, the examination of counter anions revealed that increasing size has a detrimental effect on the efficiency and reactivity (Entry 1-3, **Table 2.6**). The recent development of a Rh-catalysed asymmetric hydroacylation by Dong *et al* demonstrated that the replacement of (OTf) in favour of the less coordinating (NO_3) provided a surprising enhancement in the enantioselectivity of the transformation.[224] We decided to investigate the outcome of the carbocyclisation in presence of weakly coordinating anions, such as nitrate and sulfate. Surprisingly, the evaluation of a wide range of silver additives revealed that the sulfate anion, despite providing a lower yield, promoted a high level of enantioselectivity in the process (Entry 5, **Table 2.6**).

Table 2.6. Effect of the silver additives in the Rh-catalysed enantioselective PK reaction.[a]

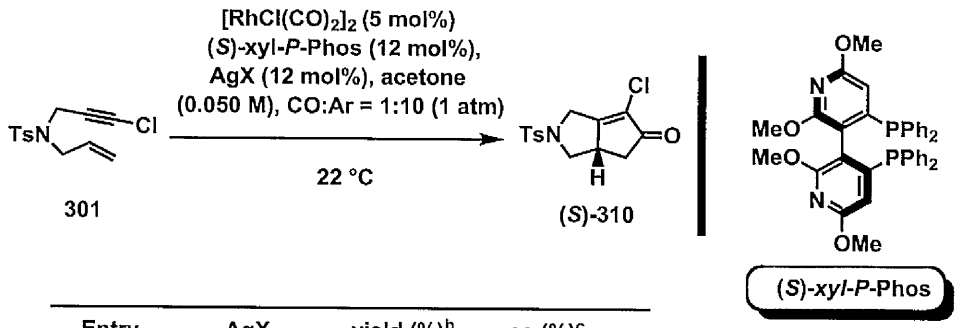

Entry	AgX	yield (%)[b]	ee (%)[c]
1	AgOTf	86	73
2	$AgBF_4$	59	61
3	$AgSbF_6$	ND	37
4	AgCN	NR	--
5	Ag_2SO_4	75	92

[a] All reactions were carried out on a 0.1 mmol scale. [b] Isolated yields. [c] Ratios of enantiomers were determined by HPLC analysis of the crude products.

Unfortunately, further application of the methodology to the analogous carbon-tethered 1,6-enyne **304** proved to be unsatisfactory in terms of reactivity and enantioselectivity (**Table 2.7**). Hence, the experimental results indicate that the nature of the tether alters the geometry of the 1,6-enyne and thereby influences the stereochemical outcome in the subsequent oxidative addition step (**Table 2.7**).

Table 2.7. Rh-catalysed enantioselective PK reaction of carbon-tethered 1,6-chlorinated enyne **304**.[a]

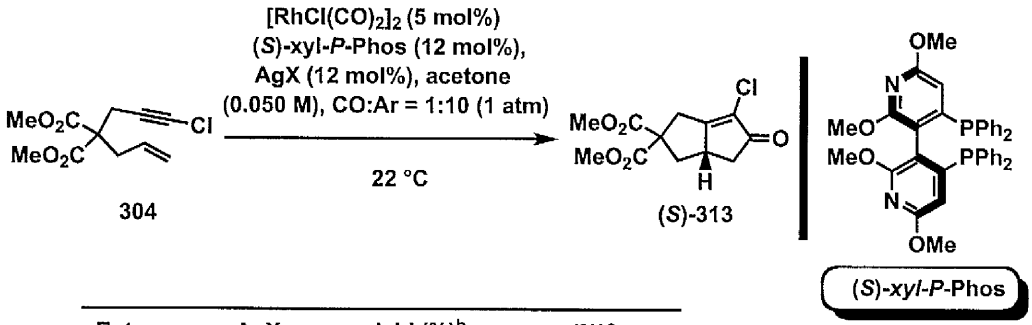

Entry	AgX	yield (%)[b]	ee (%)[c]
1	AgOTf	82	65
2	Ag_2SO_4	44	64

[a] All reactions were carried out on a 0.1 mmol scale. [b] Isolated yields. [c] Ratios of enantiomers were determined by HPLC analysis of the crude products.

In the previous investigation of the diastereoselective Rh-catalysed PK reaction of chlorinated 1,6-enynes at room temperature, the efficiency of the reaction was dramatically altered by the nature of solvents, ligands and silver additives. Hence, in order to identify an optimal combination for the enantioselective variant, the effect of the bisphosphine ligands in the presence of silver triflate and polar coordinating solvents (THF or Acetone) were investigated. Mechanistic studies by the Consiglio group[209] demonstrated that the utilisation of MeO-BIPHEP in presence of AgOTf and THF were optimal for an efficient Rh-catalysed enantioselective PK reaction. An intriguing feature with this ligand is the availability of analogues with identical chiral backbone and structural modifications on the phosphorus unit (**Figure 2.10**).

Figure 2.10. Solvias (*S*)-MeO-BIPHEP ligands.

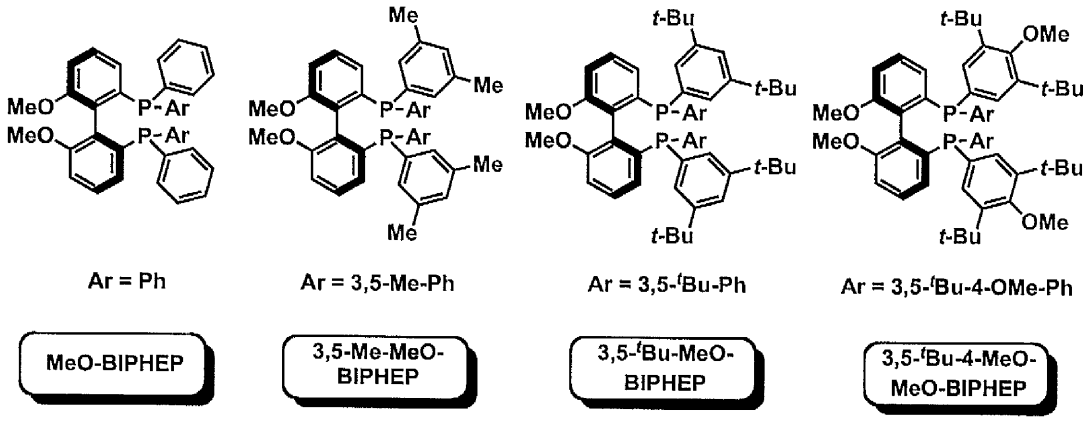

Table 2.8. Effect of BIPHEP-type ligands on the Rh-catalysed enantioselective PK reaction of enyne **301**.[a]

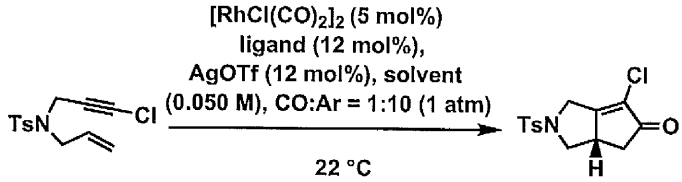

301 (*S*)-310

Entry	Solvent	Ligand	Yield (%)[b]	ee (%)[c]
1	Acetone	(*S*)-MeO-BIPHEP	65	69
2	THF	(*S*)-MeO-BIPHEP	73	70
3	"	3,5-Me-MeO-BIPHEP	78	86
4	"	3,5-^{t}Bu-MeO-BIPHEP	13	50
5	"	3,5-^{t}Bu-4-MeO-MeO-BIPHEP	NR	--

[a] All reactions were carried out on a 0.1 mmol scale. [b] Isolated yields. [c] Ratios of enantiomers were determined by HPLC analysis of the crude products.

Thus, the different substitution pattern in 3,5-Me-MeO-BIPHEP and 3,5-^{t}Bu-MeO-BIPHEP ligands would illustrate the influence of the steric environment, whereas the introduction of a methoxy moiety on the aromatic ring (3,5-^{t}Bu-4-MeO-MeO-BIPHEP) would provide a

stereoelectronic component. The analysis of the ligands indicates that (*S*)-OMe-BIPHEP provided good enantiocontrol and that THF provided increased overall yield (Entry 2, **Table 2.8**). The subsequent examination of (*S*)-3,5-Me-OMe-BIPHEP ligand demonstrated the beneficial effect of methyl substituents on the aromatic ring to impart improved efficiency and enantiocontrol (Entry 3, **Table 2.8**). In contrast, steric bulk and additional electron donating substituents proved more detrimental to the reaction rate (Entry 4 and 5, **Table 2.8**). Hence, these studies provided fundamental insights towards the identification of the optimal chiral bisphosphine for an efficient enantioselective Rh-catalysed PK reaction. For instance, a narrow dihedral was essential for achieving high reactivity and enantioselectivity (*Xyl-P*-Phos and OMe-BIPHEP). In a similar manner, lower electrondensity on the phosphorous atom was desirable, due to the problems with steric effects and electron-donating groups (3,5-^{t}Bu-4-OMe-OMe-BIPHEP). Finally, introduction of methyl substituents on the phenyl ring confers a moderate steric bulk around the phosphorous atom and provides good enantiocontrol (3,5-Me-OMe-BIPHEP).

These experimental findings led to the identification of *DM*-SEGPHOS[225] as the ideal ligand for the achievement of an efficient asymmetric manifold (Eq. 2.22). Hence, the chiral bisphosphine *DM*-SEGPHOS was selected, which has a bis(1,3-benzodioxole) backbone with a remarkably narrow dihedral angle (65.2 ° against 86 ° of BINAP) and relatively poor electron-density on the phosphorous atom ((δ (*DM*-SEGPHOS) = -12.5 ppm, δ (BINAP) = -14.4 ppm). Additionally, methyl substituents on the phenyl ring provide the desired steric environment on the phosphorous atom. Gratifyingly, this ligand provided optimal selectivity in the enantioselective Rh-catalysed PK reaction of enyne **301** (Eq. 2.22). In light of this promising result, we elected to apply these conditions to the challenging room temperature carbocyclisation of 1,6-enynes with 1,1-disubstituted alkenes. As previously pointed out, these substrates provides low in the enantioselective PK reaction, which accounts for the limited examples that have been reported. Moreover, they generally require very forcing reaction conditions which leads to side reactions and only methyl groups have been examined.

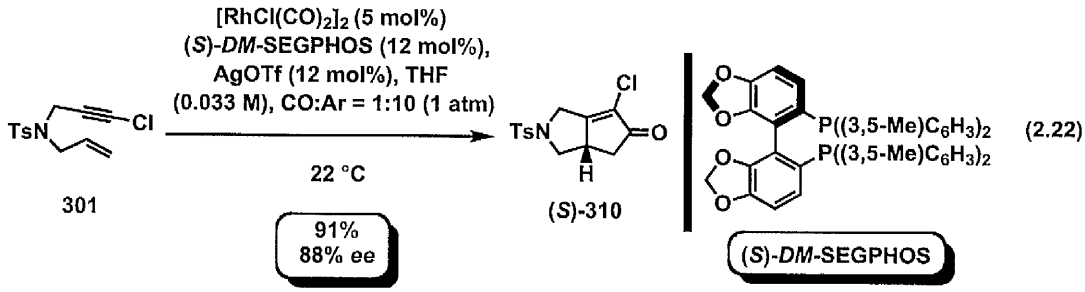

Solvent: moderately coordinating (THF, Acetone)

Ligand dihedral angle: narrow

P electrondensity: low

Silver additive: AgOTf

CO concentration: low

Table 2.9 outlines the preliminary optimisation study to probe the feasibility of the PK reaction of 1,6-enynes with 1,1-disubstituted olefins. Unfortunately, treatment of 1,6-enyne **371** and **372** (entries 1 and 2) in presence of the rhodium complex with xyl-BINAP as a ligand did not furnish any of the desired [2+2+1] cycloaddition product. Gratifyingly, replacement of alkyne terminus with a chlorine group (entry 3, **Table 2.9**) provided improved reactivity, albeit with the exclusive formation of the homodimerisation adducts **376b** and **376b'**.[226] These initial results confirmed that the replacement of the aliphatic or aromatic alkyne terminus with a chlorine moiety influences the reactivity of the PK reaction. Additionally, as observed in the previous optimisation studies, the xyl-BINAP ligand, bearing a large dihedral angle, has a low efficacy in the transformation. Hence, we were prompted to investigate the behaviour of the *DM*-SEGPHOS ligand, which provided optimal reactivity and enantioselectivity in the corresponding carbocyclisation of 1,6-enynes bearing a terminal substituted alkene unit (Eq. 2.22). Gratifyingly, this chiral bisphosphine could enhance the reactivity of chlorinated 1,6-enyne **373** in the carbocyclisation to afford the desired PK adduct **376a**, although with concomitant formation of the homodimerisation products (entry 6, **Table 2.9**). We envisaged that lower concentration would limit the formation of the undesired [2+2+2] adduct **376b** and, thereby, afford bicyclopentenone **376a** as the major product.[227]

Gratifyingly, reduction of the enyne concentration effectively circumvented the formation of the undesired homodimerisation adduct and provided the bicyclopentenone **376a** with optimal yield and excellent enantioselectivity. Hence, the chlorine group in conjunction with the optimal bisphosphine ligand *DM*-SEGPHOS provided a mild and highly selective cyclocarbonylation of 1,1-disubstituted alkenes at room temperature. This outstanding result prompted the scope of the reaction to be explored in order to verify the validity of this result for related substrates.[228]

Table 2.9. Examination of the Rh-catalysed enantioselective PK reaction of 1,6-enynes with a 1,1-disubstituted alkene.[a]

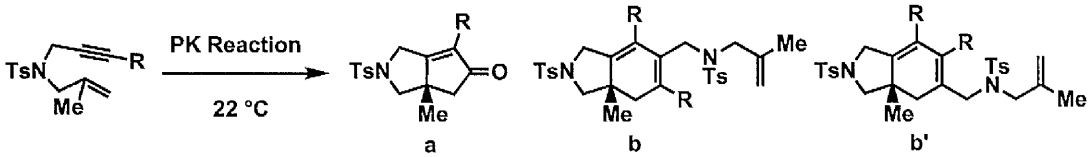

Entry	Ligand	R		[enyne] (mol/L)	Ratio a:(b+b')[b]	Yield (%)[c]		ee (%)[d]
1	(*S*)-*Xyl*-BINAP	Me	371	0.066	--	NR	374	--
2	"	Ph	372	"	--	NR	375	--
3	"	Cl	373	"	≤1:19[e]	23[e]	376	--
4	(*S*)-*DM*-SEGPHOS	Me	371	0.066	--	--	374	--
5	"	Ph	372	"	--	NR	375	--
6	"	Cl	373	"	0.8:1	87	376	ND
7	"	"	"	0.033	≥19:1	86	"	94
8	"	"		0.025	≥19:1	91	"	96

[a] All reactions (0.1 mmol) were carried out utilising $[RhCl(CO)_2]_2$ (5 mol%), AgOTf (12%), ligand (12%) in acetone at 22 °C under an atmosphere of Ar:CO = 10:1 (1 atm). [b] Ratio were determined by 500 MHz ^{1}H NMR on the crude reaction mixture. [c] Isolated yields. [d] Ratios of enantiomers were determined by HPLC analysis of the crude products. [e] 376b:376b' = 9:1, 94% ee.[226]

2.3.3. Scope of the Reaction.

In accord with this reasoning, the conditions were extended to other substituents in the alkene for the nitrogen-tethered chlorinated 1,6-enynes. Gratifyingly, replacement of the initial

methyl moiety with a wide range of substituents provided similar reactivity and enantiocontrol in the cycloaddition (entry 2-4, **Table 2.10**), albeit the CH_2OBn substituent gave a slight diminution in enantioselectivity (entry 3, **Table 2.10**). In this context, we hypothesised that the presence of a coordinating heteroatom on the aliphatic chain could interact with the metal centre and thereby, alter the stereoselective outcome of the process. A key feature of this process resides in the mild operating conditions and the possibility to employ labile functional groups that would not be tolerated under previous conditions. For example, this manifold allows the unprecedented utilisation of aliphatic silanes without any decomposition of the starting material and PK adduct (entry 4, **Table 2.10**).

Table 2.10. Scope of the reaction.[a]

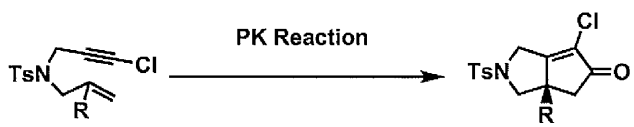

Entry	X	R		Yield (%)[b]		ee (%)[c]
1	NTs	Me	373	91	376	96
2	"	Bn	377	93	388	97
3	"	CH_2OBn	378	91	389	88
4	"	CH_2TMS	379	86	390	96
5	O	Me	380	82	391	96
6	"	Bn	381	86	392	≥99
7	"	CH_2OBn	382	83	393	92
8	"	CH_2TMS	383	81	394	98
9	$C(CO_2Me)_2$	Me	384	74	395	92
10	"	Bn	385	81	396	97
11	"	CH_2OBn	386	79	397	86
12	"	CH_2TMS	387	87	398[d]	--

[a] All reactions (0.1 mmol) were carried out utilising $[RhCl(CO)_2]_2$ (5 mol%), AgOTf (12%), ligand (12%) in acetone at 22 °C under an atmosphere of Ar:CO = 10:1 (1 atm). [b] Isolated yields. [c] Ratios of enantiomers were determined by HPLC analysis of the crude products. [d] reaction of enyne 387 provided the exclusive formation of S_N2'-type cyclisation adduct 398 (see Table 2.11)

The replacement of the nitrogen with the corresponding oxygen tether provided similar levels of reactivity and enantioselectivity (Entry 5-8). Although previous studies[169] highlighted the low reactivity of carbon tethers, the enantioselective process provides good levels of reactivity and good levels of reactivity and enantioselectivity (Entry 9-11, **Table 2.10**). Interestingly, application of the methodology to the enyne **387** did not provide any PK adduct and resulted in the preferential formation of the S_N2'-type cyclisation adduct **398** (Entry 12, **Table 2.10**).[229] Attempted optimisation of this particular example under different cyclocarbonylation conditions did not provide any PK adduct (**Table 2.11**). Interestingly, a literature survey revealed that unlike the nitrogen and oxygen tethered enynes, carbon-tethered enynes bearing an allyl silane moiety can follow a different mechanistic pathway which leads to the exclusive formation of an S_N2'-type cyclisation adduct.[230]

Table 2.11. Attempted Rh-catalysed enantioselective PK reaction of enyne **387**.

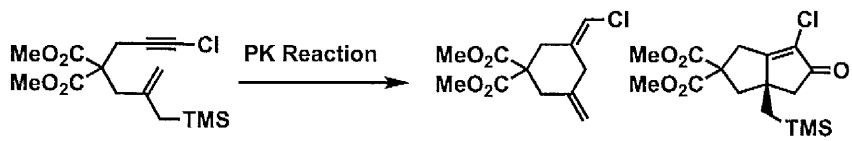

387 398 399

Entry	Method	398:399	Yield (%)	*ee* (%)
1	A	1:0	87	--
2	B	1:0	85	--
3	C	1:0	64	--

A: $[RhCl(CO)_2]_2$ (5 mol%), AgOTf (12%), *DM*-segphos (12%), acetone, Ar:CO 10:1 (1 atm), RT; B: $[RhCl(CO)_2]_2$ (5 mol%), AgOTf (12%), dppp(12%), xylene, Ar:CO 10:1 (1 atm), 120 °C; C: $[RhCl(CO)_2]_2$ (5 mol%), xylene, CO (1 atm), RT.

We also examined the feasibility of the methodology for enynes bearing a terminal substituent on the alkene. As previously outlined, the effective cyclocarbonylation of these substrates was precluded by the competitive ene-cycloisomerisation[223] and poor reactivity, due to the steric interactions between alkene terminus and metal centre. Nonetheless, Narasaka described the diastereoselective PK reaction albeit under harsh thermal conditions (Eq. 2.23).

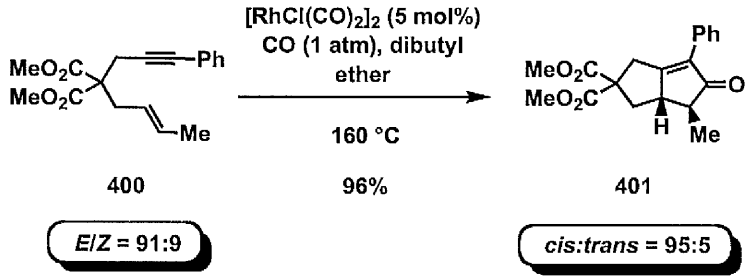

(2.23)

Moreover, these studies also demonstrated the impact of the olefin on the diastereoselectivity in the bicyclopentenone adducts, in which the *trans*-derivative **401** undergoes some equilibration. Although high temperatures were critical for the efficient formation α–substituted bicyclopentenone derivatives, the absence of an asymmetric version inspired the examination of this possibility. Disappointingly, the room temperature rhodium-catalysed PK reaction of enynes **402** and **403** provided no desired product (entry 1-2, **Table 2.12**). Interestingly, the bicyclopentenone **405** was obtained by a thermal process, employing dppp as a bisphosphine ligand (entry 3).

Table 2.12. Attempted Rh-catalysed PK reaction of 1,6-enynes bearing a *trans* olefin moiety.[a]

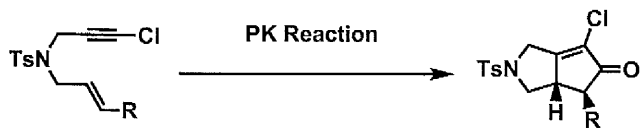

Entry	R		Yield (%)		ee (%)
1	Me	402	NR	404	--
2	Ph	403	NR	405	--
3[b]	Ph	403	34	405	--

[a] All reactions (0.1 mmol) were carried out utilising $[RhCl(CO)_2]_2$ (5 mol%), AgOTf (12%), DM-SEGPHOS (12%) in acetone (0.025M) at 22 °C under an atmosphere of Ar:CO = 10:1 (1 atm).[b] reaction was carried out utilising $[RhCl(CO)_2]_2$ (5 mol%), AgOTf (12%), dppp (12%) in *p*-xylene (0.03M) at 120 °C under an atmosphere of CO (1 atm).

A literature survey of related reactions demonstrated that terminal substituted 1,6-enynes undergo Rh-catalysed enantioselective ene-cycloisomerisation at room temperature. Interestingly, the viability of the methodology was exclusively restricted to 1,6-enynes with *cis*-alkenes (Eq. 2.24).[223]

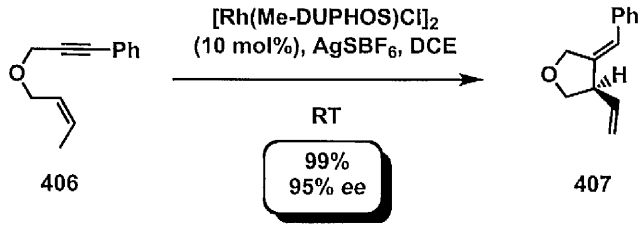

(2.24)

From a mechanistic standpoint, the Rh-catalysed PK reaction and the ene-cycloisomerisation process involve the oxidative addition of the 1,6-enyne to form a common rhodium metallacycle. We envisaged that the utilisation of a *cis*-olefin in the enyne substrate could impart a higher reactivity towards the cyclocarbonylation process and, additionally, the phenyl group suppress any ene-cycloisomerisation adduct. Gratifyingly, treatment of enyne **408** under the optimal reaction condition provided the desired adduct **409** in good yield and with outstanding diastereo- and enantioselectivity (Eq. 2.25).[231] In order to provide a rationale for the observed diastereocontrol, we computed the *trans* and *cis* rhodium metallacycles that, upon CO insertion and reductive elimination, provide the *trans*-adduct **409** and *cis*-epimer **405**.[232] (**Figure 2.11**), respectively. Analysis of the *cis* metallacycle reveals steric interactions between the phenyl substituent on the enyne and 3,5-dimethylphenyl on the phosphorous atom of the ligand. In contrast, the steric interactions between enyne and ligand in the *trans* metallacycle are minimised. Hence, steric implications can rationalise the preferential formation of the *trans* metallacycle, which in turn provides the trans adduct **409**. The racemic adduct **409** required for HPLC analysis was prepared via a standard reaction, in an analogous manner to the bicyclopentenone **405** (entry 3, **Table 2.11**).

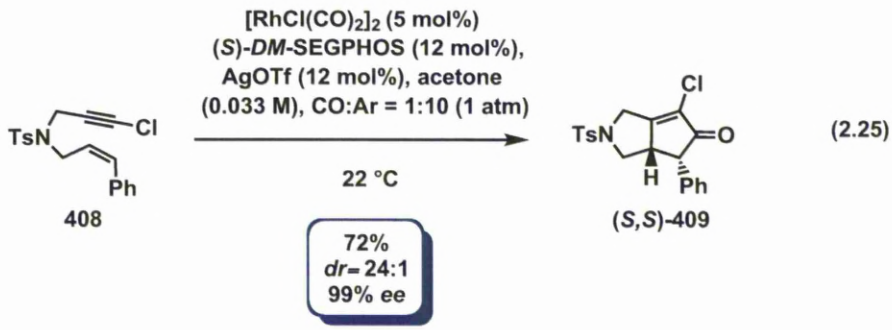

Figure 2.11. Computed metallacyclic *trans* and *cis* intermediates for the Rh-catalysed enantioselective PK reaction of enyne **408**.

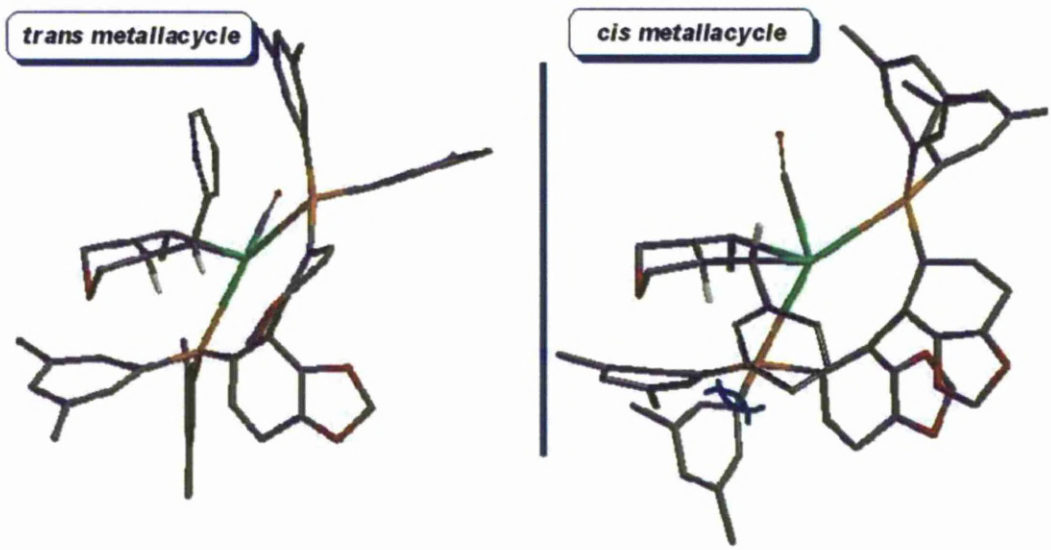

Surprisingly, the thermal Rh-catalysed cyclocarbonylation of enyne **408** did not provide any desired adduct **409**, but afforded exclusively the epimer **405** with excellent stereoselectivity in moderate yield (**Scheme 2.19**). In contrast to Narasaka studies, we envisioned that the cationic rhodium species under the thermal conditions favoured epimerisation to form the thermodynamically favoured adduct **405** (**Scheme 2.19**). An alternative scenario involves the preliminary isomerisation of *cis* enyne **408** to the analogous *trans* isomer **403**, which then provides **405** under carbonylative conditions. Gratifyingly, the room temperature conditions avoided the epimerisation and provided the desired racemic adduct **409** as a single diastereoisomer (**Scheme 2.19**).

Scheme 2.19. Thermal isomerisation in the Rh-catalysed PK reaction.

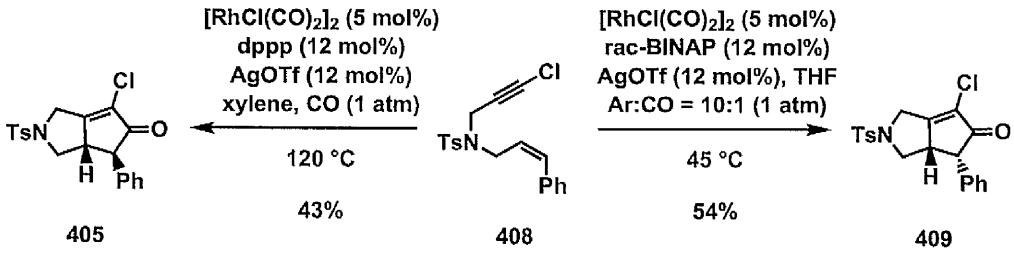

We envisioned that the epimerisation of chiral bicyclopentenone (***S,S***)-**409** would provide a convenient method to access the corresponding diastereoisomer (***S,R***)-**405**. The initial HPLC analysis of the crude mixture of (***S,S***)-**409** showed a *dr* of 99:1 in favour of the *trans*-isomer (***S,S***)-**409**, whereas the subsequent HPLC analysis of the product after chromatographic column provided a *dr* of 25:1 in favour of the *trans*-isomer. Therefore, we hypothesised that treatment of (***S,S***)-**409** with silica gel could deliver the formation of the epimer (***S,R***)-**405** with similar enantioselectivity. Gratifyingly, treatment of the *trans*-isomer (***S,S***)-**409** with silica gel furnished the *cis*-epimer (***S,R***)-**405** as a good stereocontrol. Hence, we demonstrated that the asymmetric PK reaction of *cis*-enyne **408** could be efficiently employed for the selective formation of *cis*- and *trans*- bicyclopentenone derivatives with a synthetically useful level of diastereo- and enantioselectivity.

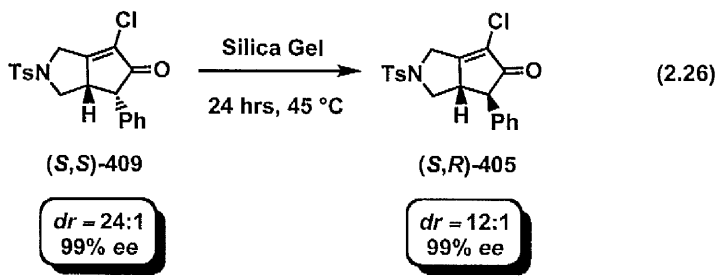

(2.26)

2.3.4. Limitations of the Reaction.

The successful development of a highly enantioselective PK reaction and the possibility to incorporate a wide range of substituents on the alkene provided the impetus to investigate to

reactivity of different olefin groups towards the cycloaddition. Treatment of a wide range of chlorinated 1,6-enynes with different olefin substituents (**410-413**) furnished none of the desired carbocyclisation adducts (**Table 2.13**). In order to circumvent this problems, we attempted to expand the scope of the enantioselective manifold by the 1,6-enynes bearing an aliphatic substituent on the *cis*-alkene unit (**Table 2.14**). Unfortunately, these substrates also did not provide any desired PK adduct. Additionally, the Rh-catalysed cyclocarbonylation of these substrates did not provide any observable formation of ene-cycloisomerisation product.

Table 2.13. Influence of alkene substitution on the Rh-catalysed enantioselective PK reaction.[a]

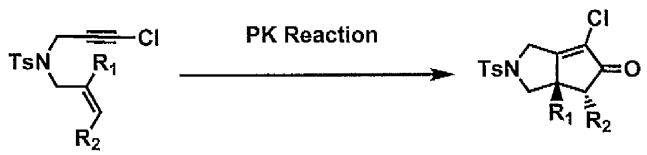

Entry	R_1	R_2		Yield (%)		ee (%)
1	Me	Me	410	NR	414	--
2	CO_2Me	H	411	NR	415	--
3	CH_2SO_2Ph	H	412	NR	416	--
4	$CH_2=C(CH_3)$	H	413	NR	417	--

[a] All reactions (0.1 mmol) were carried out utilising $[RhCl(CO)_2]_2$ (5 mol%), AgOTf (12%), DM-SEGPHOS (12%) in acetone (0.025M) at 22 °C under an atmosphere of Ar:CO = 10:1 (1 atm).

A plausible rationale for the lack of ene-cycloisomerisation adducts is presumably due to the utilisation of a bisphosphine ligand bearing a small dihedral angle in conjunction with a coordinating solvent such as acetone. In contrast, Zhang and coworkers have demonstrated that ligands with a large dihedral angle (Me-DUPHOS) using a non-coordinating solvent, such as DCE, can promote to the formation of these cycloisomerisation adducts (Eq. 2.24).[233]

Table 2.14. Influence of alkene terminus on the Rh-catalysed enantioselective PK reaction.[a]

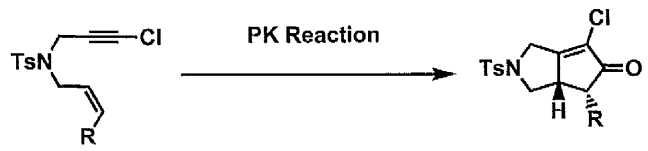

Entry	R		Yield (%)		ee (%)
1	Me	418	mixture	420	--
2	CH_2OTBS	419	NR	421	--

[a] All reactions (0.1 mmol) were carried out utilising $[RhCl(CO)_2]_2$ (5 mol%), AgOTf (12%), DM-SEGPHOS (12%) in acetone (0.025M) at 22 °C under an atmosphere of Ar:CO = 10:1 (1 atm).

Table 2.15. Rh-catalysed enantioselective PK reaction of 1,7-enynes.[a]

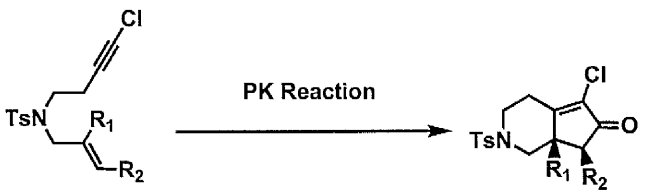

Entry	R_1	R_2		Yield (%)		ee (%)
1	Me	H	422	NR	424	--
2	$-(CH_2)_3-$		423	NR	425	--

[a] All reactions (0.1 mmol) were carried out utilising $[RhCl(CO)_2]_2$ (5 mol%), AgOTf (12%), *DM*-SEGPHOS (12%) in acetone (0.025M) at 22 °C under an atmosphere of Ar:CO = 10:1 (1 atm).

Finally we examined the feasibility of the Rh-catalysed enantioselective PK reaction with 1,7-enynes bearing substitution on the internal and terminal positions of the alkene moiety (**Table 2.15**). Although there have been significant advancements in the area, the viability of the process was largely limited to 1,6-enynes. A plausible rationale for the poor reactivity of 1,7-enynes may be due to the low aptitude to coordinate to the metal centre and/or the high energy associated for the formation a 6/5 membered ring metallacycle in the oxidative

addition step. Treatment of the 1,7-enynes **422** and **423** under the optimal conditions confirmed the low reactivity of such substrates in the carbocyclisation (**Table 2.15**).

2.3.5. Desymmetrisation of *meso*-Dienynes.

The rhodium and iridium catalysed to promote a desymmetrisation of *meso*-dienynes provides a particularly attractive strategy to generate two stereogenic centres from an achiral starting material.[219,221] In this context, the Rh-catalysed methodology could provide the corresponding PK adduct under mild conditions and with low catalyst loading (**Scheme 2.18**), albeit with poor diastereoselectivity.[221] In contrast, the Ir-catalysed manifold (**Scheme 2.14**) provided the corresponding adducts with a high level of diastereo- and enantiocontrol, albeit harsh thermal conditions and high catalyst loading were necessary to achieve an optimal reactivity.[219]

Table 2.16. Investigation of the solvent effect in the Rh-catalysed PK reaction of meso-dienyne **426**.[a]

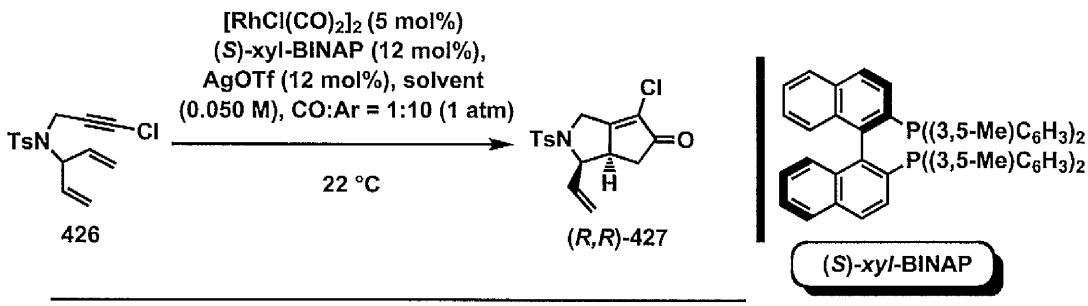

Entry	Solvent	yield (%)[b]	*dr* (%)[c]	ee (%)[c]
1	THF	ND	81:19	7
2	Acetone	34	91:9	57
3	DCE	72	96:4	77

[a] All reactions were carried out on a 0.1 mmol scale. [b] Isolated yields. [c] Ratios of stereoisomers were determined by HPLC analysis of the crude products.

As outlined in the previous optimisation study, benzene and xylene were detrimental in terms of reactivity, which is presumably due to the low solubility of the cationic rhodium complexes. As a consequence of this limitation, DCE has been widely employed due to the solubility of rhodium complexes in this solvent. Gratifyingly, switching the solvent to DCE promoted the formation of the corresponding bicyclopentenone adduct **427** in good yield and improved stereoselectivity[233], although the mechanism of the Rh-catalysed PK reaction indicates that a coordinating solvent is necessary to obtain a high degree of stereoselectivity in the process.[220] In contrast, *meso*-dienynes bears an additional C2 vinyl substituent that can coordinate to the metal centre in the oxidative addition step, thereby influencing the stereochemical outcome of the reaction.[233] Hence, the reaction does not require a coordinating solvent in order to display a high stereoselectivity and explain the switch in stereocontrol (entry 3, **Table 2.16**).[233]

Table 2.17. Effect of the silver additive in the Rh-catalysed PK reaction of meso-dienyne **424**.[a]

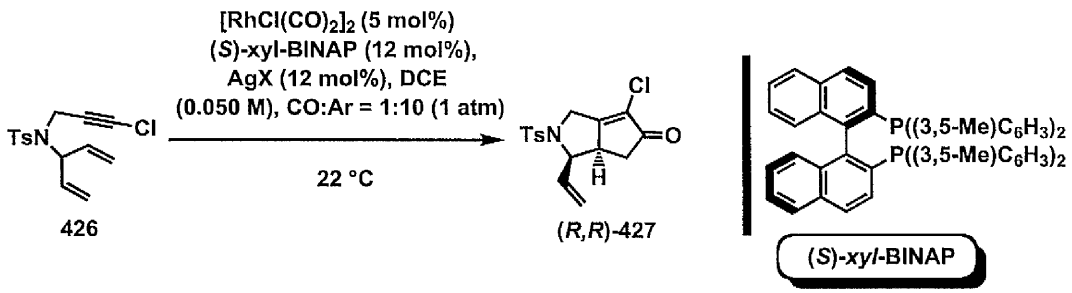

Entry	AgX	yield (%)[b]	*dr* (%)[c]	ee (%)[c]
1	$AgBF_4$	54	98:2	72
2	$AgSbF_6$	63	99:1	64
3	AgOTf	72	96:4	77

[a] All reactions were carried out on a 0.1 mmol scale. [b] Isolated yields. [c] Ratios of stereoisomers were determined by HPLC analysis of the crude products.

Additional investigations examined the influence of the counter anion on the process, which demonstrated that the triflate anion was the optimal additive for the transformation (**Table 2.17**). In light of the fact that we demonstrated a highly enantioselective Rh-catalysed PK reaction using chiral bisphosphines with a narrow dihedral angle and lowered electron density on the phosphorous atom, we elected to examine *xyl*-P-Phos in the desymmetrisation of enyne **426**. Surprisingly, the employment of this chiral bisphosphine resulted in lower stereoselectivity of the reaction (entry 2, **Table 2.18**), whereas the DIOP ligand, which displays a large dihedral angle (104 °), provided good stereocontrol.

In contrast to the enantioselective PK reaction of chlorinated 1,6-enynes, in which a smaller dihedral angle has a positive effect in the selectivity, we envisioned that ligands, which have a larger dihedral angle than BINAP, would be optimal for this process. [234]

Table 2.18. Investigation of the chiral bisphophine ligand in the Rh-catalysed PK reaction of meso-dienyne **426**.[a]

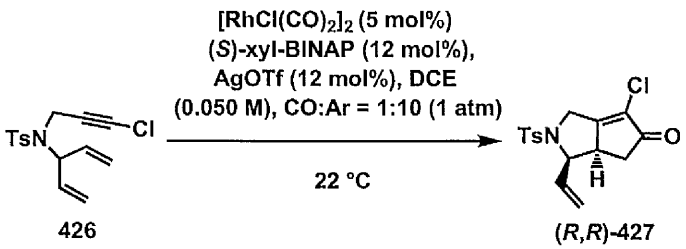

426 (*R*,*R*)-427

Entry	Ligand	yield (%)[b]	*dr* (%)[c]	*ee* (%)[c]
1	(*S*,*S*)-DIOP	52	99:1	73[d]
2	(*S*)-*xyl*-*P*-Phos	51	99:1	40
3	(*S*)-BINAP	65	96:4	64
4	(*S*)-*xyl*-BINAP	72	96:4	77

[a] All reactions were carried out on a 0.1 mmol scale. [b] Isolated yields. [c] Ratios of stereoisomers were determined by HPLC analysis of the crude products. [d] (*S*,*S*)-427 was detected as the major enantiomer.

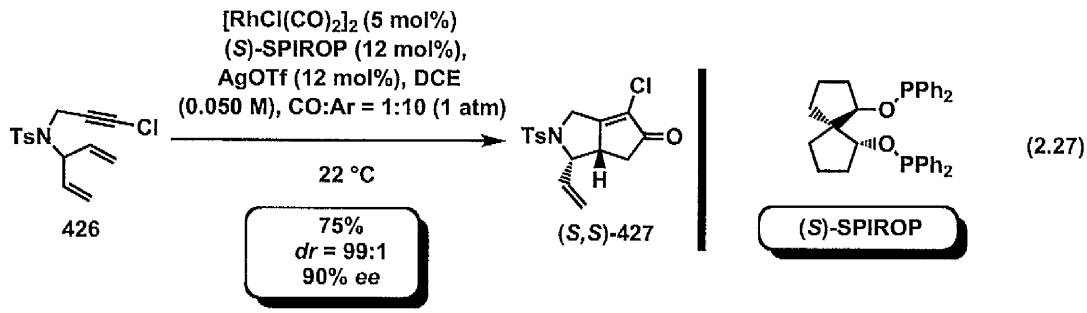

(2.27)

Gratifyingly, the spiro-type phosphite (*S*)-SPIROP promoted the desired desymmetrisation of enyne **426** with remarkable overall stereoselectivity (Eq. 2.26).[233,235] Although the stereoselectivity is comparable to the Ir-catalysed manifold (**Scheme 2.14**), this methodology avoids thermal conditions and high catalyst loadings.

2.3.6. Determination of the Absolute Configuration.

The development by our group of a highly enantioselective Rh-catalysed PK reaction showed that the alkyne terminus has a prominent influence on the reactivity and stereoselectivity of the transformation. The completion of this work involves the determination of the absolute configuration of the Pauson-Khand products by X-ray analysis. In this context, a sample of **388**, obtained by enantioselective Pauson-Khand reaction of enyne **377** (see **Table 2.10**) was recrystallised and subsequent X-ray analysis established the *S* stereochemistry of this compound (**Figure 2.12**).[236,237]

Previous studies described that bicyclopentenones undergo hydrogenation to promote a stereoselective formation of bicyclic ketones.[219] Subsequent condensation of the carbonyl moiety in presence of hydrazines provides the formation of hydrazone derivatives that display high cristallinity and, thereby, are suitable for X-ray analysis. However, as discussed in the section **1.6.6**, our previous attempts to carry out the hydrogenation of α-chloro enones resulted in recovery or decomposition of the starting material.

Figure 2.12. X-ray structure of bicyclopentenone (*S*)-377.

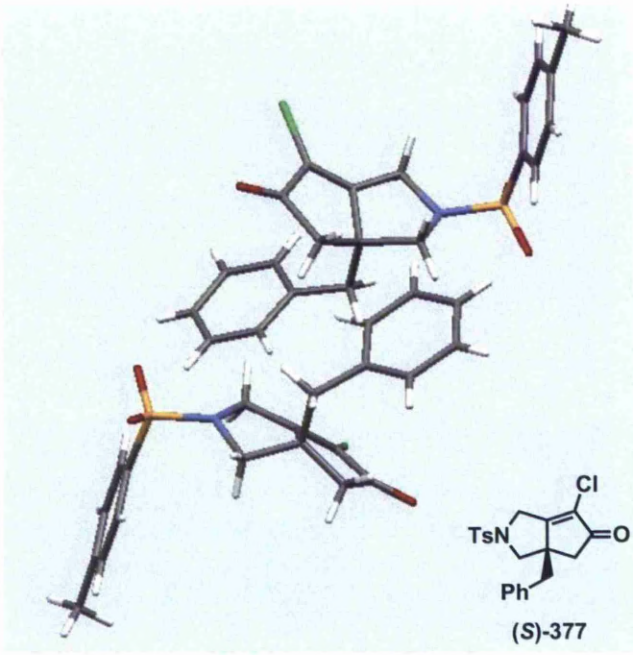

Scheme 2.20. Determination of the absolute configuration of PK adducts **409** and **427** by X-ray analysis of bicyclopentenone derivatives **429** and **431**.

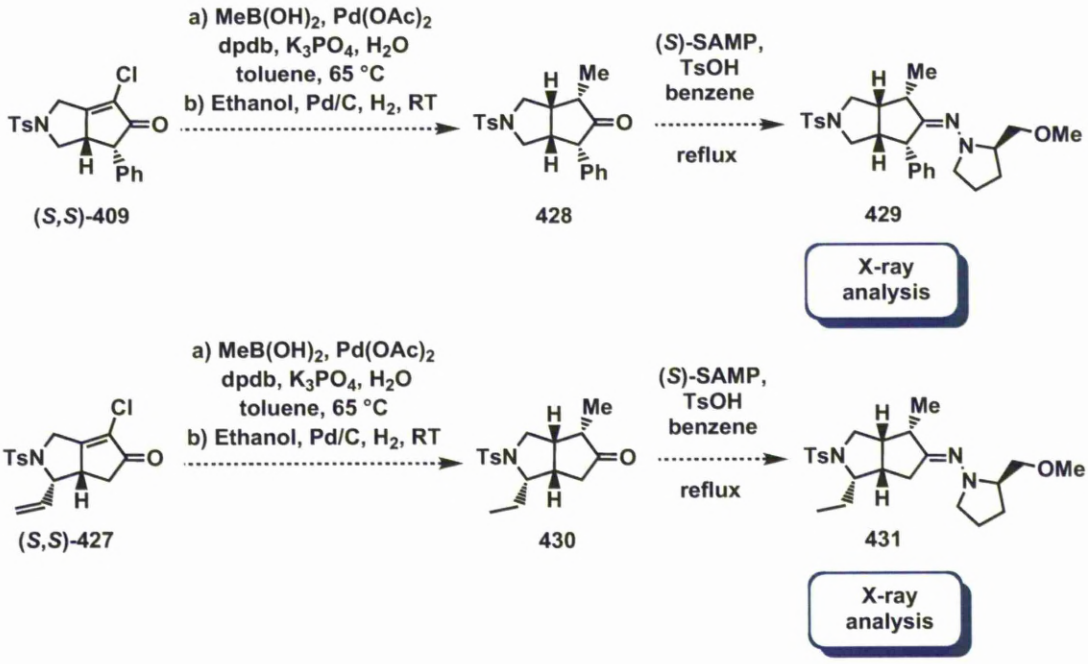

In order to prevent this drawback, a Pd-catalysed Suzuki coupling on Pauson-Khand adducts **409** and **427** could install a methyl moiety on the bicyclopentenone derivatives and reduce any decomposition process in the following hydrogenation process (**Scheme 2.20**). The corresponding ketones **428** and **430** could then undergo acid-catalysed condensation with chiral hydrazine and afford crystalline hydrazone derivatives **429** and **431** that are amenable for X-ray analysis.

2.3.7. Conclusions.

The development of a highly diastereoselective Rh-catalysed PK reaction at room temperature established the ability of the chlorine atom on the alkyne terminus to impart higher reactivity and stereoselectivity. These findings prompted the analysis of the reactivity of the chlorinated 1,6-enynes in the corresponding asymmetric manifold. A detailed study on chiral bisphosphines described that geometrical and electronic features of these ligands influence the reactivity and the stereoselectivity of the enantioselective Rh-catalysed PK reaction. Therefore, bisphosphine ligands with a narrow dihedral angle and lowered electron density on the phosphorous atom, such as SEGPHOS, provided optimal reactivity and enantioselectivity in the asymmetric manifold of chlorinated 1,6-enynes. The synergic ability of chlorinated 1,6-enynes and SEGPHOS ligand to deliver an efficient carbocyclisation process was further exploited towards substrates that display poor reactivity in the reaction, such as 1,6-enynes bearing an internal substituent on the alkyne moiety. Subsequent application of our reaction conditions to these substrates provides a remarkable opportunity to carry out a highly enantioselective PK reaction of chlorinated 1,6-enynes at room temperature. This methodology allowed the employment of a wide array of tethers and alkene substituents, thereby delivering the effective formation of bicyclopentenone derivatives with high degree of enantioselectivity. Application of this methodology to 1,6-enynes bearing a terminal substituent on the alkene moiety revealed that the *cis*-geometry on the olefin imparts high reactivity to the carbocyclisation. Additionally, a silica-promoted epimerisation allows the

preferential formation of the enantiopure diastereoisomer. Finally, the enantioselective Rh-catalysed desymmetrisation of chlorinated *meso*-dienynes provides superior diastereo- and enantioselectivity, in a preparatively more convenient process, compared to that previously reported for the Rh-catalysed variant.

2.4. Experimental.

2.4.1. General.

Unless otherwise indicated, all reactions were carried out in flame-dried glassware under atmosphere of argon. Xylene and benzene were distilled from CaH_2 and kept over sieves, under Ar atmosphere, THF was distilled from benzophenone ketyl. Dry acetone (99.8% Extra Dry, Acroseal ®) was used without any further purification under an atmosphere of argon. Acetonitrile (HPLC grade) was purchased from Fischer and kept over 3Å molecular sieves under an Ar atmosphere. All other starting materials and solvents were purchased from Acros, Aldrich, Alfa Aesar, Fluorochem or Strem and used without further purification. Catalyst $[RhCl(CO)_2]_2$ was purchased by Strem, kept in the glove box at RT and utilised entirely in the glove box. Although Strem Chemicals specifies to store the catalyst at low temperature, the storage of the catalyst in the freezer revealed to be detrimental in time. Bisphosphine ligands were purchased by Strem Chemicals, kept in the glove box at RT and utilised entirely in the glove box. Silver triflate was purchased by Strem, stored and utilised entirely in the glove box. This silver salt is highly sensitive to moisture and experimental analysis showed that the employment of wet silver triflate resulted in low yields and low ee. Cannulas are washed with acetone and kept under vacuum (p = 3 torr) for two days prior to their use in the PK reaction. Carbon monoxide gas and mixture of Ar:CO (10:1) gas were purchased by CK Gas (CO purity = 99.97%). High purity of CO (≥99.95) proved to be essential for the optimal exploitation of the PK reaction.

Thin layer chromatography (TLC) was performed on Whatman F_{254} precoated silica gel plates. Visualisation was accomplished with a UV light and/or $KMnO_4$ solution. Flash chromatography (FC) was performed using either Merck Silica Gel 60 (230-400 mesh) or Whatman Silica Gel Purasil® 60 (230-400 mesh). Solvents for extraction and FC were analytical grade. Reported solvent mixtures for TLC and FC are volume/volume mixtures. Infrared spectra were obtained on a Perkin-Elmer spectrum 100 series FTIR spectrometer. Peaks are reported in cm^{-1} with the following relative intensities: vs (very strong), s (strong), m (medium) and w (weak). Mass spectra were performed at either the University of Liverpool Mass Spectrometry Center or the EPSRC National Mass Spectrometry Service Centre, Swansea. High resolution electron-impact (EI, ionization voltages of 70 eV), chemical ionization (CI, reagent gas CH_4 or NH_3) were obtained on either an Autospec ZAB 2SE, Kratos MS-80, VG 7070E double focusing magnetic sector mass spectrometer equipped with a solid probe inlet, a QUATRO II, MAT 95, or MAT 900. The electrospray ionization (ESI) and mass spectra were obtained on a Waters micromass and LCT mass spectrometer. ^{1}H and ^{13}C NMR were recorded on a Bruker AV 500 MhZ NMR spectrometer in the indicated deuterated solvent, which were obtained from Cambridge Isotope Labs. For ^{1}H NMR, $CDCl_3$ was set to 7.26 ppm ($CDCl_3$, singlet). For ^{13}C NMR, $CDCl_3$ was set to 77.16 ppm ($CDCl_3$, center of triplet). ^{1}H data are reported in the following order: chemical shift in ppm (δ) (multiplicity, which are indicated by br (broadened), s (singlet), d (doublet), t (triplet), q (quartet), m (multiplet)); assignment of 2^{nd} order pattern, if applicable; coupling constant (*J*, Hz); integration values for all ^{13}C NMR spectra data using the descriptor *o* and *e* refer to whether the peak is odd or even respectively, and correlate to an attached proton test (APT) experiments. All liquid chromatograms were obtained on a HPLC Agilent 1200 machine with a variable UV detector. The instrument was fitted with AS-H, AD-H, OD-H, OJ-H Agilent Chiralpak analytical columns (4.6 mm x 250 mm, 5 μ).

2.4.2. Experimental Procedures.

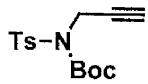

***tert*-Butyl prop-2-ynyl(tosyl)carbamate.**[238]

NaH (0.4 g, 10 mmol) was weighted into a flame-dried 250 mL flask that was then evacuated and backfilled with an argon balloon. DMF (40 mL) was added and the resulting suspension was cooled down to 0°C. After 30 minutes, a solution of 4-methyl-*N*-(prop-2-ynyl)benzenesulfonamide (1.75 g, 8.36 mmol) in DMF (20 mL) was slowly added by syringe, the ice bath was removed and the suspension was stirred for *ca* 30 minutes. Then, a solution of Boc_2O (2.20 g, 10 mmol) in DMF (20 mL) was added at RT and resulting mixture was stirred for an additional 3 hours (tlc control). The reaction was then quenched with a saturated solution of ammonium chloride (100 mL) and extracted with diethyl ether (3x 100 mL). . The combined organic layer was washed with water (2 x 200 mL) and then filtered through a short plug of silica. Removal of the solvent afforded pure *tert*-butyl prop-2-ynyl(tosyl)carbamate as a white solid (2.430 g, 94% yield).

Colour and State: white solid; mp = 79-81 °C.

^{1}H NMR (500 MHz, $CDCl_3$) δ 7.88 (d, J = 8.3 Hz, 2H), 7.29 (d, J = 8.1 Hz, 2H), 4.60 (d, J = 2.4 Hz, 2H), 2.41 (s, 3H), 2.32 (t, J = 2.4 *Hz*, 1H), 1.32 (s, 9H).

^{13}C NMR (125 MHz, $CDCl_3$) δ 150.16 (e), 144.51 (e), 136.61 (e), 129.27 (o), 128.22 (o), 85.00 (e), 78.93 (e), 72.20 (e), 35.68 (e), 27.85 (o), 21.66 (o).

IR (Neat) 3286 (m), 2990 (w), 1723 (s), 1596 (w), 1349 (s), 1155 (s), 1088 (s), 910 (m) cm^{-1}.

HRMS (ESI, $[M+Na]^+$) calcd for $C_{15}H_{19}NNaO_4S$ 332.0932, found 332.0947.

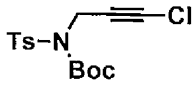

***tert*-Butyl 3-chloroprop-2-ynyl(tosyl)carbamate.**

Cesium carbonate (2.606 g, 8 mmol) and tetra-*n*-butylammonium fluoride trihydrate (0.630 g, 2 mmol) were added to a solution of *tert*-butyl prop-2-ynyl(tosyl)carbamate (1.237 g, 4 mmol) in CCl_4 (7 mL) and the reaction mixture stirred for 1 hour at room temperature. The resulting mixture was then diluted by the addition of dichloromethane (25 mL), filtered through a short pad of celite and the filtrate concentrated *in vacuo* to afford a crude oil. Purification by flash chromatography (silica gel, petroleum ether-diethyl ether, 95:5) afforded *tert*-butyl 3-chloroprop-2-ynyl(tosyl)carbamate as a pale yellow solid (1.22 g, 89% yield).

Colour and State: off-white solid; mp = 75-77 °C.

^{1}H NMR (500 MHz, $CDCl_3$) δ 7.85 (d, J = 8.3 Hz, 2H), 7.31 (d, J = 8.3 Hz, 2H), 4.60 (s, 2H), 2.43 (s, 3H), 1.34 (s, 9H).

^{13}C NMR (125 MHz, $CDCl_3$) δ 150.19 (e), 144.66 (e), 136.58 (e), 129.34 (o), 128.27 (o), 85.13 (e), 64.79 (e), 62.35 (e), 36.13 (e), 27.90 (o), 21.70 (o).

IR (Neat) 2982 (w), 2251 (w), 1728 (s), 1598 (w), 1356 (s), 1153 (s), 1088 (s), 912 (m) cm^{-1}.

HRMS (ESI, $[M+Na]^+$) calcd for $C_{15}H_{18}{}^{35}ClNNaO_4S$ 366.0543, found 366.0549.

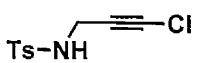

***N*-(3-Chloroprop-2-ynyl)-4-methylbenzenesulfonamide.**

Trifluoroacetic acid (2 mL, 25 mmol) was added to a solution of *tert*-butyl 3-chloroprop-2-ynyl(tosyl)carbamate (1.03 g, 3 mmol) in DCM (10 mL) and the resulting solution was stirred for 1 hour. The solution was then poured into a 100 mL Erlenmeyer flask and a solution of saturated potassium carbonate was slowly added until neutralization (pH = 7). After extraction of the aqueous layer with DCM (2 x 20 mL), the combined organic layers were dried over $MgSO_4$ and concentrated *in vacuo* to afford a crude oil. Purification by flash

chromatography (silica gel, petroleum ether-diethyl ether, 95:5)) afforded the desired *N*-(3-chloroprop-2-ynyl)-4-methylbenzenesulfonamide as a white solid (0.947 g, 89%).

Colour and State: white solid; mp = 64-66 °C

^{1}H NMR (500 MHz, $CDCl_3$) δ 7.77 (d, *J* = 8.3 Hz, 2H), 7.32 (d, *J* = 8.3 Hz, 2H), 4.97 (bs, 1H), 3.83 (d, *J* = 6.2 Hz, 2H), 2.42 (s, 3H).

^{13}C NMR (125 MHz, $CDCl_3$) δ 144.04 (e), 136.65 (e), 129.82 (o), 127.53 (o), 63.78 (e), 63.23 (e), 33.32 (e), 21.67 (o).

IR (Neat) 3257 (w), 2246 (w), 1597 (w), 1323 (m), 1156 (m), 1087 (m), 811 (m) cm^{-1}.

HRMS (ESI, $[M+Na]^+$) calcd for $C_{10}H_{10}{}^{35}ClNNaO_2S$ 266.0018, found 266.0015.

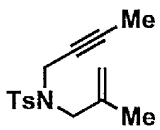

371

***N*-(But-2-ynyl)-4-methyl-*N*-(2-methylallyl)benzenesulfonamide.**[239]

A flame-dried 100 mL flask was charged with triphenylphosphine (1.18 g, 4.5 mmol) and *N*-4-methyl-*N*-(2-methylallyl)benzenesulfonamide (0.680 g, 3 mmol), evacuated and backfilled with argon. Anhydrous THF (12 mL) and but-2-yn-1-ol (0.315 g, 4.5 mmol) were added and resulting solution was placed in an ice bath for *ca* 15 minutes. Diisopropyldiazodicarboxylate (DIAD) (0.88 mL, 4.5 mmol) was added drop-wise over 5 minutes *via* syringe. The resultant reaction mixture was stirred for 18 hours, slowly warming to room temperature, then a TLC (20% diethyl ether/ petroleum ether) showed complete consumption of the secondary amine. The reaction mixture was concentrated *in vacuo* onto silica gel. Purification by flash chromatography (silica gel, petroleum ether-diethyl ether, 95:5) gel provided the desired *N*-(but-2-ynyl)-4-methyl-*N*-(2-methylallyl)benzenesulfonamide as a white solid (0.665 g, 80% yield).

Colour and State: white solid; mp = 48-50 °C

^{1}H NMR (500 MHz, $CDCl_3$) δ 7.73 (d, J = 8.2 Hz, 2H), 7.28 (d, J = 8.1 Hz, 2H), 4.94 (s, 2H), 3.96 (q, J = 2.2 Hz, 2H), 3.68 (s, 2H), 2.41 (s, 3H), 1.75 (s, 3H), 1.49 (t, J = 2.2 Hz, 3H).

^{13}C NMR (125 MHz, $CDCl_3$) δ 143.27 (e), 139.59 (e), 136.64 (e), 129.28 (o), 128.04 (o), 115.23 (e), 81.62 (e), 71.60 (e), 52.52 (e), 36.13 (e), 21.61 (o), 19.84 (o), 3.29 (o).

IR (Neat) 2920 (w), 1655 (w), 1598 (w), 1331 (m), 1159 (s), 1095 (m), 904 (m).

HRMS (ESI, $[M+Na]^+$) calcd for $C_{15}H_{19}NNaO_2S$ 300.1034, found 300.1027.

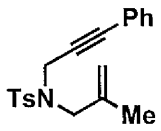

372

4-Methyl-*N*-(2-methylallyl)-*N*-(3-phenylprop-2-ynyl)benzenesulfonamide.[240]

A flame-dried 100 mL flask was charged with triphenylphosphine (1.18 g, 4.5 mmol) and *N*-4-methyl-*N*-(2-methylallyl)benzenesulfonamide (0.680 g, 3 mmol), evacuated and backfilled with argon. Anhydrous THF (12 mL) and 3-phenylprop-2-yn-1-ol (0.595 g, 4.5 mmol) were added and resulting solution was placed in an ice bath for *ca* 15 minutes. Diisopropyldiazodicarboxylate (DIAD) (0.88 mL, 4.5 mmol) was added drop-wise over 5 minutes *via* syringe. The resultant reaction mixture was stirred for 18 hours, slowly warming to room temperature, then a TLC (20% diethyl ether/ petroleum ether) showed complete consumption of the secondary amine. The reaction mixture was concentrated *in vacuo* onto silica gel. Purification by flash chromatography (silica gel, petroleum ether-diethyl ether, 9:1) gel provided the desired 4-methyl-*N*-(2-methylallyl)-*N*-(3-phenylprop-2-ynyl)benzenesulfonamide as a white solid (0.870 g, 85% yield).

Colour and State: white crystalline solid; mp = 62-64 °C

^{1}H NMR (500 MHz, $CDCl_3$) δ 7.78 (d, J = 8.2 Hz, 2H), 7.30-7.20 (m, 5H), 7.03 (d, J = 7.3 Hz, 2H), 5.01 (s, 2H), 4.26 (s, 2H), 3.80 (s, 2H), 2.33 (s, 3H), 1.81 (s, 3H).

^{13}C NMR (125 MHz, $CDCl_3$) δ 143.54 (e), 139.41 (e), 136.16 (e), 131.57 (o), 129.60 (o), 128.45 (o), 128.20 (o), 127.93 (o), 122.36 (e), 115.67 (e), 85.80 (e), 81.70 (e), 52.83 (e), 36.51 (e), 21.51 (o), 19.87 (o).

IR (Neat) 2917 (w), 1655 (w), 1598 (w), 1490 (m), 1348 (m), 1162 (s), 1097 (m), 903 (m), 659 (m).

HRMS (ESI, $[M+Na]^+$) calcd for $C_{20}H_{21}NNaO_2S$ 362.1181, found 362.1174.

General Procedure for the Preparation of Nitrogen-Tethered 1-Chloro-1,6-enynes: a flame-dried 100 mL flask was charged with triphenylphosphine (1.18 g, 4.5 mmol) and *N*-(3-chloroprop-2-ynyl)-4-methylbenzenesulfonamide (0.670 g, 3 mmol), evacuated and backfilled with argon. Anhydrous THF (12 mL) and the required alcohol (4.5 mmol) were added and resulting solution was placed in an ice bath for *ca* 15 minutes. Diisopropyldiazodicarboxylate (DIAD) (0.88 mL, 4.5 mmol) was added drop-wise over 5 minutes *via* syringe. The resultant reaction mixture was stirred for 18 hours, slowly warming to room temperature, then a TLC (20% diethyl ether/ petroleum ether) showed complete consumption of the secondary amine. The reaction mixture was concentrated *in vacuo* onto silica gel. Purification *via* flash chromatography column on silica gel (petroleum ether-diethyl ether, 95:5) provided the requisite nitrogen-tethered 1-chloro-1,6-enyne.

General Procedure for the Preparation of Oxygen- and Malonate-Tethered 1-Chloro-1,6-Enynes: a solution of the requisite 1,6-enyne (2 mmol) in THF (4 mL) was cooled to -78 °C under an argon atmosphere. LiHMDS (2.2 mL, 2.2 mmol, 1M solution in hexane) was added dropwise and the resulting suspension stirred for 20 minutes at -78 °C. Then, a solution of *p*-toluenesulfonyl chloride (0.420 g, 2.2 mmol) in THF (2 mL) was added dropwise and the reaction stirred for 4 hours at -78 °C. The resulting suspension was allowed to warm to RT and quenched with brine (10 mL) and diethyl ether (10 mL) and extracted with diethyl ether (3 x 15 mL). The organic layer was dried over $MgSO_4$, filtered and concentrated *in vacuo* to afford a crude oil. Purification by flash chromatography (silica gel, eluting with diethyl ether/hexanes) afforded the desired 1-chloro-1,6-enyne.

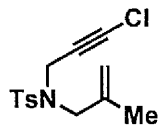

373

***N*-(3-Chloroprop-2-ynyl)-4-methyl-*N*-(2-methylallyl)benzenesulfonamide.**

Synthesised by the general procedure for the preparation of nitrogen-tethered 1-chloro-1,6-enynes (yield = 79%).

Colour and State: white crystalline solid; mp = 69-71 °C.

^{1}H NMR (500 MHz, $CDCl_3$) δ 7.72 (d, *J* = 8.3 Hz, 2H), 7.32 (d, J = 8.2 Hz, 2H), 4.97 (s, 1H), 4.95 (s, 1H), 4.02 (s, 2H), 3.68 (s, 2H), 2.43 (s, 3H), 1.75 (s, 3H).

^{13}C NMR (125 MHz, $CDCl_3$) δ 143.79 (e), 139.27 (e), 135.77 (e), 129.58 (o), 127.88 (o), 115.78 (e), 63.46 (e), 62.31 (e), 52.90 (e), 36.02 (e), 21.67 (o), 19.79 (o).

IR (Neat) 2946 (w), 2243 (w), 1597 (w), 1343 (m), 1332 (s), 1162 (s), 894 (s) cm^{-1}.

HRMS (ESI, $[M+Na]^+$) calcd for $C_{14}H_{16}{}^{35}ClNNaO_2S$ 320.0488, found 320.0497.

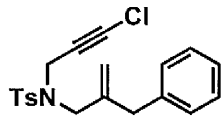

377

***N*-(2-Benzylallyl)-*N*-(3-chloroprop-2-ynyl)-4-methylbenzenesulfonamide.**

Synthesised by the general procedure for the preparation of nitrogen-tethered 1-chloro-1,6-enynes (yield = 82%).

Colour and State: white solid; mp = 71-73 °C.

^{1}H NMR (500 MHz, $CDCl_3$) δ 7.69 (d, *J* = 8.3 Hz, 2H), 7.33-7.20 (m, 7H), 5.08 (s, 1H), 4.98 (s, 1H), 4.02 (s, 2H), 3.67 (s, 2H), 3.39 (s, 2H), 2.42 (s, 3H).

^{13}C NMR (125 MHz, $CDCl_3$) δ 143.84 (e), 142.80 (e), 138.71 (e), 135.56 (e), 129.58 (o), 129.35 (o), 128.55 (o), 127.92 (o), 126.49 (o), 116.87 (e), 63.59 (e), 62.21 (e), 51.27 (e), 39.84 (e), 36.23 (e), 21.67 (o).

IR (Neat) 3029 (w), 2921 (w), 2247 (w), 1650 (w), 1597 (w), 1344 (m), 1326 (m), 1163 (s), 892 (s) cm^{-1}.

HRMS (ESI, $[M+Na]^+$) calcd for $C_{20}H_{20}{}^{35}ClNNaO_2S$ 396.0801, found 396.0789.

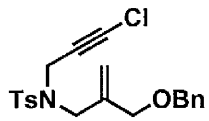

378

***N*-(2-(Benzyloxymethyl)allyl)-*N*-(3-chloroprop-2-ynyl)-4-methylbenzenesulfonamide.**

Synthesised by the general procedure for the preparation of nitrogen-tethered 1-chloro-1,6-enynes (yield = 72%).

Colour and State: white crystalline solid; mp = 39-41 °C.

^{1}H NMR (500 MHz, $CDCl_3$) δ 7.73 (d, J = 8.3 Hz, 2H), 7.40-7.27 (m, 5H), 7.32 (d, J = 8.0 Hz, 2H), 5.34 (s, 1H), 5.21 (s, 1H), 4.53 (s, 2H), 4.06 (s, 2H), 4.03 (s, 2H), 3.81 (s, 2H), 2.43 (s, 3H).

^{13}C NMR (125 MHz, $CDCl_3$) 143.89 (e), 139.85 (e), 138.21 (e), 135.60 (e), 129.63 (o), 128.55 (o), 127.93 (o), 127.90 (o), 127.80 (o), 116.88 (e), 72.75 (e), 70.65 (e), 63.72 (e), 62.31 (e), 49.31 (e), 36.46 (e), 21.69 (o).

IR (Neat) 3031 (w), 2857 (w), 2241 (m), 1598 (w), 1349 (m), 1093 (m), 903 (m)

HRMS (ESI, $[M+Na]^+$) calcd for $C_{21}H_{22}{}^{35}ClNNaO_3S$ 429.0907, found 429.0901.

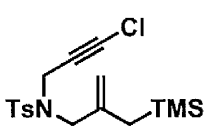

379

***N*-(3-Chloroprop-2-ynyl)-4-methyl-*N*-(2-((trimethylsilyl)methyl)allyl)benzenesulfonamide.**

Synthesised by the general procedure for the preparation of nitrogen-tethered 1-chloro-1,6-enynes (yield = 64%).

Colour and State: white solid; mp = 60-62 °C.

^{1}H NMR (500 MHz, $CDCl_3$) δ 7.72 (d, *J* = 8.3 Hz, 2H), 7.32 (d, J = 8.1 Hz, 2H), 4.86 (d, *J* = 1.0 Hz, 1H), 4.75 (s, 1H), 4.04 (s, 2H), 3.60 (s, 2H), 2.43 (s, 3H), 1.56 (s, 2H), 0.05 (s, 9H).

^{13}C NMR (125 MHz, $CDCl_3$) δ 143.75 (e), 140.93 (e), 135.90 (e), 129.57 (o), 127.91 (o), 112.57 (e), 63.41 (e), 62.48 (e), 53.16 (e), 36.07 (e), 23.03 (e), 21.67 (o), -1.38 (o).

IR (Neat) 2957 (w), 2239 (w), 1637 (w), 1598 (w), 1345 (m), 1160 (s), 1089 (m), 894 (s) cm^{-1}.

HRMS (ESI, $[M+Na]^+$) calcd for $C_{17}H_{24}{}^{35}ClNNaO_2SSi$ 392.0883, found 392.0878.

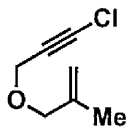

380

3-(3-Chloroprop-2-ynyloxy)-2-methylprop-1-ene.

Synthesised by the general procedure for the preparation of oxygen- and malonate-tethered 1-chloro-1,6-enynes (yield = 31%).

Colour and State: colourless liquid.

^{1}H NMR (500 MHz, $CDCl_3$) δ 4.98 (s, 1H), 4.93 (s,1H), 4.13 (s, 2H), 3.95 (s, 2H), 1.74 (s, 3H).

^{13}C NMR (125 MHz, $CDCl_3$) δ 141.38 (e), 113.20 (e), 73.82 (e), 65.67 (e), 64.35 (e), 57.41 (e), 19.55 (o).

IR (Neat) 2920 (w), 2239 (w), 1655 (w), 1353 (m), 1098 (s), 901 (m).

HRMS (CI, $[M+NH_4]^+$) calcd for $C_7H_{13}{}^{35}ClNO$ 162.0680, found 162.0681.

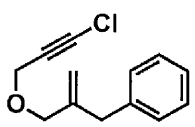

381

(2-((3-Chloroprop-2-ynyloxy)methyl)allyl)benzene.

Synthesised by the general procedure for the preparation of oxygen- and malonate-tethered 1-chloro-1,6-enynes (yield = 82%).

Colour and State: colourless liquid.

^{1}H NMR (500 MHz, $CDCl_3$) δ 7.27-7.32 (m, 2H), 7.24-7.18 (m, 3H), 5.12 (s, 1H), 4.96 (s, 1H), 4.11 (s, 2H), 3.93 (s, 2H), 3.40 (s, 2H).

^{13}C NMR (125 MHz, $CDCl_3$) δ 144.83 (e), 139.04 (e), 129.19 (o), 128.50 (o), 126.37 (o), 114.50 (e), 72.14 (e), 65.65 (e), 64.49 (e), 57.61 (e), 40.03 (e).

IR (Neat) 3028 (w), 2849 (w), 2238 (w), 1652 (w), 1495 (w), 1354 (w), 1095 (m), 907 (m).

HRMS (ESI, $[M+Na]^+$) calcd for $C_{13}H_{13}{}^{35}ClNaO$ 243.0553, found 243.0545.

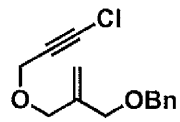

382

((2-((3-Chloroprop-2-ynyloxy)methyl)allyloxy)methyl)benzene.

Synthesised by the general procedure for the preparation of oxygen- and malonate-tethered 1-chloro-1,6-enynes (yield = 85%).

Colour and State: colourless liquid.

^{1}H NMR (500 MHz, $CDCl_3$) δ 7.39-7.28 (m, 5H), 5.27 (s, 1H), 5.25 (s, 1H), 4.52 (s, 2H), 4.15 (s, 2H), 4.09 (s, 2H), 4.04 (s, 2H).

^{13}C NMR (125 MHz, $CDCl_3$) δ 141.95 (e), 138.29 (e), 128.51 (o), 127.80 (o), 127.74 (o), 115.22 (e), 72.33 (e), 70.88 (e), 70.58 (e), 65.55 (e), 64.61 (e), 57.79 (e).

IR (Neat) 3031 (w), 2854 (w), 2238 (w), 1724 (w), 1454 (w), 1355 (w), 1092 (m), 698 (m).

HRMS (ESI, $[M+Na]^+$) calcd for $C_{14}H_{15}{}^{35}ClNaO_2$ 273.0658, found 273.0658.

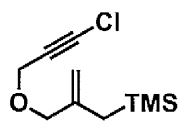

383

(2-((3-Chloroprop-2-ynyloxy)methyl)allyl)trimethylsilane.

Synthesised by the general procedure for the preparation of oxygen- and malonate-tethered 1-chloro-1,6-enynes (yield = 77%).

Colour and State: colourless liquid.

^{1}H NMR (500 MHz, $CDCl_3$) δ 4.90 (q, J = 1.6 Hz, 1H), 4.73 (s, 1H), 4.13 (s, 2H), 3.90 (s, 2H), 1.54 (s, 2H), 0.03 (s, 9H).

^{13}C NMR (125 MHz, $CDCl_3$) δ 143.13 (e), 110.15 (e), 73.94 (e), 65.75 (e), 64.41 (e), 57.46 (e), 23.39 (e), -1.28 (o).

IR (Neat) 2953 (w), 2894 (w), 2239 (w), 1637 (w), 1247 (m), 1094 (m), 843 (m).

HRMS (ESI, $[M+Na]^+$) calcd for $C_{10}H_{17}{}^{35}ClNaOSi$ 239.0635, found 239.0636.

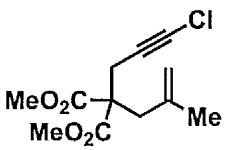

384

Dimethyl 2-(3-chloroprop-2-ynyl)-2-(2-methylallyl)malonate.

Synthesised by the general procedure for the preparation of oxygen- and malonate-tethered 1-chloro-1,6-enynes (yield = 92%).

Colour and State: pale yellow solid; mp = 38-40 °C.

^{1}H NMR (500 MHz, $CDCl_3$) δ 4.93-4.89 (m, 1H), 4.82 (s, 1H), 3.74 (s, 6H), 2.83 (s, 2H), 2.82 (s, 2H), 1.64 (s, 3H).

^{13}C NMR (125 MHz, $CDCl_3$) δ 170.61 (e), 139.81 (e), 116.59 (e), 64.65 (e), 60.86 (e), 56.55 (e), 52.97 (o), 39.89 (e), 23.28 (e), 23.18 (o).

IR (Neat) 2954 (w), 2246 (w), 1737 (s), 1647 (w), 1436 (m), 1208 (m), 1058 (m), 902 (w).

HRMS (ESI, $[M+Na]^+$) calcd for $C_{12}H_{15}{}^{35}ClNaO_4$ 281.0557, found 281.0554.

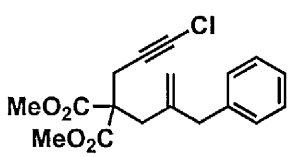

385

Dimethyl 2-(2-benzylallyl)-2-(3-chloroprop-2-ynyl)malonate.

Synthesised by the general procedure for the preparation of oxygen- and malonate-tethered 1-chloro-1,6-enynes (yield = 90%).

Colour and State: colourless oil.

^{1}H NMR (500 MHz, $CDCl_3$) δ 7.32-7.12 (m, 5H), 4.95 (s, 1H), 4.91 (s, 1H), 3.74 (s, 6H), 3.24 (s, 2H), 2.90 (s, 2H), 2.79 (s, 2H).

^{13}C NMR (125 MHz, $CDCl_3$) δ 170.53 (e), 143.25 (e), 138.97 (e), 129.19 (o), 128.50 (o), 126.44 (o), 117.54 (e), 64.64 (e), 61.17 (e), 56.91 (e), 52.98 (o), 43.53 (e), 36.89 (e), 23.32 (e).

IR (Neat) 3028 (w), 2953 (w), 2246 (w), 1736 (s), 1642 (w), 1436 (m), 1291 (m), 1201 (s), 1064 (w), 909 (w).

HRMS (ESI, $[M+Na]^+$) calcd for $C_{18}H_{19}{}^{35}ClNaO_4$ 357.0870, found 357.0871.

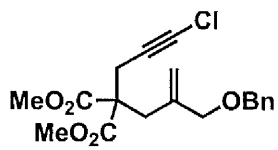

386

Dimethyl 2-(2-(benzyloxymethyl)allyl)-2-(3-chloroprop-2-ynyl)malonate.

Synthesised by the general procedure for the preparation of oxygen- and malonate-tethered 1-chloro-1,6-enynes (yield = 88%).

Colour and State: colourless oil.

^{1}H NMR (500 MHz, $CDCl_3$) δ 7.37-7.26 (m, 5H), 5.27 (q, J = 1.4 Hz, 1H), 5.07 (s, 1H), 4.47 (s, 2H), 3.84 (s, 2H), 3.69 (s, 6H), 2.90 (s, 2H), 2.85 (s, 2H).

^{13}C NMR (125 MHz, $CDCl_3$) δ 170.42 (e), 140.45 (e), 138.21 (e), 128.46 (o), 127.75 (o), 127.69 (o), 117.47 (e), 72.97 (e), 72.19 (e), 64.57 (e), 61.01 (e), 56.65 (e), 52.95 (o), 35.10 (e), 23.30 (e).

IR (Neat) 2953 (w), 2855 (w), 2245 (w), 1736 (s), 1497 (w), 1436 (m), 1291 (m), 1205 (s), 1091 (m), 917 (w).

HRMS (ESI, $[M+Na]^+$) calcd for $C_{19}H_{21}{}^{35}ClNaO_5$ 387.0975, found 387.0962.

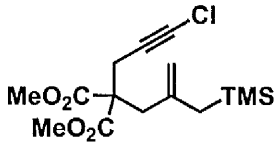

387

Dimethyl 2-(3-chloroprop-2-ynyl)-2-(2-((trimethylsilyl)methyl)allyl)malonate.

Synthesised by the general procedure for the preparation of oxygen- and malonate-tethered 1-chloro-1,6-enynes (yield = 91%).

Colour and State: colourless oil.

^{1}H NMR (500 MHz, $CDCl_3$) δ 4.68 (s, 1H), 4.64 (s, 1H), 3.73 (s, 6H), 2.87 (s, 2H), 2.73 (s, 2H), 1.42 (s, 2H), 0.02 (s, 9H).

^{13}C NMR (125 MHz, $CDCl_3$) δ 170.54 (e), 141.65 (e), 112.58 (e), 64.87 (e), 61.02 (e), 57.10 (e), 52.89 (o), 39.40 (e), 27.64 (e), 23.13 (e), -1.39 (o).

IR (Neat) 2954 (w), 2246 (w), 1740 (s), 1630 (w), 1435 (m), 1248 (m), 1181 (m), 850 (m).

HRMS (ESI, $[M+Na]^+$) calcd for $C_{15}H_{23}{}^{35}ClNaO_4Si$ 353.0952, found 353.0943.

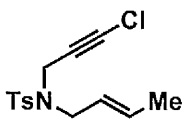

402

(*E*)-*N*-(But-2-enyl)-*N*-(3-chloroprop-2-ynyl)-4-methylbenzenesulfonamide.

Synthesised by the general procedure for the preparation of nitrogen-tethered 1-chloro-1,6-enynes (yield = 85%).

Colour and State: white solid; mp = 51-53 °C.

^{1}H NMR (500 MHz, $CDCl_3$) δ 7.68 (d, J = 8.3 Hz, 2H), 7.29 (d, J = 8.1 Hz, 2H), 5.66 (dq, J = 15.1, 6.5 Hz, 1H), 5.36-5.28 (m, 1H), 4.02 (s, 2H), 3.68 (d, J = 6.8 Hz, 2H), 2.40 (s, 3H), 1.66 (d, J = 6.5 Hz, 3H).

^{13}C NMR (125 MHz, $CDCl_3$) δ 143.67 (e), 135.73 (e), 131.82 (o), 129.50 (o), 127.76 (o), 124.52 (o), 63.23 (e), 62.50 (e), 48.68 (e), 35.94 (e), 21.57 (o), 17.77 (o).

IR (Neat) 2922 (w), 2241 (w), 1598 (w), 1347 (s), 1160 (s), 900 (s) cm^{-1}.

HRMS (ESI, $[M+Na]^+$) calcd for $C_{14}H_{16}{}^{35}ClNNaO_2S$ 320.0488, found 320.0478.

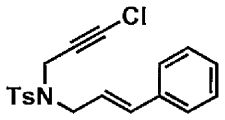

403

***N*-(3-Chloroprop-2-ynyl)-*N*-cinnamyl-4-methylbenzenesulfonamide.**

Synthesised by the general procedure for the preparation of nitrogen-tethered 1-chloro-1,6-enynes (yield = 77%).

Colour and State: white solid; mp = 57-59 °C.

^{1}H NMR (500 MHz, $CDCl_3$) δ 7.79-7.73 (m, 2H), 7.38-7.23 (m, 7H), 6.56 (d, J = 15.8 Hz, 1H), 6.08 (dt, J = 15.8, 6.9 Hz, 1H), 4.11 (s, 2H), 3.95 (dd, J = 6.6, 0.9 Hz, 1H), 2.45 (s, 3H).

^{13}C NMR (125 MHz, $CDCl_3$) δ 143.91 (e), 136.17 (e), 135.84 (e), 135.10 (o), 129.68 (o), 128.78 (o), 128.27 (o), 127.92 (o), 126.70 (o), 123.02 (o), 63.66 (e), 62.56 (e), 49.08 (e), 36.48 (e), 21.70 (o).

IR (Neat) 3028 (w), 2922 (w), 2240 (w), 1598 (w), 1348 (m), 1161 (s), 903 (s) cm^{-1}.

HRMS (ESI, $[M+Na]^+$) calcd for $C_{19}H_{18}{}^{35}ClNNaO_2S$ 382.0644, found 382.0648.

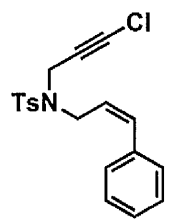

408

(*Z*)-*N*-(3-Chloroprop-2-ynyl)-4-methyl-*N*-(3-phenylallyl)benzenesulfonamide.

Synthesised by the general procedure for the preparation of nitrogen-tethered 1-chloro-1,6-enynes (yield = 80%).

Colour and State: white solid; mp = 48-50 °C.

^{1}H NMR (500 MHz, $CDCl_3$) δ 7.69 (d, J = 8.3 Hz, 2H), 7.37-7.17 (m, 7H), 6.69 (d, J = 11.7 Hz, 1H), 5.61 (dt, J = 11.7, 6.9 Hz, 1H), 4.09-4.05 (m, 4H), 2.42 (s, 3H).

^{13}C NMR (125 MHz, $CDCl_3$) δ 143.83 (e), 136.01 (e), 135.79 (e), 134.25 (o), 129.65 (o), 128.84 (o), 128.43 (o), 127.84 (o), 127.54 (o), 126.01 (o), 63.61 (e), 62.49 (e), 49.61 (e), 36.87 (e), 21.67 (o).

IR (Neat) 3025 (w), 2241 (w), 1598 (w), 1494 (w), 1347 (s), 1160 (s), 901 (s) cm^{-1}.

HRMS (ESI, $[M+Na]^+$) calcd for $C_{19}H_{18}{}^{35}ClNNaO_2S$ 382.0644, found 382.0642.

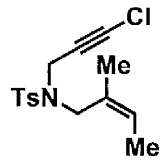

410

(*Z*)-*N*-(3-Chloroprop-2-ynyl)-4-methyl-*N*-(2-methylbut-2-enyl)benzenesulfonamide.

Synthesised by the general procedure for the preparation of nitrogen-tethered 1-chloro-1,6-enynes (yield = 75%).

Colour and State: white solid; mp = 50-52 °C.

^{1}H NMR (500 MHz, $CDCl_3$) δ 7.72 (d, J = 8.3 Hz, 2H), 7.31 (d, J = 8.1 Hz, 2H), 5.51 (q, J = 6.7 Hz, 1H), 3.95 (s, 2H), 3.75 (s, 2H), 2.42 (s, 3H), 1.69 (t, J = 1.0 Hz, 3H), 1.59 (t, J = 6.9 Hz, 3H).

^{13}C NMR (125 MHz, $CDCl_3$) δ 143.67 (e), 135.78 (e), 129.51 (o), 129.28 (e), 127.88 (o), 126.41 (o), 63.27 (e), 62.86 (e), 46.14 (e), 35.57 (e), 21.61 (o), 21.40 (o), 13.28 (o).

IR (Neat) 2967 (w), 2920 (w), 2241 (w), 1921 (w), 1597 (w), 1446 (w), 1329 (s), 1160 (s), 963 (s) cm^{-1}.

HRMS (ESI, $[M+Na]^+$) calcd for $C_{15}H_{18}{}^{35}ClNNaO_2S$ 334.0644, found 334.0639.

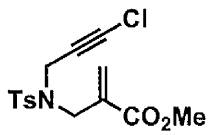

411

Methyl 2-((*N*-(3-chloroprop-2-ynyl)-4-methylphenylsulfonamido)methyl)acrylate.

Synthesised by the general procedure for the preparation of nitrogen-tethered 1-chloro-1,6-enynes (yield = 87%).

Colour and State: white solid; mp = 60-62 °C.

^{1}H NMR (500 MHz, $CDCl_3$) δ 7.75 (d, *J* = 8.3 Hz, 2H), 7.33 (d, J = 8.2 Hz, 2H), 6.40 (s, 1H), 5.93 (s, 1H), 4.09 (s, 2H), 4.04 (s, 2H), 3.77 (s, 3H), 2.44 (s, 3H).

^{13}C NMR (125 MHz, $CDCl_3$) δ 166.20 (e), 143.97 (e), 135.64 (e), 134.82 (e), 129.64 (o), 127.79 (o), 63.86 (e), 62.45 (e), 52.13 (o), 47.13 (e), 37.46 (e), 21.59 (o).

IR (Neat) 2963 (w), 2239 (w), 1717 (s), 1633 (w), 1433 (s), 1334 (m), 890 (s) cm^{-1}.

HRMS (ESI, $[M+Na]^+$) calcd for $C_{15}H_{16}{}^{35}ClNNaO_4S$ 364.0386, found 364.0383.

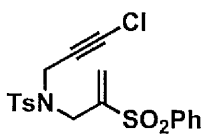

412

***N*-(3-Chloroprop-2-ynyl)-4-methyl-*N*-(2-(phenylsulfonyl)allyl)benzenesulfonamide.**

Synthesised by the general procedure for the preparation of nitrogen-tethered 1-chloro-1,6-enynes (yield = 82%).

Colour and State: white solid; mp = 135-137 °C.

^{1}H NMR (500 MHz, $CDCl_3$) δ 7.94 (d, *J* = 7.9 Hz, 2H), 7.73-7.52 (m, 5H), 7.34-7.28 (m, 2H), 5.39 (s, 1H), 5.27 (s, 1H), 3.98 (s, 2H), 3.89 (s, 2H), 3.74 (s, 2H), 2.43 (s, 3H).

^{13}C NMR (125 MHz, $CDCl_3$) δ 144.14 (e), 138.76 (e), 135.29 (e), 133.95 (o), 131.36 (e), 129.68 (o), 129.33 (o), 128.65 (o), 127.91 (o), 63.96 (e), 62.23 (e), 58.86 (e), 51.54 (e), 36.85 (e), 21.67 (o).

IR (Neat) 2924 (w), 2241 (w), 1650 (s), 1597 (w), 1447 (m), 1307 (s), 1086 (s), 906 (s) cm^{-1}.

HRMS (ESI, $[M+Na]^+$) calcd for $C_{20}H_{20}{}^{35}ClNNaO_4S_2$ 460.0420, found 460.0423.

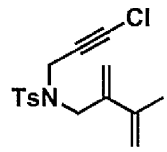

413

***N*-(3-chloroprop-2-ynyl)-4-methyl-*N*-(3-methyl-2-methylenebut-3-enyl)benzenesulfonamide.**

Synthesised by the general procedure for the preparation of nitrogen-tethered 1-chloro-1,6-enynes (yield = 79%).

Colour and State: white crystalline solid; mp = 81-83 °C.

^{1}H NMR (500 MHz, $CDCl_3$) δ 7.75 (d, *J* = 8.3 Hz, 2H), 7.33 (d, J = 8.3 Hz, 2H), 5.40 (s, 1H), 5.31 (s, 1H), 5.20 (s, 1H), 5.09 (s, 1H), 3.99 (s, 2H), 3.97 (s, 2H), 2.44 (s, 3H), 1.92 (s, 3H).

^{13}C NMR (125 MHz, $CDCl_3$) δ 143.87 (e), 141.06 (e), 140.16 (e), 135.29 (e), 129.58 (o), 128.05 (o), 117.37 (e), 115.42 (e), 63.68 (e), 62.31 (e), 49.71 (e), 36.16 (e), 21.68 (o), 21.22 (o).

IR (Neat) 2924 (w), 2240 (w), 1599 (m), 1349 (m), 1122 (s), 1093 (m), 897 (m).

HRMS (ESI, $[M+Na]^+$) calcd for $C_{16}H_{18}{}^{35}ClNNaO_2S$ 346.0644, found 346.0640.

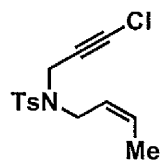

418

(*Z*)-*N*-(But-2-enyl)-*N*-(3-chloroprop-2-ynyl)-4-methylbenzenesulfonamide.

Synthesised by the general procedure for the preparation of nitrogen-tethered 1-chloro-1,6-enynes (yield = 79%).

Colour and State: white solid; mp = 70-72 °C.

^{1}H NMR (500 MHz, $CDCl_3$) δ 7.72 (d, J = 8.3 Hz, 2H), 7.32 (d, J = 8.1 Hz, 2H), 5.79-5.70 (m, 1H), 5.36-5.28 (m, 1H), 4.05 (s, 2H), 3.82 (d, J = 7.3 Hz, 2H), 2.43 (s, 3H), 1.66-1.64 (m, 3H).

^{13}C NMR (125 MHz, $CDCl_3$) δ 143.77 (e), 135.66 (e), 130.81 (o), 129.59 (o), 127.87 (o), 123.65 (o), 63.31 (e), 62.69 (e), 42.96 (e), 36.14 (e), 21.65 (o), 13.01 (o).

IR (Neat) 3026 (w), 2923 (w), 2241 (w), 1598 (w), 1347 (s), 1161 (s), 1092 (m), 908 (s) cm^{-1}.

HRMS (ESI, $[M+Na]^+$) calcd for $C_{14}H_{16}{}^{35}ClNNaO_2S$ 320.0488, found 320.0489.

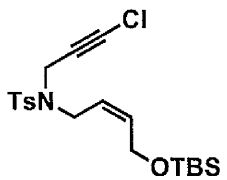

419

(*Z*)-*N*-(4-(*tert*-Butyldimethylsilyloxy)but-2-enyl)-*N*-(3-chloroprop-2-ynyl)-4-methylbenzenesulfonamide.

Synthesised by the general procedure for the preparation of nitrogen-tethered 1-chloro-1,6-enynes (yield = 71%).

Colour and State: white solid; mp = 61-63 °C.

^{1}H NMR (500 MHz, $CDCl_3$) δ 7.71 (d, J = 8.3 Hz, 2H), 7.31 (d, J = 8.0 Hz, 2H), 5.80-5.74 (m, 1H), 5.40-5.33 (m, 1H), 4.21 (dd, J = 6.0, 0.9 Hz, 2H), 4.05 (s, 2H), 3.83 (d, J = 7.2 Hz, 2H), 2.42 (s, 3H), 0.87 (s, 9H), 0.04 (s, 6H).

^{13}C NMR (125 MHz, $CDCl_3$) δ 143.83 (e), 135.63 (o), 135.59 (e), 129.60 (o), 127.83 (o), 123.92 (o), 63.46 (e), 62.55 (e), 59.10 (e), 43.56 (e), 36.32 (e), 25.94 (o), 21.62 (o), 21.65 (o), 18.35 (e), -5.22 (o).

IR (Neat) 2953 (w), 2928 (w), 2241 (w), 1598 (w), 1350 (m), 1161 (s), 1090 (m), 835 (s) cm^{-1}.

HRMS (ESI, $[M+Na]^+$) calcd for $C_{20}H_{30}{}^{35}ClNNaO_3SSi$ 450.1302, found 450.1289.

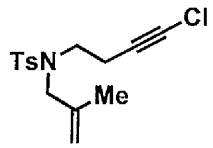

423

***N*-(4-Chlorobut-3-ynyl)-4-methyl-*N*-(2-methylallyl)benzenesulfonamide.**

Synthesised by the general procedure for the preparation of nitrogen-tethered 1-chloro-1,6-enynes (yield = 74%).

Colour and State: colourless oil.

^{1}H NMR (500 MHz, $CDCl_3$) δ 7.68 (d, J = 8.3 Hz, 2H), 7.30 (d, J = 8.2 Hz, 2H), 4.92 (s, 1H), 4.87 (s, 1H), 3.69 (s, 1H), 3.21 (t, J = 7.6 Hz, 2H), 2.42 (s, 3H), 2.40 (t, J = 7.6 Hz, 2H), 1.70 (s, 3H).

^{13}C NMR (125 MHz, $CDCl_3$) δ 143.54 (e), 140.55 (e), 136.62 (e), 129.83 (o), 127.22 (o), 115.08 (e), 66.46 (e), 59.25 (e), 55.21 (e), 46.41 (e), 21.59 (o), 19.81 (e), 19.34 (o).

IR (Neat) 2921 (w), 2245 (w), 1655 (w), 1449 (w), 1338 (m), 1158 (s), 1103 (m), 921 (m) cm^{-1}.

HRMS (ESI, $[M+Na]^+$) calcd for 334.0644 $C_{15}H_{18}{}^{35}ClNNaO_2S$, found 334.0644.

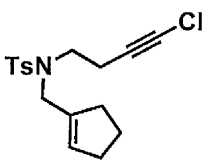

424

***N*-(4-Chlorobut-3-ynyl)-*N*-(cyclopentenylmethyl)-4-methylbenzenesulfonamide.**

Synthesised by the general procedure for the preparation of nitrogen-tethered 1-chloro-1,6-enynes (yield = 69%).

Colour and State: pale yellow oil.

^{1}H NMR (500 MHz, $CDCl_3$) δ 7.77 (d, J = 8.3 Hz, 2H), 2.28 (d, J = 8.2 Hz, 2H), 5.84 (ddd, J = 17.2, 10.7, 6.1 Hz, 2H), 5.24 (d, J = 10.4 Hz, 2H), 5.19 (d, J = 17.3 Hz, 2H), 5.03-4.96 (m, 1H), 4.04 (s, 2H), 2.42 (s, 3H).

^{13}C NMR (125 MHz, $CDCl_3$) δ 143.57 (e), 137.64 (e), 134.45 (o), 129.46 (o), 127.89 (o), 119.14 (e), 65.36 (e), 62.79 (e), 62.01 (o), 34.01 (e), 21.69 (o).

IR (Neat) 2980 (w), 2242 (w), 1597 (w), 1421 (m), 1327 (s), 1152 (s), 1091 (m), 935 (m) cm^{-1}.

HRMS (ESI, $[M+Na]^+$) calcd for $C_{17}H_{20}{}^{35}ClNNaO_2S$ 360.0801, found 360.0804.

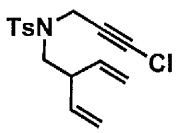

426

***N*-(3-Chloroprop-2-ynyl)-4-methyl-*N*-(2-vinylbut-3-enyl)benzenesulfonamide.**

Synthesised by the general procedure for the preparation of nitrogen-tethered 1-chloro-1,6-enynes (yield = 29%).

Colour and State: off-white solid; mp = 55-57 °C.

^{1}H NMR (500 MHz, $CDCl_3$) δ 7.68 (d, J = 8.3 Hz, 2H), 7.29 (d, J = 8.0 Hz, 2H), 5.56 (s, 1H), 3.85 (s, 2H), 3.23 (t, J = 7.6 Hz, 2H), 2.42 (s, 3H), 2.43-2.38 (m, 2H), 2.33-2.12 (m, 4H), 1.84 (quint, J = 7.6 Hz, 2H).

^{13}C NMR (125 MHz, $CDCl_3$) δ 143.44 (e), 139.41 (e), 136.85 (e), 130.16 (o), 129.75 (o), 127.27 (o), 66.56 (e), 59.23 (e), 49.06 (e), 46.26 (e), 33.19 (e), 32.51 (e), 23.20 (e), 21.62 (o), 19.55 (e).

IR (Neat) 2925 (w), 2242 (w), 2241 (w), 1598 (w), 1445 (m), 1337 (m), 1156 (s), 1096 (m) cm^{-1}.

HRMS (ESI, $[M+Na]^+$) calcd for $C_{15}H_{16}{}^{35}ClNNaO_2S$ 332.0491, found 332.0492.

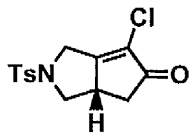

(*S*)-310

General Procedure for the Synthesis of ***(S)-310*** *by Rh-catalysed Enantioselective Pauson-Khand Reaction of 1,6-Enyne* ***301***: $[RhCl(CO)_2]_2$ (2 mg, 0.005 mmol) and the required bisphosphine ligand (0.012 mmol) were placed into a flame-dried 10 mL round-bottom flask equipped with a 10 mm stirrer bar under inert atmosphere (glove-box). The flask was removed from the glove box, equipped with an argon balloon and the specified solvent (1 mL) was added to the mixture *via* tared syringe. The resulting solution was stirred for *ca* 2 hours and subsequently transferred *via* cannula into a 10 mL round-bottom flask containing the specified silver salt (0.012 mmol). After 30 minutes, a solution of enyne **301** (0.1 mmol, 28.4 mg) in the specified solvent (1 mL) under Ar atmosphere was added to the catalyst solution *via* cannula and the argon balloon was promptly replaced with a CO balloon (10:1 Ar:CO, 1 atm). The reaction was stirred at RT (22 °C) for 48 hours. The reaction mixture was concentrated *in vacuo* onto silica gel. Purification *via* flash chromatography column (silica gel, eluting *via* a gradient 10-40% diethyl ether/hexane) provided **(*S*)-310** as a pale yellow oil.

Colour and State: pale yellow oil.

HPLC analysis (25 cm x 4.6 mm Agilent Chiral AS-H), 34% isopropanol/hexane at 1.0 mL/min, 230 nm, T = 22 °C; t_R (*major*) 62.3 min, t_R (*minor*) 47.2 min.

^{1}H NMR (500 MHz, $CDCl_3$) δ 7.72 (d, J = 8.2 Hz, 2H), 7.35 (d, J = 8.1 Hz, 2H), 4.34 (d, A of AB, J_{AB} = 17.2 Hz, 1H), 4.06-4.03 (m, 1H), 4.03 (d, B of AB, J_{AB} = 17.4 Hz, 1H), 3.21-3.15 (m, 1H), 2.76 (dd, A of ABX, J_{AB} = 18.2 Hz, J_{AX} = 6.4 Hz, 1H), 2.62 (dd, B of ABX, J_{AB} = 11.0 Hz, J_{BX} = 9.6 Hz, 1H), 2.44 (s, 3H), 2.18 (dd, B of ABX, J_{AB} = 18.2 Hz, J_{BX} = 2.9 Hz, 1H).

^{13}C NMR (125 MHz, $CDCl_3$) δ 199.09 (e), 170.70 (e), 144.53 (e), 133.26 (e), 130.25 (o), 128.69 (e), 127.59 (o), 52.69 (e), 47.17 (e), 41.60 (o), 38.50 (e), 21.71 (o).

IR (Neat) 2923 (w), 1732 (vs), 1667 (s), 1597 (m), 1345 (vs), 1161 (vs) cm^{-1}.

HRMS (CI, $[M+H]^+$) calcd for $C_{14}H_{15}{}^{35}ClNO_3S$ 312.0456, found 312.0461.

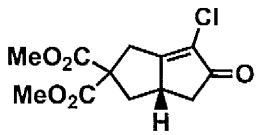

(*S*)-313

General Procedure for the Synthesis of ***(S)-313*** *by Rh-catalysed Enantioselective Pauson-Khand Reaction of 1,6-Enyne* ***304***: $[RhCl(CO)_2]_2$ (2 mg, 0.005 mmol) and (*S*)-*xyl-P*-Phos (7.8 mg, 0.012 mmol) were placed into a flame-dried 10 mL round-bottom flask equipped with a 10 mm stirrer bar under inert atmosphere (glove-box). The flask was removed from the glove box, equipped with an argon balloon and acetone (1 mL) was added to the mixture *via* tared syringe. The resulting solution was stirred for *ca* 2 hours and subsequently transferred *via* cannula into a 10 mL round-bottom flask containing the specified silver salt (0.012 mmol). After 30 minutes, a solution of enyne **304** (0.1 mmol, 24.5 mg) in acetone (1 mL) under Ar atmosphere was added to the catalyst solution *via* cannula and the argon balloon was promptly replaced with a CO balloon (10:1 Ar:CO, 1 atm). The reaction was stirred at RT (22 °C) for 48 hours. The reaction mixture was concentrated *in vacuo* onto silica gel. Purification *via* flash chromatography column (silica gel, eluting *via* a gradient 10-30% diethyl ether/hexane) provided **(*S*)-313** as a yellow oil.

Colour and State: yellow oil.

HPLC analysis (25 cm x 4.6 mm Agilent Chiral AS-H), 10% isopropanol/hexane at 0.8 mL/min, 230 nm, T = 30 °C; t_R (*major*) 14.0 min, t_R (*minor*) 15.8 min.

^{1}H NMR (500 MHz, $CDCl_3$) δ 3.80 (s, 3H), 3.77 (s, 3H), 3.38 (d, A of AB, J_{AB} = 19.7 Hz, 1H), 3.31 (d, B of AB, J_{AB} = 19.6 Hz, 1H), 3.16-3.10 (m, 1H), 2.84 (dd, A of ABX, J_{AB} = 12.9 Hz, J_{AX} = 7.3 Hz, 1H), 2.81 (ddd, A of ABMX, J_{AB} = 18.2 Hz, J_{AM} = 6.3 Hz, J_{AX} = 0.8 Hz, 1H), 2.25 (dd, B of ABX, J_{AB} = 18.2 Hz, J_{AX} = 2.9 Hz, 1H), 1.78 (*app.* t, J = 12.8 Hz, 1H).

^{13}C NMR (125 MHz, $CDCl_3$) δ 200.78 (e), 176.93 (e), 171.68 (e), 170.86 (e), 127.81 (e), 60.60 (e), 53.61 (o), 53.46 (o), 42.59 (o), 40.55 (e), 39.36 (e), 34.56 (e).

IR (Neat) 2956 (m), 2925 (w), 1733 (vs), 1655 (s), 1262 (s), 955 (m) cm^{-1}.

HRMS (CI, $[M+H]^+$) calcd for $C_{12}H_{14}{}^{35}ClO_5$ 273.0524, found 273.0531.

General Procedure for the Rh-catalysed Enantioselective Pauson-Khand Reaction of Chlorinated 1,6-Enynes: $[RhCl(CO)_2]_2$ (2 mg, 0.005 mmol) and *DM*-SEGPHOS (8.7 mg, 0.012 mmol) were placed into a flame-dried 10 mL round-bottom flask equipped with a 10 mm stirrer bar under inert atmosphere (glove-box). The flask was removed from the glove box, equipped with an argon balloon and acetone (2 mL) was added to the mixture *via* tared syringe. The resulting yellow clear solution was stirred for *ca* 2 hours and subsequently transferred *via* cannula into a 10 mL round-bottom flask containing silver triflate (3.2 mg, 0.012 mmol). The resulting solution was stirred for an additional 30 minutes with precipitation of silver chloride and formation of an orange solution. Then, a solution of the required enyne (0.1 mmol) in acetone (2mL) under Ar atmosphere was added to the catalyst solution *via* cannula and the argon balloon was promptly replaced with a CO balloon (10:1 Ar:CO, 1 atm). The reaction was stirred at RT (22 °C) until consumption of the starting 1,6-enyne (t.l.c. control). The reaction mixture was concentrated *in vacuo* onto silica gel. Purification *via* FCC (silica gel, eluting *via* a gradient 10-50% diethyl ether/hexane) provided the desired bicyclopentenone adduct.

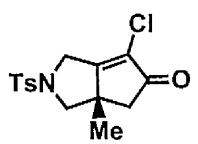

376a

(*S*)-6-Chloro-3a-methyl-2-tosyl-2,3,3a,4-tetrahydrocyclopenta[*c*]pyrrol-5(1*H*)-one.

Synthesised by the general procedure for the Rh-catalysed enantioselective Pauson-Khand reaction of chlorinated 1,6-enynes (t = 3 days, yield = 91%).

Colour and State: Pale yellow foam; *Selectivity:* 96% *ee.* $[\alpha]_D^{20}$ -6.5 (c = 0.5, CH_2Cl_2).

HPLC analysis (25 cm x 4.6 mm Agilent Chiral AS-H), 34% isopropanol/hexane at 1.0 mL/min, 230 nm, T = 22 °C; t_R (*major*) 52.6 min, t_R (*minor*) 25.2 min.

^{1}H NMR (500 MHz, $CDCl_3$) δ 7.73 (d, J = 8.1 Hz, 2H), 7.36 (d, J = 8.1 Hz, 2H), 4.34 (d, A of AB, J_{AB} = 16.8 Hz, 1H), 4.07 (d, B of AB, J_{AB} = 16.8 Hz, 1H), 3.72 (d, A of AB, J_{AB} = 9.2 Hz, 1H), 2.81 (d, B of AB, J_{AB} = 9.2 Hz, 1H), 2.53 (d, A of AB, J_{AB} = 17.8 Hz, 1H), 2.44 (s, 3H), 2.39 (d, B of AB, J_{AB} = 17.8 Hz, 1H), 1.25 (s, 3H).

^{13}C NMR (125 MHz, $CDCl_3$) δ 198.74 (e), 173.89 (e), 144.45 (e), 133.63 (e), 130.20 (o), 127.68 (e), 127.53 (o), 58.28 (e), 47.15 (e), 46.92 (e), 45.97 (e), 25.25 (o), 21.71 (o).

IR (Neat) 2923 (w), 2255 (w), 1731 (m), 1667 (m), 1348 (m), 1157 (m), 1094 (m), 910 (m).

HRMS (ESI, $[M+Na]^+$) calcd for $C_{15}H_{16}{}^{35}ClNNaO_3S$ 348.0437, found 348.0430.

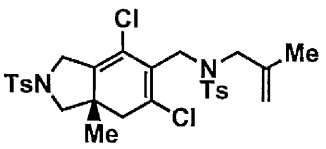

376b

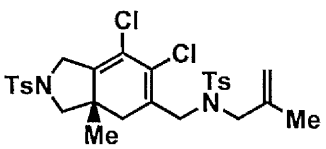

376b'

(*S*)-*N*-((4,6-Dichloro-7a-methyl-2-tosyl-2,3,7,7a-tetrahydro-1*H*-isoindol-5-yl)methyl)-4-methyl-*N*-(2-methylallyl)benzenesulfonamide 376b (Table 2.9, entry 3).

$[RhCl(CO)_2]_2$ (2 mg, 0.005 mmol) and (*S*)-*xyl*-BINAP (8.8 mg, 0.012 mmol) were placed into a flame-dried 10 mL round-bottom flask equipped with a 10 mm stirrer bar under inert atmosphere (glove-box). The flask was removed from the glove box, equipped with an argon balloon and acetone (1 mL) was added to the mixture *via* tared syringe. The resulting solution was stirred for *ca* 2 hours and subsequently transferred *via* cannula into a 10 mL round-bottom flask containing silver triflate (3.1 mg, 0.012 mmol). After 30 minutes, a solution of enyne **373** (0.1 mmol, 29.8 mg) in acetone (0.5 mL) under Ar atmosphere was added to the catalyst solution *via* cannula and the argon balloon was promptly replaced with a CO balloon (10:1 Ar:CO, 1 atm). The reaction was stirred at RT (22 °C) for 48 hours. The reaction

mixture was concentrated *in vacuo* onto silica gel. Purification *via* flash chromatography column (silica gel, eluting *via* a gradient 10-30% diethyl ether/hexane) provided a mixture of **376b** and **376b'** (**376b**:**376b'** = 9:1) as a yellow oil.

Colour and State: yellow oil. *Selectivity **376b**:* 94% *ee.* $[\alpha]_D^{20} + 60.1 (c = 0.5, CH_2Cl_2)$.

HPLC analysis (25 cm x 4.6 mm Agilent Chiral AS-H), 34% isopropanol/hexane at 1.0 mL/min, 230 nm, T = 22 °C; t_R = 50.5 min (*major*), t_R (*minor*) = 36.3 min.

^{1}H NMR (500 MHz, $CDCl_3$) δ 7.73-7.65 (m, 4H), 7.36 (d, J = 7.9 Hz, 2H), 7.31 (d, J = 7.9 Hz, 2H), 4.96 (s, 1H), 4.83 (s, 1H), 4.36 (dd, J = 13.3, 2.3 Hz, 1H), 4.21 (d, A of AB, J_{AB} = 16.0 Hz, 1H), 4.07 (d, B of AB, J_{AB} = 13.3 Hz, 1H), 3.81 (d, B of AB, J_{AB} = 16.1 Hz, 1H), 3.70 (d, A of AB, J_{AB} = 16.3 Hz, 1H), 3.65 (d, A of AB, J_{AB} = 8.7 Hz, 1H), 3.52 (d, B of AB, J_{AB} = 16.3 Hz, 1H), 2.86 (d, B of AB, J_{AB} = 8.7 Hz, 1H), 2.72 (d, A of AB, J_{AB} = 16.4 Hz, 1H), 2.56 (s, 3H), 2.55 (s, 3H), 2.43 (d, B of AB, J_{AB} = 16.7 Hz, 1H), 1.76 (s, 3H), 1.29 (s, 3H).

^{13}C NMR (125 MHz, $CDCl_3$) δ 144.20 (e), 143.69 (e), 140.79 (e), 137.81 (e), 132.53 (e), 130.03 (o), 129.79 (o), 127.90 (o), 127.80 (o), 125.67 (e), 121.08 (e), 112.48 (e), 61.91 (e), 54.13 (e), 50.23 (e), 47.52 (e), 43.73 (e), 43.61 (e), 21.75 (o), 21.71 (o), 21.47 (o), 20.35 (o).

HRMS (ESI, $[M+Na]^+$) calcd for $C_{28}H_{32}{}^{35}ClN_2NaO_4S$ 619.1078, found 619.1075.

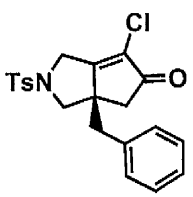

388

((*S*)-3a-Benzyl-6-chloro-2-tosyl-2,3,3a,4-tetrahydrocyclopenta[*c*]pyrrol-5(1*H*)-one.

Synthesised by the general procedure for the Rh-catalysed enantioselective Pauson-Khand reaction of chlorinated 1,6-enynes (t = 3 days, yield = 93%).

Colour and State: white crystalline solid; mp = 131-133 °C. *Selectivity:* 97% *ee.*

$[\alpha]_D^{20}$ -46.7 (c = 0.3, CH_2Cl_2).

HPLC analysis (25 cm x 4.6 mm Agilent Chiral AD-H), 15% isopropanol/hexane at 1.0 mL/min, 230 nm, T = 25 °C; t_R (*major*): 29.2 min, t_R (*minor*) min. 46.6.

^{1}H NMR (500 MHz, $CDCl_3$) δ 7.75 (d, J = 8.3 Hz, 2H), 7.37 (d, J = 8.0 Hz, 2H), 7.38-7.23 (m, 3H), 7.05-7.01 (m, 2H), 4.47 (d, A of AB, J_{AB} = 16.9 Hz, 1H), 4.08 (d, B of AB, J_{AB} = 16.9 Hz, 1H), 3.96 (d, A of AB, J_{AB} = 9.4 Hz, 1H), 2.98 (d, A of AB, J_{AB} = 13.6 Hz, 1H), 2.76 (d, A of AB, J_{AB} = 17.8 Hz, 1H), 2.72 (d, B of AB, J_{AB} = 9.2 Hz, 1H), 2.70 (d, B of AB, J_{AB} = 13.3 Hz, 1H), 2.45 (s, 3H), 2.14 (d, B of AB, J_{AB} = 17.8 Hz, 1H).

^{13}C NMR (125 MHz, $CDCl_3$) δ 198.00 (e), 171.80 (e), 144.54 (e), 135.40 (e), 133.52 (e), 133.49 (e), 130.26 (o), 129.15 (o), 128.82 (o), 127.63 (o), 127.59 (o), 56.37 (e), 51.81 (e), 46.37 (e), 44.30 (e), 42.48 (e), 21.74 (o).

IR (Neat) 3029 (w), 2924 (w), 1731 (m), 1667 (w), 1346 (m), 1164 (m), 1093 (m), 669 (m).

HRMS (ESI, $[M+Na]^+$) calcd for $C_{21}H_{20}{}^{35}ClNNaO_3S$ 424.0750, found 424.0751.

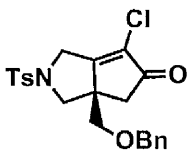

389

(*R*)-3a-(Benzyloxymethyl)-6-chloro-2-tosyl-2,3,3a,4-tetrahydrocyclopenta[*c*]pyrrol-5(1*H*)-one.

Synthesised by the general procedure for the Rh-catalysed enantioselective Pauson-Khand reaction of chlorinated 1,6-enynes (t = 3 days, yield = 91%).

Colour and State: yellow oil. *Selectivity:* 88% *ee.* $[\alpha]_D^{20}$ -19.1 (c = 0.4, CH_2Cl_2).

HPLC analysis (25 cm x 4.6 mm Agilent Chiral AD-H), 10% isopropanol/hexane at 1.0 mL/min, 230 nm, T = 22 °C; t_R (*major*): 28.3 min, t_R (*minor*) min. 38.5.

^{1}H NMR (500 MHz, $CDCl_3$) δ 7.70 (d, J = 8.2 Hz, 2H), 7.38-7.25 (m, 5H), 7.23-7.15 (m, 2H), 4.39 (d, A of AB, J_{AB} = 12.2 Hz, 1H), 4.33 (d, B of AB, J_{AB} = 12.2 Hz, 1H), 4.15 (d, A of AB, J_{AB} = 16.7 Hz, 1H), 4.07 (d, B of AB, J_{AB} = 16.7 Hz, 1H), 3.86 (d, A of AB, J_{AB} = 9.8 Hz, 1H), 3.34 (d, A of AB, J_{AB} = 9.0 Hz, 1H), 3.11 (d, B of AB, J_{AB} = 9.0 Hz, 1H), 2.85 (d, B of AB, J_{AB} = 9.8 Hz, 1H), 2.71 (d, A of AB, J_{AB} = 17.6 Hz, 1H), 2.43 (s, 3H), 2.23 (d, B of AB, J_{AB} = 17.6 Hz, 1H).

^{13}C NMR (125 MHz, $CDCl_3$) δ 198.39 (e), 168.71 (e), 144.29 (e), 137.15 (e), 133.53 (e), 130.09 (o) (e), 129.52 (e), 128.57 (o), 128.03 (o), 127.64 (o), 127.41 (o), 73.39 (e), 71.63 (e), 54.19 (e), 51.86 (e), 46.16 (e), 43.91 (e), 21.60 (o).

IR (Neat) 3029 (w), 2924 (w), 1731 (m), 1667 (w), 1346 (m), 1164 (m), 1093 (m), 669 (m).

HRMS (ESI, $[M+Na]^+$) calcd for $C_{22}H_{22}{}^{35}ClNNaO_4S$ 454.0856, found 454.0837.

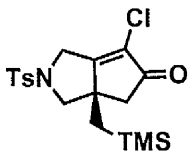

390

(*R*)-6-Chloro-2-tosyl-3a-((trimethylsilyl)methyl)-2,3,3a,4-tetrahydrocyclopenta[*c*]pyrrol-5(1*H*)-one.

Synthesised by the general procedure for the Rh-catalysed enantioselective Pauson-Khand reaction of chlorinated 1,6-enynes (t = 3 days, yield = 86%).

Colour and State: transparent oil; *Selectivity:* 96% *ee*. $[\alpha]_D^{20}$ -13.0 (c = 0.5, CH_2Cl_2).

HPLC analysis (25 cm x 4.6 mm Agilent Chiral AS-H), 34% isopropanol/hexane at 1.0 mL/min, 230 nm, T = 22 °C; t_R (*major*) 21.0 min, t_R (*minor*) 14.7 min.

^{1}H NMR (500 MHz, $CDCl_3$) δ 7.73 (d, J = 8.3 Hz, 2H), 7.36 (d, J = 8.0 Hz, 2H), 4.31 (d, A of AB, J_{AB} = 16.6 Hz, 1H), 4.02 (d, B of AB, J_{AB} = 16.6 Hz, 1H), 3.76 (d, A of AB, J_{AB} = 9.1 Hz, 1H), 2.71 (d, B of ABX, J_{AB} = 9.1, 0.8 Hz, 1H), 2.56 (d, A of AB, J_{AB} = 18.0 Hz, 1H),

2.44 (s, 3H), 2.35 (d, B of AB, J_{AB} = 18.0 Hz, 1H), 1.17 (d, A of AB, J_{AB} = 14.8 Hz, 1H), 0.76 (d, B of AB, J_{AB} = 14.8 Hz, 1H), 0.01 (s, 9H).

^{13}C NMR (125 MHz, $CDCl_3$) δ 198.89 (e), 175.37 (e), 144.45 (e), 133.61 (e), 130.21 (o), 127.56 (e), 127.40 (o), 59.27 (e), 49.41 (e), 46.38 (e), 46.06 (e), 16.64 (e), 26.64 (o), 21.71 (o).

IR (Neat) 2953 (w), 1731 (m), 1667 (m), 1349 (m), 1163 (m), 1093 (m), 845 (m).

HRMS (ESI, $[M+Na]^+$) calcd for $C_{18}H_{24}{}^{35}ClNNaO_3SSi$ 420.0832, found 408.0833.

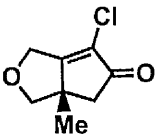

391

(*S*)-6-Chloro-3a-methyl-3a,4-dihydro-1*H*-cyclopenta[*c*]furan-5(3*H*)-one.

Synthesised by the general procedure for the Rh-catalysed enantioselective Pauson-Khand reaction of chlorinated 1,6-enynes (t = 2 days, yield = 82%).

Colour and State: pale yellow oil; *Selectivity:* 96% *ee*. $[\alpha]_D^{20}$ -15.0 (c = 0.5, CH_2Cl_2).

HPLC analysis (25 cm x 4.6 mm Agilent Chiral OJ-H), 15% isopropanol/hexane at 0.9 mL/min, 230 nm, T = 30 °C; t_R (*major*) 30.0 min, t_R (*minor*) 27.1 min.

^{1}H NMR (500 MHz, $CDCl_3$) δ 4.71 (d, A of AB, J_{AB} = 16.6 Hz, 1H), 4.59 (d, B of AB, J_{AB} = 16.6 Hz, 1H), 4.01 (d, A of AB, J_{AB} = 8.2 Hz, 1H), 3.46 (d, B of AB, J_{AB} = 8.2 Hz, 1H), 2.57 (d, A of AB, J_{AB} = 17.6 Hz, 1H), 2.48 (d, B of AB, J_{AB} = 17.6 Hz, 1H), 1.36 (s, 3H).

^{13}C NMR (125 MHz, $CDCl_3$) δ 200.15 (e), 178.86 (e), 126.22 (e), 77.16 (e), 64.23 (e), 48.53 (e), 46.23 (e), 24.69 (o).

IR (Neat) 2928 (w), 2857 (w), 1727 (m), 1662 (m), 1449 (w), 1206 (m), 1024 (m), 890 (m).

HRMS (CI, $[M+H]^+$) calcd for $C_8H_{10}{}^{35}ClO_2$ 173.0364, found 173.0365.

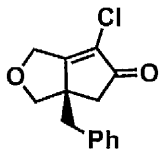

392

(*S*)-3a-Benzyl-6-chloro-3a,4-dihydro-1*H*-cyclopenta[*c*]furan-5(3*H*)-one.

Synthesised by the general procedure for the Rh-catalysed enantioselective Pauson-Khand reaction of chlorinated 1,6-enynes (t = 2 days, yield = 86%).

Colour and State: pale yellow oil; *Selectivity:* ≥99% *ee.* $[\alpha]_D^{20}$ -88.0 (c = 0.5, CH_2Cl_2).

HPLC analysis (25 cm x 4.6 mm Agilent Chiral AD-H), 10% isopropanol/hexane at 0.5 mL/min, 230 nm, T = 22 °C; t_R (*major*) 15.7 min, t_R (*minor*) 18.1 min.

^{1}H NMR (500 MHz, $CDCl_3$) δ 7.32-7.23 (m, 3H), 7.09-7.05 (m, 2H), 4.78 (d, A of AB, J_{AB} = 16.6 Hz, 1H), 4.65 (d, B of AB, J_{AB} = 16.6 Hz, 1H), 4.24 (d, A of AB, J_{AB} = 8.6 Hz, 1H), 3.47 (d, B of AB, J_{AB} = 8.6 Hz, 1H), 2.98 (d, A of AB, J_{AB} = 13.6 Hz, 1H), 2.84 (d, B of AB, J_{AB} = 13.6 Hz, 1H), 2.78 (d, A of AB, J_{AB} = 17.6 Hz, 1H), 2.26 (d, B of AB, J_{AB} = 17.6 Hz, 1H).

^{13}C NMR (125 MHz, $CDCl_3$) δ 199.36 (e), 176.47 (e), 136.00 (e), 130.27 (o), 128.70 (o), 127.52 (e), 127.45 (o), 75.64 (e), 64.69 (e), 53.16 (e), 43.72 (e), 42.24 (e).

IR (Neat) 2921 (w), 2855 (w), 1729 (m), 1662 (m), 1454 (w), 1039 (m), 958 (m), 705 (m).

HRMS (ESI, $[M+Na]^+$) calcd for $C_{14}H_{13}{}^{35}ClNaO_2$ 271.0502, found 271.0503.

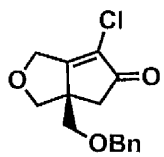

393

(*S*)-3a-(Benzyloxymethyl)-6-chloro-3a,4-dihydro-1*H*-cyclopenta[*c*]furan-5(3*H*)-one.

Synthesised by the general procedure for the Rh-catalysed enantioselective Pauson-Khand reaction of chlorinated 1,6-enynes (t = 2 days, yield = 83%).

Colour and State: pale yellow oil; *Selectivity:* 92% *ee.* $[\alpha]_D^{20}$ -11.2 (c = 0.5, CH_2Cl_2).

HPLC analysis (25 cm x 4.6 mm Agilent Chiral AD-H), 10% isopropanol/hexane at 0.7 mL/min, 230 nm, T = 22 °C; t_R (*major*) 12.7 min, t_R (*minor*) 14.1 min.

^{1}H NMR (500 MHz, $CDCl_3$) δ 7.37-7.23 (m, 5H), 4.58 (d, A of AB, J_{AB} = 16.6 Hz, 1H), 4.54 (d, B of AB, J_{AB} = 16.9 Hz, 1H), 4.53 (d, A of AB, J_{AB} = 12.2 Hz, 1H), 4.48 (d, B of AB, J_{AB} = 12.1 Hz, 1H), 4.19 (d, A of AB, J_{AB} = 8.7 Hz, 1H), 3.58 (d, A of AB, J_{AB} = 8.9 Hz, 1H), 3.47 (d, B of AB, J_{AB} = 8.7 Hz, 1H), 3.31 (d, B of AB, J_{AB} = 8.9 Hz, 1H), 2.81 (d, A of AB, J_{AB} = 17.5 Hz, 1H), 2.34 (d, B of AB, J_{AB} = 17.5 Hz, 1H).

^{13}C NMR (125 MHz, $CDCl_3$) δ 199.91 (e), 173.70 (e), 137.51 (e), 128.69 (o), 128.32 (e), 128.13 (o), 127.88 (o), 73.65 (e), 73.60 (e), 71.16 (e), 64.60 (e), 53.59 (e), 43.34 (e).

IR (Neat) 2857 (w), 1730 (m), 1662 (m), 1454 (w), 1237 (w), 1095 (m), 1025 (m), 739 (m).

HRMS (ESI, $[M+Na]^+$) calcd for $C_{15}H_{15}{}^{35}ClNaO_3$ 301.0607, found 301.0608.

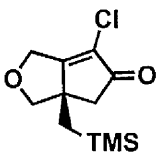

394

(*R*)-6-chloro-3a-((trimethylsilyl)methyl)-3a,4-dihydro-1*H*-cyclopenta[*c*]furan-5(3*H*)-one. Synthesised by the general procedure for the Rh-catalysed enantioselective Pauson-Khand reaction of chlorinated 1,6-enynes (t = 2 days, yield = 81%).

Colour and State: transparent oil; *Selectivity:* 98% *ee.* $[\alpha]_D^{20}$ +4.9 (c = 0.3, CH_2Cl_2).

HPLC analysis (25 cm x 4.6 mm Agilent Chiral AS-H), 10% isopropanol/hexane at 1.0 mL/min, 230 nm, T = 22 °C; t_R (*major*) 17.4 min, t_R (*minor*) 19.6 min.

^{1}H NMR (500 MHz, $CDCl_3$) δ 4.68 (d, A of AB, J_{AB} = 16.4 Hz, 1H), 4.56 (d, B of AB, J_{AB} = 16.4 Hz, 1H), 4.05 (d, A of AB, J_{AB} = 8.2 Hz, 1H), 3.38 (d, B of ABX, J_{AB} = 8.2 Hz, J_{BX} = 1.3 Hz, 1H), 2.60 (d, A of AB, J_{AB} = 17.8 Hz, 1H), 2.44 (d, B of AB, J_{AB} = 17.8 Hz, 1H), 1.26 (d, A of AB, J_{AB} = 14.9 Hz, 1H), 0.9 (d, B of ABX, J_{AB} = 1.2 Hz, J_{BX} = 1.2 Hz, 1H), 0.05 (s, 9H).

^{13}C NMR (125 MHz, $CDCl_3$) δ 200.25 (e), 180.30 (e), 126.11 (e), 76.91 (e), 64.31 (e), 50.77 (e), 45.80 (e), 26.22 (e), 0.16 (o).

IR (Neat) 2954 (w), 1728 (s), 1661 (m), 1451 (w), 1250 (m), 955 (m), 839 (s).

HRMS (ESI, $[M+Na]^+$) calcd for $C_{11}H_{17}{}^{35}ClNaO_2Si$ 267.0584, found 267.0577.

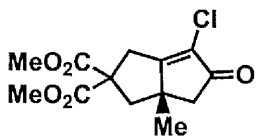

395

(*S*)-Dimethyl 6-chloro-3a-methyl-5-oxo-3,3a,4,5-tetrahydropentalene-2,2(1*H*)-dicarboxylate.

Synthesised by the general procedure for the Rh-catalysed enantioselective Pauson-Khand reaction of chlorinated 1,6-enynes (t = 3 days, yield = 74%).

Colour and State: pale yellow oil; *Selectivity:* 92% *ee*. $[\alpha]_D^{20}$ -82.82 (c = 0.5, CH_2Cl_2).

HPLC analysis (25 cm x 4.6 mm Agilent Chiral AS-H), 15% isopropanol/hexane at 0.9 mL/min, 230 nm, T = 30 °C; t_R (*major*) 25.2 min, t_R (*minor*) 15.7 min.

^{1}H NMR (500 MHz, $CDCl_3$) δ 3.82 (s, 3H), 3.75 (s, 3H), 3.55 (d, A of AB, J_{AB} = 18.3 Hz, 1H), 3.30 (d, B of AB, J_{AB} = 18.3 Hz, 1H), 2.65 (d, A of AB, J_{AB} = 13.7 Hz, 1H), 2.55 (d, A of AB, J_{AB} = 17.7 Hz, 1H), 2.48 (d, B of AB, J_{AB} = 17.7 Hz, 1H), 2.27 (d, B of AB, J_{AB} = 13.8 Hz, 1H), 1.18 (s, 3H).

^{13}C NMR (125 MHz, $CDCl_3$) δ 200.49 (e), 179.79 (e), 171.91 (e), 171.48 (e), 126.87 (e), 60.01 (e), 53.65 (o), 53.63 (o), 50.19 (e), 47.96 (e), 45.01 (e), 33.62 (e), 26.78 (o).

IR (Neat) 2956 (w), 1731 (m), 1655 (m), 1435 (w), 1261 (m), 1167 (m), 1065 (w), 955 (w).

HRMS (ESI, $[M+Na]^+$) calcd for $C_{13}H_{15}{}^{35}ClNaO_5$ 309.0506, found 309.0506.

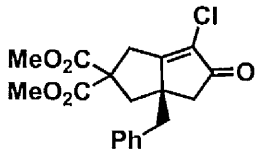

396

(*S*)-dimethyl 3a-benzyl-6-chloro-5-oxo-3,3a,4,5-tetrahydropentalene-2,2(1H)-dicarboxylate.

Synthesised by the general procedure for the Rh-catalysed enantioselective Pauson-Khand reaction of chlorinated 1,6-enynes (t = 3 days, yield = 81%).

Colour and State: pale yellow oil; *Selectivity:* 97% *ee.* $[\alpha]_D^{20}$ -129.4 (c = 0.5, CH_2Cl_2)

HPLC analysis (25 cm x 4.6 mm Agilent Chiral AS-H), 10% isopropanol/hexane at 0.9 mL/min, 230 nm, T = 22 °C; t_R (*major*) 27.2 min, t_R (*minor*) 31.1 min.

^{1}H NMR (500 MHz, $CDCl_3$) δ 7.30-7.20 (m, 3H), 7.03-6.90 (m, 2H), 3.85 (s, 3H), 3.76 (s, 3H), 3.61 (d, A of AB, J_{AB} = 18. Hz, 1H), 3.37 (d, B of AB, J_{AB} = 18.1 Hz, 1H), 2.85 (d, A of AB, J_{AB} = 14.1 Hz, 1H), 2.79 (d, A of AB, J_{AB} = 17.7 Hz, 1H), 2.78 (d, A of AB, J_{AB} = 13.7 Hz, 1H), 2.67 (d, B of AB, J_{AB} = 13.7 Hz, 1H), 2.33 (d, B of AB, J_{AB} = 14.2 Hz, 1H), 2.28 (d, B of AB, J_{AB} = 17.7 Hz, 1H).

^{13}C NMR (125 MHz, $CDCl_3$) δ 199.61 (e), 177.07 (e), 171.97 (e), 171.46 (e), 135.91 (e), 130.24 (o), 128.58 (o), 128.27 (e), 127.38 (o), 60.02 (e), 53.71 (o), 53.68 (e), 52.32 (e), 47.44 (e), 43.89 (e), 43.47 (e), 34.01 (e).

IR (Neat) 2954 (w), 1727 (s), 1655 (m), 1435 (m), 1259 (m), 1165 (m), 957 (m), 705 (m).

HRMS (ESI, $[M+Na]^+$) calcd for $C_{19}H_{19}{}^{35}ClNaO_5$ 385.0819, found 385.0813.

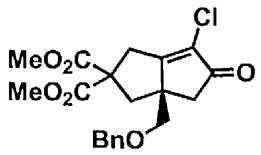

397

(*R*)-dimethyl 3a-(benzyloxymethyl)-6-chloro-5-oxo-3,3a,4,5-tetrahydropentalene-2,2(1*H*)-dicarboxylate.

Synthesised by the general procedure for the Rh-catalysed enantioselective Pauson-Khand reaction of chlorinated 1,6-enynes (t = 3 days, yield = 79%).

Colour and State: bright yellow oil. *Selectivity:* 86% *ee.* $[\alpha]_D^{20}$ -67.25 (c = 0.5, CH_2Cl_2).

HPLC analysis (25 cm x 4.6 mm Agilent Chiral AS-H), 10% isopropanol/hexane at 1.0 mL/min, 230 nm, T = 22 °C; t_R (*major*) 25.6 min, t_R (*minor*) 42.7 min.

^{1}H NMR (500 MHz, $CDCl_3$) δ 7.37-7.20 (m, 5H), 4.45 (d, A of AB, J_{AB} = 12.2 Hz, 1H), 4.41 (d, B of AB, J_{AB} = 12.2 Hz, 1H), 3.73 (s, 3H), 3.69 (s, 3H), 3.37 (d, A of AB, J_{AB} = 17.9 Hz, 1H), 3.29 (d, A of AB, J_{AB} = 9.0 Hz, 1H), 3.28 (d, B of AB, J_{AB} = 18.0 Hz, 1H), 3.27 (d, B of AB, J_{AB} = 9.1 Hz, 1H), 2.77 (d, A of AB, J_{AB} = 14.2 Hz, 1H), 2.67 (d, A of AB, J_{AB} = 17.4 Hz, 1H), 2.36 (d, B of AB, J_{AB} = 17.4 Hz, 1H), 2.27 (d, B of AB, J_{AB} = 14.2 Hz, 1H.

^{13}C NMR (125 MHz, $CDCl_3$) δ 200.03 (e), 175.83 (e), 171.72 (e), 171.46 (e), 137.42 (e), 128.61 (e), 128.51 (o), 128.05 (e), 127.89 (e), 74.42 (e), 73.51 (e), 60.42 (e), 53.58 (o), 53.40 (o), 52.36 (e), 46.83 (e), 40.98 (e), 34.65 (e).

IR (Neat) 2954 (w), 1727 (s), 1655 (m), 1454 (w), 1435 (m), 1256 (m), 1166 (m), 1091 (m), 960 (m).

HRMS (ESI, $[M+Na]^+$) calcd for $C_{20}H_{21}{}^{35}ClNaO_6$ 415.0924, found 415.0924.

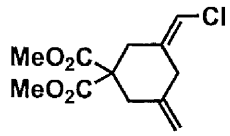

398

(*E*)-Dimethyl 3-(chloromethylene)-5-methylenecyclohexane-1,1-dicarboxylate.

Synthesised by the general procedure for the Rh-catalysed enantioselective Pauson-Khand reaction of chlorinated 1,6-enynes (t = 24 h, yield = 87%).

^{1}H NMR (500 MHz, $CDCl_3$) δ 5.90 (s, 1H), 4.88 (s, 1H), 4.84 (d, J = 0.8 Hz, 1H), 3.71 (s, 6H), 3.03 (d, J = 1.0 Hz, 2H), 2.78 (s, 2H), 2.75 (s, 2H).

^{13}C NMR (125 MHz, $CDCl_3$) δ 170.64 (e), 140.52 (e), 135.52 (e), 113.03 (e), 112.77 (o), 56.78 (e), 52.92 (o), 39.65 (e), 38.01 (e), 36.37 (e).

IR (Neat) 3079 (w), 2955 (w), 1733 (s), 1655 (m), 1433 (m), 1243 (m), 894 (m).

HRMS (ESI, $[M+Na]^+$) calcd for $C_{12}H_{15}{}^{35}ClNaO_4$ 281.0557, found 281.0558.

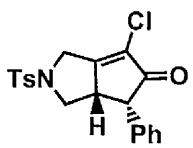

(*S*,*S*)-409

(3a*S*,4*S*)-6-Chloro-4-phenyl-2-tosyl-2,3,3a,4-tetrahydrocyclopenta[*c*]pyrrol-5(1*H*)-one.

Synthesised by the general procedure for the Rh-catalysed enantioselective Pauson-Khand reaction of chlorinated 1,6-enynes (t = 3 days, yield = 72%).

Colour and State: pale yellow oil; *Selectivity: dr* = 24:1, 99% *ee*. $[\alpha]_D^{20}$ - 26.9 (c = 0.25, CH_2Cl_2).

HPLC analysis (25 cm x 4.6 mm Agilent Chiral AD-H), 10% isopropanol/hexane at 1 mL/min, 230 nm, T = 22 °C; t_R (*major*) 48.8 min, t_R (*minor*) 31.8 min.

^{1}H NMR δ (500 MHz, $CDCl_3$) 7.62 (d, J = 8.30 Hz, 2H), 7.38-7.20 (m, 5H), 6.84-6.78 (m, 2H), 4.36 (d, A of AB, J_{AB} = 17.4 Hz, 1H), 4.14 (d, B of AB, J_{AB} = 17.5 Hz, 1H), 4.05 (d, J = 6.7 Hz, 1H), 3.55-3.47 (m, 2H), 2.45 (s, 3H), 2.35-2.27 (m, 1H).

^{1}H NMR δ (500 MHz, CD_3CN) 7.63 (d, J = 8.3 Hz, 2H), 7.47-7.24 (m, 5H), 6.90-6.83 (m, 2H), 4.41 (ddd, J = 17.5, 1.5, 0.9 Hz, 1H), 4.21 (dd, J = 17.5, 1.6 Hz, 1H), 4.1 (d, J = 7.0 Hz, 1H), 3.63-3.55 (m, 1H), 3.47 (*app* t, J = 9.2 Hz, 1H), 2.46 (s, 3H), 2.26 (dd, J = 11.2, 9.7 Hz, 1H).

^{13}C NMR (125 MHz, $CDCl_3$) δ 200.25 (e), 170.98 (e), 144.42 (e), 135.20 (e), 133.48 (e), 130.16 (o), 129.22 (o), 128.57 (e), 128.23 (o), 128.05 (o), 127.55 (o), 53.16 (o), 49.08 (e), 47.69 (e), 46.84 (o), 21.74 (o).

IR (Neat) 3030 (w), 2924 (w), 1727 (m), 1655 (m), 1497 (w), 1343 (m), 1158 (s), 1090 (m), 953 (m).

HRMS (ESI, $[M+Na]^+$) calcd for $C_{20}H_{18}{}^{35}ClNNaO_3S$ 410.0594, found 410.0594.

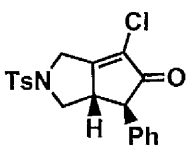

(*S*,*R*)-405

(3a*S*,4*R*)-6-Chloro-4-phenyl-2-tosyl-2,3,3a,4-tetrahydrocyclopenta[*c*]pyrrol-5(1*H*)-one. **(*S*,*S*)-409** (19.4 mg, 0.05 mmol) was placed into a flame-dried 10 mL round-bottom flask equipped with a 10 mm stirrer bar and silica gel (1 g) was added. The resulting solid mixture was stirred in a preheated bath at 45 °C for *ca.* 24 hrs. Then, the bath was removed and the solid mixture was allowed to cool at room temperature. DCM (4 mL) was added into the flask, the resulting suspension was stirred for *ca* 5 minutes. The suspension was then passed through a glass pipette equipped with cotton plug, and the residual silica gel was further washed with DCM (2 x 3 mL). Removal of the solvent *in vacuo* afforded **(*S*,*R*)-405** as a pale yellow oil (18.1 mg, 93%).

Colour and State: pale yellow oil; *Selectivity: dr* = 12:1, 99% *ee.* $[\alpha]_D^{20}$ -16.2 (c = 0.2, CH_2Cl_2).

HPLC analysis (25 cm x 4.6 mm Agilent Chiral AD-H), 10% isopropanol/hexane at 1 mL/min, 230 nm, T = 22 °C; t_R (*major*) 40.0 min, t_R (*minor*) 71.8 min.

^{1}H NMR δ (500 MHz, $CDCl_3$) 7.75 (d, J = 8.20 Hz, 2H), 7.40-7.25 (m, 5H), 7.11 (d, J = 7.0 Hz, 2H), 4.42 (dd, A of ABX, J_{AB} = 17.5, J_{AX} = 0.9 Hz, 1H), 4.16-4.11 (m, 2H), 3.40-3.32 (m, 2H), 2.80 (*app* t, J = 9.9 Hz, 1H), 2.45 (s, 3H).

^{1}H NMR δ (500 MHz, CD_3CN) 7.78 (d, J = 8.3 Hz, 2H), 7.48-7.30 (m, 5H), 7.18-7.15 (m, 2H), 4.43 (dd, J = 17.5, 1.0 Hz, 1H), 4.13 (d, J = 17.4, 1H), 4.03 (dd, J = 9.2, 8.4 Hz, 1H), 3.49 (d, J = 3.7 Hz, 1H), 3.38-3.30 (m, 1H), 2.93 (dd, J = 10.7, 9.7 Hz, 1H), 2.46 (s, 3H).

^{13}C NMR (125 MHz, $CDCl_3$) δ 198.82 (e), 168.79 (e), 144.60 (e), 135.87 (e), 133.36 (e), 130.28 (o), 129.21 (o), 128.18 (o), 128.08 (o), 127.68 (o), 127.55 (e), 57.05 (o), 52.51 (e), 50.51 (o), 47.27 (e), 21.74 (o).

IR (Neat) 3030 (w), 2925 (w), 1731 (m), 1667 (m), 1597 (w), 1347 (m), 1162 (s), 1093 (m), 953 (m).

HRMS (ESI, $[M+Na]^+$) calcd for $C_{20}H_{18}{}^{35}ClNNaO_3S$ 410.0594, found 410.0591.

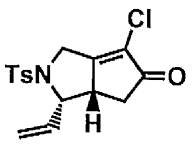

(*S*,*S*)-427

(3*S*,3a*S*)-6-Chloro-2-tosyl-3-vinyl-2,3,3a,4-tetrahydrocyclopenta[*c*]pyrrol-5(1*H*)-one.

$[RhCl(CO)_2]_2$ (2 mg, 0.005 mmol) and (*S*)-SPIROP (6.3 mg, 0.012 mmol) were placed into a flame-dried 10 mL round-bottom flask equipped with a 10 mm stirrer bar under inert atmosphere (glove-box). The flask was removed from the glove box, equipped with an argon balloon and DCE (1 mL) was added to the mixture *via* tared syringe. The resulting solution was stirred for *ca* 2 hours and subsequently transferred *via* cannula into a 10 mL round-

bottom flask containing AgOTf (3.1 mg, 0.012 mmol). After 30 minutes, a solution of enyne **426** (0.1 mmol, 31 mg) in DCE (1 mL) under Ar atmosphere was added to the catalyst solution *via* cannula and the argon balloon was promptly replaced with a CO balloon (10:1 Ar:CO, 1 atm). The reaction was stirred at 22 °C for 3 days. The reaction mixture was concentrated *in vacuo* onto silica gel. Purification *via* flash chromatography column (silica gel, eluting *via* a gradient 10-40% diethyl ether/hexane) provided **(*S*,*S*)-427** as a pale yellow oil (25 mg, 75%).

Colour and State: pale yellow oil; *Selectivity: dr* = 99:1, 90% *ee*. $[\alpha]_D^{20}$ 28.6 (c = 0.25, CH_2Cl_2).

HPLC analysis (25 cm x 4.6 mm Agilent Chiral AD-H), 10% isopropanol/hexane at 1 mL/min, 230 nm, T = 22 °C; t_R (*major*) 40.0 min, t_R (*minor*) 41.8 min.

^{1}H NMR δ (500 MHz, $CDCl_3$) 7.75 (d, J = 8.3 Hz, 2H), 7.33 (d, J = 8.1 Hz, 2H), 5.35-5.22 (m, 3H), 4.76-4.70 (m, 1H), 4.37 (dd, *J* = 17.0. 0.6 Hz, 1H), 4.22 (d, A of AB, *J* =17.0 Hz, 1H), 3.19 (dddd, *J* = 9.8, 6.6, 3.3, 1.8 Hz, 1H), 2.59 (ddd, *J* = 18.7, 6.6, 0.7 Hz, 1H), 2.43 (s, 3H), 2.26 (dd, A of ABX, *J* = 18.6, 3.0 Hz, 1H).

^{13}C NMR (125 MHz, $CDCl_3$) δ 199.57 (e), 170.02 (e), 144.26 (e), 135.72 (e), 130.83 (o), 130.04 (o), 128.76 (e), 127.55 (o), 121.04 (e), 63.43 (o), 46.23 (e), 45.46 (o), 35.99 (e), 21.72 (o).

IR (Neat) 2927 (w), 1732 (m), 1669 (m), 1598 (w), 1346 (m), 1159 (s), 1093 (m), 815 (m).

HRMS (ESI, $[M+Na]^+$) calcd for $C_{16}H_{16}{}^{35}ClNNaO_3S$ 360.0437, found 360.0421.

2.5. References.

182. Knowles, W. S.; Sabacky, M. J. *Chem. Commun.* **1968**, 1445.

183. Horner, L.; Siegel, H.; Buthe, H. *Angew. Chem. Int. Ed.* **1968**, *7*, 942.

184. For recent reviews on chiral phosphine ligands, see: a) Tang, W.; Zhang, X. *Chem. Rev.* **2003**, *103*, 3029; b) Gridnev, I. D.; Imamoto, T. *Acc. Chem. Res.* **2004**, *37*, 633; c)

Cui, X.; Burgess, K. *Chem. Rev.* **2005**, *105*, 3272. d) Knowles, W. S.; Noyori, R. *Acc. Chem. Res.* **2007**, *40*, 1238. e) Minnaard, A. J.; Feringa, B. L.; Lefort, L.; de Vries, J. G. *Acc. Chem. Res.* **2007**, *40*, 1267; f) Zhang, W.; Chi, Y.; Zhang, X. *Acc. Chem. Res.* **2007**, *40*, 1278.

185. Kagan, H. B.; Dang, T.-P. *J. Am. Chem. Soc.* **1972**, *94*, 6429.

186. a) Vineyard, B. D.; Knowles, W. S.; Sabacky, M. J.; Bachman, G. L.; Weinkauff, O. J. *J. Am. Chem. Soc.* **1977**, *99*, 5946; b) Knowles, W. S. *Acc. Chem. Res.* **1983**, *16*, 106; c) Knowles, W. S. *Angew. Chem. Int. Ed.* **2002**, *41*, 1998.

187. a) Miyashita, A.; Yasuda, A.; Takaya, H.; Toriumi, K.; Ito. T.; Souchi, T.; Noyori, R. *J. Am. Chem. Soc.* **1980**, *102*, 7932; b) Miyashita, A.; Takaya, H.; Souchi, T.; Noyori, R. *Tetrahedron* **1984**, *40*, 1245; c) Noyori, R.; Ohta, M.; Hsiao, Y.; Kitamura, M.; Ohta, T.; Takaya, H. *J. Am. Chem. Soc.* **1986**, *108*, 7117; d) Noyori, R.; Ohkuma, T.; Kitamura, M.; Takaya, H.; Sayo, N.; Kumobayashi, H.; Akutagawa, S. *J. Am. Chem. Soc.* **1987**, *109*, 5856; e) Ohkuma, T.; Ooka, H.; Ikariya, T.; Noyori, R. *J. Am. Chem. Soc.* **1995**, *117*, 10417.

188. Jeulin, S.; Duprat de Paule, S.; Ratovelomanana-Vidal, V.; Genet, J.-P.; Champion, N.; Dellis, P. *Proc. Natl. Acad. Sci. U.S.A.* **2004**, *101*, 5799.

189. a) Burk, M. J. *J. Am. Chem. Soc.* **1991**, *113*, 8518; b) Burk, M. J.; Feaster, J. E.; Nugent, W. A.; Harlow, R. L. *J. Am. Chem. Soc.* **1993**, *115*, 10125; c) Burk, M. *Acc. Chem. Res.* **2000**, *33*, 363.

190. a) Togni, A.; Breutel, C.; Schnyder, A.; Spindler, F.; Landert, H.; Tijani, A. *J. Am. Chem. Soc.* **1994**, *116*, 4062; b) Blaser, H.-U.; Brieden, W.; Pugin, B.; Spindler, F.; Studer, M.; Togni, A. *Top. Catal.* **2002**, *19*, 3.

191. McGarrity, J.; Spindler, F.; Fuchs, R.; Eyer, M. (LONZA AG), EP-A 624587 A2, **1995**; *Chem. Abstr.* **1995**, *122*, P81369q.

192. a) Blaser, H.-U. *Adv. Synth. Catal.* **2002**, *344*, 17; b) Blaser, H.-U.; Buser, H.-P.; Coers, K.; Hanreich, R.; Jalett, H.-P.; c) Jelsch, E.; Pugin, B.; Schneider, H.-D.; Spindler, F.; Wegmann, A. *Chimia* **1999**, *53*, 275.

193. a) Claver, C.; Fernandez, E.; Gillon, A.; Heslop, K.; Hyett, D. J.; Martorell, A.; Orpen, A. G.; Pringle, P. G. *Chem. Commun.* **2000**, 961; b) Reetz, M. T.; Mehler, G. *Angew. Chem., Int. Ed.* **2000**, *39*, 3889; c) van den Berg, M.; Minnaard, A. J.; Schudde, E. P.; van Esch, J.; de Vries, A. H. M.; de Vries, J. G.; Feringa, B. L. *J. Am. Chem. Soc.* **2000**, *122*, 11539.

194. a) Berk, S. C.; Grossman, R. B.; Buchwald, S. L. *J. Am. Chem. Soc.* **1994**, *116*, 8593; b) Hicks, F. A.; Berk, S. C.; Buchwald, S. L. *J. Am. Chem. Soc.* **1996**, *118*, 9450; c) Hicks, F. A.; Kablaoui, N. M.; Buchwald, S. L. *J. Am. Chem. Soc.* **1999**, *121*, 5881.

195. a) Hicks, F. A.; Buchwald, S. L. *J. Am. Chem. Soc.* **1996**, *118*, 11688; b) Hicks, F. A.; Buchwald, S. L. *J. Am. Chem. Soc.* **1999**, 121, 7029; c) Sturla, S. J.; Buchwald, S. L. *J. Org. Chem.* **1999**, *64*, 5547; d) Sturla, S. J.; Buchwald, S. L. *Organometallics* **2002**, *21*, 739.

196. a) Hiroi, K.; Watanabe, T.; Kawagishi, R.; Abe, I. *Tetrahedron: Asymmetry* **2000**, *11*, 797; b) Hiroi, K.; Watanabe, T.; Kawagishi, R.; Abe, I. *Tetrahedron Lett.* **2000**, *41*, 891.

197. a) Gibson, S. E.; Kaufmann, K. A. C.; Loch, J. A.; Steed, J. W.; White, A. J. P. *Chem. Eur. J.* **2005**, *11*, 2566; b) Gibson, S. E.; Hardick, D. J.; Haycock, P. R.; Kaufmann, K. A. C.; Miyazaki, A.; Tozer, M. J.; White, A. J. P. *Chem. Eur. J.* **2007**, *13*, 7099.

198. Sturla, S. J.; Buchwald, S. L. *J. Org. Chem.* **2002**, *67*, 3398.

199. a) Verdaguer, X.; Moyano, A.; Pericas, M. A.; Riera, A.; Greene, A. E.; Piniella, J. F.; Alvarez-Larena, A. *J. Organomet. Chem.* **1992**, *433*, 305; b) Castro, J.; Moyano, A.; Pericas, M. A.; Riera, A.; Greene, A. E. *Tetrahedron: Asymmetry* **1994**, *5*, 307.

200. Konya, D.; Robert, F.; Gimbert, Y.; Greene, A. E. *Tetrahedron Lett.* **2004**, *45*, 6975.

201. a) Verdaguer, X.; Moyano, A.; Pericàs, M.A.; Riera, A.; Maestro, M.A.; Mahía, J. *J. Am. Chem. Soc.* **2000**, *122*, 10242; b) Solà, J.; Riera, A..; Verdaguer, X ; Maestro, M. A. *J. Am. Chem. Soc.* **2005**, *127*, 13629.

202. Liu, G.; Cogan, D. A; Ellman, J. A. *J. Am. Chem. Soc.* **1997**, *119*, 9913.

203. a) Solà, J.; Revés, M.; Riera, A.; Verdaguer, X. *Angew. Chem. Int. Ed.* **2007**, *46*, 5020; b) Revés, M.; Achard, T.; Solà, J.; Riera, A.; Verdaguer, X. *J. Org. Chem.* **2008**, *73*,

7080; c) Ji, Y.; Riera, A.; Verdaguer, X. *Org. Lett.* **2009**, *11*, 4346.

204. a) Shibata, T.; Takagi, K. *J. Am. Chem. Soc.* **2000**, *122*, 9852; Shibata, T.; b) Toshida, N.; Yamasaki, M.; Maekawa, S.; Takagi, K. *Tetrahedron* **2005**, *61*, 9974.

205. Kwong, F. Y.; Lee, H. W.; Lam, W. H.; Qiu, L.; Chan, A. S. C. *Tetrahedron: Asymmetry* **2006**, *17*, 1238.

206. a) Lightfoot, A.; Schnider, P.; Pfaltz, A. *Angew. Chem. Int. Ed.* **1998**, *37*, 2897; b) Helmchen, G.; Pfaltz, A. *Acc. Chem. Res.* **2000**, *33*, 336.

207. Lu, Z.-L.; Neumann, E.; Pfaltz, A. *Eur. J. Org. Chem.* **2007**, 4189.

208. Jeong, N.; Sung, B. K.; Choi, Y. K. *J. Am. Chem. Soc.* **2000**, *122*, 6771.

209. Schmid, T. M.; Consiglio, G. *Chem. Commun.* **2004**, 2318.

210. a) Kim, D. E.; Choi, C.; Kim, I. S.; Jeulin, S.; Ratovelomanana-Vidal, V.; Genet, J. P.; Jeong, N. *Synthesis* **2006**, 4053; b) Kim, D. E.; Choi, C.; Kim, I. S.; Jeulin, S.; Ratovelomanana-Vidal, V.; Genet, J. P.; Jeong, N. *Adv. Synth. Catal.* **2007**, *349*, 1999.

211. Fan, B. M.; Li, S; Xie, J.-H.; Wang, L.-X; Tu, Y.-Q.; Zhou, Q.-L., *Science in China: Series B Chemistry* **2006**, *49*, 81.

212. Fan, B.-M.; Xie, J.-H.; Li, S.; Tu, Y.-Q.; Zhou, Q.-L. *Adv. Synth. Catal.* **2005**, *347*, 759.

213. Morimoto, T.; Fuji, K.; Tsutsumi, K.; Kakiuchi, K. *J. Am. Chem. Soc.* **2002**, *124*, 3806.

214. Shibata, T.; Toshida, N.; Takagi, K. *Org. Lett.* **2002**, *4*, 1619.

215. Shibata, T.; Toshida, N.; Takagi, K. *J. Org. Chem.* **2002**, *67*, 7446.

216. a) Fuji, K.; Morimoto, T.; Tsutsumi, K.; Kakiuchi, *Angew. Chem. Int. Ed.* **2003**, *42*, 2409; b) Fuji, K.; Morimoto, T.; Tsutsumi, K.; Kakiuchi, K. *Tetrahedron Lett.* **2004**, *45*, 9163.

217. Kwong, F. Y.; Li, Y. M.; Lam, W. H.; Qiu, L.; Lee, H. W.; Yeung, C. H.; Chan, K. S. Chan, A. S. C. *Chem. Eur. J.* **2005**, *11*, 3872.

218. Kwong, F. Y.; Lee, H. W.; Qiu, L.; Lam, W. H.; Li, Y. M.; Kwong, H. L.; Chan, A. S. C. *Adv. Synth. Catal.* **2005**, *347*, 1750.

219. Jeong, N.; Kim, D. H.; Choi, J. H. *Chem. Commun.* **2004**, 1134.

220. Kim, D. E.; Choi, C.; Kim, I. S.; Jeulin, S.; Ratovelomanana-Vidal, V.; Genet, J. P.; Jeong, N. *Adv. Synth. Catal.* **2008**, *350*, 2695.

221. Kim, D. E.; Kim, I. S.; Ratovelomanana-Vidal, V.; Genet, J. P.; Jeong, N. *J. Org. Chem.* **2008**, *73*, 7985.

222. The stereochemical assignment for bicyclopentenone **(*S*)-310** was initially based on the work of Jeong and coworkers (ref. 221) and later confirmed by X-ray analysis of adduct **388** (*vide* section **2.3.6.**).

223. Cao, P.; Zhang, X. *Angew. Chem. Int. Ed.* **2000**, *39*, 4104.

224. Phan, D. H. T.; Kim, B.; Dong, V. M. *J. Am. Chem. Soc.* **2009**, *131*, 15608.

225. SEGPHOS-type ligands were previously unemployed in the asymmetric Rh-catalysed. For the application of SEGPHOS ligands in the Rh-catalysed ene cycloisomerisation, see: Tanaka, K.; Otake, Y.; Hirano, M. *Org. Lett.* **2007**, *9*, 3953.

226. The enantioselective PK reaction of enyne **373** (entry 3, **Table 2.9.**) provided a mixture of homodimerisation products **376b** and **376c** in a ratio of 9:1. The regiochemistry of adduct **376b** was determined by HSQC and HMBC analysis.

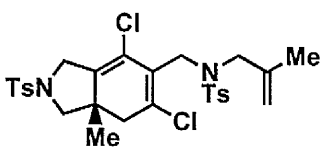

376b

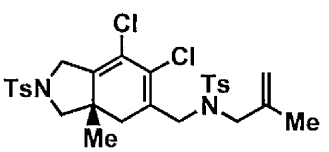

376c

227. The absolute stereochemistry for the products of the enantioselective PK reaction of chlorinated 1,6-enynes was confirmed by X-ray analysis of adduct **388** (*vide* section **2.3.6.**).

228. Ricci, P.; Evans, P. A. *manuscript in preparation.*

229. The alkene geometry of the S_N2'-type cyclisation adduct **398** was confirmed by HMBC and NOE analysis.

230. Fernandez-Rivas, C.; Mendez, M.; Nieto-Oberhuber, C.; Echavarren, A. M. *J. Org. Chem.* **2002**, *67*, 5197.

231. The relative stereochemistry of adducts **405** and **409** was confirmed by NOESY

analysis.

232. Calculations of the *cis* and *trans* equilibrium conformers were performed by means of Spartan Wavelength Software (Hartree-Fock 3.21 G* level). Tosyl moiety and hydrogen atoms are omitted for clarity.

233. The relative and absolute stereochemistry of adduct **427** has been tentatively assigned as *(R,R)* on the basis of the previous works of Jeong and coworkers on the desymmetrisation of *meso*-dienynes by Pauson-Khand reaction.[219.,221] However, as showed by Jeong, the relative and absolute stereochemistry is highly dependent on the catalyst and solvent employed in the reaction (see **Scheme 2.14**) and thereby, we cannot establish the stereochemistry of adduct **427** by simple comparison with previous works. Hence, the determination of the relative and absolute stereochemistry of the product **427** must be assigned by X-ray analysis of this product or, alternatively, X-ray analysis on a derivative of Pauson-Khand product **427** (*vide* section **2.3.6.**).

234. Cheng, X.; Zhang, Q.; Xie, J.-H.; Wang, L.-X.; Zhou, Q.-L. *Angew. Chem. Int. Ed.* **2005**, *44*, 1118.

235. HPLC analysis showed that the utilisation of (*S*)-*xyl*-BINAP as a ligand in the Rh-catalysed desymmetrisation reaction of **426** provides **(*R*,*R*)-427** as the major enantiomer, while the utilisation of (*S*)-SPIROP as a ligand in the reaction provides **(*S*,*S*)-427** as the major enantiomer.

236. A sample of **(*S*)-388** (80 mg) in a 10 mL vial was dissolved in DCM (1 mL) and hexane (4 mL) was slowly added dropwise on top of the DCM layer. The vial was closed with a cap and left at room temperature. After two days, formation of transparent crystals of **(*S*)-388** was observed. Then, the vial was opened and the solvent was allowed to evaporate slowly over one day.

237. X-ray analysis of compound **(*S*)-388** has been performed by Dr Craig Robertson (X-ray service supervisor, Department of Chemistry, University Liverpool). The unrefined X-ray analysis (**Figure 2.12**) has provided the absolute configuration for the compound **(*S*)-388**. The complete refinement of the structure is still in progress and full data of the X-ray

analysis will be included in this PhD thesis.

238. Oppolzer, W.; Stammen, B. *Tetrahedron*, **1997**, *53*, 3577.

239. Kitamura, T.; Sato, Y.; Mori, M. *Adv. Synth. Catal.* **2002**, *344*, 678.

240. Kim, S. Y.; Chung, Y. K. *J. Org. Chem.* **2010**, *75*, 1281.